POLSKIE TOWARZYSTWO MIKROBIOLOGÓW
POLISH SOCIETY OF MICROBIOLOGISTS

Polish Journal of Microbiology

2019

Polish Journal of Microbiology
formerly Acta Microbiologica Polonica
2019, Vol. 68, No 2

CONTENTS

INSTRUCTIONS FOR AUTHORS
Instructions for authors: https://www.exeley.com/journal/polish_journal_of_microbiology

Ministry of Science
and Higher Education

Republic of Poland

Purchase of DOI numbers for articles and implementation
of a modern publication platform
for the Polish Journal of Microbiology are funded with the financial support
of the Ministry of Science and Higher Education
under agreement No. 659/P-DUN/2018 for science dissemination activities.

Polish Journal of Microbiology
2019, Vol. 68, No 2, 153–164
https://doi.org/10.33073/pjm-2019-028

MINIREVIEW

The State of Research on Antimicrobial Activity of Cold Plasma

IWONA NIEDŹWIEDŹ[1], ADAM WAŚKO[1], JOANNA PAWŁAT[2] and MAGDALENA POLAK-BERECKA[1]*

[1] Department of Microbiology, Biotechnology and Human Nutrition, University of Life Sciences in Lublin, Lublin, Poland
[2] Faculty of Electrical Engineering and Computer Science, Lublin University of Technology, Lublin, Poland

Submitted 17 January 2019, revised 15 April 2019, accepted 17 April 2019

Abstract

Microbiological contamination is a big challenge to the food industry, medicine, agriculture, and environmental protection. For this reason, scientists are constantly looking for alternative methods of decontamination, which ensure the effective elimination of unwanted biological agents. Cold plasma is a new technology, which due to its unique physical and chemical properties becomes a point of interest to a growing group of researchers. The previously conducted experiments confirm its effective action, e.g. in the disinfection of skin wounds, air, and sewage treatment, as well as in food preservation and decontamination. The reactive compounds present in the plasma: high-energy electrons, ionized atoms and molecules, and UV photons are the key factors that cause an effective reduction in the number of microorganisms. The mechanism and effectiveness of the cold plasma are complex and depend on the process parameters, environmental factors and the type and properties of the microorganisms that are to be killed. This review describes the current state of knowledge regarding the effectiveness of the cold plasma and characterizes its interaction with various groups of microorganisms based on the available literature data.

Key words: biofilm, cellular response, cold plasma, mycotoxin, viruses

Introduction

Cold plasma (CP) or nonthermal plasma (NTP) and, in particular, cold atmospheric plasma (CAP) is gaining increasing scientists' interest, given the possibility of application thereof in medicine (Boudam and Moisan 2010; Isbary et al. 2010; Vandamme et al. 2010; Metelmann et al. 2018), food industry (Afshari and Hosseini 2014; Hojnik et al. 2017, Pignata et al. 2017), agriculture, and environmental protection (Bogaerts and Neyts 2018; Pawłat et al. 2018a; 2018b; Siddique et al. 2018). Many investigations have confirmed the positive effect of the plasma on the anticancer therapy (Kim et al. 2009; Vandamme et al. 2010), disinfection of skin wounds (Isbary et al. 2010; Lademann et al. 2011), surgical instruments and materials in contact with food (Boudam and Moisan 2010; Dasan et al. 2017b), purification of air, water, wastewater, and sewage, as well as preservation and decontamination of food (Gallagher et al. 2007; Korachi et al. 2009; Pawłat 2013; Chizoba Ekezie et al. 2017; Wolny-Koładka et al. 2017). Such a broad spectrum of the cold plasma applications is associated with its ability to inactivate biological factors as viruses (Terrier et al. 2009; Su et al. 2018), bacteria (Isbary et al. 2010; Samoń et al. 2014; Kartaschew et al. 2016), spores (Deng et al. 2006; Boudam and Moisan 2010), yeasts (Korachi et al. 2009; Metelmann et al. 2018), or fungi (Bayliss et al. 2012; Panngom et al. 2014; Siddique et al. 2018).

William Crookes discovered plasma in 1879 while the concept of the plasma was first used in the article by Irving Langmuir's entitled "Oscillations in ionized gases" in 1928. Since then, plasma physics has become an important field of research. The plasma processing is used from the seventies when it was used to etch semiconductor materials. Then, in the 1980s, it was used in the computer industry, especially in the production of miniaturized circuits. In the last decade of the twentieth century, there has been a development of the plasma generation technology at an atmospheric pressure, which allowed to eliminate the expensive vacuum chambers. This has resulted in wider applications of

* Corresponding author: M. Polak-Berecka, Department of Microbiology, Biotechnology and Human Nutrition, University of Life Sciences in Lublin, Lublin, Poland; e-mail address: **magdalena.polak-berecka@up.lublin.pl**

cold plasma in medicine, environmental protection and food preservation (Misra et al. 2016).

Plasma, which is regarded as the fourth state of matter is a type of ionized gas containing many charged particles (OH^-, H_2O^+, electrons), reactive compounds (reactive oxygen species – ROS, which include hydroxyl radical, superoxide anion hydrogen peroxide, and reactive nitrogen species – RNS, i.e., peroxynitrite), the molecules in the excited and basic states, and UV photons (UVB, UVC) (Brisset and Pawłat 2016; Bruggeman et al. 2016).

Plasma can be classified according to the generation conditions, i.e. atmospheric pressure (low-pressure plasma, high-pressure plasma), temperature (low-temperature plasma, high-temperature plasma), and the composition of plasma-generating gas (one-component plasma, multi-component plasma) (Dzimitrowicz et al. 2015; Bourke et al. 2017). The division of the plasma due to the temperature depends on the temperature of the electrons (T_e). The high-temperature plasma is characterized by $T_e = 10^6 \sim 10^8$ K, whereas for the low-temperature plasma the T_e value is in the range from 10^4 to 10^5 K (Fridman et al. 2005). In addition, the low-temperature plasma is divided into thermal and non-thermal plasma due to the thermodynamic equilibrium. Inactivation of biological factors uses a non-thermal plasma that is characterized by a thermodynamic imbalance. Therefore, the electrons have a higher temperature than the temperature of the neutral particles (T_n), and the temperature of the gas (T_g), and thus, the temperature of the process increases slightly (Laskowska et al. 2016; Liao et al. 2017).

Non-equilibrium plasma (with temperatures of electrons substantially exceeding the temperatures of the other gas components) can be generated with the use of various electric discharges, e.g. corona, microwave, gliding arc, and dielectric barrier discharges as plasma sources. As a result of these discharges, the energy from the electric field is collected by electrons as a result of their collision, and only part of the energy is transferred to neutral molecules which results in the formation of the $T_e \geq T_n$ state, characterized by non-thermal plasma. The type of the plasma source has directed the effect on the composition and the number of components generated by the plasma and determines the technological application of the plasma. The temperature of the plasma is extremely important in the processing of the materials that are sensitive to high temperatures. The optimization of the power supply system, an appropriate geometry of the discharge system, and the type of gas are essential when active agents generated by cold plasma (e.g. reactive compounds), whose temperature does not exceed several tens of degrees Celsius, have to be standardized. For the applications in agriculture, food industry, and medicine, the dielectric barrier discharges (DBD) and plasma jets are used most frequently for the generation of cold plasma due their simple structure and ease of modification (Pawłat et al. 2016; Bourke et al. 2017).

The mechanism involved in the cold plasma sterilization process has not yet been elucidated. The numerous attempts made by scientists confirm the inactivation of virus particles and microbial cells by the plasma, but the relationships between them have not been explored in details (Liao et al. 2017). The reactive compounds, high-energy electrons, ionized atoms and particles, and UV radiation are involved in the process of biological inactivation (Bourke et al. 2017). When in contact with biological material, the compounds derived from oxygen or nitrogen, i.e., O, O_2, O_3, OH·, NO, and NO_2 are characterized by high reactivity. Their effects include oxidation of membrane lipids and proteins, which results in the disturbances of the proper membrane function and, finally, the disruption of the cell membrane (Afshari and Hosseini 2014). Membrane integrity is highly influenced by electrostatic forces. The charged particles generated by the plasma accumulate on the outer side of the membrane, thereby leading to its disintegration (Liao et al. 2017). The discontinuity of the cell surface structures can also be an effect of the electroporation process. This phenomenon involves an increase in the number of the existing cell micropores and the emergence of new ones induced by the pulsed electric field (Wiktor et al. 2013). The degradation of DNA caused by UV radiation could also be involved in the inactivation of microorganisms. Photons present in the plasma can alter the structure of the nucleic acids, leading to the formation of nitrogen base dimers and impairment of DNA replication capacity (Beggs 2002; Liao et al. 2017). The contribution of each of the mechanisms and their effectiveness in biological inactivation vary and depend primarily on the parameters of the plasma generation process, environmental factors, and the type and properties of the microorganisms (Fig. 1) (Bayliss et al. 2012).

The aim of this review is to present the current knowledge on the antimicrobial activity of the plasma and to discuss the molecular mechanism of interactions between cold atmospheric plasma and various groups of microorganisms.

Effect of cold plasma on viruses

The cold plasma technology becomes a promising solution for inactivation of pathogenic viruses that cause infections in humans, animals, and plants (Bourke et al. 2017). The specific mechanisms of CP inactivation of viruses have not been elucidated yet. The studies carried out so far demonstrated that exposure to cold plasma can lead to the modification and/or degradation of proteins, nucleic acids, and lipids of viral envelopes (Pradeep and Chulkyoon 2016). The

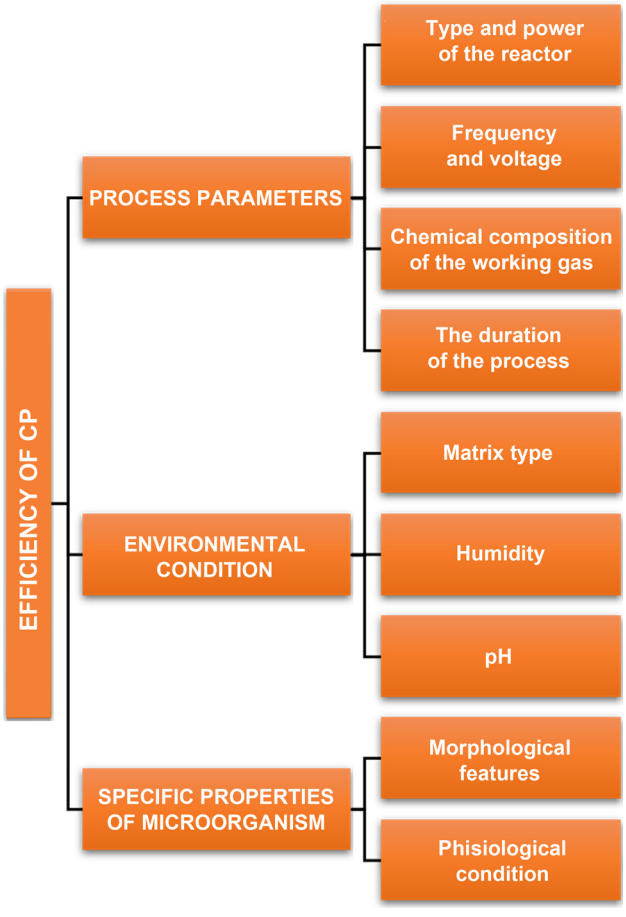

Fig. 1. Factors influencing the effectiveness of decontamination using cold plasma. Based on Liao et al. 2017.

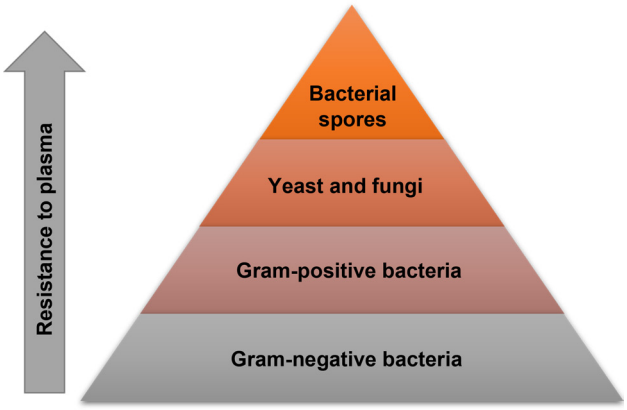

Fig. 2. Pyramid of the sensitivity of microorganisms to plasma*. Based on Klämpfl T.G. et al. 2012; and Liao et al. 2017.

* Sensitivity of individual groups of microorganisms can vary depending on the conditions of the process.

researches on the impact of the plasma on bacteriophages (a λ phage model system) suggested that the damage of capsid proteins is directly involved in the inactivation of viruses (Yasuda et al. 2010).

Cold plasma has been demonstrated to inactivate animal viruses. Terrier et al. (2009) investigated three types of viruses with the considerable clinical importance, which cause respiratory infections, e.g. respiratory syncytial virus (RSV), human parainfluenza virus type 3 (HPIV-3), and influenza A virus subtype H5N2. The plasma generated with air as the working gas contributed to a significant decrease in the titer of all viruses tested. Researchers indirectly associated this finding with the presence of ozone in the generated plasma that induces the protein damage and lipid peroxidation. The effect of the plasma on adenoviruses was analyzed by Zimmermann et al. (2011), who used 4.7-kV micro-discharges for the generation of the plasma. These viruses have double-stranded DNA (dsDNA) and exhibit low sensitivity to physical and chemical factors. They are causative agents of ophthalmological, respiratory, and gastrointestinal diseases. Using a green fluorescent protein (GFP) and a firefly luciferase, the researchers demonstrated that both viral infectivity and replication were inhibited. The activity of reactive nitrogen species (RNS) and their intermediates was proposed as a mechanism of the plasma effect on the DNA structure and immunogenicity of the virus. Some investigations were focused on the susceptibility of noroviruses (NoV), which cause gastrointestinal infections and pose a major problem in the food industry. Ahlfeld et al. (2015) studied the effect of CP on the inactivation of NoV from fecal samples. They treated the samples with a plasma stream and evaluated the effectiveness of inactivation at a variable time of the process. They achieved 1.23 log and 1.69 log reduction in the viral titer after 10 and 15 minutes, respectively (Bourke et al. 2017). The recent research also suggests that plasma-activated solutions (PASs) can contribute to effective decontamination. The effectiveness of inactivation of the Newcastle disease virus (ND) by the plasma-activated solutions (H_2O, 0.9% NaCl, 0.3% H_2O_2) was assessed. The scanning electron microscope's (SEM) images revealed morphological changes in virus particles, and the reduction of their titer and RNA degradation have also been shown (Su et al. 2018).

Effect of cold plasma on microbial cells

Microorganisms are a key target in the investigation of the plasma efficiency, as susceptibility to the sterilization process may vary between microorganisms, even within species and strains (Fig. 2). It largely depends on the structure of cellular envelopes and the microbial growth phase (Liao et al. 2017).

Bacteria

The exact mechanism of inactivation of bacterial cells by cold plasma is still unknown, although the issue has been extensively studied. Permeabilisation of

the cell membrane or cell wall leading to leakage of intracellular components, i.e. potassium, nucleic acids, and proteins, is regarded as one of the mechanisms of inactivation of this group of microorganisms. Furthermore, inactivation of bacteria occurs via the oxidative damage to intracellular proteins and DNA related to the effect of the plasma compounds (Mai-Prochnow et al. 2014). The overall mechanisms of microbial inactivation with plasma reactive species are presented in Fig. 3. The impact of the plasma stream on the external bacterial structures was investigated by Laroussi et al., who use the plasma generated with dielectric barrier discharge (DBD) against *Escherichia coli* and *Bacillus subtilis* cells. For Gram-negative *E. coli* with a cell wall composed of an outer membrane and thin peptidoglycan (murein), there was substantial damage to the membrane resulting in the cytoplasm leakage. The authors suggest that the visible changes resulted from the electrostatic rupture of the outer membrane. In turn, the microscopic image of Gram-positive *B. subtilis* cells with a thick cell wall did not show the significant morphological modifications and the decontamination was most probably due to interactions of reactive compounds with the intracellular components. The differences in the effect of the plasma on this microbial group are related to a different structure of cell walls in these microorganisms (Laroussi et al. 2003). A comprehensive analysis of chemical modifications induced by CAP in the structure of Gram-positive (*B. subtilis*) and Gram-negative (*E. coli*) bacteria was performed by Kartaschew et al. (2016) with use of a Fourier Transform Infrared Spectroscopy (FTIR) technique. The spectral images revealed that the plasma caused an increase in the number of symmetric stretching vibrations that reveal the formation of carboxylic groups (COO^-). The investigators also noted the spectra in the absorbance range of 1720 cm^{-1} that indicate the formation of carbonyl groups (C = O) related to the presence of aldehydes, ketones, or acids. The resulting signals were associated with the destruction of the cell wall and cellular membrane by ROS. Another phenomenon induced by the activity of the plasma is the change of the cell membrane potential. This leads to disturbances in the function of the protonomotoric force and, consequently, abnormal ATP synthesis and the impairment of cell metabolism and division (Brun et al. 2018).

The changes in the membrane integrity may have a direct effect on DNA, mainly through the discontinuation of interactions with membrane proteins and formation of pores in the cell membrane by which nucleic acids can be released from the cell (Coutinho et al. 2018). Plasma-induced release of DNA is possible after the prior DNA fragmentation, and the effectiveness of this process depends on the conformation of the nucleic acid. In comparison with linear DNA, its supercoiled circular form is regarded as the resistant form of the nucleic acids (Moreau et al. 2008; Alkawareek et al. 2014). In general, it is believed that the plasma effect on DNA is a result of the activity of both reactive compounds and UV photons (Coutinho et al. 2018). In the cell, the DNA-protein crosslinks (DPCs) can be formed, which lead to the formation of hard-to-repair damage. Reactive oxygen and nitrogen species produced by the plasma oxidize proteins by the generation of hydroperoxide groups in their structure, which can form strong intramolecular crosslinks with the nucleic acids. In the experiment conducted by Guo et al. (2018), *E. coli* cells after treatment with the plasma stream with an air and 1% He were subjected to two versions of a Comet assay (with and without proteinase K) to assess the formation of DPC in DNA of the analyzed bacterium. In the fluorescent DNA image of the cells treated with the plasma,

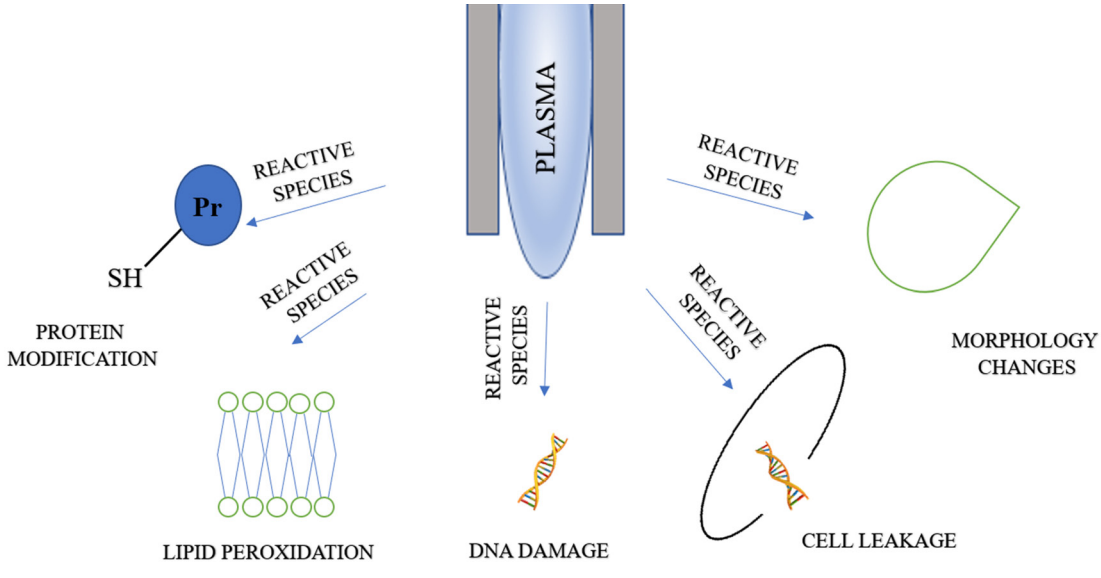

Fig. 3. Mechanisms of microbial inactivation with plasma reactive species. Based on Bourke et al. 2017.

the researchers observed short "tails" indicating the damaged fragments without proteinase treatment, and much longer tails after the treatment with proteinase. This suggested the presence of DPC crosslinks, which were destroyed by the enzyme digesting the proteins. Then, the proteins were by the CsCl density gradient ultracentrifugation, treated with a nuclease, and their analysis revealed a higher concentration and diversity of the proteins than in the samples that were not treated with the plasma. This may be another piece of evidence supporting the hypothesis that the plasma-induced damage to nucleic acids is a result of the protein-DNA covalent bonding. An important issue is the CP effect on the genes encoding antibiotic resistance. The resistance of methicillin-resistant *Staphylococcus aureus* (MRSA) is associated with the *mecA* gene, which encodes protein *PBP2a* characterized by low affinity to β-lactam antibiotics. The most recent investigations of the CP applications for inactivation of *S. aureus* MRSA demonstrated that the cumulative energy delivered to the surface of the plasma-treated sample was 0.12 kJ/cm^2 and 0.35 kJ/cm^2, respectively, when air was used as the working gas. Five-log reduction in the number of *S. aureus* MRSA was observed even at the lower energy values, whereas higher values (0.35 kJ/cm^2) were required for more effective degradation of the resistance gene. The isolated *mecA* gene exhibited higher sensitivity to the plasma activity compared to the intracellular gene. This is closely related to the protective effect of cell constituents, which are the first to interact with the reactive plasma components (Liao et al. 2018). The investigations also highlighted the changes in the membrane potential and integrity induced by the various intensities of the plasma activity. After application of the plasma treatment with a cumulative energy level of 0.12 kJ/cm^2, the authors observed that a membrane potential coefficient was close to the depolarization value (Liao et al. 2018).

The use of cold plasma leads to the degradation of cellular proteins. Large proteins (50–90 kDa) are destroyed as the first. It was revealed by analysis of the samples where the concentration of the proteins with a molecular mass below 25 kDa increased after the plasma treatment (Hosseinzadeh Colagar et al. 2013). The probable mechanism of the degradation consists of the destruction of hydrogen, sulfide, and peptide bonds by reactive compounds present in the plasma. This results in the changes of the primary, secondary, and tertiary protein structure that lead to a decline in the enzymatic activity of the cell (Mai-Prochnow et al. 2014). Recently, researchers have investigated the effect of CP on proteins in thermophilic bacteria that pose a serious problem in the food industry due to their high resistance to the classical decontamination methods, i.e. high temperature or chemical denaturing agents. Attri et al. (2018) treated a highly stable MTH 1880 protein from the thermophilic bacterium *Methanobacterium thermoautotrophicum* with CP generated by DBD and analyzed it with the circular dichroism (CD), fluorescence, and nuclear magnetic resonance (NMR) spectroscopy techniques. Additionally, molecular dynamics (MD) simulation was carried out for both the native and plasma-treated protein. The investigators achieved a partial destabilization of MTH protein only after a long time of exposure to CP (20 min), which resulted in a decrease of 5°C in its melting point and an increase in its susceptibility to thermal denaturation. To elucidate the mechanism of the plasma effect on cellular proteins, the proteomic profile of *Salmonella enteritidis* was determined and as the result, 1096 proteins were identified with 249 of them present only in the plasma-treated samples and nine only in control samples. Under the impact of CP, the proteins that were overexpressed came mainly from the carbohydrate and nucleotide metabolism pathways and were associated with RNA transcription. It indicates an increased energy metabolism in cells as a defense response of bacteria (Ritter et al. 2018). The plasma-induced changes in bacterial metabolism were reported by Laroussi et al. (2003), who demonstrated the reduced utilization of L-lactic acid and increased consumption of D-sorbitol (Moreau et al. 2008). Interestingly, the effect of plasma on microorganisms does not always lead to cell death but can also reduce their metabolism, therefore, the cells do not undergo division and become viable but not culturable (VBNC). Dolezalova et al. (2015) treated a suspension of *E. coli* cells with the plasma and measured bacterial viability with a conventional culture method and by assessment of the fluorescent images of the cells stained with the LIVE/DEAD kits. The result of the former method suggested a 7.0-log reduction of the number of cells, whereas a reduction of only 1.0 log was indicated with the latter technique. These findings suggest that the plasma may induce the VBNC state of the cells.

Spores. Through evolutionary adaptation, bacterial spores have acquired the possibility to survive in adverse environmental conditions. They are characterized by resistance to disinfectants, chemical sterilants, drying processes, and thermal inactivation. This poses a serious threat to food and pharmaceutical industries as well as medicine, where spores are a permanent source of contamination (Liao et al. 2017). The major cause of such high resistance of spores is their structure, which differs substantially from that of vegetative forms of bacteria. Spores are composed of impermeable outer layers creating a specific barrier for the external factors. Additionally, they are characterized by low water content, which accounts for approximately 15% of the entire cell (Olesiak and Stępniak 2012). The interior of the spore contains a rigid structure, i.e. an inner membrane permeable only to small molecules (< 200 Daltons). When

the membrane is damaged, dipicolinic acid (DPA) is released and endospore germination is not induced. DPA ensures considerably higher (up to 50-fold) resistance to UV radiation in spores (Olesiak and Stępniak 2012). In the very core of the spore, the DNA protection function against chemical and physical agents is fulfilled by small acid-soluble SASP proteins, which are closely related to the nucleic acids (Kądzielska et al. 2012). The precise mechanism of the plasma effect on spores has not been clarified to date. Some researchers suggest that spores are inactivated mainly via interactions between the reactive plasma compounds and the external spore structures (Hong et al. 2009). The morphological changes in *B. subtillis* endospores induced by various CF-related factors were presented by Deng et al. (2006) on scanning electron microscopy (SEM) images. The changes in the spore size, leakage of the cytoplasm content, and final membrane disruption were observed. These results suggest that oxidation by reactive oxygen species is the main factor contributing to the reduction of the number of viable *B. subtilis* cells, whereas the electric field, UV photons, and charged particles play a minor role in this process. Other investigators demonstrated that inactivation of endospores was primarily caused by damage to their outer layers resulting in leakage of DPA and hydration of the core (Tseng et al. 2012). The importance of the external structures for resistance to cold plasma was analyzed by Raguse et al. (2016), who investigated wild-type *B. subtilis* spores and mutants deficient in some surface structures. Additionally, the investigators examined the effect of the gas applied on the effectiveness of sterilization. Their results indicated a substantial impact of surface structures and the type of gas on the resistance of spores. A mixture of oxygen and argon was the most effective in inactivation of bacterial spores, as it caused significant damage to the external layers. In contrast, the mutants deficient in surface structures exhibited the highest sensitivity to plasma. The recent studies conducted by Connor et al. (2017) also have emphasized the impact of environmental conditions on plasma efficiency. The studies on the resistance of *Clostridium difficile* spores to plasma were conducted in three different environments (the spores suspended in water and dry spores with or without 0.03% BSA). The greatest reduction in the spore number in the shortest time was observed in a dry environment. In contrast, organic matter and moist environment extended the time of the spore inactivation by plasma (Klampf et al. 2014).

Another aspect that should be explored more deeply is the mechanism of CP effect on sporal DNA. There is a contradictory data on the effect of UV photons generated in the sterilization process on nucleic acids. The results of investigations conducted by Tseng et al. (2012) did not show DNA degradation in *B. subtilis* spores after a 20-min exposure to the plasma. This finding can be supported by the conclusion reported by Fiebrandt et al. (2016), who suggested that cell layers absorb UV radiation, thereby protecting DNA from damage. This mechanism is plausible given the structure of spores. Surface structures of spores are characterized by a high content of proteins with amino acid side chains forming endogenous chromophores. These compounds can be the main target of photooxidation, thereby protecting the cell interior from harmful radiation.

Some investigations have indicated that the plasma inactivates spores by the impact on key metabolic proteins. In their study, Dobrynin et al. (2010) suggested that reactive oxygen species penetrating the cell interior could cause oxidation of proteins involved in germination or inactivate germination receptors located in the inner membrane of spores. In turn, Wang et al. (2011) compared the kinetics of germination of the cold plasma-treated *B. subtilis* spores and untreated spores. They conducted the experiments in an environment enriched with nutrient germinants (L-valine) and non-nutrient germinants (dodecylamine, Ca^{2+}DPA). Their results indicated the potential inactivation effects of the plasma on germination receptors but the germination induced by L-valine was inhibited.

Bacterial biofilm. Many microorganisms live in the environment as biofilms rather than free-living organisms. Biofilm was defined as the cells adhering to a solid surface and surrounded by an extracellular matrix produced by them (Czapka et al. 2018). Such populations exhibit higher resistance to adverse external factors (antibiotics, temperature, and pH); therefore, they pose a serious challenge in both medicine and food industry (Maciejewska et al. 2016). There are numerous reports demonstrating the sensitivity of biofilms to CF; however, the time required for full inactivation thereof is longer than for planktonic cells (Mai-Prochnow et al. 2014; Flynn et al. 2015). This was confirmed by Jahid et al. (2014), who compared the effect of CP on planktonic *Aeromonas hydrophila* cells and bacterial biofilm on the surface of lettuce. The experiment showed that a 15-s plasma treatment was sufficient to reduce the number of planktonic populations by >5 logs. In contrast, the cell population on the lettuce surface was substantially reduced after a 5-min process of the plasma treatment (Jahid et al. 2014; Bourke et al. 2017). The extracellular matrix constitutes approx. 90% of biofilm and its presence largely determines the effectiveness of sterilization processes (Czyzewska-Dors et al. 2018). The matrix composition varies and depends on species of microorganisms forming the biofilm. The basic components of the extracellular matrix are polysaccharides, lipids, proteins, and nucleic acids. These compounds constitute a protective barrier against antibiotics or temperature as well as photons, reactive

compounds, and charged particles in the plasma. Since these agents have to penetrate the protective layer, the biofilm inactivation time is prolonged (Mai-Prochnow et al. 2014). The results of investigations conducted by Ermolaeva et al. (2011) demonstrated the differences in the survival of bacteria in different biofilm layers, suggesting that the effectiveness of CP depends on the biofilm thickness. Microscopic evaluation of the viability of *P. aeruginosa* biofilm showed a greater number of bacterial cells in its deeper layers. This probably explains the proportional decline of the sterilization effectiveness with the increasing biofilm thickness. Another determinant of the sterilization effectiveness is the species of biofilm-forming microorganisms. This issue was investigated by Mai-Prochnow et al. (2016) who compared the effects of CP on bacterial biofilm formed by Gram-positive *B. subtillis* and Gram-negative *P. aeruginosa*. Almost complete reduction of the bacteria in Gram-negative biofilm was observed in contrast to Gram-positive biofilm where a 10-min plasma treatment resulted in <1 log reduction. The presence of reactive oxygen compounds contributing to the cell wall disintegration in the emission spectra suggests that the cell wall thickness may be correlated with the duration of the cold-plasma inactivation. In conclusion, the sterilants present in the plasma inactivate biofilms through damage to the extracellular matrix, cell wall, cellular membrane, and internal cell structures. They can also induce the VBNC state in the cells (Ziuzina et al. 2015; Bourke et al. 2017).

Bacterial cell response to cold-plasma treatment. Elucidation of mechanisms of cell response to the cold plasma treatment is an important issue and requires further exploration. Hitherto, the changes in gene transcription and expression induced by exposure of cells to plasma have been already analyzed. The available scientific publications demonstrated a potential increase in the expression of SOS regulon, oxidation-related genes, and the genes encoding DNA repair processes. In turn, the expression of housekeeping genes was reduced (Sharma et al. 2009; Roth et al. 2010). Sharma et al. investigated the effect of plasma on genomic DNA in *E. coli* and performed a microarray analysis of the samples after 2-min plasma exposure. The increased expression of the gene involved in superoxide radical scavenging (*katG*) and the *recA* gene responsible for DNA recombination and repair was noted (Sharma et al. 2009). Similar results were reported by Roth et al. (2010) who analyzed the samples of highly radiation-resistant bacteria (*Deinococcus radiodurans*) and found an increase in the expression of the genes involved in DNA repair, oxidative stress responses, and cell wall synthesis. The process of the nucleic acids repair may result in the emergence of mutations that will determine increased resistance to CP. UV radiation, which induces the formation of nitrogen base dimers in nucleic acids is the main mutagenic factor. On the other hand, ROS and RNS present in the plasma exert a destructive effect on cellular components; thus, contribute to bacterial death and minimize the conservation of mutation effects (Boxhammer et al. 2013).

Yeast

Yeasts, which are a valuable source of many enzymes, are widely used in food biotechnology and microbiology in both fermentation and food-enrichment processes (Krzyczkowska et al. 2008). With their low pathogenicity as well as a unique structure and properties, some yeast species, e.g. *Saccharomyces cerevisiae* or *Schizosaccharomyces pombe* have become an inseparable element of molecular biology, serving as a model for an eukaryotic organism. Furthermore, a simple and cost-efficient culture of yeasts has contributed to the increasing interest in these organisms as objects for the elucidation of the effect of CP on cells (Wawrzycka 2011). The experiments were performed by Nishime and coworkers (2017) on the effectiveness of the plasma generated by DBD discharges with helium addition against various microorganisms. The researchers studied *Enterococcus faecalis* (Gram-positive) and *P. aeruginosa* (Gram-negative) bacteria as well as *Candida albicans* yeasts. They reported an inactivating effect of the plasma on all of the microorganisms investigated. Nevertheless, in comparison with the bacterial cells, *C. albicans* exhibited higher resistance, which can be explained mainly by the differences in their cell structure. In turn, the investigations conducted by Colonna et al. (2017) were focused on the effect of the plasma generated with dry air and a gas mixture (65% O_2, 30% CO_2, 5% N_2) on *S. cerevisiae* cells at a different density of cellular suspension and duration of the exposure. The results confirmed a correlation between the effectiveness of sterilization and the process parameters. For the samples with higher cellular density, a longer timer of exposure of the suspension to the plasma was required for a complete cell degradation. Moreover, the reduction effect monitored at various time points indicated higher efficiency of a plasma stream with a gas mixture. The effect of environmental conditions on the effectiveness of inactivation was examined by Ryu et al. (2013), who observed a decrease of the number of *S. cerevisiae* cells suspended in different media (water, saline, and YPD). The most serious CP-induced damage to membrane lipids and genomic DNA was observed in yeast cells suspended in water. This was associated with the highest content of hydroxyl radicals generated in the water medium during the process.

Polcic et al. (2018), who used genetic mutants of yeasts to identify the role of oxidative stress and apoptosis

in the decontamination process made an attempt at the elucidation of the mechanisms of CP effect on *S. cerevisiae*. The results of the experiments indicated higher susceptibility of strains with superoxide dismutase deficiency than those deprived of the key components of the apoptotic pathway, as their sensitivity to the plasma activity did not change. This proves that reactive oxygen species are one of the most important factors involved in the inactivation of yeast cells, and the apoptosis process itself does not play a key role in this case. An important issue requiring comprehensive investigations is the impact of CP on intracellular proteins. The treatment of *S. cerevisiae* with argon plasma was found to lead to protein ubiquitination and formation of the insoluble protein aggregates in the yeast cytoplasm. These researchers also underlined the potential of the CP-induced generation of endoplasmic reticulum (ER) stress, which is characteristic of eukaryotic cells. This was confirmed by an increase in the activity of the endoplasmic reticulum transmembrane protein Ire1p induced by accumulation of unfolded proteins in ER (Itooka et al. 2018). As demonstrated in many research reports, the cold-plasma technique can be used for inactivation of enzymes (Li et al. 2011; Surowsky et al. 2013; Tolouie et al 2017; Tolouie et al. 2018). The authors suggest that the ability of plasma to inhibit enzymes is associated with loss of the protein secondary structure. It is an effect of interactions with reactive compounds generated in the gas used in the process (Misra et al. 2016). Colonna et al. (2017) investigated the impact of CP on enzymes produced by yeasts in a study on the plasma generated with dry air. Their analyses were focused on *S. cerevisiae* yeast invertase, which lost its activity at a level of > 96% after 75 s of the treatment.

Fungi

Plant diseases caused by fungal pathogens pose a serious crisis in agriculture, as they cause huge economic losses worldwide. As demonstrated in the recent research reports, the cold-plasma technology can become an alternative plant protection method either by inactivating fungal cells or improving the resistance of infected hosts (Dasan et al. 2017a; Siddique et al. 2018). The investigations that confirmed the susceptibility of this microbial group to the CP activity have been conducted by many researchers (Suhem et al. 2013; Sohbatzadeh et al. 2016; Nikmaram et al. 2018). Some of them suggested that the inactivation of fungal cells using CP mainly involves the production of reactive compounds which seems to have their destructive effect on the cell wall and inner membrane of fungi (Ye et al. 2012; Lu et al. 2014; Dasan et al. 2016; Dasan et al. 2017a). In their study, Ye et al. (2012) assessed the effect of the plasma (working gas: air) generated by corona discharges on the cells of *Penicillium expansum*, i.e. one of the most important pathogens causing spoilage of the stored fruit. SEM images revealed disruption of the external structures of *P. expansum*, which resulted in cytoplasmic leakage. In turn, an analysis of transmission electron microscopy (TEM) images indicated the plasma-induced alterations in the cell, i.e. an increased volume of the protoplasm, stretching of vacuoles, and disintegration of the membrane, which contributed to cell lysis.

Besides their impact on external structures and intracellular organelles, the reactive compounds present in the plasma and the generated UV radiation cause damage to nucleic acids and oxidation of proteins and lipids. Lu et al. (2014) have investigated the effect of CP on *Cladosporium fulvum* by determination of the concentration of malondialdehyde (MDA), i.e. the basic product of lipid peroxidation. The findings reported confirmed the hypothesis that the activity of sterilizing agents in fungal cells triggers the peroxidation process. The similar observations were reported by another research team investigating the effect of CP generated at atmospheric pressure on *Aspergillus flavus* cells. The investigators determined the activity of thiobarbituric acid (TBA) in the samples, which showed a linkage between the membrane damage and lipid oxidation process (Simoncicova et al. 2018).

The other mechanism that may reduce the number of fungal cells is apoptosis or necrosis, as suggested by Panngom et al. (2014) to identify the mechanism of inactivation of *Fusarium oxysporum* cells, the authors stained the cells with Annexin V and propidium iodide and treated them with argon plasma for 1, 5, and 10 min. The numbers of viable, necrotic, and apoptotic cells were analyzed with flow cytometry. The majority of the cells were propidium iodide-stained after 5- and 10-min of the treatment with CP. This indicates that the necrosis process was the main mechanism of inactivation of the fungal cells.

An important aspect that requires further research is the increase in resistance to fungal pathogens in the plasma-treated plants. The experiments conducted by Filatova et al. (2016) demonstrated a substantially reduced incidence of diseases caused by *Fusarium* spp. and *Ustilago maydis* in wheat, lupine, and maize after exposure of the seeds to CP. The stimulating and fungicidal effect of the plasma resulted in an increase in the yield of the spring wheat, maize, and lupine seeds by 4–6%, 1.5–2%, and 20–40%, respectively, in comparison with the control. After additional assays that should be carried out in the future, CP may become an alternative to chemical plant protection agents, which may effectively minimize the negative impact of fungicides on the environment (Siddique et al. 2018).

Cold-plasma inactivation of mycotoxins. The UN Food and Agriculture data indicate that 25% of world

crops are contaminated with mycotoxins produced by fungi during plant growth or crop storage. *Aspergillus*, *Fusarium*, and *Penicillium* molds are the major producers of toxic secondary metabolites, including aflatoxin, fumonisin, zearalenone, ochratoxin, and deoxynivalenol, which are most toxic to mammals. The elimination of these compounds from food products is problematic due to their high thermostability; for instance, the temperature of aflatoxin degradation ranges from 237 to 306°C (Pankaj et al. 2017). The latest physicochemical methods that can potentially be used for elimination of mycotoxins include the cold-plasma sterilization (Ouf et al. 2015; Hojnik et al. 2017; Pankaj et al. 2017; Shi et al.2017). There is a possibility of the complete degradation and reduction of aflatoxin B1 (AFB_1), deoxy nivalenol (DON), and nivalenol (NIV) cytotoxicity with the use of argon plasma generated by microwave discharges (Hojnik et al. 2017). The reduction of the toxicity of these compounds may result from structural changes induced by the sterilization process. Wang et al. (2015) applied low-temperature radio-frequency plasma and reported 88.3% reduction in AFB_1 concentration after a 10-minute process. The analysis of degradation products revealed five different compounds characterized by loss of the double bond between C8 and C9 in the furan ring. Besides its effect on the standard mycotoxin solutions, the plasma has been found to exert a reductive effect on the compounds contained in food products (Ouf et al. 2015; Siciliano et al. 2016; Shi et al. 2017). Aflatoxins present in hazelnuts were decontaminated using CP (1000 W, 12 min), which resulted in an over 70% decline in the AFB_1 concentration (Siciliano et al. 2016). In turn, the concentration of this maize contaminant was reduced by 62% and 82% after the 1- and 10-min plasma treatments, respectively (Shi et al. 2017). However, the atmospheric plasma treatment of contaminated nuts did not allow complete removal of the mycotoxin. The best results were obtained with the highest power (1150 W) and the longest operating time (12 min), which enabled the reduction of AFB1 approx. by 70%. Given the high efficiency of degradation of standard mycotoxin solutions and mycotoxins contained in food, the cold plasma method is becoming a promising solution that may replace conventional techniques in the future. In addition to the high efficiency of compound degradation, the relatively low cost of the process, as well as environmental safety, also favor the use of CP (Hojnik et al. 2017).

Summary

The cold plasma technology is becoming a promising solution with the potential to replace conventional techniques of decontamination of food products, medical materials, and air in the future. This technique has many advantages, e.g. high efficiency in reducing the viral particles load and the number of microorganisms, formation of non-toxic by-products, and a relatively low cost of the process (Liao et al. 2016). Although many studies focused on this issue, the precise molecular mechanism of the plasma effect on cells of different microbial groups has not been clarified yet. The available reports on the possibility of induction of VBNC state in some bacteria raise doubts about the safety of this sterilization method (Dolezalova and Lukes 2015). In addition, this technology has some disadvantages, i.e. a small working surface and poor permeability. In food products, this technique may cause increased lipid oxidation, increased acidity of the product, reduced color intensity and decrease in firmness of fruits (Misra et al. 2016; Chizoba Ekezie et al. 2017). Therefore, it is necessary to conduct further research that will allow for the optimization of process parameters, explain the doubts concerning the biting mechanisms of plasma operation and promote the application of cold plasma in the industry with no negative effects on human health or the environment.

ORCID
Iwona Niedźwiedź 0000-0003-1832-9528
Adam Waśko 0000-0001-9329-1043
Magdalena Polak-Berecka 0000-0003-3832-8610

Conflict of interest

The authors do not report any financial or personal connections with other persons or organizations, which might negatively affect the contents of this publication and/or claim authorship rights to this publication.

Literature

Afshari R, Hosseini H. Non-thermal plasma as a new food preservation method, its present and future prospect. J Paramed Sci. 2014;5:116–120.

Ahlfeld B, Li Y, Boulaaba A, Binder A, Schotte U, Zimmermann JL, Morfill G, Klein G. Inactivation of a foodborne norovirus outbreak strain with nonthermal atmospheric pressure plasma. MBio. 2015 Feb 27;6(1):e02300–e02314. doi:10.1128/mBio.02300-14 Medline

Alkawareek MY, Alshraiedeh NH, Higginbotham S, Flynn PB, Algwari QT, Gorman SP, Graham WG, Gilmore BF. Plasmid DNA damage following exposure to atmospheric pressure nonthermal plasma: kinetics and influence of oxygen admixture. Plasma Med. 2014;4(1-4):211–219. doi:10.1615/PlasmaMed.2015011977

Attri P, Han J, Choi S, Choi EH, Bogaerts A, Lee W. CAP modifies the structure of a model protein from thermophilic bacteria: mechanisms of CAP-mediated inactivation. Sci Rep. 2018 Dec; 8(1):10218. doi:10.1038/s41598-018-28600-w Medline

Bayliss DL, Walsh JL, Iza F, Shama G, Holah J, Kong MG. Complex responses of microorganisms as a community to a flowing atmospheric plasma. Plasma Process Polym. 2012 Jun;9(6):597–611. doi:10.1002/ppap.201100104

Beggs CB. A quantitative method for evaluating the photoreactivation of ultraviolet damaged microorganisms. Photochem Photobiol Sci. 2002 Jun 7;1(6):431–437. doi:10.1039/b202801h Medline

Bogaerts A, Neyts EC. Plasma technology: an emerging technology for energy storage. ACS Energy Lett. 2018 Apr 13;3(4):1013–1027. doi:10.1021/acsenergylett.8b00184

Boudam MK, Moisan M. Synergy effect of heat and UV photons on bacterial-spore inactivation in an N_2 –O_2 plasma-afterglow sterilizer. J Phys D Appl Phys. 2010 Jul 28;43(29):295202. doi:10.1088/0022-3727/43/29/295202

Bourke P, Ziuzina D, Han L, Cullen PJ, Gilmore BF. Microbiological interactions with cold plasma. J Appl Microbiol. 2017 Aug;123(2):308–324. doi:10.1111/jam.13429 Medline

Boxhammer V, Li YF, Köritzer J, Shimizu T, Maisch T, Thomas HM, Schlegel J, Morfill GE, Zimmermann JL. Investigation of the mutagenic potential of cold atmospheric plasma at bactericidal dosages. Mutat Res-Gen Tox En. 2013;753(1):23–28.

Brisset JL, Pawłat J. Chemical effects of air plasma species on aqueous solutes in direct and delayed exposure modes: discharge, post-discharge and plasma activated water. Plasma Chem Plasma Process. 2016 Mar;36(2):355–381. doi:10.1007/s11090-015-9653-6

Bruggeman PJ, Kushner MJ, Locke BR, Gardeniers JGE, Graham WG, Graves DB, Hofman-Caris RCHM, Maric D, Reid JP, Ceriani E, et al. Plasma–liquid interactions: a review and roadmap. Plasma Sources Sci Technol. 2016 Sep 30;25(5):053002. doi:10.1088/0963-0252/25/5/053002

Brun P, Bernabè G, Marchiori C, Scarpa M, Zuin M, Cavazzana R, Zaniol B, Martines E. Antibacterial efficacy and mechanisms of action of low power atmospheric pressure cold plasma: membrane permeability, biofilm penetration and antimicrobial sensitization. J Appl Microbiol. 2018 Aug;125(2):398–408. doi:10.1111/jam.13780 Medline

Chizoba Ekezie F-G, Sun DW, Cheng JH. A review on recent advances in cold plasma technology for the food industry: current applications and future trends. Trends Food Sci Technol. 2017 Nov; 69:46–58. doi:10.1016/j.tifs.2017.08.007

Colonna W, Wan Z, Pankaj SK, Keener KM. High-voltage atmospheric cold plasma treatment of yeast for spoilage prevention. Plasma Med. 2017;7(2):97–107. doi:10.1615/PlasmaMed.2017019201

Connor M, Flynn PB, Fairley DJ, Marks N, Manesiotis P, Graham WG, Gilmore BF, McGrath JW. Evolutionary clade affects resistance of *Clostridium difficile* spores to Cold Atmospheric Plasma. Sci Rep. 2017 Dec;7(1):41814. doi:10.1038/srep41814 Medline

Coutinho NM, Silveira MR, Rocha RS, Moraes J, Ferreira MVS, Pimentel TC, Freitas MQ, Silva MC, Raices RSL, Ranadheera CS, et al. Cold plasma processing of milk and dairy products. Trends Food Sci Technol. 2018 Apr;74:56–68. doi:10.1016/j.tifs.2018.02.008

Czapka T, Maliszewska I, Olesiak-Bańska J. Influence of atmospheric pressure non-thermal plasma on inactivation of biofilm cells. Plasma Chem Plasma Process. 2018 Nov;38(6):1181–1197. doi:10.1007/s11090-018-9925-z

Czyzewska-Dors E, Dors A, Pomorska-Mól M. Właściwości biofilmu bakteryjnego warunkujące oporność na antybiotyki oraz metody jego zwalczania. Zycie Wet. 2018;93(11):765–771.

Dasan BG, Boyaci IH, Mutlu M. Nonthermal plasma treatment of *Aspergillus* spp. spores on hazelnuts in an atmospheric pressure fluidized bed plasma system: impact of process parameters and surveillance of the residual viability of spores. J Food Eng. 2017a Mar;196:139–149. doi:10.1016/j.jfoodeng.2016.09.028

Dasan BG, Mutlu M, Boyaci IH. Decontamination of Aspergillus flavus and *Aspergillus parasiticus* spores on hazelnuts via atmospheric pressure fluidized bed plasma reactor. Int J Food Microbiol. 2016 Jan;216:50–59. doi:10.1016/j.ijfoodmicro.2015.09.006 Medline

Dasan BG, Onal-Ulusoy B, Pawłat J, Diatczyk J, Sen Y, Mutlu M. A new and simple approach for decontamination of food contact surfaces with gliding arc discharge atmospheric non-thermal plasma. Food Bioprocess Technol. 2017b Apr;10(4):650–661. doi:10.1007/s11947-016-1847-2

Deng X, Shi J, Kong MG. Physical mechanisms of inactivation of *Bacillus subtilis* spores using cold atmospheric plasmas. IEEE Trans Plasma Sci. 2006 Aug;34(4):1310–1316. doi:10.1109/TPS.2006.877739

Dobrynin D, Fridman G, Mukhin YV, Wynosky-Dolfi MA, Rieger J, Rest RF, Gutsol AF, Fridman A. Cold plasma inactivation of *Bacillus cereus* and *Bacillus anthracis* (anthrax) spores. IEEE Trans Plasma Sci. 2010 Aug;38(8):1878–1884. doi:10.1109/TPS.2010.2041938

Dolezalova E, Lukes P. Membrane damage and active but nonculturable state in liquid cultures of *Escherichia coli* treated with an atmospheric pressure plasma jet. Bioelectrochemistry. 2015 Jun;103:7–14. doi:10.1016/j.bioelechem.2014.08.018 Medline

Dzimitrowicz A, Jamróz P, Nowak P. Sterylizacja za pomocą niskotemperaturowej plazmy, generowanej w warunkach ciśnienia atmosferycznego. Postepy Mikrobiol. 2015;54(2):195–200.

Ermolaeva SA, Varfolomeev AF, Chernukha MY, Yurov DS, Vasiliev MM, Kaminskaya AA, Moisenovich MM, Romanova JM, Murashev AN, Selezneva II, et al. Bactericidal effects of non-thermal argon plasma *in vitro*, in biofilms and in the animal model of infected wounds. J Med Microbiol. 2011 Jan 01;60(1):75–83. doi:10.1099/jmm.0.020263-0 Medline

Fiebrandt M, Lackmann JW, Raguse M, Moeller R, Awakowicz P, Stapelmann K. VUV absorption spectroscopy of bacterial spores and DNA components. Plasma Phys Contr Fusion. 2017 Jan 01; 59(1):014010. doi:10.1088/0741-3335/59/1/014010

Filatova I, Azharonok V, Lyushkevich V, Zhukovsky A, Mildažienė V, Pauzaite G, Zukiene RAM. 2016. The effect of presowing plasma seeds treatment on germination, plants resistance to pathogens and crop capacity. Paper presented at: 1st International Workshop on Plasma Agriculture; Camden, NJ.

Flynn PB, Higginbotham S, Alshraiedeh NH, Gorman SP, Graham WG, Gilmore BF. Bactericidal efficacy of atmospheric pressure non-thermal plasma (APNTP) against the ESKAPE pathogens. Int J Antimicrob Agents. 2015 Jul;46(1):101–107. doi:10.1016/j.ijantimicag.2015.02.026 Medline

Fridman A, Chirokov A, Gutsol A. Non-thermal atmospheric pressure discharges. J Phys D Appl Phys. 2005 Jan 21;38(2):R1–R24. doi:10.1088/0022-3727/38/2/R01

Gallagher MJ, Vaze N, Gangoli S, Vasilets VN, Gutsol AF, Milovanova TN, Anandan S, Murasko DM, Fridman AA. Rapid inactivation of airborne bacteria using atmospheric pressure dielectric barrier grating discharge. IEEE Trans Plasma Sci. 2007 Oct; 35(5):1501–1510. doi:10.1109/TPS.2007.905209

Guo L, Zhao Y, Liu D, Liu Z, Chen C, Xu R, Tian M, Wang X, Chen H, Kong MG. Cold atmospheric-pressure plasma induces DNA – protein crosslinks through protein oxidation. Free Radic Res. 2018 Jul 03;52(7):783–798. doi:10.1080/10715762.2018.1471476 Medline

Hojnik N, Cvelbar U, Tavčar-Kalcher G, Walsh J, Križaj I. Cold atmospheric pressure plasma versus "classic" decontamination. Toxins (Basel). 2017 Apr 28;9(5):151. doi:10.3390/toxins9050151 Medline

Hong YF, Kang JG, Lee HY, Uhm HS, Moon E, Park YH. Sterilization effect of atmospheric plasma on *Escherichia coli* and *Bacillus subtilis* endospores. Lett Appl Microbiol. 2009 Jan;48(1):33–37. doi:10.1111/j.1472-765X.2008.02480.x Medline

Hosseinzadeh Colagar A, Memariani H, Sohbatzadeh F, Valinataj Omran A. Nonthermal atmospheric argon plasma jet effects on *Escherichia coli* biomacromolecules. Appl Biochem Biotechnol. 2013 Dec;171(7):1617–1629. doi:10.1007/s12010-013-0430-9 Medline

Isbary G, Morfill G, Schmidt HU, Georgi M, Ramrath K, Heinlin J, Karrer S, Landthaler M, Shimizu T, Steffes B, et al. A first prospective randomized controlled trial to decrease bacterial

load using cold atmospheric argon plasma on chronic wounds in patients. Br J Dermatol. 2010 May;163(1):78–82. doi:10.1111/j.1365-2133.2010.09744.x Medline

Itooka K, Takahashi K, Kimata Y, Izawa S. Cold atmospheric pressure plasma causes protein denaturation and endoplasmic reticulum stress in *Saccharomyces cerevisiae.* Appl Microbiol Biotechnol. 2018 Mar;102(5):2279–2288. doi:10.1007/s00253-018-8758-2 Medline

Jahid IK, Han N, Ha SD. Inactivation kinetics of cold oxygen plasma depend on incubation conditions of *Aeromonas hydrophila* biofilm on lettuce. Food Res Int. 2014 Jan;55:181–189. doi:10.1016/j.foodres.2013.11.005

Kądzielska J, Obuch-Woszczatyński P, Pituch H, Młynarczyk G. *Clostridium perfringens* jako czynnik etiologiczny biegunki poantybiotykowej. Postepy Mikrobiol. 2012;51(1):17–25.

Kartaschew K, Baldus S, Mischo M, Bründermann E, Awakowicz P, Havenith M. Cold atmospheric-pressure plasma and bacteria: understanding the mode of action using vibrational microspectroscopy. J Phys D Appl Phys. 2016 Sep 21;49(37):374003. doi:10.1088/0022-3727/49/37/374003

Kim GC, Kim GJ, Park SR, Jeon SM, Seo HJ, Iza F, Lee JK. Air plasma coupled with antibody-conjugated nanoparticles: a new weapon against cancer. J Phys D Appl Phys. 2009 Feb 07;42(3):032005. doi:10.1088/0022-3727/42/3/032005

Klämpfl TG, Isbary G, Shimizu T, Li YF, Zimmermann JL, Stolz W, Schlegel J, Morfill GE, Schmidt HU. Cold atmospheric air plasma sterilization against spores and other microorganisms of clinical interest. Appl Environ Microbiol. 2012 Aug 01;78(15):5077–5082. doi:10.1128/AEM.00583-12 Medline

Klämpfl TG, Shimizu T, Koch S, Balden M, Gemein S, Li YF, Mitra A, Zimmermann JL, Gebel J, Morfill GE, et al. Decontamination of nosocomial bacteria including *Clostridium difficile* spores on dry inanimate surface by cold atmospheric plasma. Plasma Process Polym. 2014 Oct;11(10):974–984. doi:10.1002/ppap.201400080

Korachi M, Turan Z, Şentürk K, Şahin F, Aslan N. An investigation into the biocidal effect of high voltage AC/DC atmospheric corona discharges on bacteria, yeasts, fungi and algae. J Electrost. 2009 Jul;67(4):678–685. doi:10.1016/j.elstat.2009.03.002

Krzyczkowska J, Stolarzewicz I, Bellok D, Bellok M, Białecka-Florjańczyk E. Wpływ modyfikacji pożywki na biokatalityczne właściwości drożdży. Żywn Nauka Technol Jakość. 2008;15(5):299–306.

Lademann O, Kramer A, Richter H, Patzelt A, Meinke MC, Roewert-Huber J, Czaika V, Weltmann K-D, Hartmann B, Koch S. Antisepsis of the follicular reservoir by treatment with tissue-tolerable plasma (TTP). Laser Phys Lett. 2011 Apr;8(4):313–317. doi:10.1002/lapl.201010123

Laroussi M, Mendis DA, Rosenberg M. Plasma interaction with microbes. New J Phys. 2003;5(1):41.1–41.10.

Laskowska M, Bogusławska-Wąs E, Kowal P, Hołub M, Dąbrowski W. Skuteczność wykorzystania niskotemperaturowej plazmy w mikrobiologii i medycynie. Postepy Mikrobiol. 2016;55(2):172–181.

Li HP, Wang LY, Li G, Jin LH, Le PS, Zhao HX, Xing XH, Bao CY. Manipulation of lipase activity by the helium radio-frequency, atmospheric-pressure glow discharge plasma jet. Plasma Process Polym. 2011 Mar 22;8(3):224–229. doi:10.1002/ppap.201000035

Liao X, Cullen PJ, Liu D, Muhammad AI, Chen S, Ye X, Wang J, Ding T. Combating *Staphylococcus aureus* and its methicillin resistance gene (*mecA*) with cold plasma. Sci Total Environ. 2018 Dec;645:1287–1295. doi:10.1016/j.scitotenv.2018.07.190 Medline

Liao X, Liu D, Xiang Q, Ahn J, Chen S, Ye X, Ding T. Inactivation mechanisms of non-thermal plasma on microbes: A review. Food Control. 2017 May;75:83–91. doi:10.1016/j.foodcont.2016.12.021

Lu Q, Liu D, Song Y, Zhou R, Niu J. Inactivation of the tomato pathogen *Cladosporium fulvum* by an atmospheric-pressure cold plasma jet. Plasma Process Polym. 2014 Nov;11(11):1028–1036. doi:10.1002/ppap.201400070

Maciejewska M, Bauer M, Dawgul M. Nowoczesne metody zwalczania biofilmu bakteryjnego. Postepy Mikrobiol. 2016;55(1):3–11.

Mai-Prochnow A, Clauson M, Hong J, Murphy AB. Gram positive and Gram negative bacteria differ in their sensitivity to cold plasma. Sci Rep. 2016 Dec;6(1):38610. doi:10.1038/srep38610 Medline

Mai-Prochnow A, Murphy AB, McLean KM, Kong MG, Ostrikov KK. Atmospheric pressure plasmas: infection control and bacterial responses. Int J Antimicrob Agents. 2014 Jun;43(6):508–517. doi:10.1016/j.ijantimicag.2014.01.025 Medline

Metelmann HR, Seebauer C, Miller V, Fridman A, Bauer G, Graves DB, Pouvesle J-M, Rutkowski R, Schuster M, Bekeschus S, et al. Clinical experience with cold plasma in the treatment of locally advanced head and neck cancer. Clin Plasma Med. 2018 Mar;9:6–13. doi:10.1016/j.cpme.2017.09.001

Misra NN, Pankaj SK, Segat A, Ishikawa K. Cold plasma interactions with enzymes in foods and model systems. Trends Food Sci Technol. 2016 Sep;55:39–47. doi:10.1016/j.tifs.2016.07.001

Misra NN, Schlüter O, Cullen PJ. Plasma in food and agriculture. Amsterdam (Netherlands): Academic Press. 2016. p. 1–16.

Moreau M, Orange N, Feuilloley MGJ. Non-thermal plasma technologies: new tools for bio-decontamination. Biotechnol Adv. 2008 Nov;26(6):610–617. doi:10.1016/j.biotechadv.2008.08.001 Medline

Nikmaram H, Rezaei Kanavi M, Ghoranneviss M, Balagholi S, Ahmadieh H, Roshandel D, Amini M. Cold atmospheric pressure plasma jet for the treatment of *Aspergillus keratitis.* Clin Plasma Med. 2018 Mar;9:14–18. doi:10.1016/j.cpme.2017.12.075

Nishime TMC, Borges AC, Koga-Ito CY, Machida M, Hein LRO, Kostov KG. Non-thermal atmospheric pressure plasma jet applied to inactivation of different microorganisms. Surf Coat Tech. 2017 Feb;312:19–24. doi:10.1016/j.surfcoat.2016.07.076

Olesiak P, Stępniak L. Skuteczność wybranych związków dezynfekcyjnych wobec przetrwalników *Bacillus.* Inżynieria i Ochrona Środowiska. 2012;15:41–50.

Ouf SA, Basher AH, Mohamed AAH. Inhibitory effect of double atmospheric pressure argon cold plasma on spores and mycotoxin production of *Aspergillus niger* contaminating date palm fruits. J Sci Food Agric. 2015 Dec;95(15):3204–3210. doi:10.1002/jsfa.7060 Medline

Pankaj SK, Shi H, Keener KM. A review of novel physical and chemical decontamination technologies for aflatoxin in food. Trends Food Sci Technol. 2018 Jan;71:73–83. doi:10.1016/j.tifs.2017.11.007

Panngom K, Lee SH, Park DH, Sim GB, Kim YH, Uhm HS, Park G, Choi EH. Non-thermal plasma treatment diminishes fungal viability and up-regulates resistance genes in a plant host. PLoS One. 2014 Jun 9;9(6):e99300. doi:10.1371/journal.pone.0099300 Medline

Pawłat J, Kwiatkowski M, Terebun P, Murakami T. RF-powered atmospheric-pressure plasma jet in surface treatment of high-impact polystyrene. IEEE Trans Plasma Sci. 2016 Mar;44(3):314–320. doi:10.1109/TPS.2015.2436061

Pawłat J, Starek A, Sujak A, Kwiatkowski M, Terebun P, Budzeń M. Effects of atmospheric pressure plasma generated in GlidArc reactor on *Lavatera thuringiaca* L. seeds' germination. Plasma Process Polym. 2018a Feb;15(2):1700064. doi:10.1002/ppap.201700064

Pawłat J, Starek A, Sujak A, Terebun P, Kwiatkowski M, Budzeń M, Andrejko D. Effects of atmospheric pressure plasma jet operating with DBD on *Lavatera thuringiaca* L. seeds' germination. PLoS One. 2018b Apr 9;13(4):e0194349. doi:10.1371/journal.pone.0194349 Medline

Pawłat J. Atmospheric pressure plasma jet for decontamination purposes. Eur Phys J Appl Phys. 2013;61:1–11.

Pignata C, D'Angelo D, Fea E, Gilli G. A review on microbiological decontamination of fresh produce with nonthermal plasma. J Appl Microbiol. 2017 Jun;122(6):1438–1455. doi:10.1111/jam.13412 Medline

Polčic P, Pakosová L, Chovančíková P, Machala Z. Reactive cold plasma particles generate oxidative stress in yeast but do not trigger apoptosis. Can J Microbiol. 2018 Jun;64(6):367–375. doi:10.1139/cjm-2017-0753 Medline

Pradeep P, Chulkyoon M. Non-thermal plasmas (NTPs) for inactivation of viruses in abiotic environment. Res J Biotechnol. 2016;11:91–96.

Raguse M, Fiebrandt M, Denis B, Stapelmann K, Eichenberger P, Driks A, Eaton P, Awakowicz P, Moeller R. Understanding of the importance of the spore coat structure and pigmentation in the *Bacillus subtilis* spore resistance to low-pressure plasma sterilization. J Phys D Appl Phys. 2016 Jul 20;49(28):285401. doi:10.1088/0022-3727/49/28/285401

Ritter AC, Santi L, Vannini L, Beys-da-Silva WO, Gozzi G, Yates J 3rd, Ragni L, Brandelli A. Comparative proteomic analysis of foodborne *Salmonella* Enteritidis SE86 subjected to cold plasma treatment. Food Microbiol. 2018 Dec;76:310–318. doi:10.1016/j.fm.2018.06.012 Medline

Roth S, Feichtinger J, Hertel C. Response of *Deinococcus radiodurans* to low-pressure low-temperature plasma sterilization processes. J Appl Microbiol. 2010 Jun;109(5):1521–1530. doi:10.1111/j.1365-2672.2010.04771.x Medline

Ryu YH, Kim YH, Lee JY, Shim GB, Uhm HS, Park G, Choi EH. Effects of background fluid on the efficiency of inactivating yeast with non-thermal atmospheric pressure plasma. PLoS One. 2013 Jun 14;8(6):e66231. doi:10.1371/journal.pone.0066231 Medline

Samoń R, Czapiński J, Grządziel J, Płonka M, Pawłat J, Diatczyk J. Ocena działania bakteriobójczego niskotemperaturowej plazmy nierównowagowej generowanej w reaktorze RF. Eur J Med Technol. 2014;2:17–26.

Sharma A, Collins G, Pruden A. Differential gene expression in *Escherichia coli* following exposure to nonthermal atmospheric pressure plasma. J Appl Microbiol. 2009 Nov;107(5):1440–1449. doi:10.1111/j.1365-2672.2009.04323.x Medline

Shi H, Ileleji K, Stroshine RL, Keener K, Jensen JL. Reduction of aflatoxin in corn by high voltage atmospheric cold plasma. Food Bioprocess Technol. 2017 Jun;10(6):1042–1052. doi:10.1007/s11947-017-1873-8

Siciliano I, Spadaro D, Prelle A, Vallauri D, Cavallero M, Garibaldi A, Gullino M. Use of cold atmospheric plasma to detoxify hazelnuts from aflatoxins. Toxins (Basel). 2016 Apr 26;8(5):125. doi:10.3390/toxins8050125 Medline

Siddique SS, Hardy GESJ, Bayliss KL. Cold plasma: a potential new method to manage postharvest diseases caused by fungal plant pathogens. Plant Pathol. 2018 Jun;67(5):1011–1021. doi:10.1111/ppa.12825

Šimončicová J, Kaliňáková B, Kováčik D, Medvecká V, Lakatoš B, Kryštofová S, Hoppanová L, Palušková V, Hudecová D, Ďurina P, et al. Cold plasma treatment triggers antioxidative defense system and induces changes in hyphal surface and subcellular structures of *Aspergillus flavus*. Appl Microbiol Biotechnol. 2018 Aug;102(15): 6647–6658. doi:10.1007/s00253-018-9118-y Medline

Sohbatzadeh F, Mirzanejhad S, Shokri H, Nikpour M. Inactivation of *Aspergillus flavus* spores in a sealed package by cold plasma streamers. J Theor Appl Phys. 2016 Jun;10(2):99–106. doi:10.1007/s40094-016-0206-z

Su X, Tian Y, Zhou H, Li Y, Zhang Z, Jiang B, Yang B, Zhang J, Fang J. Inactivation efficacy of non-thermal plasma activated solutions against Newcastle disease virus. Appl Environ Microbiol. 2018 Feb 23;84(9):e02836-17. doi:10.1128/AEM.02836-17

Suhem K, Matan N, Nisoa M, Matan N. Inhibition of *Aspergillus flavus* on agar media and brown rice cereal bars using cold atmospheric plasma treatment. Int J Food Microbiol. 2013 Feb;161(2): 107–111. doi:10.1016/j.ijfoodmicro.2012.12.002 Medline

Surowsky B, Fischer A, Schlueter O, Knorr D. Cold plasma effects on enzyme activity in a model food system. Innov Food Sci Emerg Technol. 2013 Jul;19:146–152. doi:10.1016/j.ifset.2013.04.002

Terrier O, Essere B, Yver M, Barthélémy M, Bouscambert-Duchamp M, Kurtz P, VanMechelen D, Morfin F, Billaud G, Ferraris O, et al. Cold oxygen plasma technology efficiency against different airborne respiratory viruses. J Clin Virol. 2009 Jun;45(2): 119–124. doi:10.1016/j.jcv.2009.03.017 Medline

Tolouie H, Mohammadifar MA, Ghomi H, Hashemi M. Cold atmospheric plasma manipulation of proteins in food systems. Crit Rev Food Sci Nutr. 2018;58(15):2583–2597. doi:10.1080/10408398.2017.1335689 Medline

Tolouie H, Mohammadifar MA, Ghomi H, Yaghoubi AS, Hashemi M. The impact of atmospheric cold plasma treatment on inactivation of lipase and lipoxygenase of wheat germs. Innov Food Sci Emerg Technol. 2018 Jun;47:346–352. doi:10.1016/j.ifset.2018.03.002

Tseng S, Abramzon N, Jackson JO, Lin WJ. Gas discharge plasmas are effective in inactivating *Bacillus* and *Clostridium* spores. Appl Microbiol Biotechnol. 2012 Mar;93(6):2563–2570. doi:10.1007/s00253-011-3661-0 Medline

Vandamme M, Robert E, Pesnel S, Barbosa E, Dozias S, Sobilo J, Lerondel S, Le Pape A, Pouvesle JM. Antitumor effect of plasma treatment on U87 glioma xenografts: preliminary results. Plasma Process Polym. 2010 Mar 22;7(3-4):264–273. doi:10.1002/ppap.200900080

Wang G, Zhang P, Setlow P, Li Y. Kinetics of germination of wet-heat-treated individual spores of *Bacillus* species, monitored by Raman spectroscopy and differential interference contrast microscopy. Appl Environ Microbiol. 2011 May 15;77(10):3368–3379. doi:10.1128/AEM.00046-11 Medline

Wang SQ, Huang GQ, Li YP, Xiao JX, Zhang Y, Jiang WL. Degradation of aflatoxin B1 by low-temperature radio frequency plasma and degradation product elucidation. Eur Food Res Technol. 2015 Jul;241(1):103–113. doi:10.1007/s00217-015-2439-5

Wawrzycka D. Drożdże jako model w badaniach chorób neurodegeneracyjnych. Postepy Hig Med Dosw. 2011 Jun 2;65:328–337. doi:10.5604/17322693.945767

Wiktor A, Śledź M, Nowacka M, Witrowa-Rajchert D. Możliwości zastosowania niskotemperaturowej plazmy w technologii żywności. Żywn Nauka Technol Jakość. 2013. 5:5–14.

Wolny-Koładka K, Pawłat J, Terebun P, Kwiatkowski M, Diatczyk J. Ocena możliwości zastosowania plazmy niskotemperaturowej w celu higienizacji zmieszanych odpadów komunalnych służących do produkcji paliwa alternatywnego. Przegl Elektrotechn. 2017 Nov 5;1(11):211–215. doi:10.15199/48.2017.11.43

Yasuda H, Miura T, Kurita H, Takashima K, Mizuno A. Biological evaluation of DNA damage in bacteriophages inactivated by atmospheric pressure cold plasma. Plasma Process Polym. 2010 Mar 22;7(3-4):301–308. doi:10.1002/ppap.200900088

Ye S, Song X, Liang JL, Zheng S, Lin Y. Disinfection of airborne spores of *Penicillium expansum* in cold storage using continuous direct current corona discharge. Biosyst Eng. 2012 Oct;113(2): 112–119. doi:10.1016/j.biosystemseng.2012.06.013

Zimmermann JL, Dumler K, Shimizu T, Morfill GE, Wolf A, Boxhammer V, Schlegel J, Gansbacher B, Anton M. Effects of cold atmospheric plasmas on adenoviruses in solution. J Phys D Appl Phys. 2011 Dec 21;44(50):505201. doi:10.1088/0022-3727/44/50/505201

Ziuzina D, Boehm D, Patil S, Cullen PJ, Bourke P. Cold plasma inactivation of bacterial biofilms and reduction of quorum sensing regulated virulence factors. PLoS One. 2015 Sep 21;10(9):e0138209. doi:10.1371/journal.pone.0138209 Medline

Polish Journal of Microbiology
2019, Vol. 68, No 2, 165–171
https://doi.org/10.33073/pjm-2019-016

ORIGINAL PAPER

Hand, Foot, and Mouth Disease Caused by Coxsackievirus A6: A Preliminary Report from Istanbul

AYSE N. CEYLAN[1], OZDEN TUREL[2], BILGE SUMBUL GULTEPE[1], ELIF INAN[2], AYSEL VEHAPOGLU TURKMEN[2] and MEHMET Z. DOYMAZ[1, 3]*

[1] Bezmialem Vakif University, Department of Medical Microbiology, Istanbul, Turkey
[2] Bezmialem Vakif University, Department of Pediatrics, Istanbul, Turkey
[3] Bezmialem Vakif University, Beykoz Institute of Life Sciences and Biotechnology (BILSAB), Istanbul, Turkey

Submitted 1 October 2018, revised 7 January 2019, accepted 7 January 2019

Abstract

Hand, foot, and mouth disease (HFMD) is caused by various serotypes of *Enterovirus* genus. Coxsackievirus A16 (CV-A16) and enterovirus A71 (EV-A71) were known to be the only responsible agents for these epidemics; however, this opinion was challenged after the detection that coxsackievirus A6 (CV-A6) was the responsible species for the outbreak in Finland in 2008. HFMD is frequently seen in Turkey, and no detailed study on its clinical and microbiological epidemiology has previously been reported. The present study addresses this question. Twenty-seven patient samples collected between 2015 and 2017 were included in the study. Typing was conducted by RT-PCR and the sequencing applied directly to patient's samples and as well as to the viral cultures with pan-enterovirus and serotype-specific primers. The presence of *Enterovirus* in 12 of 27 HFMD samples was shown with RT-PCR. The causative agent for three of these 12 samples was CV-A16, one of the most frequent two serotypes around the world, and the remaining nine samples was CV-A6. The findings of the study are relevant since it pertains to the molecular epidemiology of HFMD in Turkey, a gateway country where different serotypes might be circulating and transmitted. The findings also support the notion that CV-A6 cases are rising in number, which has caused more severe clinical features and widespread rashes in recent outbreaks.

Key words: hand foot and mouth disease, HFMD, enterovirus, coxsackievirus A6, coxsackievirus A16

Introduction

Hand, foot, and mouth disease (HFMD) is a viral and febrile disease frequently seen in children, generally presenting with a mild course and accompanied by oral rash and rashes on palmar surfaces of hand and feet (Kliegman and Geme 2015). Cases of HFMD are seen all over the world; however, epidemics with serious complications that result in deaths are reported mostly from Western Pacific Region countries (WHO 2011). *Enterovirus* A species are responsible for more than 90% of HFMD cases. Coxsackievirus A (CV-A) 2, 3, 5, 6, 7, 8, 10, 12, 14, 16, and enterovirus A71 (EV-A71) belong to this group. It is known that epidemics are induced by CV-A16 and EV-A71, while other enteroviruses may cause sporadic cases (Mao et al. 2014; Bian et al. 2015).

CV-A6 was identified, for the first time, as the causative agent for HFMD in an epidemic that emerged in Finland in 2008 (Österback et al. 2009). Following this, the identification of CV-A6 as the major causative agent for HFMD epidemics continued to occur in France, Spain and other European countries in 2009–2011 (Bracho et al. 2011; Mirand et al. 2012). HFMD epidemics caused by CV-A6 were also reported in the Western Pacific Region and the Americas after 2009 (CDC 2012; Chen et al. 2012; Fujimoto et al. 2012; Fonseca et al. 2014; Han et al. 2014; Hu et al. 2015). More severe clinical course and widespread skin rashes were seen in cases caused by CV-A6, different from typical HFMD (Romero 2017).

Cases with no severe clinical course can be diagnosed with clinical findings without the need for microbiological diagnostic tests. However, certain serotypes may lead to severe disease (Romero 2017). Serotypes may vary within and among countries. Therefore, determination of the causative serotype is important for public health as well as for the design and implementation of the preventive measures. Recent increases

* Corresponding author: M.Z. Doymaz, Bezmialem Vakif University Adnan Menderes Bulvari, Fatih, Istanbul, Turkey;
e-mail: mzdoymaz@bezmialem.edu.tr

in movements of people between countries and continents could be influential in the spread of different viral serotypes. Full identification of the causative organism could also provide information for the vaccine development studies in addition to its epidemiological importance (WHO 2011).

The published research on HFMD in Turkey has been generally towards the clinical aspects of the disease (Ekinci et al. 2013; Demirhan et al. 2016; Bucak et al. 2017). Apart from a single case study, no detailed investigations on the viral agent itself have been conducted (Kiratli et al. 2017). In this investigation, we aimed to determine the serotype distribution in HFMD cases in children.

Experimental

Materials and Methods

Patient Selection. Our study cohort consisted of children applied to the outpatient clinics of the Pediatric Infectious Disease Department of Bezmialem Vakif University Hospital between January 2015 and November 2017. These consecutive patients were selected who complained of fever and rash on the hands, mouths or on the body including the legs (Fig. 1, 2 and 3) and who were later clinically diagnosed with HFMD. An approval from Bezmialem Vakıf University Ethics Committee for Experimentation Involving Human Subjects was obtained before the study and informed consent was obtained from all families of the subjects.

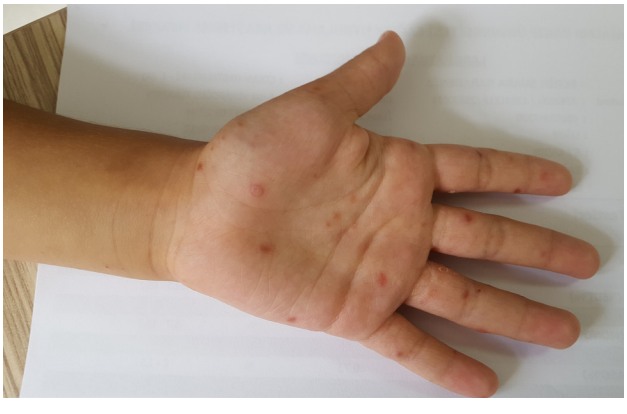

Fig. 1. Patients with typical lesions on the hands.

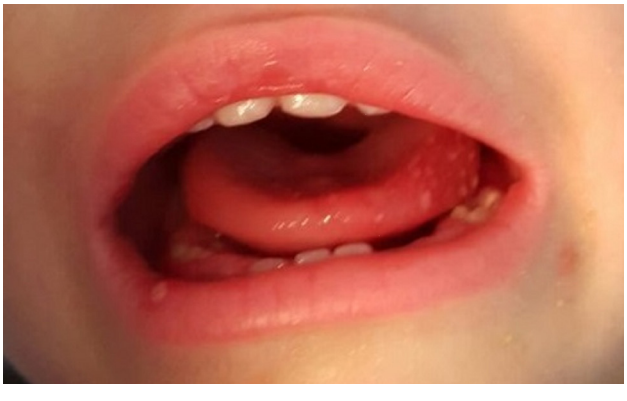

Fig. 2. Patients with mouth ulcers.

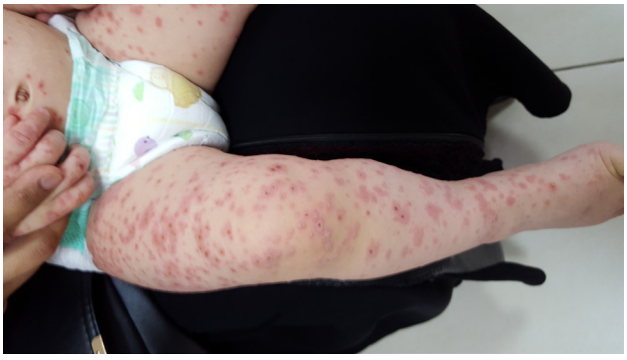

Fig. 3. Patient with generalized lesions on the legs.

Sample Collection and Storage. Samples were taken from at least two lesions in oral mucosa or trunk of patients with clinical symptoms of HFMD. Sterile cotton swabs wetted with saline (0.9% NaCl) were used for sampling. The samples were stored at –80°C in 1.5 ml sterile tubes containing phosphate buffered saline (PBS) until further processed.

RNA isolation. Direct-zol RNA MiniPrep Kit (Zymo Research, Irvine, CA, USA) was used for nucleic acid extraction directly from patient samples and from supernatants obtained after viral culture. Manufacturer's instructions were followed for the entire procedure.

Reverse transcription. SensiFAST cDNA Synthesis Kit (Bioline, London, UK) was used to synthesize cDNA from isolated viral RNAs using random primers and the manufacturer's instructions were followed at all steps. cDNA was purified from reverse transcription products with Zymo Research DNA Clean & Concentrator™-5 kit in accordance with the manufacturer's instructions.

Designing primers and PCR. Pan-enterovirus primers specific to the *Enterovirus* genus targeting 5'UTR were designed for nested-PCR on basis of previously published studies (Ge et al. 2013). In addition, specific primers targeting VP1 gene were used for EV-A71 and CV-A16 (Table I). A commercial kit (Illustra™ Hot Start Master Mix, GE Healthcare, Buckinghamshire, UK) was used for PCR. The reaction mixture contained 0.5 µmol forward primer, 0.5 µmol reverse primer, 1 µl (1–4 µg/µl) post clean-up purified cDNA, and 22 µl DNase-RNase free water added to the master mix kept ready in PCR tubes. Veriti® thermal cycler (Applied Biosystems, Foster City, CA, USA), was programmed as 94°C for 3 min initial incubation, 30 cycles of 94°C for 30 sec, 59°C for 30 sec, 72°C for 30 sec and 72°C for 5 min in order to amplify the Pan-EV, CV-A16 and EV-A71 specific products.

Table I
Primers used for PCR.

Target Serotype	Orientation	Sequence
Pan-EV-5'UTR Outer	Forward	5'-CYTTGTGCGCCTGTTTT-3'
	Reverse	5'-ATTGTCACCATAAGCAGCC-3'
Pan-EV-5'UTR-Inner	Forward	5'-CAAGYACTTCTGTMWCCCC-3'
	Reverse	5'-CCCAAAGTAGTCGGTTCC-3'
EV-A71-VP1	Forward	5'-AGAGCATGATTGAGACACG-3'
	Reverse	5'-RTCTTTCTCYTGTTTGTGTTC-3'
CV-A16-VP1	Forward	5'-TGCAGACATGATTGACCAG-3'
	Reverse	5'-TGCCTACAGTTCTGATGCTA-3'

The amplification products and the 100 bp marker were loaded into 1.5% agarose gel, electrophoresed for 40 minutes under 80 V, and analyzed in Molecular Imager Gel Doc XR System (BioRad, Hercules, CA, U.S.A.) imaging device.

Cell culture. Vero E6 cells were cultured *in vitro* with DMEM (Gibco, Thermo Fisher Scientific, Waltham, MA, USA) containing 10% fetal bovine serum (Gibco) in 5% CO_2 medium at 37°C. Samples were filtered through 0.45 µm filters and then added to monolayers of Vero E6 cell cultures. The infected cells were examined after 3 days of incubation for evaluation of *Enterovirus* specific cytopathic effects. Reverse-transcription PCR was performed with cell culture supernatants to confirm the PCR results of the patient samples.

Sanger sequencing and phylogenetic analysis. The sequencing of the amplified product was carried out by the Sentegen Biyotek (Ankara, Turkey) to determine the serotype of *Enterovirus* detected in the samples.

The sequences of PCR products were assembled and edited using BioEdit version 7.0.5 (http://www.mbio.ncsu.edu/BioEdit/bioedit.html). This sequence was compared with the sequences deposited in GenBank of the National Center for Biotechnology Information (NCBI) by means of the BLASTN 2.2.19 option. The consensus sequence was compiled in a FASTA file for the phylogenetic analysis and aligned with the Clustal W 1.8.1. profile mode included in the Mega 4.0.2 (https://www.megasoftware.net/mega4/) software.

Results

Eleven of 27 children included in the study were female and 16 were male. The ages ranged from 4 months to 9 years, and 21 of the 27 children were aged between 1 and 3 years (78%). Eighteen of the patients (67%) applied to the hospital during the summer months. In the cohorts, neither systemic blisters nor high fever was noted. None of our patients needed hospitalization. There were no severe complications such as meningitis and encephalitis. Only three of 27 patients applied to the hospital with nail shedding after the recovery period of approximately six weeks.

A total of 27 patient samples, 15 from the 2015–2016 season and 12 from 2017, were included in the study. The nested PCR results of 12 patients, sampled in 2015–2016, revealed products with a length of 530 and 389 bp (Fig. 4 and 5) that corresponded to the pan-enterovirus outer and inner primers, respectively. This finding was interpreted as proof of the *Enterovirus* content in the samples. No positive results were observed after PCR performed with the species-specific primers targeting CV-A16 and EV-A71 viruses. To confirm the presence of enteroviral genetic material, all 12 PCR positive

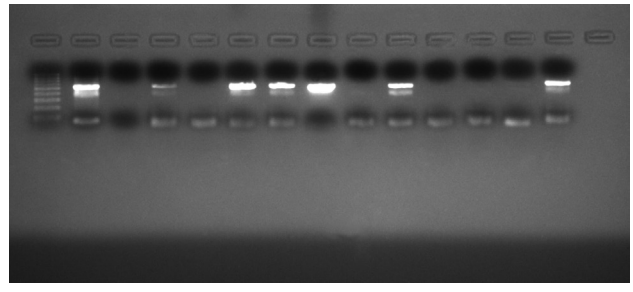

Fig. 4. The samples were subjected to the pan-enterovirus specific nested PCR with outer primers where 530 bp products were amplified. Left to right, line 1: 100 bp marker, lines 2 to 5: HFM-2 to HFM-5, line 6: HFM-7, line 7: HFM-9, lines 8 to 14: HFM-10 to HFM-16.

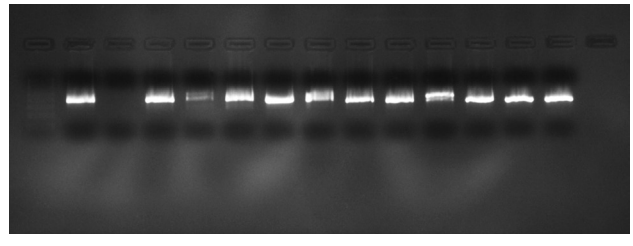

Fig. 5. The samples were subjected to the pan-enterovirus specific nested PCR with inner primers where 389 bp products were amplified. Left to right, line 1: 100 bp marker, lines 2 to 5: HFM-2 to HFM-5, line 6: HFM-7, line 7: HFM-9, lines 8 to 14: HFM-10 to HFM-16.

Table II
Phylogenetic identities of the coxsackievirus A isolates, based on VP1 sequences.

Isolate code	Primer	Nearest phylogenetic neighbours	Identity percentage
HFM-2	153 F/ 541 R	Coxsackievirus A6	99%
HFM-5	153 F/ 541 R	Coxsackievirus A6	99%
HFM-9	153 F/ 541 R	Coxsackievirus A6	99%
HFM-10	153 F/ 541 R	Coxsackievirus A6	99%
HFM-11	153 F/ 541 R	Coxsackievirus A6	99%
HFM-12	153 F/ 541 R	Coxsackievirus A6	99%
HFM-14	153 F/ 541 R	Coxsackievirus A6	99%
HFM-15	153 F/ 541 R	Coxsackievirus A6	99%
HFM-16	153 F/ 541 R	Coxsackievirus A6	99%
HFM24	153 F/ 541 R	Coxsackievirus A16	99%
HFM25	153 F/ 541 R	Coxsackievirus A16	99%
HFM26	153 F/ 541 R	Coxsackievirus A16	97%

products were sequenced. Sequencing revealed that nine of these samples were consistent with the CV-A6 sequences but the remaining samples were not (Table II). Afterward, a confirmatory species-specific PCR affirmed that the samples were indeed CV-A6 (Fig. 6).

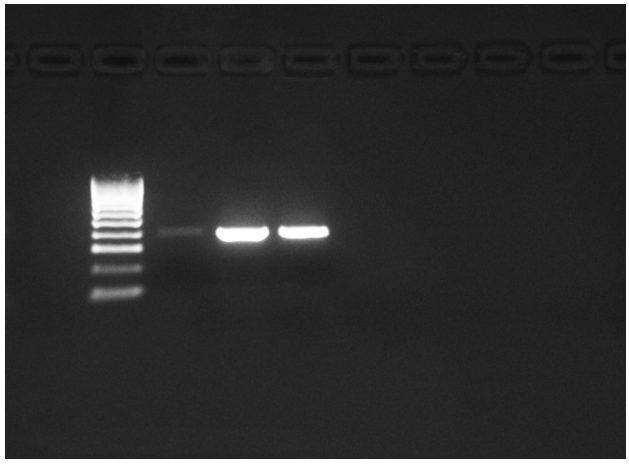

Fig. 6. CV-A6 specific primers amplified products of approximately 645 bp.

Twelve patient samples from 2017, were amplified by PCR and seven samples were positive for *Enterovirus*. These samples were directly subjected to sequencing without serotype-specific PCR for EV-A71 and CV-A16, since the previous samples were negative. Three of the seven samples were CV-A16 according to the results of sequencing (Fig. 7).

All the samples were inoculated into the Vero E6 cell line and characteristic cytopathic effects were noticed after 3-days incubation. The supernatant samples were collected and the PCR test was carried out with pan-enterovirus primers (data not shown). It was noticed that the results were compatible with the PCR performed directly from the patient samples.

Discussion

Hand, foot, and mouth disease epidemics are mostly caused by EV-A71 and CV-A16. Recently, CV-A6 has been identified as the agent of epidemics causing severe forms of the disease with general skin involvement. Similar epidemics that started in Finland in 2008 were also reported from Singapore in 2009, France and Taiwan in 2010, and the USA, Cuba, Spain, Japan, and China in 2011 (Bian et al. 2015). In this study, CV-A6 was found to be the causative agent in 75% of the cases what was confirmed by sequencing (Table III). This result is consistent with the current literature that reports an increase

Table III
The patients' samples and their positivity for coxsackievirus A6 and A16.

Year	No. of samples	*Enterovirus* positivity	Coxsackievirus A6 positivity	Coxsackievirus A16 positivity
2015–2016	15	12	9	0
2017	12	7	0	3
Total	27	19	9	3

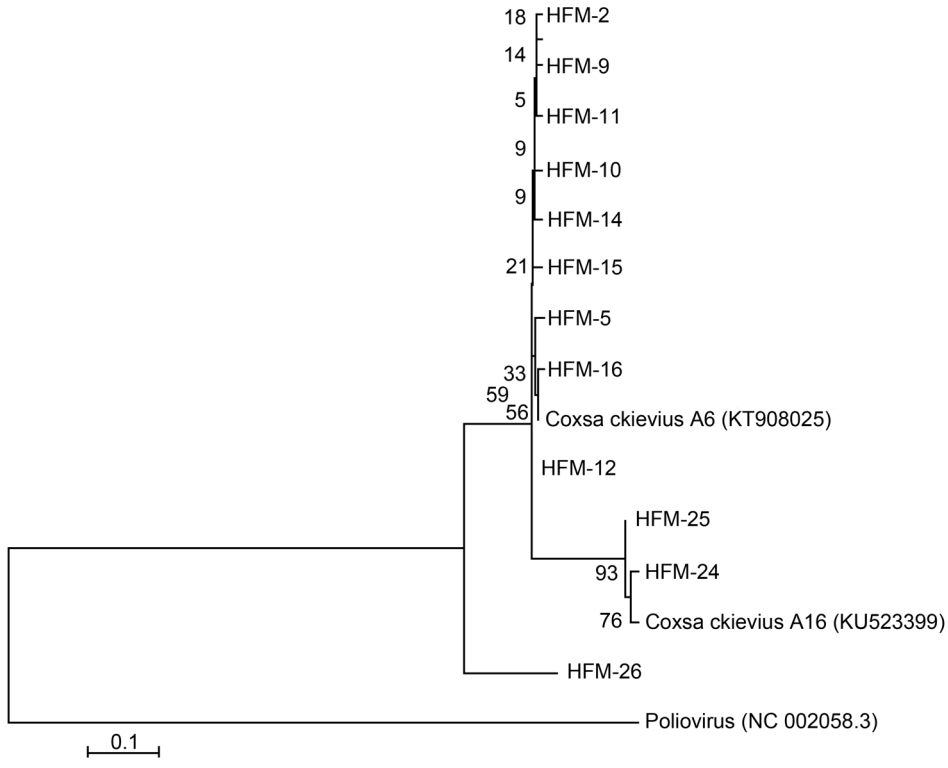

Fig. 7. Phylogenetic analysis of clinical isolates. Phylogenetic analysis of coxsackievirus A6 nucleotide sequences that were obtained using 153F ve 541R primers, showed the relationships between the clinical CV-A6 and the CV-A16 isolate selected from the GenBank. A scale bar indicates branch distances. The phylogenetic tree was constructed using neighbour-joining method and validated with 1000 pseudo-replicates. Poliovirus (NC 002058.3) was selected as out-group.

in CV-A6 incidence (Bian et al. 2015). HFMD is not a mandatory disease to report to public health authorities in Turkey. Therefore, complete data on the causative agents of the cases throughout the country is not yet known. Only a single case study identifying the causative agent was reported from Turkey (Kiratli et al. 2017). In that study, the identification of CV-16 in a 39 years old male patient was performed. The present study identified CV-A16 in 25% of the pediatric samples (Table III). A study conducted in China between 2011 and 2015 on 2130 samples positive for *Enterovirus* demonstrated that CV-A16 was identified in 32%, and EV-A71 – in 30% of the samples (Sun et al. 2017). It has been reported that EV-A71 infections may lead to neurological complications (e.g. aseptic meningitis, acute flaccid paralysis, and brainstem encephalitis), and mortality. All of the cases in our study were from outpatient services and no EV-A71 was identified in any patients. The literature reported severe cases with CV-A6 but none of our patients had a complicated course of the disease and needed hospitalization (Yang et al. 2014). Another clinical feature of CV-A6 is onychomadesis, (Wei et al. 2011) and in our cohorts, only one of the confirmed CV-A6 cases was re-admitted to the hospital at the 6th week after the discharge with complaints of onychomadesis.

The frequency of HFMD emergences peak twice in a year in countries with a tropical climate; however, it can be observed throughout the year. It exhibits a single annual rise in summer or fall in countries located at higher latitudes (Blomqvist et al. 2010; Huang et al. 2015; Wang et al. 2017). In Turkey, individual studies showed that the frequency of HFMD rises during summer (Topkarcı 2013; Uğraş et al. 2014; Yorulmaz and Onat 2017). In parallel with the previous research, in the present study, it has been observed that the majority of HFMD cases (67%) applied to our hospital during summer months.

Hand, foot, and mouth disease frequently affects children under the age of 5. Previous studies show that more than half of the individuals affected by epidemics were aged between 1 and 3 years (Montes et al. 2013; Huang et al. 2015). Seventy-eight percent of 27 children included in the current study was aged between 1 and 3 years. Epidemiological studies investigating HFMD have shown that the incidence is 1.5–2 times higher among boys compared to girls (Huang et al. 2015; Sun et al. 2017). In this study, similarly, the ratio of boys/girls was 16/11.

One of the limitations of the current study is that our cohorts were from a single city and the numbers of the patient were rather small. Therefore, our result might not reflect the overall HFMD epidemiology of all country. Secondly, only 12 sequencing results could be used to make the evolutionary trees to establish the

relationship of the CV-A6, or CV-A16 in Turkey in relation to others in the world. Therefore further studies including samples from various regions of Turkey with a larger sampling might shed a better light on the dissemination as well as the phylogenetic relationships of these viral agents. Nevertheless, the data presented in the current study reports for the first time a detailed investigation about the presence of previously unnoticed serotypes on an important public health agent.

Geographically, Turkey acts as a gateway between Asia and Europe, and receives an influx of tourists from various countries across the world during summer months, the time that the incidence of HFMD peaks. Therefore, the establishment of a national surveillance system for HFMD and identification of causative serotype agents are important from an epidemiological point of view as well as for the planning and execution of preventive measures including vaccination. Our investigation and reporting might be useful in guiding these efforts.

Acknowledgements

We thank Hamid Ceylan Ph.D. for Blast Search assistance.

Conflict of interest

The authors do not report any financial or personal connections with other persons or organizations, which might negatively affect the contents of this publication and/or claim authorship rights to this publication.

Literature

Bian L, Wang Y, Yao X, Mao Q, Xu M, Liang Z. Coxsackievirus A6: a new emerging pathogen causing hand, foot and mouth disease outbreaks worldwide. Expert Rev Anti Infect Ther. 2015 Sep 02;13(9):1061–1071. doi:10.1586/14787210.2015.1058156 Medline

Blomqvist S, Klemola P, Kaijalainen S, Paananen A, Simonen ML, Vuorinen T, Roivainen M. Co-circulation of coxsackieviruses A6 and A10 in hand, foot and mouth disease outbreak in Finland. J Clin Virol. 2010 May;48(1):49–54. doi:10.1016/j.jcv.2010.02.002 Medline

Bracho MA, González-Candelas F, Valero A, Córdoba J, Salazar A. Enterovirus co-infections and onychomadesis after hand, foot, and mouth disease, Spain, 2008. Emerg Infect Dis. 2011 Dec;17(12): 2223–2231. doi:10.3201/eid1712.110395 Medline

Bucak İH, Tepe B, Almiş H, Köse A, Turgut M. Joint diagnosis of pediatric and dermatology clinics: Prospective observation of thirty-nine patients with hand, foot and mouth disease (in Turkish). Turkderm-Turk Arch Dermatol Venereology. 2017;51:41–45. doi:10.4274/turkderm.22804

Centers for Disease Control and Prevention (CDC). Notes from the field: severe hand, foot, and mouth disease associated with coxsackievirus A6 – Alabama, Connecticut, California and Nevada, November 2011 – February 2012. MMWR Morb Mortal Wkly Rep. 2012 Mar 30;61(12):213–214. Medline

Chen YJ, Chang SC, Tsao KC, Shih SR, Yang SL, Lin TY, Huang YC. Comparative genomic analysis of coxsackievirus A6 strains of different clinical disease entities. PLoS One. 2012 Dec 26;7(12):e52432. doi:10.1371/journal.pone.0052432 Medline

Demirhan B, Demirbaş Z, Sari T, Toprak A, Navruz M. Hand-foot-mouth disease in 14 years-old: A Case Report. Turk J Fam Med & Prim Care. 2016;10(1):49–51. doi:10.5455/tjfmpc.209819

Ekinci AP, Erbudak E, Baykal C. A significant increase in the frequency of hand-foot-mouth disease in Istanbul in June 2012 (in Turkish). Turkderm-Turk Arch Dermatol Venereology. 2013; 47(4):192. doi:10.4274/turkderm.19942

Fonseca MC, Sarmiento L, Resik S, Martínez Y, Hung LH, Morier L, Piñón A, Valdéz O, Kourí V, González G. Coxsackievirus A6 and enterovirus 71 causing hand, foot and mouth disease in Cuba, 2011–2013. Arch Virol. 2014 Sep;159(9):2451–2455. doi:10.1007/s00705-014-2071-x Medline

Fujimoto T, Iizuka S, Enomoto M, Abe K, Yamashita K, Hanaoka N, Okabe N, Yoshida H, Yasui Y, Kobayashi M, et al. Hand, foot, and mouth disease caused by coxsackievirus A6, Japan, 2011. Emerg Infect Dis. 2012 Feb;18(2):337–339. doi:10.3201/eid1802.111147 Medline

Ge S, Yan Q, He S, Zhuang S, Niu J, Xia N. Specific primer amplification of the VP1 region directed by 5' UTR sequence analysis: enterovirus testing and identification in clinical samples from hand-foot-and-mouth disease patients. J Virol Methods. 2013 Nov;193(2):463–469. doi:10.1016/j.jviromet.2013.06.009 Medline

Han JF, Xu S, Zhang Y, Zhu SY, Wu DL, Yang XD, Liu H, Sun BX, Wu XY, Qin CF. Hand, foot, and mouth disease outbreak caused by coxsackievirus A6, China, 2013. J Infect. 2014 Sep;69(3):303–305. doi:10.1016/j.jinf.2014.03.015 Medline

Hu YQ, Xie GC, Li DD, Pang LL, Xie J, Wang P, Chen Y, Yang J, Cheng WX, Zhang Q, et al. Prevalence of coxsackievirus A6 and enterovirus 71 in hand, foot and mouth disease in Nanjing, China in 2013. Pediatr Infect Dis J. 2015 Sep;34(9):951–957. doi:10.1097/INF.0000000000000794 Medline

Huang X, Wei H, Wu S, Du Y, Liu L, Su J, Xu Y, Wang H, Li X, Wang Y, et al. Epidemiological and etiological characteristics of hand, foot, and mouth disease in Henan, China, 2008–2013. Sci Rep. 2015 Aug;5(1):8904. doi:10.1038/srep08904 Medline

Kiratli K, Topal Y, Saat B, Kemer S, Cevik E. Hand-foot-mouth Disease in an Immunocompetent Adult. CausaPedia. 2017;6(1):1–5.

Kliegman S, Geme SS. Nelson Textbook of Pediatrics, 2-Volume Set, 20th ed. Amsterdam (the Netherlands): Elsevier Inc.; 2015.

Mao Q, Wang Y, Yao X, Bian L, Wu X, Xu M, Liang Z. Coxsackievirus A16: epidemiology, diagnosis, and vaccine. Hum Vaccin Immunother. 2014 Feb;10(2):360–367. doi:10.4161/hv.27087 Medline

Mirand A, Henquell C, Archimbaud C, Ughetto S, Antona D, Bailly JL, Peigue-Lafeuille H. Outbreak of hand, foot and mouth disease/herpangina associated with coxsackievirus A6 and A10 infections in 2010, France: a large citywide, prospective observational study. Clin Microbiol Infect. 2012 May;18(5):E110–E118. doi:10.1111/j.1469-0691.2012.03789.x Medline

Montes M, Artieda J, Piñeiro LD, Gastesi M, Diez-Nieves I, Cilla G. Hand, foot, and mouth disease outbreak and coxsackievirus A6, northern Spain, 2011. Emerg Infect Dis. 2013 Apr;19(4):676. doi:10.3201/eid1904.121589 Medline

Österback R, Vuorinen T, Linna M, Susi P, Hyypiä T, Waris M. Coxsackievirus A6 and hand, foot, and mouth disease, Finland. Emerg Infect Dis. 2009 Sep;15(9):1485–1488. doi:10.3201/eid1509.090438 Medline

Romero JR. Hand, foot, and mouth disease and herpangina: an overview [Internet]. Waltham (USA): UpToDate; 2017 [cited 2018 Sep 12]. Available from: https://www.uptodate.com/contents/hand-foot-and-mouth-disease-and-herpangina

Sun Z, Zhang G, Guo P, Liu J, Gao Q, Xu X, Gong L. Epidemiological characterizations, pathogen spectrum and molecular

characteristics of Coxsackievirus A16 from patients with HFMD in Yantai, Shandong, China between 2011 and 2015. Hum Vaccin Immunother. 2017 Aug 03;13(8):1831–1838. doi:10.1080/21645515.2017.1318233 Medline

Topkarcı Z. A clinical and demographic properties of hand-foot-mouth disease. Medical Journal of Bakirköy. 2013;9(1):12–15. doi:10.5350/BTDMJB201309103

Uğraş M, Küçük Ö, Biçer S, Çöl D, Giray T, Erdağ GÇ, Yalvaç Z, Yüce B, Vitrinel A. İki yıllık periyot içinde el-ayak-ağız hastalığı olan çocukların değerlendirilmesi. J Kartal TR. 2014;25:34–38. doi:10.5505/jkartaltr.2014.48568

Wang P, Zhao H, You F, Zhou H, Goggins WB. Seasonal modeling of hand, foot, and mouth disease as a function of meteorological variations in Chongqing, China. Int J Biometeorol. 2017 Aug; 61(8):411–1419. doi:10.1007/s00484-017-1318-0 Medline

Wei SH, Huang YP, Liu MC, Tsou TP, Lin HC, Lin TL, Tsai CY, Chao YN, Chang LY, Hsu CM. An outbreak of coxsackievirus A6 hand, foot, and mouth disease associated with onychomadesis in Taiwan, 2010. BMC Infect Dis. 2011 Dec;11(1):346. doi:10.1186/1471-2334-11-346 Medline

World Health Organization (WHO). A guide to clinical management and public health response for hand, foot and mouth disease (HFMD). Manila (Philippines):WHO Regional Office for the Western Pacific. 2011.

Yang F, Yuan J, Wang X, Li J, Du J, Su H, Zhou B, Jin Q. Severe hand, foot, and mouth disease and coxsackievirus A6-Shenzhen, China. Clin Infect Dis. 2014 Nov 15;59(10):1504–1505. doi:10.1093/cid/ciu624 Medline

Yorulmaz A, Onat NK. Clinical and Demographic Properties of Hand-Foot and Mouth Disease. J Clin Anal Med. 2017 May 01; 8(3):219–222. doi:10.4328/JCAM.4821

Polish Journal of Microbiology
2019, Vol. 68, No 2, 173–183
https://doi.org/10.33073/pjm-2019-017

ORIGINAL PAPER

Evaluation of a *Salmonella* Strain Isolated from Honeybee Gut as a Potential Live Oral Vaccine Against Lethal Infection of *Salmonella* Typhimurium

HASSAN ZAFAR[1]*, SAJJAD UR RAHMAN[1], SULTAN ALI[1] and MUHAMMAD TARIQ JAVED[2]

[1] Institute of Microbiology, University of Agriculture, Faisalabad, Punjab, Pakistan
[2] Department of Veterinary Pathology, University of Agriculture, Faisalabad, Punjab, Pakistan

Submitted 9 October 2018, revised 16 January 2019, accepted 19 January 2019

Abstract

In this research, *Salmonella* species were isolated from the animal, insect and human enteric sources in Faisalabad, Punjab, Pakistan. These species were characterized by different microbiological and molecular techniques including polymerase chain reaction (PCR) by amplification of the 16S rRNA gene. Furthermore, sequencing of the amplicons confirmed all ten isolates as *Salmonella* strains. The antigenic cross-reactivity was found maximum between the HB1 (strain isolated from honeybee) antiserum and its antigen with an antibody titer of 1:128, while the HB1 antiserum showed a cross-reactive titer range of 1:8 to 1:64. On the basis of the highest geometric mean titer (GMT) shown by the antiserum of the HB1 antigen, it was selected as the best candidate for a cross-reactive live *Salmonella* oral antigen. Moreover, the HB1 antigen was used a live oral antigen (1×10^{10} CFU/ml) in a safety test in rabbits and proved to be avirulent. During the animal trial, three different oral doses of the HB1 live oral antigen were evaluated in four different rabbits' groups (R1, R2, R3, and R4). The dose number 2 of 0.5 ml (two drops orally and repeated after one week) gave the best GMT measured by indirect hemagglutination (IHA) as compared to the other two doses, while R4 group was kept as control. Results of the challenge protection test also validated the efficacy of the double dose of the HB1 live vaccine, which gave the highest survival percentage. Results of this study lay the foundation for a potential cross-reactive live oral *Salmonella* vaccine that has proved to be immunogenic in rabbits.

Key words: *Salmonella*, antigen, cross-reactivity, 16S rRNA gene, geometric mean titer

Introduction

Globally, every year millions of humans and animals become victims of *Salmonella*-related infections. Both developed and underdeveloped countries are equally affected by these infections, and each year millions of dollars are exhausted on epidemiological studies, prevention, and treatment (Eng et al. 2015). In spite of advancements and improvements in hygiene and sanitation in many countries, *Salmonella*-related infections are still on the rise (Coburn et al. 2007; Crump et al. 2015). The most common manifestation of *Salmonella* infection is gastroenteritis followed by enteric fever and bacteremia (Majovicz et al. 2010; Medalla et al. 2017)

The genus *Salmonella* is a rod-shaped, Gram-negative, facultative anaerobe and a member of the family Enterobacteriaceae, it has two species *Salmonella enterica* and S*almonella bongori* (Kidgell et al. 2002; Coburn et al. 2007); for a review about the taxonomy of the genus *Salmonella* see Brenner et al. (2000). Division of *Salmonella* subspecies into serotypes was done on the basis of lipopolysaccharide, flagellar and carbohydrate structures (Naier et al. 2014). Both humans and animals can acquire the *S. enterica* serovars orally (McClelland et al. 2001). However, the manifestation of disease caused by these pathogens depends upon various factors such as host susceptibility, immune status of the host and the pathogenic serovar involved (Hauser et al. 2010).

The four major disease syndromes caused by *S. enterica* include diarrhea/enterocolitis, typhoid fever, bacteremia and chronic asymptomatic carriage (Bhan et al. 2005; Karon et al. 2007; Crump et al. 2015). The primary route of spread of *S*. Typhi in humans is the fecal-oral route. According to the latest World Health Organization (WHO) data from 2018, each year 11–20 million

* Corresponding author: H. Zafar, Institute of Microbiology, University of Agriculture, Faisalabad, Punjab, Pakistan; **e-mail: hassanzafaruaf@gmail.com**

people get sick from typhoid fever, and between 128 000 to 161 000 people die due to the disease (WHO 2018). More than 90% of enteric fever cases occur in Asia alone (Crump et al. 2004), with Pakistan, Bangladesh, and Nepal being the most affected (Brooks et al. 2005; Karkey et al. 2013). If a suitable treatment regime is not adopted for the typhoid patients there is a 12–30% increase in the mortality, while in treated cases the survival rate can be up to 99% (Ochiai et al. 2008). Over the years, antimicrobial resistance in *Salmonella* serotypes has emerged as a serious health problem worldwide (Chiu et al. 2002). For more insight about antimicrobial resistance in *Salmonella* see Threlfall (2002), Foley et al. (2008), Kariuki et al. (2015).

Consumption of food or fluids contaminated with *Salmonella* result in infection in both humans and animals (Escobedo et al. 2011). After entry into the intestine, the bacteria attach, invade, and proliferate in the enterocytes of the gut-associated lymphoid tissue (GALT) (Monack et al. 2004). This can result in a diseased or carrier state and can also stimulate the induction of various immune responses (mucosal and systemic). However, these immune responses can be suppressed with avirulent invasive *Salmonella*, which can facilitate the establishment of a carrier state (Curtiss et al. 1993; Burton et al. 2014). It is possible to attenuate *Salmonella* strains by the introduction of various mutations. The main purpose of oral immunization of animals with avirulent *Salmonella* serotypes is usually not associated with suppression, but with the stimulation of cellular and humoral immune responses (Coburn et al. 2007). Animals injected with killed vaccines or bacterins exhibit short-lived humoral immunity, and this also does not stimulate the induction of mucosal and cellular immune response. Moreover, live *Salmonella* oral vaccines are better suited as vaccine candidates as they provide long-lasting immunity (Behnsen et al. 2015).

In many countries licensed typhoid vaccines are being used against typhoid fever. However, systemic reactions have developed in around 25–40% of patients (Eng et al. 2015). The majority of recipients of the typhoid vaccine have been either children or young adults. The Ty21a is an oral attenuated *Salmonella* vaccine, but it has not been adopted by countries due to its high cost (Fraser et al. 2007). Another vaccine used in the prevention of typhoid fever is Vi capsular polysaccharide subunit vaccine, but it has not shown positive results in children under the age of two years (Yang et al. 2001). Recently, a conjugate vaccine using O-polysaccharide (OSP) of *S*. Typhi and *S*. Paratyphi A conjugated with Diphtheria toxoid (DT) was used in a vaccine trial in mice. The trials confirmed the immunogenic potential of the conjugate vaccine (Ali et al. 2014). In the case of animals including poultry, various *Salmonella* vaccines are also in practice worldwide (Desin et al. 2013; Gayet et al. 2017).

Salmonella Typhimurium is a non-typhoidal serovar, which infects a wide range of animal hosts and humans (Feasey et al. 2012). Despite various attempts, an appropriate licensed vaccine against *S*. Typhimuirum for human use has not yet been approved (Ortiz et al. 2014). However, various vaccines (live, attenuated, subunit) are under the process of development, these vaccines may have the ability to induce a long-term cross-protective prophylaxis against non-typhoidal *Salmonella* serotypes (Sanapala et al. 2017). The aim of this study was to search out a *Salmonella* species that could be used as a potential live cross-reactive antigen against infection of *S*. Typhimurium in a rabbit model and could have the potential to be used as a live vaccine for future experiments.

For this purpose, a mass scale isolation of *Salmonella* species from different enteric sources was done using various microbiological and molecular tools. Initially, the whole cell antigen of all the identified strains was used in an immunological assay to determine the cross-reactivity. The best cross-reactive antigen was also evaluated for its avirulent potential in animal trials. Finally, the live antigen was tested for cross-protection against lethal challenge by *S*. Typhimurium (ATCC 14028) in an animal trial.

Experimental

Materials and Methods

Sample collection. Between June and July of 2016, a total of 90 samples were randomly collected from various enteric sources. These stool and fecal samples were collected from various veterinary hospitals, poultry/livestock farms and hospital facilities (Allied hospital, District headquarter hospital, Faisalabad) in the district of Faisalabad, Punjab, Pakistan (Table I). In the case of insects, honeybees were selected for sampling, the droppings were not clearly visible by the naked eye, so the gut contents were taken as samples. The samples were collected through sterile cotton swabs in different collection tubes containing Cary Blair transport medium (Oxoid, UK). All the samples were transported immediately to Institute of Microbiology, University of Agriculture, Faisalabad, Pakistan for further processing.

Isolation and identification of *Salmonella* isolates. For pre-enrichment, the samples were suspended in phosphate buffer water (PBW) with the necessary volume of medium used to make a 1/10 dilution of each sample. Tetrathionate broth (TTB) (Oxoid, UK) was used for the primary enrichment of the fecal/stool/droppings samples, with 1 g of the sample in 10 ml of

Table I
Details of collection of the fecal/stool/dropping samples along with location of the sampling.

Species	Sample size	Average weight (gm)	Location of the sample collection
Human	15	7	Allied Hospital, Faisalabad, Pakistan. District Headquarters Hospital, Faisalabad, Pakistan
Cat	15	5	Department of Clinical Medicine and Surgery, University of Agriculture, Faisalabad, Pakistan
Sheep	15	4	Livestock farm, University of Agriculture, Faisalabad, Pakistan Department of Clinical Medicine and Surgery, University of Agriculture, Faisalabad, Pakistan
Honey bee	15	0.2	Botanical garden, University of Agriculture, Faisalabad, Pakistan Department of Entomology, University of Agriculture, Faisalabad, Pakistan
Poultry birds	15	3	Poultry farms, University of Agriculture, Faisalabad, Pakistan
Horse	15	8	Brooke Hospital, University of Agriculture, Faisalabad, Pakistan

TTB and incubated at 37°C for 48 hours. After enrichment, the subculturing was performed on *Salmonella-Shigella* agar (SSA) (Oxoid, UK), and further confirmation was done on Bismuth Sulphite Agar (BSA) (Oxoid, UK). In the case of SSA, the Petri plates were incubated for 24 hours, and the BSA plates were incubated for 48 hours at 37°C (Andrews et al. 1998). Visual examination of the colonies in the growth media was performed. Presumptive *Salmonella* colonies were straw colored with black centers on SSA and black colored colonies on BSA.

For further biochemical characterization, a biochemical kit RapID™ ONE (Remel R8311006) (ThermoFisher Scientific, USA) was used. Prior to inoculation into the kit, the well-differentiated colonies were picked up by a sterilized inoculating loop from both SSA plates and BSA plates and were inoculated into the Remel inoculation fluid (2 ml). The turbidity of the fluid was matched with the McFarland standard scale and was equal to 2.0 McFarland standard. The fluid containing the growth was then transferred to the wells of the kit and incubated at 37°C for 4 hours. The Rapid one panel (kit) contains 18 reaction cavities that provide a total test score of 19. The cavities 15–17 required the addition of two reagents, 1) RapID One reagent (ρ-dimeth ylaminocinnamaldehyde), the enzymatic hydrolysis of the acrylamide substrate releases free β-naphtylamine which is detected by this reagent 2) RapID Indole reagent (ρ-dimethylaminocinnamaldehyde, hydrochloric acid, and demineralized water), detects formation of indole. Scores were evaluated using the following link http://www.remel.com/ERIC/Home.aspx. *Salmonella* Typhimuirum (ATCC 14028) was used as a control for the validation of kit results.

Molecular identification by amplification of 16S rRNA genes. The ten isolates that were confirmed as *Salmonella* species from the biochemical tests were further subjected to polymerase chain reaction (PCR) by amplifying the 16S rRNA gene and further sequencing of the amplicons. The DNA extraction was performed using Genomic Isolate II DNA extraction kit (Bio line, London, UK) by following the instructions provided in the user manual for cultured cells. The NANODROP 8000 spectrophotometer (Thermo Scientific, USA) was used for the quantification of the DNA concentration in the samples.

For the amplification of the 16S rRNA gene of the isolates, PCR was done with primers 27 F (5'-AGAGTTTGATCCTGGCTCAG-3') and 1492 R (5'-GGTTACCTTGTTACGACTT-3'). For PCR, the conditions of the thermal cycler were set at initial denaturation at 96°C for 3 min, followed by 32 amplification cycles of 30 s at 94°C, 30 s at 52°C and 1 min at 70°C, followed by a final extension at 70°C for 10 min (Sipos et al. 2007). For gel electrophoresis, a marker (kb ladder, University of California, San Diego, USA), of 4 kbp size was used. The amplicons were further purified using QIAquick Kit (Qiagen, Germany). The pure PCR products were placed in ice boxes for transport and were sent for sequencing to the biotechnology company TSINGKE, China.

Phylogenetic analysis. The sequences obtained of all ten *Salmonella* isolates were screened against the National Center of Biotechnology (NCBI) database using the Basic Local Alignment Search Tool (BLAST). After BLAST confirmed all ten sequences to be *Salmonella*; these sequences and two *S. bongori* strains (as out-groups) were used to construct a phylogenetic tree using the Molecular Evolutionary Genetic Analysis (MEGA X) software (Kumar et al. 2018)

Preparation of antigen for the raising of antiserum in rabbits. The purified colonies of *Salmonella* strains were cultured in tryptic soy broth for 48 hours at 37°C. Cultures were transferred to Eppendorf tubes and were centrifuged at 800 × g. The supernatant was discarded, and the pellet was resuspended in phosphate buffer saline (PBS). Using the McFarland standard, a standard of 0.5 McFarland was maintained. The antigens in the bacterial culture were inactivated by the addition of 0.3% formalin, and an equal volume of Montanide adjuvant ISA 206VQ (SEPPIC) was added in the suspension and was mixed gently. The final count of

Table II
Schedule of *Salmonella* antigen inoculation for the raising of antibodies against *Salmonella* strains.

Salmonella antigen	Day 1 = 1st shot (0.2 ml)		Day 7 = 1st booster (0.5 ml)		Day 14th = 2nd booster (0.5 ml)	
	HR1	C	HR1	C	HR1	C
TY1	0.2	0.2	0.5	0.5	0.5	0.5
TY2	0.2	0.2	0.5	0.5	0.5	0.5
TY3	0.2	0.2	0.5	0.5	0.5	0.5
HB1	0.2	0.2	0.5	0.5	0.5	0.5
HB11	0.2	0.2	0.5	0.5	0.5	0.5
SP6	0.2	0.2	0.5	0.5	0.5	0.5
CT7	0.2	0.2	0.5	0.5	0.5	0.5
PB2	0.2	0.2	0.5	0.5	0.5	0.5
PB9	0.2	0.2	0.5	0.5	0.5	0.5
HE13	0.2	0.2	0.5	0.5	0.5	0.5

HR1 = Group 1 of rabbits given antigen, C = control group given normal saline

the Montanide adjuvanted antigens was 1×10^{10} CFU/ml and they were preserved at 4°C.

Protocol for raising antiserum against *Salmonella* strains. For the raising of antisera, twenty specific pathogen free (SPF) Chinchilla rabbits having an average weight of 3 kg were selected. Following all the bioethical and biosafety measures as approved by the Institutional Biosafety Committee of UAF, the rabbits were reared at the animal house of the Institute of Microbiology, UAF. The rabbits were divided into two groups HR1 and HC, with each group having ten rabbits in it (Table II). On the first day, 0.2 ml of the prepared antigens were injected intraperitoneally into rabbits of the group HR1, while 0.2 ml of normal saline was injected into the rabbits of group HC as described in. On the 7th day a booster dose of 0.5 ml was given to the rabbits of HR1, while 0.5 ml of normal saline was given to group C. On the 14th day a repeat of the booster dose for the group HR1 was done with 0.5 ml being injected again, while the group C rabbits were injected with 0.5 ml normal saline. The antiserum raised against the whole cell antigens of the *Salmonella* strains was collected on the 21st day of the experiment.

Microtiter plate agglutination test. This modified assay test was performed to check the antibody titer levels resultant from the antiserum reacting with the different *Salmonella* antigens (Barsoum and Awad 1972). It was performed in a 96-well microtiter plate in a triplicate with average readings presented in the Results section. A volume of 50 µl of tryptic soy broth was layered in each of the wells of the microtiter plate, 50 µl of the antiserum raised from all of the strains was layered at the start of each well and two-fold dilutions were done until the last well. A volume of 50 µl of the antigens from all of the isolates was mixed in a sequence. The plate was incubated for 12 hours at 37°C. A smooth mat shape at the bottom of the well indicated a positive reaction, while a negative reaction was indicated by button formation of the antigen at the bottom of the wells. The last serum dilution where agglutination was visible was considered the agglutination endpoint. Agglutination antibody titers were measured as the inverse of the greatest dilution that still yielded agglutination. For the geometric mean titer (GMT), the arithmetic means of the logarithms of the last positive serum dilution were considered.

Safety studies for evaluation of HB1 live antigen. Preserved cultures of HB1 strain were refreshed in tryptone soy broth (TSB). Colony count was performed, and a separate final suspension of 10^{10} CFU/ml was prepared. The *Salmonella* antigen (HB1) was maintained to a 0.5 McFarland standard and kept in phosphate buffer saline (PBS) (pH 7.2). As a preservative, honey (2%) was added and no inactivation of the antigen was done. The safety studies were conducted according to the international standards of antigen evaluation (Fedson 2005). Three different groups of healthy rabbits with five rabbits in each (SR1, SR2, and SR3) were maintained. All the containment facilities and biosafety measures were adopted according to instructions provided by Biosafety Level 2 (BSL2) laboratories Institute of Microbiology, University of Agriculture, Faisalabad, Pakistan. In the group, SR1 rabbits were given a single oral dose of 0.5 ml (1×10^{10} CFU/ml) followed by normal feed and fodder. In the group, SR2 an oral dose of 1 ml (1×10^{10} CFU/ml) was given along with normal feed and fodder. Rabbits in SR3 were controls and 0.5 ml of normal saline was orally given to the animals in this group. The body temperature of all groups was measured and dropping samples were collected after every 24 hours till the 7th day of

the experiment. The *Salmonella* viable count was also performed on droppings for evaluation of the recovery of the HB1 live antigen.

Comparative immune response evaluation of live *Salmonella* antigen (HB1) using three different dose levels in rabbits. Four groups of healthy rabbits (10 in each) were maintained in the laboratory animal housing facility attached to the IOM, UAF. Three different dose levels of the HB1 antigen (0.5 ml) were given separately to each group including group R1 with two drops orally (a single dose), group R2 was given two drops orally and repeated after one week (a double dose) and group R3 was given two drops and repeated after alternate days for three times (a triple dose). The group R4 rabbits were kept as inoculated control. All the rabbits were maintained according to the institutional ethics committee recommendation and offered fresh water with feed and fodder *ad-libitum*.

For the detection of antibodies, the titer indirect hemagglutination test (IHAT) of Smith et al. (1977) was used with minor modifications. The live *Salmonella* antigen (HB1) was used to sensitize RBC's using chromium chloride for antigen binding. Two-fold serial dilutions of sera were made in microtitration plate and antiserum raised against HB1 live antigen was placed. The serum raised against HB1 live antigen was diluted separately, and 2% sensitized RBC's were added into 50 µl diluted serum after thorough mixing and were incubated at 37°C for 30 minutes. The different settling of RBC's was interpreted as positive and the compact button formation of RBC's at bottom wells was indicated as negative.

Challenge protection test. Three groups of rabbits R1, R2 and R3 were given an LD50 dose of *S.* Typhimurium (ATCC 14028) (1×10^4 CFU/ml), while the fourth group (R4) was given normal saline and used as a control. The survival percentage for the duration of 70 days and statistical analysis for determination of survival percentage was done using the software GraphPad Prism version 7 (GraphPad Software Inc., USA).

Results

Morphological and biochemical results. The colonies were moderately large (range of 0.5–1.5 mm diameter) convex, glistening and round in shape. In addition, the suspected colonies of *Salmonella* were straw colored with black centers due to the production of hydrogen sulphide (H_2S) on SSA. Typical straw-colored colonies with black centered colonies were further plated for confirmation on BSA. The suspected *Salmonella* colonies were completely black when grown on BSA.

The biochemical characterization of the *Salmonella* isolates was done using a Remel Rapid ID kit (ThermoFisher Scientific, USA) and the results were given in Table III. All ten isolates were confirmed as *S. enterica* (Salmonella I from RapID instruction manual). For quality control, a reference strain of *S.* Typhimurium ATCC 14028 was also tested.

Table III
Results of biochemical characterization by Remel RapID™ and the analysis by ERIC software.

Salmonella isolate	RapID No.	Percentage ID	Spp. identification
TY1	0320410	99.45%	*Salmonella* I
TY2	0320410	99.45%	*Salmonella* I
TY3	0320410	99.45%	*Salmonella* I
HB1	2360410	99.9%	*Salmonella* I
HB11	6363210	99.9%	*Salmonella* I
SP6	6360400	99.9%	*Salmonella* I
CT7	6160400	75.5%	*Salmonella* I
PB2	2300010	98.10%	*Salmonella* I
PB9	2300010	98.10%	*Salmonella* I
HE13	6360400	99.9%	*Salmonella* I
S. Typhimurium ATCC 14028	6360410	99.9%	*Salmonella* I

Molecular characterization of isolates. The DNA extracted from the *Salmonella* isolates was quantified using Nanodrop 8000 spectrophotometer (Thermo Scientific, USA). After DNA quantification the DNA samples were subjected to molecular characterization by PCR and further sequencing of the amplicons. For PCR the 16S rRNA gene was amplified. All ten isolates gave a band in the range of 1.4 kbp after gel electrophoresis shown in Fig. 1. Sequences of all ten isolates were

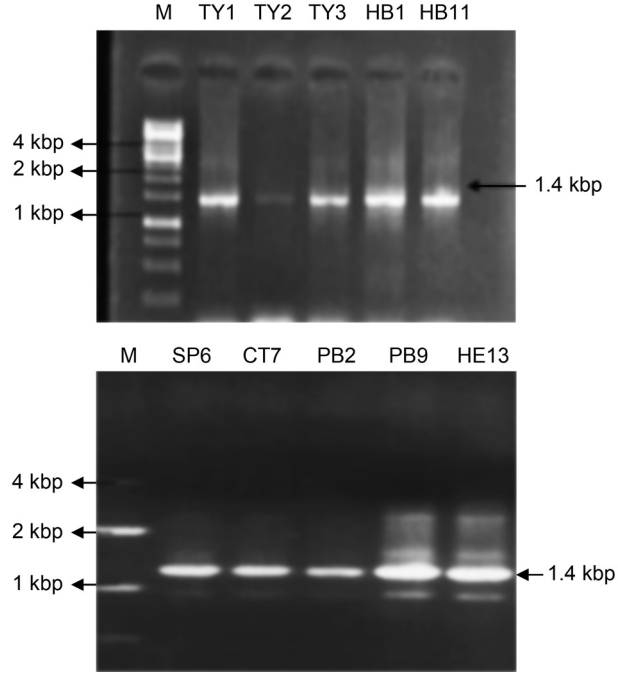

Fig. 1. Amplicons of 1.4 kbp are visible for each *Salmonella* isolate. According to literature, the universal primer (27F, 1492R) gives a PCR product of 1.4 kbp or 1.5 kpb. M is the marker used of 4 kbp size.

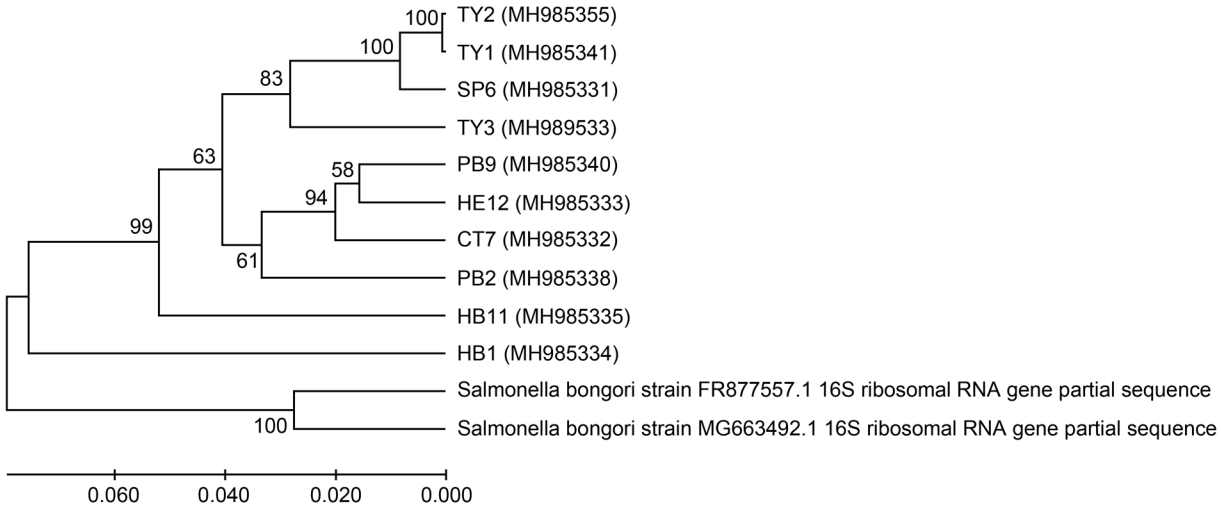

Fig. 2. The phylogenetic tree constructed by MEGA X, with the 16S rRNA sequences of the 10 *Salmonella* strains and two out-groups of *Salmonella bongori*. The UPGMA method was used with 2000 bootstrap replications, bootstrap percentages are indicated on nodes. The ten *Salmonella* species in this study are denoted as previously in this study along with their NCBI accession numbers. Evolutionary distances were computed using the Maximum Composite Likelihood method and they are provided in the units of number of base substitutions per site. The rate variation among sites was modeled with a gamma distribution (shape parameter = 2). All positions containing gaps and missing data were eliminated. There were a total of 1034 positions in the final dataset.

submitted to NCBI and were allotted following accession numbers; TY1 (MH985341), TY2 (MH985355), TY3 (MH989533), HB1 (MH985334), HB11 (MH985335), SP (MH985331), CT (MH985332), PB2 (MH985338), PB9 (MH985340), HE13 (MH985333). According to the BLAST, the results the three human isolates TY1, TY2 and TY3 had top four hits of *S.* Typhi strains, while HB1, HB11, CT7, HE13, and SP6 had more hits of *S.* Typhimurium with good scores. In case of the poultry isolates PB2 and PB9 both had top hits of *S.* Gallinarum strains.

Phylogenetic analysis of DNA sequences is important in determining evolutionary relationships between species of both prokaryotes and eukaryotes. In this study, an evolutionary tree was constructed by using the Molecular Evolutionary Genetics Analysis (MEGA X) program. The tree construction was based on the *Salmonella* 16s rRNA sequences obtained in this study and two out-groups of *S. bongori*. According to the tree results (Fig. 2), the sequences were denoted as previously along with their NCBI accession. Alignment of the sequences was done using Multiple Sequence Comparison by Log-Expectation (MUSCLE). The statistical method used for inference of evolutionary history was the Unweighted Pair Group Method and Arithmetic Mean (UPGMA).

Looking at the tree in Fig. 2, various clades can be observed. Two of the strains isolated from humans; TY1 and TY2 shared the most common ancestor (gene) forming a monophyletic clade, also the 16S rRNA genes of the third strain (TY3) isolated from humans and that of the SP6 strain isolated from sheep were closer to TY1 and TY2 from an evolutionary standpoint. Another monophyletic clade of the HE 13 strain isolated from horse and the poultry isolate PB9 was present in the tree, the second poultry isolate PB9 and the strain (CT7) isolated from cat seemed more related to this clade. The two strains (HB1 and HB11) isolated from honeybee were also similar to each other with respect to their position in the tree.

***Salmonella* plate agglutination test.** The test was performed to determine the homologous and heterologous antibody titer among individual antigens and their antiserum. The assay was performed in a 96-well microtiter plate. All the cumulative results of antigen and antiserum reactions along with all possible combinations (homologous and heterologous) are presented in Table IV. The HB1 antiserum exhibited significant ($p < 0.0001$) cross-reactivity by giving the highest geometric mean titer among all strains (Fig. 3).

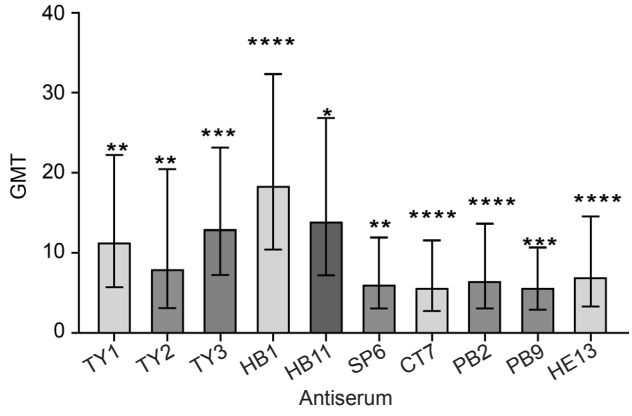

Fig. 3. Geometric mean titers of the antiserum against ten different strains.
Bars indicate the GMT (± SEM) at 95% Confidence Interval (CI) (*$p < 0.05$, **$p < 0.01$, ***$p < 0.001$ and ****$p < 0.0001$).

Table IV
The immunological cross-reactivity assay for the *Salmonella* strains with homologous and heterologous antibody titers and geometric mean titers.

	Antiserum									
Antigen	TY1	TY2	TY3	HB1	HB11	SP6	CT7	PB2	PB9	HE13
TY1	1:64	1:32	1:16	1:16	1:16	1:2	1:4	1:2	1:4	1:8
TY2	1:16	1:64	1:32	1:16	1:32	1:4	1:8	1:4	1:2	1:4
TY3	1:16	1:32	1:64	1:8	1:16	1:4	1:2	1:2	1:4	1:2
HB1	1:32	1:16	1:16	1:128	1:32	1:16	1:8	1:16	1:8	1:16
HB11	1:16	1:8	1:16	1:32	1:64	1:8	1:4	1:4	1:8	1:4
SP6	1:4	1:2	1:4	1:16	1:8	1:32	1:2	1:8	1:4	1:2
CT7	1:4	1:2	1:8	1:8	1:16	1:4	1:64	1:8	1:4	1:8
PB2	1:8	1:4	1:8	1:16	1:8	1:16	1:8	1:64	1:16	1:8
PB9	1:4	1:2	1:8	1:16	1:4	1:2	1:4	1:8	1:32	1:8
HE13	1:8	1:14	1:8	1:16	1:4	1:4	1:4	1:4	1:2	1:64
GMT	11.31	8	13	18.38	13.93	6.063	5.657	6.498	5.657	6.964

Safety evaluation of HB1 live antigen. Zero mortalities were observed among the rabbits of the two groups SR1, SR2 immunized with different doses of HB1 live antigen (1×10^{10} CFU/ml). Overall, in the ten rabbits, no physical abnormalities were observed, while the feed intake remained normal throughout the seven days with no apparent weight loss. Colony count was performed on the feces of the five rabbits throughout the experiment and recovery of the *Salmonella* HB1 live antigen from the five rabbits was shown to be between 1×10^3 to 1×10^5 CFU/ml for SR1, and 1×10^5 to 1×10^8 CFU/ml for SR2. The complete results for the two immunized groups and the controls (SR3) given normal saline are given in Table SI of the Supplementary information.

Immune response in rabbits to different doses of HB1 live antigen. The rapidity of the immune response was similar for the groups R2 and R3 with a GMT of 12.1 for both groups 10 days post vaccination. For the group R2, which were given the double dose, the highest GMT of 119.4 was observed at 40 days post-vaccination; while the lowest GMT of 8 was observed at 70 days post-vaccination. The group R1, given the single dose of HB1 antigen, initially exhibited low immune response with a GMT of 9.1 and 17.1 at 10 and 20 days post vaccination (Table V). However, there was a rise in the immune response of the rabbits with a GMT of 73.5 at 50 days post vaccination. The lowest GMT of 6.6 was recorded at 70 days post-vaccination. The group R3, given tripe dose of the HB1 live antigen, showed a strong immune response at 40 days post vaccination with a GMT of 122.4, and the lowest GMT of 5.8 at 70 days post-vaccination.

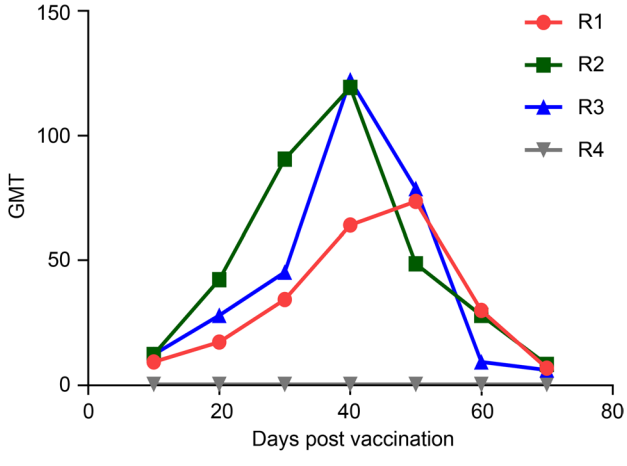

Fig. 4. Comparative indirect hemagglutination titers GMT in the three vaccinated groups and the control group during the 70-days animal trial.

Results of challenge protection test. Protective efficacy of the three different doses of HB1 live antigen in rabbits (R1 = single dose, R2 = double dose, R3 = triple dose, and R4 = control) was evaluated against LD50 dose of *S.* Typhimurium (ATCC 14028) (1×10^4 CFU/ml) for a duration of 70 days post immunization. The LD 50 dose was determined using the method of Reed and Muench (1938). The survival rates of the four groups

Table V
Geomean mean titers of the sera from four group of rabbits immunized with the live HB1 antigen.

Days post vaccination	R1	R2	R3	R4
10	9.1	12.1	12.1	–
20	17.1	42.2	27.8	–
30	34.2	90.5	45.2	–
40	64	119.4	122.4	–
50	73.5	48.5	78.7	–
60	29.8	27.8	9.1	–
70	6.6	8	5.8	–

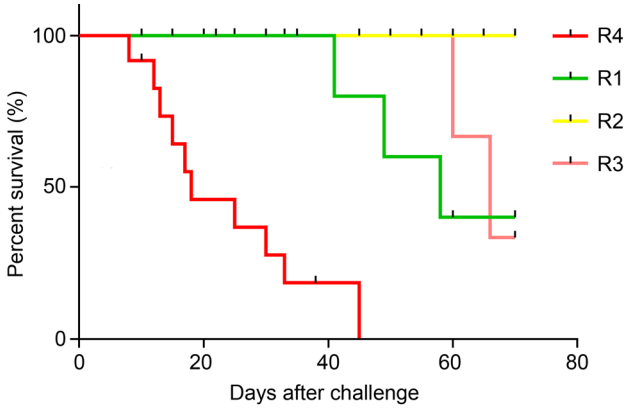

Fig. 5. Survival rate of four groups of rabbits immunized. All four groups were subjected to LD_{50} of *S.* Typhimurium. The three groups (R1, R2, and R3), immunized with different doses of HB1 live antigen, showed a significance increase ($p < 0.0001$) in the survival time in comparison to the control group (R4). Each group consisted of 10 rabbits. Kaplan Meier graph was generated by GraphPad Prism 7.

(each group included ten rabbits) are given in Fig. 5 in the form of a Kaplan Meier graph (it is also given in Table SIII as percentage protection). The three vaccinated groups that received three different doses (HB1 live antigen) had significantly longer survival rates as compared to the control (R4; given normal saline, NS), $^{****}p < 0.0001$. All the rabbits injected with NS succumbed to the *Salmonella* infection by day 45th day of the test. However, the R2 had zero mortalities throughout the 70-day period of the test, while R1 and R3 had three and two mortalities, respectively. The double dose of the HB1 live antigen (0.5 ml) proved to be the most efficient dose in the challenge protection test.

Discussion

Salmonella-related infections are a major disease threat in Southeast Asian countries including Pakistan. With antibiotic resistance in *Salmonella* strains increasing at an alarming rate, the role of antimicrobial therapy for treating infections appears to be ineffective in the battle against multi-drug-resistant (MDR) strains. Moreover, the situation could be altered by effective strategies that include: caution in the excessive use of antimicrobials, better diagnostic techniques and the finding of effective novel antimicrobials. Vaccines have been elected as a suitable measure to prevent the occurrence of *Salmonella* infections. The present research was designed to evaluate the antigenic cross-reactivity of *Salmonella* strains isolated from different human and animal sources in Faisalabad, Punjab, Pakistan. The predetermined goal of the research was to find an avirulent *Salmonella* strain, whose live antigen would prove to be a potential candidate for the development of a live oral cross-reactive vaccine. The vaccine would be trialed in an animal model for evaluation of efficacy.

There was a variation among the prevalence percentage of the *Salmonella* strains isolated from different hosts. The highest prevalence was found in humans with a percentage of 20%, followed by the honey bee (13%), poultry birds (13%), and cat, sheep, and horse, all three having prevalence percentage of 6%. In Pakistan, prevalence studies on *Salmonella* have regularly pointed towards the higher prevalence of *S.* Typhi in human subjects (Ochiai et al. 2008). In another prevalence study in Karachi, Pakistan, the prevalence percentage of *S.* Typhi from human subjects was reported to be 9.1% (Siddiqui et al. 2015). The prevalence percentage of *S.* Typhi in the human subjects in this study was the highest among all the *Salmonella* strains. Orji et al. 2004, have reported a high prevalence of *S.* Gallinarum and *S.* Pullorum in poultry birds in Pakistan with a combined percentage prevalence of around 12% for both strains. In our study, one strain of both Salmonella serovars was found with a combined prevalence percentage of 13%. Interestingly, in our study the occurrence of two *Salmonella* strains from the gut of honeybee was unexpected. The honeybee nests selected were not situated in the vicinity of any sewer, however, the contact of the bees with any animal feces cannot be ruled out. Also, Tarpy et al. (2014), have reported the presence of members of the Enterobacteriaceae family in the gut microbiome of the honeybee, which was one of the main reasons why we chose honeybee in our insect category for the sampling of *Salmonella* spp.

The targeting of the 16S rRNA gene in bacteria for numerous phylogenetic and taxonomic studies is becoming quite common. There are several reasons why the scientific community has resorted to this gene as the housekeeping marker, i) it is ubiquitous in all bacteria, and may exist as a multigene family or an operon, ii) the sequence of the gene is highly conserved, indicating that random sequence changes could be more useful in determining evolutionary pathways iii) the size (1400–1500 bp) of the 16S rRNA gene makes it a suitable candidate for bioinformatics analysis (Janda and Abbot 2007). Based on the sequencing results generated after the amplification of the 16S rRNA given in the Results section, the ten isolates were confirmed to be *Salmonella* strains. Previous results of Trkov and Avgustin (2003), also validated the success of the primers 27F, 1492R used in this study for the amplification of the 16S rRNA gene of different strains of *S. enterica*. The phylogenetic analysis of the sequences yielded interesting evolutionary relationships among the ten strains (sequences submitted to NCBI) of this study.

The scientific community has envisioned a cross-reactive live vaccine for enteric bacteria (Chedid et al. 1968). Various reports (Chacana and Trezolo, 2006;

Matluva et al. 2013) have confirmed the cross-immunity induced by live *Salmonella* vaccines in animal models. However, a live vaccine is only considered effective against an intracellular pathogen such as *Salmonella*, if it can induce both systemic (IgG) and mucosal (IgA) immune responses. In the present research, the double dose (two drops of 0.5 ml and repeated after one week) of the HB1 vaccine gave the best protection in the rabbits in response to LD50 of *S*. Typhimurium, as indicated by the challenge protection test. However, a shortcoming of this study was the determination of the type of humoral immune response (either systemic or mucosal) taking place in the rabbits. As *Salmonella* is an enteric pathogen, IgA is more likely to be the dominant player in the protective immune response after secretion into the gut lumen. As IgG (systemic antibodies) are more likely to combat *Salmonella* bacteria, which have left infected cells and migrated to other tissues, thus initiating new infections (Nandre et al. 2015).

Preliminary results do support the avirulent live HB1 strain to be a highly effective cross-reactive live vaccine in rabbits, which works in a dose-dependent manner. However, due to certain limitations, the exact mechanism of this cross-protection elicited by the vaccine could not be established. It has been recognized that live *Salmonella* strains are detected by the host immune system through the surface exposed antigens, as cell envelope shields the internal antigens (Burton et al. 2014). The mechanism of action of the HB1 live vaccine could be synonymous to the above-mentioned hypothesis. According to literature, most of the identified cross-protective antigens of *Salmonella* are surface exposed (Baumann 2014). On the cell surface of *Salmonella*, lipopolysaccharide (LPS) has been considered the main component to induce cross-reactive antibodies in the host. Various experiments have been performed on the complete core LPS and truncated LPS of *Salmonella* strains along with their cross-protection (Nnalue 1999). However, literature reported previously, supports the argument that the common outer membrane proteins (OMPs) such as OmpD and the core LPS *Salmonella* can induce cross-protection. As the core region of the LPS in *Salmonella* serotypes is highly conserved; this could be a candidate for studies that could help explain the cross-protection induced by the HB1 vaccine. However, the role of cell-mediated immune (CMI) responses cannot be overlooked as live oral *Salmonella* vaccines have been shown to elicit cross-reactivity by stimulating these CMI responses in the host, and future studies on the CMI responses induced by HB1 vaccine would be helpful.

Various avirulent live attenuated *Salmonella* mutants have been used as vaccine candidates in the past. These mutants have certain gene knockouts for attenuation and have been extensively studied. The use of attenuated strains bears various advantages such as the ability to carry heterologous antigens and to induce humoral, cellular and mucosal immune responses. However, the HB1 strain was not attenuated due to the lack of genomic information about the strain and the safety evaluation test gave us the notion to use it as a whole live antigen. For the preservation of the HB1 vaccine honey (2%) was used. However, how this preservative affected the vaccine should be evaluated in future studies. Various preservatives are used in vaccine preservation; some of these include aluminum salts, thimerosal (mercury-containing preservative), human serum albumin, and formaldehyde. Future studies could be performed using various preservatives and checking the stability of the vaccine (a stability trial was conducted whose results are given in the Supplementary file).

This research could prove to be just the tip of a huge iceberg with numerous areas yet to be explored. However, it does lay down the foundation of a *Salmonella* strain that has shown significant cross-reactivity against homologous and heterologous strains and significant efficacy as a vaccine against lethal infection by *S*. Typhimuirum. First of all, a future perspective should be the whole genome sequencing of the strain, as this study just confirmed the HB1 isolate as a *Salmonella* strain by sequencing of the 16S rRNA gene. A whole genome sequence would certainly be helpful in the identification of the suitable conserved antigens in comparison with already sequenced *Salmonella* strains. After comparative genomics of the strains, the development of HB1 strain mutants may be plausible, and these mutants could also be evaluated as future vaccine candidates in comparison to the wild type. In addition, the proteomic analysis including 3-D structural analysis of the structure of the proteins of the HB1 strain could also be helpful in identifying the amino acid differences that might be critical for the cross-reactivity of the antigens of the strain.

The animal model included specific pathogen free (SPF) Chinchilla rabbits infected with LD50 dose of *S*. Typhimuirum (animal pathogen). However, future studies could be orchestrated involving mice infected with other *Salmonella* strains, and to check if the cross-reactive HB1 vaccine still provides significant cross-protection. In this regard, the prospective studies could involve humanized mice (Mian et al. 2011) infected with *S*. Typhi strains. These mice have been used to mimic *S*. Typhi infections and have proven to be a valuable tool in studying the pathogenesis of *S*. Typhi. Future research could apprehend if the HB1 vaccine could provide similar cross-protection against *S*. Typhi strains in humanized mice.

Conclusion

The HB1 live oral antigen (double dose) elicited a strong immune response in the rabbits used in the animal trial, this vaccine could also prove to be a good

candidate as a potential vaccine in animals against other strains of *S.* Typhimurium. Overall, this study does support the notion that the HB1 vaccine can be an effective live oral vaccine that may provide cross-protection against other *Salmonella* strains in an animal model and may also be tested for immunoprotection against *S.* Typhi in a humanized mouse model. However, only rigorous future experiments would be able to corroborate the claims about the immunoprotection potential of the HB1 live oral antigen.

Acknowledgments

The authors acknowledge the funding of the International Research Program (IRSIP) funded by the Higher Education Commission (HEC) of Pakistan. In addition, we appreciate the technical support from members of the Sajjad-ur-Rahman Lab, Institute of Microbiology, University of Agriculture, Faisalabad.

Conflict of interest

The authors do not report any financial or personal connections with other persons or organizations, which might negatively affect the contents of this publication and/or claim authorship rights to this publication.

Literature

Ali A, An SJ, Cui C, Haque A, Carbis R. Synthesis and immunogenicity evaluation of *Salmonella enterica* serovar Paratyphi A O-specific polysaccharide conjugated to diphtheria toxoid. Hum Vaccin Immunother. 2014 Jun 04;10(6):1494–1498. doi:10.4161/hv.28130 Medline

Andrews WH, Wang H, Jacobson A, Hammack T. Chapter 5. *Salmonella*. In: Bacteriological Analytical Manual (BAM) 8th ed. Silver Spring (USA): U.S. Food and Drug Administration. 1998.

Barsoum IS, Awad AY. Microtiter plate agglutination test for *Salmonella* antibodies. Appl Microbiol. 1972 Feb;23(2):425–426 Medline

Behnsen J, Perez-Lopez A, Nuccio SP, Raffatellu M. Exploiting host immunity: the *Salmonella* paradigm. Trends Immunol. 2015 Feb;36(2):112–120. doi:10.1016/j.it.2014.12.003 Medline

Bhan MK, Bahl R, Bhatnagar S. Typhoid and paratyphoid fever. Lancet. 2005 Aug;366(9487):749–762. doi:10.1016/S0140-6736(05)67181-4 Medline

Brenner FW, Villar RG, Angulo FJ, Tauxe R, Swaminathan B. *Salmonella* nomenclature. J Clin Microbiol. 2000 Jul;38(7):2465–2467 Medline

Brooks WA, Hossain A, Goswami D, Sharmeen AT, Nahar K, Alam K, Ahmed N, Naheed A, Nair GB, Luby S, et al. Bacteremic typhoid fever in children in an urban slum, Bangladesh. Emerg Infect Dis. 2005 Feb;11(2):326–329. doi:10.3201/eid1102.040422 Medline

Burton NA, Schürmann N, Casse O, Steeb AK, Claudi B, Zankl J, Schmidt A, Bumann D. Disparate impact of oxidative host defenses determines the fate of *Salmonella* during systemic infection in mice. Cell Host Microbe. 2014 Jan;15(1):72–83. doi:10.1016/j.chom.2013.12.006 Medline

Chacana PA, Terzolo HR. Protection conferred by a live *Salmonella* Enteritidis vaccine against fowl typhoid in laying hens. Avian Dis. 2006 Jun;50(2):280–283. doi:10.1637/7463-102705R.1 Medline

Chedid L, Parant M, Parant F, Boyer F. A proposed mechanism for natural immunity to enterobacterial pathogens. J Immunol. 1968 Feb;100(2):292–306. Medline

Chiu CH, Wu TL, Su LH, Chu C, Chia JH, Kuo AJ, Chien MS, Lin TY. The emergence in Taiwan of fluoroquinolone resistance in *Salmonella enterica* serotype choleraesuis. N Engl J Med. 2002 Feb 07;346(6):413–419. doi:10.1056/NEJMoa012261 Medline

Coburn B, Grassl GA, Finlay BB. *Salmonella*, the host and disease: a brief review. Immunol Cell Biol. 2007 Feb;85(2):112–118. doi:10.1038/sj.icb.7100007 Medline

Crump JA, Luby SP, Mintz ED. The global burden of typhoid fever. Bull World Health Organ. 2004 May;82(5):346–353. Medline

Crump JA. Building the case for wider use of typhoid vaccines. Vaccine. 2015 Jun;33 Suppl 3:C1–C2. doi:10.1016/j.vaccine.2015.04.033 Medline

Curtiss R 3rd, Kelly SM, Olu Hassan J. Live oral avirulent *Salmonella* vaccines. Vet Microbiol. 1993 Nov;37(3-4):397–405. doi:10.1016/0378-1135(93)90038-9 Medline

Desin TS, Köster W, Potter AA. *Salmonella* vaccines in poultry: past, present and future. Expert Rev Vaccines. 2013 Jan;12(1):87–96. doi:10.1586/erv.12.138 Medline

Feasey NA, Dougan G, Kingsley RA, Heyderman RS, Gordon MA. Invasive non-typhoidal salmonella disease: an emerging and neglected tropical disease in Africa. Lancet. 2012 Jun;379(9835):2489–2499. doi:10.1016/S0140-6736(11)61752-2 Medline

Fedson DS. Preparing for pandemic vaccination: an international policy agenda for vaccine development. J Public Health Policy. 2005 Apr;26(1):4–29. doi:10.1057/palgrave.jphp.3200008 Medline

Foley SL, Lynne AM. Food animal-associated Salmonella challenges: pathogenicity and antimicrobial resistance1. J Anim Sci. 2008 Apr 01;86(14) suppl_14:E173–E187. doi:10.2527/jas.2007-0447 Medline

Fraser A, Paul M, Goldberg E, Acosta CJ, Leibovici L. Typhoid fever vaccines: systematic review and meta-analysis of randomised controlled trials. Vaccine. 2007 Nov;25(45):7848–7857. doi:10.1016/j.vaccine.2007.08.027 Medline

Gayet R, Bioley G, Rochereau N, Paul S, Corthésy B. Vaccination against *Salmonella* Infection: the Mucosal Way. Microbiol Mol Biol Rev. 2017 Sep;81(3):e00007-17. doi:10.1128/MMBR.00007-17 Medline

Gonzalez-Escobedo G, Marshall JM, Gunn JS. Chronic and acute infection of the gall bladder by Salmonella Typhi: understanding the carrier state. Nat Rev Microbiol. 2011 Jan;9(1):9–14. doi:10.1038/nrmicro2490 Medline

Hauser E, Tietze E, Helmuth R, Junker E, Blank K, Prager R, Rabsch W, Appel B, Fruth A, Malorny B. Pork contaminated with *Salmonella enterica* serovar 4,[5],12:i:-, an emerging health risk for humans. Appl Environ Microbiol. 2010 Jul 15;76(14):4601–4610. doi:10.1128/AEM.02991-09 Medline

Janda JM, Abbott SL. 16S rRNA gene sequencing for bacterial identification in the diagnostic laboratory: pluses, perils, and pitfalls. J Clin Microbiol. 2007 Sep 01;45(9):2761–2764. doi:10.1128/JCM.01228-07 Medline

Kariuki S, Gordon MA, Feasey N, Parry CM. Antimicrobial resistance and management of invasive *Salmonella* disease. Vaccine. 2015 Jun;33 Suppl 3:C21–C29. doi:10.1016/j.vaccine.2015.03.102 Medline

Karkey A, Thwaites GE, Baker S. The evolution of antimicrobial resistance in *Salmonella* Typhi. Curr Opin Gastroenterol. 2018 Jan;34(1):25–30. doi:10.1097/MOG.0000000000000406 Medline

Karon AE, Archer JR, Sotir MJ, Monson TA, Kazmierczak JJ. Human multidrug-resistant *Salmonella* Newport infections, Wisconsin, 2003–2005. Emerg Infect Dis. 2007 Nov;13(11):1777–1780. doi:10.3201/eid1311.061138 Medline

Kidgell C, Reichard U, Wain J, Linz B, Torpdahl M, Dougan G, Achtman M. *Salmonella* typhi, the causative agent of typhoid fever, is approximately 50,000 years old. Infect Genet Evol. 2002 Oct;2(1):39–45. doi:10.1016/S1567-1348(02)00089-8 Medline

Kumar S, Stecher G, Li M, Knyaz C, Tamura K. MEGA X: Molecular Evolutionary Genetics Analysis across Computing Platforms. Mol Biol Evol. 2018 Jun 01;35(6):1547–1549. doi:10.1093/molbev/msy096 Medline

Majowicz SE, Musto J, Scallan E, Angulo FJ, Kirk M, O'Brien SJ, Jones TF, Fazil A, Hoekstra RM. International Collaboration on Enteric Disease 'Burden of Illness' Studies. The global burden of nontyphoidal *Salmonella* gastroenteritis. Clin Infect Dis. 2010 Mar 15;50(6):882–889. doi:10.1086/650733 Medline

Matulova M, Havlickova H, Sisak F, Babak V, Rychlik I. SPI1 defective mutants of *Salmonella enterica* induce cross-protective immunity in chickens against challenge with serovars Typhimurium and Enteritidis. Vaccine. 2013 Jun;31(31):3156–3162. doi:10.1016/j.vaccine.2013.05.002 Medline

McClelland M, Sanderson KE, Spieth J, Clifton SW, Latreille P, Courtney L, Porwollik S, Ali J, Dante M, Du F, et al. Complete genome sequence of *Salmonella enterica* serovar Typhimurium LT2. Nature. 2001 Oct;413(6858):852–856. doi:10.1038/35101614 Medline

Medalla F, Gu W, Mahon BE, Judd M, Folster J, Griffin PM, Hoekstra RM. Estimated incidence of antimicrobial drug-resistant nontyphoidal *Salmonella* infections, United States, 2004–2012. Emerg Infect Dis. 2016 Jan;23(1):29–37. doi:10.3201/eid2301.160771 Medline

Mian MF, Pek EA, Chenoweth MJ, Coombes BK, Ashkar AA. Humanized mice for *Salmonella typhi* infection: new tools for an old problem. Virulence. 2011 May;2(3):248–252. doi:10.4161/viru.2.3.16133 Medline

Monack DM, Mueller A, Falkow S. Persistent bacterial infections: the interface of the pathogen and the host immune system. Nat Rev Microbiol. 2004 Sep;2(9):747–765. doi:10.1038/nrmicro955 Medline

Nair A, Balasaravanan T, Malik SVS, Mohan V, Kumar M, Vergis J, Rawool DB. Isolation and identification of *Salmonella* from diarrheagenic infants and young animals, sewage waste and fresh vegetables. Vet World. 2015 May;8(5):669–673. doi:10.14202/vetworld.2015.669-673 Medline

Nandre RM, Lee D, Lee JH. Cross-protection against *Salmonella* Typhimurium infection conferred by a live attenuated *Salmonella* Enteritidis vaccine. Can J Vet Res. 2015 Jan;79(1):16–21. Medline

Nnalue NA. All accessible epitopes in the *Salmonella* lipopolysaccharide core are associated with branch residues. Infect Immun. 1999 Feb;67(2):998–1003. Medline

Ochiai RL, Acosta CJ, Danovaro-Holliday MC, Baiqing D, Bhattacharya SK, Agtini MD, Bhutta ZA, Canh DG, Ali M, Shin S, et al. Domi Typhoid Study Group. a study of typhoid fever in five Asian countries: disease burden and implications for controls. Bull World Health Organ. 2008 Apr 1;86(4):260–268. doi:10.2471/BLT.06.039818 Medline

Orji MU, Onuigbo HC, Mbata TI. Isolation of *Salmonella* from poultry droppings and other environmental sources in Awka, Nigeria. Int J Infect Dis. 2005 Mar;9(2):86–89. doi:10.1016/j.ijid.2004.04.016 Medline

Ortiz D, Siegal EM, Kramer C, Khandheria BK, Brauer E. Nontyphoidal cardiac salmonellosis: two case reports and a review of the literature. Tex Heart Inst J. 2014 Aug;41(4):401–406. doi:10.14503/THIJ-13-3722 Medline

Reed LJ, Muench H. A simple method of estimating fifty percent end point. Am J Hyg. 1938;27:8739–8744.

Sanapala S, Mosca L, Wang S, Curtiss R. Comparative evaluation of Salmonella Typhimurium vaccines derived from UK-1 and 14028S: importance of inherent virulence. PLoS One. 2018 Sep 7; 13(9):e0203526. doi:10.1371/journal.pone.0203526 Medline

Siddiqui TR, Bibi S, Mustufa MA, Ayaz SM, Khan A. High prevalence of typhoidal Salmonella enterica serovars excreting food handlers in Karachi-Pakistan: a probable factor for regional typhoid endemicity. J Health Popul Nutr. 2015 Dec;33(1):27–33. doi:10.1186/s41043-015-0037-6 Medline

Smith PJ, Harvey CN, Hebert CN. Diagnosis of bovine salmonellosis II. Application of the indirect haemagglutination test to the diagnosis of *Salmonella* dublin infection. Br Vet J. 1977 Sep; 133(5):509–517. doi:10.1016/S0007-1935(17)33994-5 Medline

Tarpy DR, Mattila HR, Newton ILG. Development of the honey bee gut microbiome throughout the queen-rearing process. Appl Environ Microbiol. 2015 May 01;81(9):3182–3191. doi:10.1128/AEM.00307-15 Medline

Threlfall EJ. Antimicrobial drug resistance in *Salmonella*: problems and perspectives in food- and water-borne infections. FEMS Microbiol Rev. 2002 Jun;26(2):141–148. doi:10.1111/j.1574-6976.2002.tb00606.x Medline

Trkov M, Avgustin G. An improved 16S rRNA based PCR method for the specific detection of *Salmonella enterica.* Int J Food Microbiol. 2003 Jan 15;80(1):67–75. doi:10.1016/S0168-1605(02)00138-1 Medline

World Health Organization (WHO). Report on *Salmonella.* 2018.

Yang HH, Wu CG, Xie GZ, Gu QW, Wang BR, Wang LY, Wang HF, Ding ZS, Yang Y, Tan WS, et al. Efficacy trial of Vi polysaccharide vaccine against typhoid fever in south-western China. Bull World Health Organ. 2001;79(7):625–631. Medline

Supplementary materials are available on the journal's website.

Polish Journal of Microbiology
2019, Vol. 68, No 2, 185–191
https://doi.org/10.33073/pjm-2019-018

ORIGINAL PAPER

Evaluation of The Pathogenic Potential of Insecticidal *Serratia marcescens* Strains to Humans

EDYTA KONECKA, JOANNA MOKRACKA, SYLWIA KRZYMIŃSKA and ADAM KAZNOWSKI

Department of Microbiology, Faculty of Biology, Adam Mickiewicz University in Poznań, Poland

Submitted 27 November 2018, revised 17 January 2019, accepted 19 January 2019

Abstract

We observed the death of insect caterpillars of *Spodoptera exigua* in the laboratory culture line and identified *Serratia marcescens* as the bacterial causative agent of the insect death. We confirmed that *S. marcescens* had insecticidal activity against *S. exigua* and caused high mortality of larvae. The LC_{50} values of *S. marcescens* CFU per 1 cm^2 of insect diet surface were similar for all isolates. Our research reports novel strains with high pesticidal activity as candidates for future research on a new bioinsecticide. As bioinsecticides cannot be harmful to non-target organisms, we determined the pathogenic properties of *S. marcescens* to humans. We proved the ability of *S. marcescens* to damage mammalian epithelial cells. All strains had cytopathic effects to Vero cells with a cytotoxic index ranging from 51.2% ± 3.8% to 79.2% ± 4.1%. We found that all of the strains excreted catecholate siderophore – enterobactin. All isolates were resistant to sulfamethoxazole, tobramycin, gentamicin, cefepime, and aztreonam. We did not observe the ESBL phenotype and the integrons' integrase genes. Resistance to sulfamethoxazole was due to the presence of the *sul1* or *sul2* gene. The use of resistant *S. marcescens* strains that are pathogenic to humans in plant protection may cause infections difficult to cure and lead to the spread of resistance genes. The results of our study emphasize the necessity of determination of the safety to vertebrates of the bacteria that are proposed to serve as biocontrol agents. The novelty of our study lies in the demonstration of the indispensability of the bacteria verification towards the lack of hazardous properties to humans.

Key words: bioinsecticide, insecticidal activity, pathogenicity, pesticide safety, *Serratia marcescens*

Introduction

Due to the growing resistance of insects to synthetic pesticides, there is an urgent need for new biopreparations. *Serratia marcescens* is a species of Gram-negative rods (Hejazi and Falkiner 1997) that produces substances useful in different branches of industry and medicine (Siva et al. 2012). Some *S. marcescens* strains have been recognized as opportunistic or facultative pathogens of insects. They cause lethal septicemia after penetration into the hemocoel. The first step of pathogenesis is the colonization of epithelial cells. After adhesion to the cells, the bacteria produce potential virulence factors, including extracellular toxins which are probably the most common factors of *S. marcescens* pathogenicity (Grimont and Grimont 2006). The pathogenicity of *S. marcescens* to insects makes these bacteria an interesting tool in the search of the new biological control preparation applied in plant protection. Liquid culture of *S. marcescens* had potential use as a biocontrol factor against insect pest of Lepidoptera *Plutella xylostella* (Jeong et al. 2010), *Heliothis virescens* (Sikorowski et al. 2001) and *Helicoverpa armigera* (Mohan et al. 2011). Additionally, *S. marcescens* could reduce the development of fungus and thus inhibit the appearance of some diseases of crops. The bacteria have an antagonistic effect towards plant pathogen belonging to oomycetes – *Phytopthora parasitica* – the causative agent of a disease known as gummosis (de Queiroz and de Melo 2006). It has been demonstrated that the whole *S. marcescens* cells (Sikorowski et al. 2001; Jeong et al. 2010; Mohan et al. 2011) as well as their isolated components (Khanafari et al. 2006; Patil et al. 2011; Aggarwal et al. 2015) had putative usefulness in biocontrol on condition that they are safe for non-target organisms.

As the whole bacterial cells could have a harmful effect on vertebrates, more desirable are the components produced by bacteria. The bioactive substances that may play an important role in plant protection produced by *S. marcescens* include several virulence agents:

* Corresponding author: E. Konecka, Department of Microbiology, Faculty of Biology, Adam Mickiewicz University in Poznań, Poland; **e-mail: edkon@amu.edu.pl**

prodigiosin (Patil et al. 2011) and chitinase (Mohan et al. 2011; Aggarwal et al. 2015) among them. Prodigiosin synthesized by *S. marcescens* is active against insects of Coleoptera (Bidari et al. 2018) and Diptera. It has also medical utility due to antitumor, immunomodulating, antimycotic (Khanafari et al. 2006), and antibacterial features (Samrot et al. 2011). It induces apoptosis in some cancer cell lines, such as acute human T-cell leukemia hepatocellular cancer, breast cancer, and the TNF-stimulated cervix carcinoma (Khanafari et al. 2006). It can also be used as an inhibition agent of protozoan species (Grimont and Grimont 2006). Moreover, *S. marcescens* synthesizes substances active against *Pectobacteria* spp. that causes the soft rot disease of plant *Amorphophallus konjac* (Wu et al. 2012). None of the previous studies on the usefulness of *S. marcescens* in plant protection included the determination of pathogenic potential to humans of *S. marcescens* strains and evaluation of their safety to vertebrates.

The same factors which make *S. marcescens* the putative biological control organisms are these that in humans could facilitate bacterial cells adhesion, protect from host's immune system and allow for tissue penetration. The pathogenicity factors include the fimbriae, the production of siderophores, the presence of cell wall antigens, the ability to resist to the bactericidal action of serum, the production of proteases and the cell-contact toxins that facilitate bacterial invasion, induce cytotoxicity and apoptosis of host cells (Franczek et al. 1986; Krzymińska et al. 2012).

Additionally, the antibiotic resistance of the strains should be considered due to the possibility of the spread of the genes conferring drug resistance. Antibiotic resistance genes are often incorporated into mobile structures such as plasmids, transposons, and integrons. The latter are genetic structures that capture and incorporate resistance gene cassettes and transform them into the functional genes (Cambray et al. 2010).

We have observed the death of beet armyworm *Spodoptera exigua* Hübner (Lepidoptera: Noctuidae) larvae in the laboratory culture line of this insect pest. This encouraged us to isolate and identify the bacterial causative agent of the insects' death and evaluate its utility in plant protection against pests. We estimated the 50% lethal concentration (LC_{50}) of the microorganisms for *S. exigua* larvae to confirm the pathogenicity of the bacterial strains for insects. According to the Integrated Pest Management program (Directive 2009/128/WE of the European Parliament and the Council of the European Union), application of insecticidal biopreparations should come with the lowest risk to human health (Matyjaszczyk 2018). Biological pest management can be aiming to maintain food and human safety (Mosa et al. 2016). Therefore, we decided to evaluate if the bacteria that caused the insect death are safe for humans. We examined the cytotoxic activity of the isolates to mammalian epithelial cells and the ability to produce siderophores. Moreover, the strains were verified for antimicrobial susceptibility and the presence of integrons.

Experimental

Materials and Methods

Bacterial strains. Eight *S. marcescens* isolates (MPU Si1 – MPU Si8) were used in this study. They were isolated from dead caterpillars of *Spodoptera exigua* cultured in the laboratory culture line in September 2009. In order to determine the clonal relationship of isolates, thirteen additional strains were included in the study as a comparative samples: *S. marcescens* strain MPU Si9 obtained from a dead larva of *Agrotis segetum* reared in the same laboratory three months earlier, eight *S. marcescens* strains (MPU S11, MPU S14, MPU S15, MPU S26, MPU S32, MPU S40, MPU S41, MPU S47) isolated from clinical specimens, one *S. odorifera* (MPU Se128/7) cultured from sewage, one *S. ficaria* (MPU S49), one strain of *Enterobacter cloacae* (MPU E39a) from clinical specimens, and *Pseudomonas aeruginosa* (MPU Pb5/4) from the intestinal tract of a wild boar.

Bacteria isolation and identification. Dead caterpillars were swabbed with 90% ethanol, homogenized in BHI medium (Difco) and incubated at 30°C for 24h. Then, the bacterial suspension was spread on BHI agar medium and after 24-hour incubation, the bacteria were characterized based on the morphology of colonies. Identification of bacteria was performed by API 20E tests according to the manufacturer's instruction (bioMérieux, France).

Clonal relationship. Bacterial typing was conducted by REP-PCR with primers REP1I and REP2I for repetitive extragenic palindromic sequences (Moura et al. 2007). One bacterial colony was suspended in 25 µl of sterile distilled water and heated at 98°C for 5 min. Two microliters of DNA were added to PCR mixture containing PCR buffer with $NH_4(SO_4)_2$, 0.5 µM of each primer (Oligo.pl, Poland), 200 µM of dNTP mix, 2.5 mM of $MgCl_2$, and 0.5 U of Allegro DNA polymerase (Novazym, Poland). PCR amplification involved an initial denaturation at 94°C for 3 min followed by 35 cycles at 94°C for 1 min, 40°C for 1 min, 72°C for 90, and a final extension at 72°C for 8 min.

Amplification products were electrophoresed in 1.5% NOVA Mini agarose gel (Novazym, Poland). The similarity of bacteria DNA profiles was estimated with Dice coefficient and a dendrogram was created by the unweighted pair group method with average linkages (UPGMA).

Pathogenicity of *S. marcescens* strains for insects. The pathogenicity of *S. marcescens* strains against *S. exigua* caterpillars was determined. Insects originated from laboratory culture line reared at 26°C, 40–60% relative humidity, and a 16:8 (light: dark) period in the Department of Microbiology, Adam Mickiewicz University, Poznań.

The bioassay on insects was conducted according to Jeong et al. (2010), Mohan et al. (2011), and Sikorowski et al. (2001). *S. marcescens* isolates were grown in nutrient agar (Biocorp, Poland) at 30°C for 24 h. One bacterial colony was suspended in 1 ml of 0.85% NaCl. Five different volumes: 2.5 µl, 5 µl, 10 µl, 20 µl, 40 µl of the suspension were spread on pieces (5 mm diameter, 3 mm hight) of semisynthetic diet for *S. exigua* rearing as described by McGuire et al. (1997). The pieces of diet were placed separately in transparent polystyrene multi-well plates. Caterpillars in L1 instar were placed onto the diet – one larva per one well with one diet piece. Each *S. marcescens* CFU number was tested against 30 larvae (three replications with 10 insects each). Simultaneously, the number of CFU per milliliter was determined by the spread plate method. The volume of 100 µl of a bacterial colony suspension in 1 ml of 0.85% NaCl, and additionally the volume of 100 µl of five dilutions of the suspension (10^{-1}, 10^{-2}, 10^{-3}, 10^{-4}, and 10^{-5}) were spread on BHI agar (each dilution on two plates with medium). After the overnight incubation at 37°C, the colonies were counted and the number of CFU per milliliter was calculated. As we mentioned above different volumes of the suspension were spread on pieces (5 mm diameter, 3 mm height) of semisynthetic diet for insect rearing. The pieces had a shape of a cylinder and the formula for the surface area is πr^2. Knowing the value of the surface area in cm^2, the volume of bacterial suspension spread on the medium, and the number of CFU per milliliter, we calculated CFU/cm^2.

As a positive control, a strain of *Bacillus thuringiensis* subsp. *kurstaki* HD1 from biopesticide Foray was used. Foray contains bacterial endospores (spores) and protein crystals and is dedicated for plant protection against lepidopteran pests. The *B. thuringiensis* was cultured in medium developed for bacteria sporulation by Lecadet and Dedonder (1971). Spores and crystals were applied to insects in the same way as *S. marcescens*. As a negative control, 0.85% NaCl was used.

Infected insects were reared at 26°C, 40–60% relative humidity, and a 16:8 (light: dark) period. The number of dead insects was estimated after 7 days. The LC_{50} [*S. marcescens* CFU per 1 cm^2 of insect diet surface] against insects was calculated by a probit analysis according to Finney, based on the mortality (%) in the control sample, by using BioStat ver. 5.8.4.3 software (AnalystSoft Inc.).

Cytotoxic activity to epithelial cells by MTT assay. African monkey kidney (Vero) cells were cultured in Eagle Minimum Essential Medium (EMEM, Sigma) with 5% fetal calf serum (FCS, Sigma) containing 2 mM glutamine, 50 IU of penicillin per milliliter, streptomycin (100 µg/ml) and nystatin (1 mg/ml). The cells were seeded (1×10^4 per well) and incubated at 37°C in an atmosphere with 5% CO_2.

The strains were cultured in Luria-Bertani medium (LB, Difco) at 37°C for 24 h with shaking at 300 rpm. The supernatants were centrifuged at $3000 \times g$ for 30 min and sterilized through 0.22 µm-pore size membrane filters Millex-GV (Millipore) (Krzymińska et al. 2010).

The epithelial cell monolayer was incubated with bacterial culture filtrates for 24 h at 37°C. As a negative control, the cells were infected with a nonpathogenic *E. coli* K-12C600 supernatant. The cytotoxicity was assessed quantitatively by monitoring the mitochondrial reduction of 3-(4,5-dimethylthiazol-2-yl)-2,5-diphenyltetrazolium bromide (MTT, Sigma) (Krzymińska et al. 2009). The data were presented as means ± standard deviation (SD) from two independent experiments performed in duplicate.

Siderophore production. *Serratia* sp. strains were verified for the production of siderophores by chrome azurol S (CAS) assay (Schwyn and Neilands 1987). The type of the siderophore excreted was identified in cross-feeding assays with the following indicators: enterobactin indicator – *Salmonella typhimurium* TA 2700, aerobactin and rhodotorulic acid indicator – *Escherichia coli* LG 1522, rhizoferrin and α-keto acids indicator – *Morganella morganii* SBK 3 (Reissbrodt and Rabsch 1988), and yersiniabactin indicator – *Yersinia enterocolitica* 5030 (Haag et al. 1993). Additionally, the presence of siderophore receptors for yersiniabactin, aerobactin and glycosylated enterobactin – salmochelin, encoded respectively by the *fyuA*, *iutA* and *iroN* genes, was assessed by PCR. All PCR reagents were purchased from Novazym (Poland). PCR amplification conditions and sequences of primers have been previously published (Karch et al. 1999; Johnson et al. 2000; Johnson and Stell 2000). The PCR products were separated in 1.5% agarose gel. All experiments were performed in triplicate.

Antimicrobial susceptibility. The susceptibility of the isolates to 20 antibiotics representing nine classes was determined according to the standard disk diffusion method recommended by The European Committee on Antimicrobial Susceptibility Testing (EUCAST 2014). The antimicrobials comprised: amikacin (30 µg), tobramycin (10 µg), netilmicin (10 µg), gentamicin (10 µg), ticarcillin (75 µg), ciprofloxacin (5 µg), norfloxacin (10 µg), cefotaxime (5 µg), ceftaroline (5 µg), ceftazidime (10 µg), cefoperazone (10 µg), cefepime (30 µg), co-trimoxazole (25 µg), trimethoprim (5 µg), sulfamethoxazole (200 µg), piperacillin (30 µg), piperacillin/

tazobactam (30–60 µg), aztreonam (30 µg), imipenem (10 µg), and meropenem (10 µg). The production of extended spectrum β-lactamases (ESBL) was determined in the double-disc synergy test. All antibiotic discs were provided by Oxoid. Amplifications of three genes conferring resistance to sulfonamides (*sul1*, *sul2*, *sul3*), were conducted in a 25-µl volume with PCR buffer with $NH_4(SO_4)_2$, 0.5 µM of each primer (Oligo. pl), 200 µM of dNTP mix, 2.5 mM of $MgCl_2$, 0.5 U of DreamTaq polymerase (Thermo Scientific), and 200 ng of genomic DNA. The PCR conditions consisted of initial denaturation at 94°C, 3 min, followed by 35 cycles at 94°C for 45 s, annealing (varied; 46–60°C) for 45 s, 72°C for 90 s, with a final extension at 72°C for 7 min (Pei et al. 2006).

Presence of integrons. The integron integrase genes were detected by multiplex PCR with primers targeting three classes of the integrase genes *intI1*, *intI2* and *intI3* (Dillon et al. 2005). PCR amplifications were performed in a 25-µl volume with 2.5 µl of 10 × PCR buffer with $NH_4(SO_4)_2$, 0.25 µM of each primer, 100 µM of dNTP mix, 2.5 mM of $MgCl_2$, 1 U of DreamTaq polymerase (Thermo Scientific), and 200 ng of genomic DNA. Amplification involved an initial denaturation (94°C, 5 min) followed by 30 cycles of denaturation (94°C, 1 min), annealing (59°C, 1 min) and extension (72°C, 1 min), with a final extension step (72°C, 8 min).

Results

Bacteria identification. The strains isolated from insects were Gram-negative rods identified as *Serratia marcescens* with API 20E system. On the agar medium, the bacteria formed circular, raised, shiny, and smooth colonies. All isolates produced the pigment that made the colonies red.

Clonal relationship. Molecular typing revealed three groups of bacteria with 100% similarity of DNA patterns (Supplementary Fig. S1). Cluster 1 consisted of three isolates: MPU Si4, MPU Si5, and MPU Si7. Three strains MPU Si1, MPU Si2, and MPU Si3 formed cluster 2. Isolates MPU Si6 and MPU Si8 were gathered in cluster 3. These groups comprised *S. marcescens* isolates cultured from dead *S. exigua* insects. The similarity between cluster 1 and 2 was equal to 92%. Group 3 was similar to 1 and 2 in 85%. *S. marcescens* MPU Si9 isolated from the intestinal tract of *A. segetum* cultured in the same laboratory as *S. exigua* but in different time showed 66% similarity with *S. marcescens* isolates originated from *S. exigua*. DNA pattern of *S. marcescens* isolated from *A. segetum* was similar in 70% to the strain cultured from a clinical specimen.

Pathogenicity of *S. marcescens* strains for insects. *S. marcescens* isolates revealed insecticidal activity against *S. exigua* caterpillars and caused high mortality of larvae. The LC_{50} values of *S. marcescens* were similar and ranged from 7.6×10^5 to 5.6×10^6 CFU per 1 cm^2 of the insect diet surface. The toxicities of *S. marcescens* strains were higher than the activity of spore-crystal preparation of *B. thuringiensis* from Foray bioinsecticide (Table I).

Table I
Pathogenicity of *S. marcescens* and *B. thuringiensis* to *S. exigua*.

Strain	LC_{50} (CFU/cm^2)	95% Fiducial limits
MPU Si1	4×10^6	$2 \times 10^6 - 4.3 \times 10^7$
MPU Si2	4.2×10^6	$2 \times 10^6 - 1.1 \times 10^8$
MPU Si3	5×10^6	$2.1 \times 10^6 - 3.8 \times 10^8$
MPU Si4	2×10^6	$5.6 \times 10^5 - 7.6 \times 10^6$
MPU Si5	4.5×10^6	$9.2 \times 10^5 - 2.3 \times 10^7$
MPU Si6	5.6×10^6	$9.2 \times 10^5 - 3.3 \times 10^7$
MPU Si7	7.6×10^5	$2 \times 10^5 - 2.8 \times 10^6$
MPU Si8	2.5×10^6	$1.3 \times 10^6 - 2.4 \times 10^7$
B. thuringiensis	1.7×10^7	$3.6 \times 10^6 - 3 \times 10^7$

Cytotoxicity of *S. marcescens* strains. After 24 h of incubation with the strain culture supernatants, we observed cytopathic effects such as rounding and shrinking of the Vero cells. These changes were followed by the gradual destruction of the monolayer. All strains were cytotoxic to Vero cells (Table II). The highest cytotoxicity in a range from 76.6 to 79.2% was observed for five strains. Three isolates revealed cytotoxic activity, causing death from 54.9 to 59.7% of Vero cells. The supernatant of non-pathogenic control, *E. coli* K-12C600 did not cause the cytopathic effect.

Siderophore production. In the standard method of Schwyn and Neilands (1987), all *S. marcescens* strains demonstrated the production of iron chelators. Biological assays with indicator strains deficient in siderophore synthesis but capable of acquiring exogenous iron chelators indicated that all of the strains excreted catecholate siderophore – enterobactin. The PCR results showed that the strains did not have the receptor genes for yersiniabacin, aerobactin or salmochelin.

Table II
Cytotoxic activity of *S. marcescens* strains isolated from insects.

Strain	Cytotoxic index (%)
MPU Si1	79.2 ± 4.1*
MPU Si2	77.6 ± 2.8
MPU Si3	77.5 ± 3.1
MPU Si4	58.5 ± 2.5
MPU Si5	76.6 ± 1.9
MPU Si6	78.3 ± 3.7
MPU Si7	59.7 ± 2.1
MPU Si8	54.9 ± 3.8

* Mean percentage of cytotoxicity ± SD, measured by MTT assay

Table III
Antibiotic resistance of *S. marcescens* strains isolated from insects.

Isolate	Antimicrobial resistance profile
MPU Si1	SUL*
MPU Si2	SUL
MPU Si3	SUL
MPU Si4	SUL
MPU Si5	TOB, FEP, SUL
MPU Si6	SUL
MPU Si7	GEN, TOB, SUL
MPU Si8	SUL

*ATM – aztreonam, GEN – gentamicin, SUL – sulfamethoxazole, TOB – tobramycin

Antimicrobial susceptibility and presence of integrons. The strains were resistant toward one to three antimicrobials (Table III). All isolates were resistant to sulfamethoxazole. Moreover, they were resistant to antibiotics belonging to aminoglycosides: tobramycin (22.2%) and gentamicin (11.1%), cephalosporins: cefepime (11.1%) and monobactams: aztreonam (11.1%). We did not observe an ESBL phenotype and the integron integrases genes. Resistance to sulfamethoxazole of all strains was due to the presence of the *sul1* or *sul2* gene.

Discussion

In recent years some microbial insect pathogens have become useful in protecting crops against pests. Application of natural enemies of insects could be the long-term and suitable strategy. There is still a need to search for an effective and safe biopreparation against harmful crop pests, and entomopathogens of hazardous insects could be employed in the development of the biopreparations (Bahar and Demirbağ 2007; Nuñez-Valdez et al. 2008). *S. marcescens* strains are proposed to be used as biocontrol agents because of their insecticidal activity against lepidopteran larvae (Sikorowski et al. 2001; Jeong et al. 2010; Mohan et al. 2011) of all developmental stages (Aggarwal et al. 2015). However, the proposal mentioned above ignored the issue of bacterial safety for humans and other non-target vertebrates. We observed the death of insect caterpillars of *S. exigua* and *A. segetum* in the laboratory culture lines. We isolated and identified the bacterial causative agent of dead insect and determined the pathogenic properties of insecticidal *S. marcescens* strains to humans.

For determining the possible clonality of strains, we applied the REP-PCR typing method to determine the genetic similarity of Gram-negative rods (Rasschaert et al. 2005; Henriques et al. 2006; Moura et al. 2007; Czajkowski et al. 2010; Mokracka et al. 2011). The analysis revealed a high similarity of all *S. marcescens* isolates cultured from *S. exigua* intestinal track. DNA profiles of strains that caused infections of *S. exigua* varied significantly from that of the strain infecting *A. segetum*. The strains made three clusters, yet we did not treat them as clones as they differed in resistance profiles and cytotoxic activity.

We confirmed entomopathogenicity of *S. marcescens* isolates. The insecticidal activity of strains indicates the usefulness of the bacteria in plant protection. The low values of LC_{50} of *S. marcescens* against caterpillars in comparison with LC_{50} of spore-crystal preparation of *B. thuringiensis* from Foray suggested the possibility to create a novel biopesticide based on *S. marcescens* with high activity against lepidopteran pests. However, the preparation could not have harmful effect for non-target organisms, so we examined the cytotoxic activity of the isolates to mammalian epithelial cells, determined the siderophore production, antimicrobial susceptibility, and the presence of integrons in *S. marcescens* genomes.

We observed that culture filtrates of *S. marcescens* strains isolated from insects were capable of damaging mammalian epithelial cell line. Escobar et al. (2001) have reported that supernatants of *S. marcescens* isolates from plants and insects were cytotoxic to epithelial cell lines. Strains originated from the stomach of *Rhodnius prolixus* larvae revealed hemolytic activity (Azambuja et al. 2004). Toxin production by entomopathogenic strains is still not clearly defined. Hertle (2005) has suggested that hemolysin produced by *S. marcescens* strains (ShlA) is the major cytolysin in the pathogenesis of the bacteria. The toxin induces the formation of pores in erythrocytes and eukaryotic nucleated cells, which results in osmotic lysis. Moreover, the bacteria produce extracellular lecithinase, proteinase, and chitinase that play a role in their virulence for insects (Grimont and Grimont 2006). Similar cytotoxic destruction of epithelial cells has been observed for strains isolated from human specimens (Krzymińska et al. 2010). The results presented in this study suggested that extracellular factors produced by the isolates could be responsible for the destruction of the epithelial barrier, which could pose a potential risk to human health.

Iron sequestration involving siderophores is a recognized factor essential for bacterial pathogenicity. Deletion of siderophore biosynthetic genes leads to loss of pathogenicity in a mouse infection model, and also affects maturation of biofilms, surface motility, activation of exotoxins and synthesis of other virulence factors (Vokes et al. 1999; Visca et al. 2007; Mossialos and Amoutzias 2009). Enterobactin, which is a prototypical catecholate siderophore with the highest known affinity for iron, was excreted by all *S. marcescens* strains (Supplementary Table SI). Its role in pathogenesis is limited, as in host it is bound by siderocalin (lipocalin 2, Lcn2)

that inhibits bacterial iron acquisition (Flo et al. 2004). Other siderophores like structurally distinct yersiniabactin or salmochelin, which is glycosylated enterobactin, deliver iron to bacteria despite the presence of Lcn2, yet we did not find receptors for these chelators.

We did not find integrons in the genomes in *S. marcescens* strains although all of them were resistant to sulfamethoxazole, suggesting the presence of class 1 integrons, which have the *sul*1 gene at the 3' integron end. The resistance to sulfamethoxazole was determined by the *sul1* or *sul2* genes that code for dihydropteroate synthases, which are not inhibited by sulfonamides (Pei et al. 2006). The resistance of single strains to aztreonam and cefepime may be the result of overproduction of β-lactamase and resistance to aminoglycosides, which is often noted in clinical strains of *S. marcescens*. It is most frequently determined by the presence of the plasmid-mediated aminoglycoside-modifying enzymes. Both the *sul* genes and those conferring resistance to β-lactams and aminoglycosides may reside on mobile genomic elements and be spread *via* horizontal gene transfer (Stokes and Gillings 2011).

Our research confirmed the potential pathogenicity to humans of *S. marcescens* strains lethal for insect pests. We decided to undertake this issue because *S. marcescens* is proposed to be a useful bioinsecticide (Sikorowski et al. 2001; Jeong et al. 2010; Mohan et al. 2011; Aggarwal et al. 2015); however, the pesticidal biopreparations cannot be harmful to non-target organisms. The ability of *S. marcescens* to damage mammalian epithelial cell line and to employ siderophore-mediated strategies of iron acquisition eliminates the bacterial cells to be used as a bioinsecticide. Using the antimicrobial resistant, potentially pathogenic to humans *S. marcescens* strains in plant protection may cause human infections difficult to cure and lead to the spread of resistance genes. We emphasize the necessity of determining the safety to vertebrates of the bacteria that are proposed to be used as a biocontrol preparation for reducing the number of insects. Yet, it is worth mentioning that bacterial strains harmful for pests could be a source of novel genes or factors useful in controlling insect pests. In our further studies, the insecticidal factors-coding genes in *S. marcescens* strains will be identified, cloned and expressed in *E. coli* cells (Baranek et al. 2015). After isolation and purification of the genes' products, their insecticidal activity against lepidopteran pests will be determined.

ORCID
Edyta Konecka 0000-0002-2334-8857

Conflict of interest

The authors do not report any financial or personal connections with other persons or organizations, which might negatively affect the contents of this publication and/or claim authorship rights to this publication.

Literature

Aggarwal C, Paul S, Tripathi V, Paul B, Khan MA. Chitinolytic activity in *Serratia marcescens* (strain SEN) and potency against different larval instars of *Spodoptera litura* with effect of sublethal doses on insect development. BioControl. 2015 Oct;60(5):631–640. doi:10.1007/s10526-015-9674-3

Azambuja P, Feder D, Garcia ES. Isolation of *Serratia marcescens* in the midgut of *Rhodnius prolixus*: impact on the establishment of the parasite *Trypanosoma cruzi* in the vector. Exp Parasitol. 2004 May;107(1-2):89–96. doi:10.1016/j.exppara.2004.04.007 Medline

Bahar A, Demirbağ Z. Isolation of pathogenic bacteria from *Oberea linearis* (Coleptera: Cerambycidae). Biologia. 2007 Jan 1;62(1): 13–18. doi:10.2478/s11756-007-0009-4

Baranek J, Kaznowski A, Konecka E, Naimov S. Activity of vegetative insecticidal proteins Vip3Aa58 and Vip3Aa59 of *Bacillus thuringiensis* against lepidopteran pests. J Invertebr Pathol. 2015 Sep;130:72–81. doi:10.1016/j.jip.2015.06.006 Medline

Bidari F, Shams-Bakhsh M, Mehrabadi M. Isolation and characterization of a *Serratia marcescens* with insecticidal activity from *Polyphylla olivieri* (Col.: Scarabaeidae). J Appl Entomol. 2018 Feb; 142(1-2):162–172. doi:10.1111/jen.12421

Cambray G, Guerout AM, Mazel D. Integrons. Annu Rev Genet. 2010 Dec;44(1):141–166. doi:10.1146/annurev-genet-102209-163504 Medline

Patil CD, Patil SV, Salunke BK, Salunkhe RB. Prodigiosin produced by *Serratia marcescens* NMCC46 as a mosquito larvicidal agent against *Aedes aegypti* and *Anopheles stephensi.* Parasitol Res. 2011 Oct;109(4):1179–1187. doi:10.1007/s00436-011-2365-9 Medline

Czajkowski R, de Boer WJ, Velvis H, van der Wolf JM. Systemic colonization of potato plants by a soilborne, green fluorescent protein-tagged strain of *Dickeya* sp. biovar 3. Phytopathology. 2010 Feb;100(2):134–142. doi:10.1094/PHYTO-100-2-0134 Medline

Dillon B, Thomas L, Mohmand G, Zelynski A, Iredell J. Multiplex PCR for screening of integrons in bacterial lysates. J Microbiol Methods. 2005 Aug;62(2):221–232. doi:10.1016/j.mimet.2005.02.007 Medline

Escobar MM, Carbonell GV, Beriam LOS, Siqueira WJ, Yano T. Cytotoxin production in phytopathogenic and entomopathogenic *Serratia marcescens*. Rev Latinoam Microbiol. 2001 Oct-Dec;43(4): 165–170 Medline.

EUCAST. Breakpoint tables for interpretation of MICs and zone diameters, version 4.0. The European Committee on Antimicrobial Susceptibility Testing. 2014.

Flo TH, Smith KD, Sato S, Rodriguez DJ, Holmes MA, Strong RK, Akira S, Aderem A. Lipocalin 2 mediates an innate immune response to bacterial infection by sequestrating iron. Nature. 2004 Dec 16;432(7019):917–921. doi:10.1038/nature03104 Medline

Franczek SP, Williams RP, Hull SI. A survey of potential virulence factors in clinical and environmental isolates of *Serratia marcescens.* J Med Microbiol. 1986 Sep 01;22(2):151–156. doi:10.1099/00222615-22-2-151 Medline

Grimont F, Grimont PAD. The genus *Serratia*. In: Dworkin M, Falkow S, Rosenberg E, Schleifer KH, Stackebrandt E, editors. The Proaryotes, 3rd ed. Berlin (Germany): Springer Verlag; 2006. p. 219–244.

Haag H, Hantke K, Drechsel H, Stojiljkovic I, Jung G, Zähner H. Purification of yersiniabactin: a siderophore and possible virulence factor of *Yersinia enterocolitica*. J Gen Microbiol. 1993 Sep 01; 139(9):2159–2165. doi:10.1099/00221287-139-9-2159 Medline

Henriques IS, Fonseca F, Alves A, Saavedra MJ, Correia A. Occurrence and diversity of integrons and β-lactamase genes among ampicillin-resistant isolates from estuarine waters. Res Microbiol. 2006 Dec;157(10):938–947. doi:10.1016/j.resmic.2006.09.003 Medline

Hertle R. The family of *Serratia* type pore forming toxins. Curr Protein Pept Sci. 2005 Aug 01;6(4):313–325. doi:10.2174/1389203054546370 Medline

Hejazi A, Falkiner FR. *Serratia marcescens*. J Med Microbiol. 1997 Nov 01;46(11):903–912. doi:10.1099/00222615-46-11-903 Medline

Jeong HU, Mun HY, Oh HK, Kim SB, Yang KY, Kim I, Lee HB. Evaluation of insecticidal activity of a bacterial strain, *Serratia* sp. EML-SE1 against diamondback moth. J Microbiol. 2010 Aug; 48(4):541–545. doi:10.1007/s12275-010-0221-9 Medline

Johnson JR, Russo TA, Tarr PI, Carlino U, Bilge SS, Vary JC Jr, Stell AL. Molecular epidemiological and phylogenetic associations of two novel putative virulence genes, *iha* and $iroN_{E.\ coli}$, among *Escherichia coli* isolates from patients with urosepsis. Infect Immun. 2000 May 01;68(5):3040–3047. doi:10.1128/IAI.68.5.3040-3047.2000 Medline

Johnson JR, Stell AL. Extended virulence genotypes of *Escherichia coli* strains from patients with urosepsis in relation to phylogeny and host compromise. J Infect Dis. 2000 Jan;181(1):261–272. doi:10.1086/315217 Medline

Khanafari A, Assadi MM, Fakhr FA. Review of prodigiosin, pigmentation in *Serratia marcescens*. Online J Biol Sci. 2006 Jan 1;6(1): 1–13. doi:10.3844/ojbsci.2006.1.13

Karch H, Schubert S, Zhang D, Zhang W, Schmidt H, Olschläger T, Hacker J. A genomic island, termed high-pathogenicity island, is present in certain non-O157 Shiga toxin-producing *Escherichia coli* clonal lineages. Infect Immun. 1999 Nov;67(11):5994–6001. Medline

Krzymińska S, Mokracka J, Koczura R, Kaznowski A. Cytotoxic activity of *Enterobacter cloacae* human isolates. FEMS Immunol Med Microbiol. 2009 Aug;56(3):248–252. doi:10.1111/j.1574-695X.2009.00572.x Medline

Krzymińska S, Raczkowska M, Kaznowski A. Cytotoxic activity of *Serratia marcescens* clinical isolates. Pol J Microbiol. 2010;59(3): 201–205. Medline

Krzymińska S, Ochocka K, Kaznowski A. Apoptosis of epithelial cells and macrophages due to nonpigmented *Serratia marcescens* strains. Scientific World Journal. 2012;2012:1–8. doi:10.1100/2012/679639 Medline

Lecadet MM, Dedonder R. Biogenesis of the crystalline inclusion of *Bacillus thuringiensis* during sporulation. Eur J Biochem. 1971 Nov;23(2):282–294. doi:10.1111/j.1432-1033.1971.tb01620.x Medline

Matyjaszczyk E. "Biorationals" in integrated pest management strategies. J Plant Dis Prot. 2018 Dec;125(6):523–527. doi:10.1007/s41348-018-0180-6

McGuire MR, Galan-Wong LJ, Tamez-Guerra P. Bioassay of *Bacillus thuringiensis* against lepidopteran larvae. In: Lacey LA, editor. Manual of techniques in insect pathology. San Diego (USA): Academic Press; 1997. p. 91–99.

Mohan M, Selvakumar G, Sushil SN, Bhatt JC, Gupta HS. Entomopathogenicity of endophytic *Serratia marcescens* strain SRM against larvae of *Helicoverpa armigera* (Noctuidae: Lepidoptera). World J Microbiol Biotechnol. 2011 Nov;27(11):2545–2551. doi:10.1007/s11274-011-0724-4

Mokracka J, Koczura R, Jabłońska L, Kaznowski A. Phylogenetic groups, virulence genes and quinolone resistance of integron-bearing *Escherichia coli* strains isolated from a wastewater treatment plant. Antonie van Leeuwenhoek. 2011 May;99(4):817–824. doi:10.1007/s10482-011-9555-4 Medline

Mosa WFAEG, Sas Paszt L, Frąc M, Trzciński P. Microbial products and biofertilizers in improving growth and productivity of apple – A review. Pol J Microbiol. 2016 Aug 26;65(3):243–251. doi:10.5604/17331331.1215599 Medline

Mossialos D, Amoutzias G. Role of siderophores in cystic fibrosis pathogenesis: foes or friends? Int J Med Microbiol. 2009 Feb;299(2): 87–98. doi:10.1016/j.ijmm.2008.06.008 Medline

Moura A, Henriques I, Ribeiro R, Correia A. Prevalence and characterization of integrons from bacteria isolated from a slaughterhouse wastewater treatment plant. J Antimicrob Chemother. 2007 Oct 03;60(6):1243–1250. doi:10.1093/jac/dkm340 Medline

Nuñez-Valdez ME, Calderón MA, Aranda E, Hernández L, Ramírez-Gama RM, Lina L, Rodríguez-Segura Z, Gutiérrez MC, Villalobos FJ. Identification of a putative Mexican strain of *Serratia entomophila* pathogenic against root-damaging larvae of Scarabaeidae (Coleoptera). Appl Environ Microbiol. 2008 Feb 01; 74(3): 802–810. doi:10.1128/AEM.01074-07 Medline

de Queiroz BPV, de Melo IS. Antagonism of *Serratia marcescens* towards *Phytophthora parasitica* and its effects in promoting the growth of citrus. Braz J Microbiol. 2006 Dec;37(4):448–450. doi:10.1590/S1517-83822006000400008

Pei R, Kim SC, Carlson KH, Pruden A. Effect of River Landscape on the sediment concentrations of antibiotics and corresponding antibiotic resistance genes (ARG). Water Res. 2006 Jul;40(12):2427–2435. doi:10.1016/j.watres.2006.04.017 Medline

Rasschaert G, Houf K, Imberechts H, Grijspeerdt K, De Zutter L, Heyndrickx M. Comparison of five repetitive-sequence-based PCR typing methods for molecular discrimination of *Salmonella enterica* isolates. J Clin Microbiol. 2005 Aug 01;43(8):3615–3623. doi:10.1128/JCM.43.8.3615-3623.2005 Medline

Reissbrodt R, Rabsch W. Further differentiation of Enterobacteriaceae by means of siderophore-pattern analysis. Zentralbl Bakteriol Mikrobiol Hyg A. 1988 May;268(3):306–317. doi:10.1016/S0176-6724(88)80015-4 Medline

Samrot AV, Chandana K, Senthilkumar P, Kumar GN. Optimization of prodigiosin production by *Serratia marcescens* SU-10 and evaluation of its bioactivity. Int Res J Biotechnol. 2011;2:128–133.

Schwyn B, Neilands JB. Universal chemical assay for the detection and determination of siderophores. Anal Biochem. 1987 Jan;160(1): 47–56. doi:10.1016/0003-2697(87)90612-9 Medline

Sikorowski PP, Lawrence AM, Inglis GD. Effects of *Serratia marcescens* on rearing of the tabacco budworm (Lepidoptera: Noctuide). Am Entomol (Lanham Md). 2001;47(1):51–60. doi:10.1093/ae/47.1.51

Siva R, Subha K, Bhakta D, Ghosh AR, Babu S. Characterization and enhanced production of prodigiosin from the spoiled coconut. Appl Biochem Biotechnol. 2012 Jan;166(1):187–196. doi:10.1007/s12010-011-9415-8 Medline

Stokes HW, Gillings MR. Gene flow, mobile genetic elements and the recruitment of antibiotic resistance genes into Gram-negative pathogens. FEMS Microbiol Rev. 2011 Sep;35(5):790–819. doi:10.1111/j.1574-6976.2011.00273.x Medline

Visca P, Imperi F, Lamont IL. Pyoverdine siderophores: from biogenesis to biosignificance. Trends Microbiol. 2007 Jan;15(1):22–30. doi:10.1016/j.tim.2006.11.004 Medline

Vokes SA, Reeves SA, Torres AG, Payne SM. The aerobactin iron transport system genes in *Shigella flexneri* are present within a pathogenicity island. Mol Microbiol. 1999 Jul;33(1):63–73. doi:10.1046/j.1365-2958.1999.01448.x Medline

Wu J, Liu X, Diao Y, Ding Z, Hu Z. Authentication and characterization of a candidate antagonistic bacterium against soft rot of *Amorphophallus konjac*. Crop Prot. 2012 Apr;34:83–87. doi:10.1016/j.cropro.2011.12.008

Supplementary materials are available on the journal's website.

Polish Journal of Microbiology
2019, Vol. 68, No 2, 193–201
https://doi.org/10.33073/pjm-2019-019

ORIGINAL PAPER

An Investigation of Petrol Metabolizing Bacteria Isolated from Contaminated Soil Samples Collected from Various Fuel Stations

FATIMA MUCCEE and SAMINA EJAZ*

Department of Biochemistry and Biotechnology, The Islamia University of Bahawalpur, Bahawalpur, Pakistan

Submitted 1 December 2018, revised 29 January 2019, accepted 31 January 2019

Abstract

The present study aimed to isolate the high-efficiency petrol metabolizing thermophilic bacteria from petrol contaminated soil samples. Isolation was carried out through enrichment culture, serial dilution and pour plate methods using the petrol supplemented minimal salt media. The isolated bacteria were analyzed to document growth behavior, petrol removal efficiencies, antibiotic resistance profile, and biochemical characteristics. The 16S rRNA based phylogenetic analysis helped to reveal the identity of isolated bacterial species and construct the phylogenetic trees. Total nine bacteria were isolated, out of which three (IUBP2, IUBP3, IUBP5) were identified as *Brevibacillus formosus*, one (IUBP1) was found similar to *Brevibacillus agri*, four (IUBP7, IUBP8, IUBP13, and IUBP14) shared homology with *Burkholderia lata*, and one (IUBP15) with *Burkholderia pyrrocinia*. All the isolates were fast growing and exhibited considerable petrol degradation potential. The highest petrol removal efficiency (69.5% ± 13.44/6 days) was recorded for the strain IUBP15 at a petrol concentration of 0.1% (v/v). All bacteria studied (100%) were positive for esculinase and phosphatase. Many strains exhibited positive responses for arginine dehydrolase (22%), β-naphthylamidase (11%), β-D-glucosaminide (33%), mannitol (55%), sorbitol (66%) and inulin (88%) fermentation test. While all were sensitive to the antibiotics, some of them were found resistant against chloramphenicol and oxacillin. The remarkable biochemical characteristics and considerable petrol removal potential (40–70%) highlights utilization of the bacteria isolated for petrol bioremediation, mineralization of organophosphates, dairy and food industry, and also as biofertilizers and biocontrol agents.

Key words: bioremediation, minimal salt media, green technology, gasoline and 16S rRNA profiling

Introduction

Petrol, also known as gasoline, is a mixture of alkanes (4–8%), alkenes (2–5%), isoalkanes (20–40%), cycloalkanes (3–7%), cycloalkenes (1–4%) and aromatics (20–50%). Aromatics include benzene, toluene, ethylbenzene, and xylene (BTEX). Some other substances like oxygen, sulfur, nitrogen, and metals are also present in low concentrations (Silva et al. 2018). Petrol is obtained during the distillation and refinement of petroleum. The hydrocarbon constituents of petrol due to their adverse impact on the environment and human health have been classified as the priority pollutants by the Environment Protection Agency (Varjani 2017; Yuniati 2018).

Petrol contains various volatile compounds like propane, butane, benzene, toluene, ethylbenzene, and xylene which are ultimately transferred to the atmosphere. The workers of the petroleum industry and petrol pumps are at high risk of exposure to these gasoline components (Rappaport et al. 1987; Cruz et al. 2017; Ekpenyong and Asuquo 2017). Petrol may also intrude indoor spaces from underground storage facilities and may lead to the explosion and serious health hazards after inhalation. Through oil spills, petrol enters the ecosystem and its use as fossil fuel also exerts an adverse impact on the biosphere. It is burned and oxidized in engines of motor vehicles to provide energy for transportation. The incomplete oxidation of petrol generates hydrocarbons which contribute to global warming.

Acute and chronic exposure to petrol hydrocarbons may occur through ingestion, inhalation as well as dermal route and result in various health hazards. Light-chain volatile compounds: toluene, ethylbenzene, and xylene, considered ototoxic compounds, are capable to damage the auditory system. Benzene has no safe

* Corresponding author: S. Ejaz, Department of Biochemistry and Biotechnology, The Islamia University of Bahawalpur, Bahawalpur, Pakistan; **e-mail: saminaejazsyed@yahoo.com, samina.ejazsyed@iub.edu.pk**

exposure limit and it is a proved carcinogen (Silva et al. 2018). Gasoline hydrocarbons also affect the respiratory system (Sekkal et al. 2012). Other systemic health effects include the hematological, immunological, reproductive, dermatological, central nervous system, and renal pathologies (Ekpenyong and Asuquo 2017). The associated environmental hazards include contamination of soil and groundwater resources in addition to decreased agricultural productivity (Thapa et al. 2012; Perera 2017).

In order to minimize health-related hazards, the decontamination of the environmental sources from petrol hydrocarbons is indispensable. For this purpose, various physicochemical approaches like thermal desorption, incineration, landfilling, and solvent extraction have been employed (Jain et al. 2011). These techniques suffer from certain limitations like high cost, labor-intensive, incomplete removal of pollutants, land disturbance, and inherent hazard of aggravating the prevailing situation etc. So, the physicochemical methods are being replaced by green technologies, which employ biological means for the purpose of decontamination. Use of bacteria for the removal of petrol is the most cost-effective technique providing required efficacy. The hydrocarbon decomposing bacteria, which are available commercially in freeze-dried forms, propagate to at least 2×10^8 colony forming unit per milliliter (CFU/ml) and they are considered suitable for bioremediation (Thapa et al. 2012). Some of these bacteria with capability of degrading petrol components are: *Flavobacterium* spp., *Rhodococcus* spp., *Serratia* spp., *Pseudomonas putida* HM346961, *Dietzia* spp., *Alcaligenes* spp., *Nocardia* spp., *Micrococcus* spp., *Burkholderia* spp., *Pseudomonas aeruginosa*, and *Bacillus pumilus* MVSV3 (Ridgway et al. 1990; Lu et al. 2006a; Avanzi et al. 2015; Mujahid et al. 2015; Morlett-Chávez et al. 2017; Chen et al. 2017; Surendra et al. 2017; Satyam et al. 2018).

Although the literature reports isolation and characterization of several bacteria capable of metabolizing different gasoline constituents, however, the bacteria reported so far are capable of metabolizing the limited number of gasoline constituents, which proves them less efficient for gasoline remediation. These bacteria metabolize different hydrocarbons of petroleum and oil but very few efficiently degrade multiple petrol constituents simultaneously. Moreover, the bacteria which can degrade some aromatic compounds fail to metabolize the aliphatic compounds and *vice-versa* (Fida et al. 2017; Zhao et al. 2017). A few earlier reported bacterial species capable of degrading multiple hydrocarbons have been studied only in the presence of a particular hydrocarbon and not in the petrol saturated environment (Guermouche M'rassi et al. 2015). It limits their potential of being used as petrol bioremediating agents. Such bacteria can only be effective in the form of consortium (Gurav et al. 2017; Sarkar et al. 2017; Bacosa et al. 2018). In order to achieve optimal degradation, the use of bacterial consortium consisting of bacteria capable of metabolizing different fractions/ constituents of petrol has been recommended (Patowary et al. 2016). This phenomenon is referred to as co-metabolism and is highly advantageous for effective degradation of mixtures, like petrol (Battikhi 2014). Bioremediation is not an omnipotent technology and is affected by several environmental factors. Moreover, the large-scale application of consortium, containing a wide range of bacterial species, for the purpose of bioremediation may encounter the problem of providing favorable conditions for optimum growth of diverse bacteria found in a consortium (Xu et al. 2018). In contrast to this, use of bacteria having the potential of degrading multiple constituents of petrol simultaneously in petrol saturated environment may result in increased bacterial access to the numerous carbon sources and more efficient bioremediation (Vignesh et al. 2016). The study presented in this manuscript was initiated to isolate bacteria capable of surviving in high gasoline environments and efficiently removing gasoline by the simultaneous breakdown of multiple gasoline components.

We tried to explore the highly efficient eco-friendly (i.e., lacking drug resistance and pathogenicity) petrol metabolizing bacteria, exhibiting fast growth rate, and capable of metabolizing multiple constituents of petrol.

Bioremediation is an eco-friendly technology which requires the selection of environmentally friendly bacteria lacking pathogenicity and drug resistance (Händel et al. 2013). Up to our knowledge, the literature already published does not contain any information regarding virulence status of petrol metabolizing bacteria (Lu et al. 2006b; Asiedu et al. 2014). During the present study to justify the future application as a bioremediating agent, we documented the antibiotics resistance potential of the isolated petrol metabolizing bacteria.

Constant spilling of petrol at the gas stations contaminates the surrounding soil which thus could be the rich reservoir of the petrol utilizing bacteria. Although various studies have reported the isolation of petrol metabolizing bacteria from the petrol-contaminated soil of petrol pumps, no one has explored our native sources. Moreover, under different habitats bacteria may employ unique degradative pathways and enzymes for remediation (Copley 2009; Bagga et al. 2015; Mujahid et al. 2015; Abou-Shanab et al. 2016). We, therefore, hypothesized that we might have found some unusual petrol metabolizing bacteria expressing novel petrol degradative enzymes and associated metabolic pathways in petrol contaminated soil of indigenous fuel stations. It was further speculated that the accomplishment of the proposed study may serve as a road map to revive petrol contaminated environmental resources.

Experimental

Materials and Methods

Screening of petrol metabolizing bacteria. For initial screening of petrol metabolizing bacteria, minimal salt media (MSM) was used. This medium contained; KH_2PO_4, 1 g; K_2HPO_4, 1 g; NH_4NO3, 1 g; $MgSO_4$, 0.2 g; $CaCl_2$, 0.02 g; $FeCl_3$ (0.5 M), 2 drops per 1000 ml of distilled water, and 100 µl petrol in 100 ml of medium (Ozyurek and Bilkay 2017). Initially, 1 g of soil sample was added to the medium (50 ml) and incubated for one week in shaker adjusted at 50°C and at 250 rpm. After a week, this culture was used as inoculum and added to a freshly prepared minimal salt medium supplemented with petrol. The culture was incubated in incubator shaker under the same conditions. The enrichment process was repeated for six weeks. After enrichment, the serial dilutions were prepared and each dilution (100 µl) was spread on petrol supplemented MSM agar medium solidified in Petri plates. Followed by spreading, the Petri plates were incubated at 50°C and the isolates exhibiting optimum growth were stored in the form of glycerol stock for future use.

Morphology. The colony morphology on agar medium and response to Gram staining and colony forming units (CFUs) of each bacterial isolate were documented.

Growth characteristics. The growth of bacteria was monitored turbidometrically (OD_{600}) by measuring absorbance at regular time intervals using UV-visible spectrophotometer. To better reflect the growth behavior, optical density was plotted versus time.

Biochemical characterization. The Remel RapID STR System (Thermo Scientific) was used for biochemical characterization of the isolated bacteria. This system included various qualitative biochemical tests like arginine dehydrolase test, esculinase test, sorbitol fermentation test, mannitol fermentation test, inulin fermentation test, raffinose fermentation test, ρ-nitrophenyl-α,D-galactosidase test, ρ-Nitrophenyl-α,D-glucosidase test, tyrosine β-naphthylamidase test, ρ-nitrophenyl-n-acetyl-β,D-glucosaminidase test, pyrrolidonyl peptidase test and lysine β-naphthylamidase test.

Quantitative study of petrol degradation by isolates. For the assessment of petrol degrading potential of the bacteria isolated, petrol supplemented MSM (50 ml) was added in 250 ml Erlenmeyer flask containing 1% (v/v) of the aqueous solution of 2, 6-dichlorophenolindophenol (DCPIP), a redox indicator. Overnight grown bacterial cultures (1 ml) were added as inoculum in the culture flask and incubated at 50°C and 250 rpm for seven days. The culture was collected after different time intervals and centrifuged (6000 rpm) at 4°C. The pelleted cells were discarded, and an absorbance of the supernatant was measured at 600 nm to assess the color change against a blank (Ozyurek and Bilkay 2017). DCPIP serves as a redox indicator and its decolorization or color change in petrol supplemented medium is a measure of petrol metabolizing capability of bacteria (Marchand et al. 2017).

Antibiotic sensitivity profiling. All isolated bacteria were subjected to disc diffusion antibiotic sensitivity assay (Bauer et al. 1966). Bacteria were tested against antibiotics teicoplanin (30 µg/disc), linezolid (10 µg/disc), linezolid (30 µg/disc), oxacillin (1 µg/disc) and chloramphenicol (30 µg/disc).

Molecular analysis. For molecular analysis, bacterial genomic DNA was extracted using organic method (Maniatis et al. 1982). For PCR (Polymerase Chain Reaction) amplification of 16S rDNA gene, specific primers F1 and R1 were designed (Table SI). The PCR (50 µl) reaction mixture contained; 5 µl of 10 × PCR buffer (Mg^{2+} free), 5 µl of $MgCl_2$, 1 µl of 10 mM dNTPs, 2 µl of 10 pM forward primer, 2 µl of 10 pM reverse primer, 0.25 µl of Taq DNA polymerase, 50 ng of template DNA and 29.75 µl of nuclease-free water. The conditions used for PCR amplification were as follows: initial denaturation (95°C, 5 min), 38 cycles consisting of denaturation (94°C, 40 seconds), annealing (58°C, 40 seconds) and extension (72°C, 30 seconds), followed by a final extension of 10 min at 72°C. Amplification of target DNA was confirmed by agarose gel electrophoresis and PCR amplicons purified using Monarch DNA Gel Extraction Kit (Cat# T1020S) were sent to Macrogen, Korea for the DNA sequencing. The obtained FASTA sequences were subjected to BLASTN analysis (http://blast.ncbi.nlm.nih.gov/blast/Blast.cgi) which aligned study sequences with the sequences available in the non-redundant nucleotide database of NCBI (National Center for Biotechnology Information). Once the taxonomic affiliation of bacterial sequences was revealed, 16S rRNA gene sequences were submitted to NCBI Genbank database. Accession numbers were assigned (Table I). Multiple sequence alignments of 16S rRNA gene sequences of isolated bacteria and the closely related bacterial sequences available in the NCBI database were carried out using Clustal omega multiple sequence alignment algorithms available at http://www.clustal.org/mbed.tgz. Results of multiple sequence alignment analysis were used to construct bootstrapped maximum composite likelihood neighbor-joining trees using Mega 7 software.

Sequences of nine isolates have been submitted to NCBI and accession numbers assigned are: IUBP1 (MH368051), IUBP2 (MH023312), IUBP3 (MH023313), IUBP5 (MH023314), IUBP7 (MH368052), IUBP8 (MH368053), IUBP13 (MH368054), IUBP14 (MH368055) and IUBP15 (MH368057) (Table I).

Table I
Phylogenetic analysis of petrol metabolizing bacteria.

Group	Isolate	Accession No.	Closest phylogenetic relative	Similarity	URLs
Group I	IUBP2	MH023312	*Brevibacillus formosus* strain NBRC 15716	100%	https://www.ncbi.nlm.nih.gov/nuccore/MH023312.1
	IUBP3	MH023313	*Brevibacillus formosus* strain NBRC 15716	100%	https://www.ncbi.nlm.nih.gov/nuccore/MH023313.1
	IUBP5	MH023314	*Brevibacillus formosus* strain NBRC 15716	100%	https://www.ncbi.nlm.nih.gov/nuccore/MH023314.1
Group II	IUBP1	MH368051	*Brevibacillus agri* strain NBRC 15538	100%	https://www.ncbi.nlm.nih.gov/nuccore/MH368051
Group III	IUBP7	MH368052	*Burkholderia lata strain 383*	99%	https://www.ncbi.nlm.nih.gov/nuccore/MH368052.1
	IUBP8	MH368053	*Burkholderia lata strain 383*	99%	https://www.ncbi.nlm.nih.gov/nuccore/MH368053.1
	IUBP13	MH368054	*Burkholderia lata strain 383*	99%	https://www.ncbi.nlm.nih.gov/nuccore/MH368054.1
	IUBP14	MH368055	*Burkholderia lata strain 383*	99%	https://www.ncbi.nlm.nih.gov/nuccore/MH368055.1
Group IV	IUBP15	MH368057	*Burkholderia pyrrocinia* strain LMG 14191	98%	https://www.ncbi.nlm.nih.gov/nuccore/MH368057

Results

Morphology. Nine petrol metabolizing bacteria were isolated from the soil sample of a petrol pump through enrichment culture technique. All isolated bacteria were found to be Gram-positive bacilli. The number of the bacteria was enumerated (Table SII).

Molecular analysis. The molecular study used as the first level of screening classified nine petrol metabolizing bacteria into four groups (Fig. 1). Group I included three isolates IUBP2, IUBP3 and IUBP5 exhibiting similarity to *Brevibacillus formosus*. Group II consisted of only one isolate IUBP1 homologous to *Brevibacillus agri*. Four isolates sharing homology with *Burkholderia lata* were included in Group III. While Group IV, a group of *Burkholderia pyrrocinia* comprised of one isolate IUBP15 (Table I).

Phylogenetic analysis. To trace the phylogenetic history of the isolated bacteria, the phylogenetic trees were constructed. The isolates IUBP7, 8, 13, 14 and 5 were assigned to genus *Burkholderia*. Study of the evolutionary relationship revealed that IUBP15 shared common ancestry with *B. pyrrocinia* (Accession number NR 118075.1) and *Burkholderia ambifaria* (Accession number NR 118051.1). Moreover, they shared the same clade with a strong (93) bootstrap value. While IUBP8,

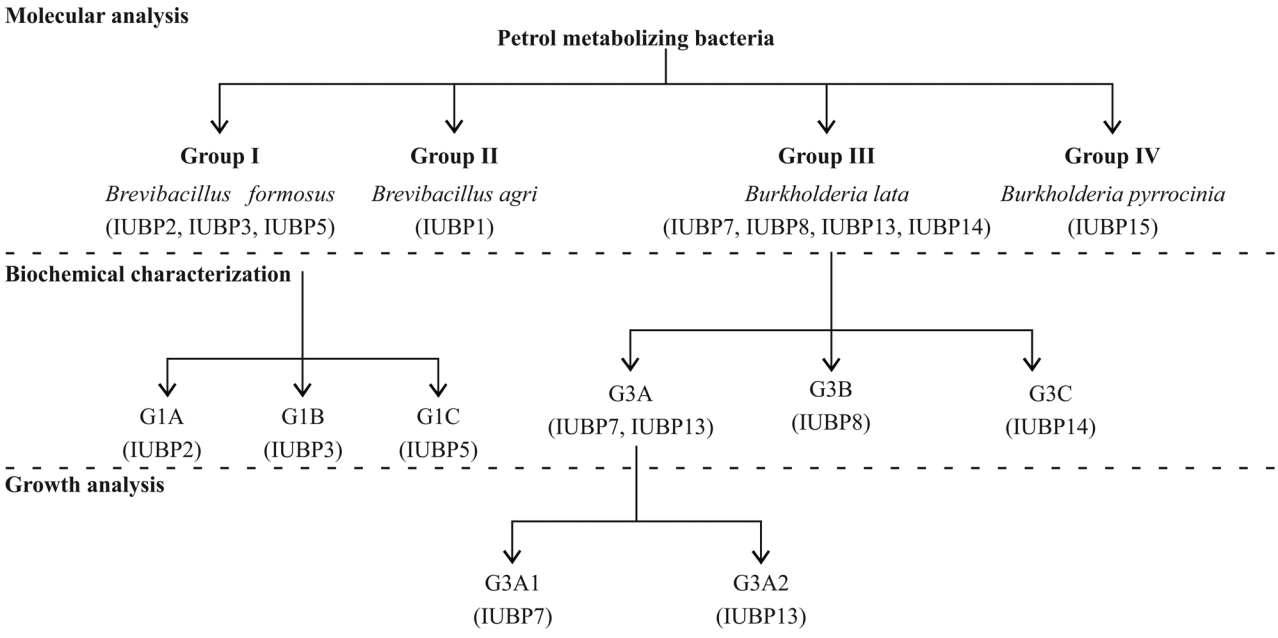

Fig. 1. Characteristics of petrol metabolizing bacteria based upon molecular, biochemical and growth curve analysis. The ribotyping, biochemical, growth behavior analysis helped to discriminate among the bacteria isolated.

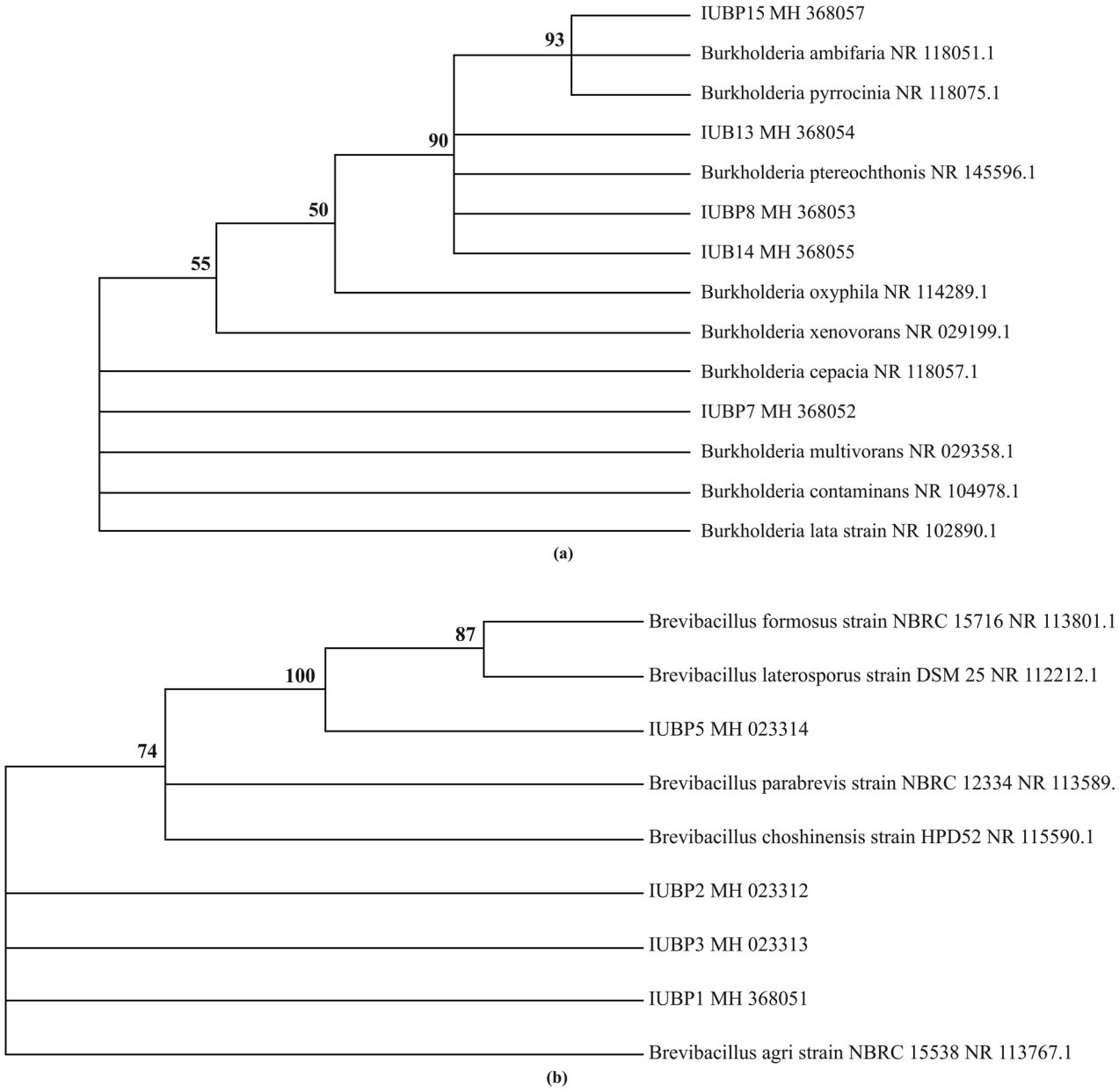

Fig. 2. A) Phylogenetic tree of petrol metabolizing bacteria exhibiting homology with *Burkholderia*.
B) Phylogenetic tree of petrol metabolizing bacteria exhibiting homology with *Brevibacillus*.

13 and 14 were found closely related to each other as they originated from the same lineage with strong bootstrap value (90). However, IUBP7 distantly related to the other isolates of genus *Burkholderia* (Fig. 2A).

Molecular analysis placed isolates IUBP1, 2, 3 and 5 in genus *Brevibacillus*. As per evolutionary study, IUBP5 shared clade (bootstrap value = 87) with *B. formosus* strain NBRC 15716 (Accession number NR 113801.1) and *Brevibacillus laterosporus* strain DSM (Accession number NR 112212.1). While IUBP1, IUBP2, and IUBP3 shared the same clade with each other and with *B. agri* strain NBRC 15538 (Accession number NR 113767.1) (Fig. 2B).

Biochemical characterization. The isolated bacteria were biochemically characterized through fourteen tests (Table SIII and Fig. S1) and all were found negative for raffinose fermentation (RAF) test, D-galactoside (GAL) test, tyrosine β-naphthylamide (TYR) test, D-glucoside (GLU) test, lysine β-naphthylamide (LYS) test and pyrrolidine β-naphthylamide (PYR) test. All bacteria were esculinase and phosphatase producers. While only two (IUBP3 and 14) were arginine dehydrolase producers. Five isolates (IUBP2, 3, 7, 13 and 15) were capable of fermenting mannitol and six (IUBP2, 3, 5, 7, 13 and 15) were noticed to be sorbitol fermenting and all except IUBP1 were inulin fermenting. Only one bacterium, IUBP1, was found positive for hydroxyproline β-naphthylamidase and three (IUBP2, 3 and 8) were examined to be glucosaminidase producers. The biochemical analysis helped to differentiate between the

members of the group I and group III. All the members of the group I and two members of the group III (IUBP8 and 14) were distinctive from each other. However, IUBP7 and IUBP13 were biochemically similar and thus placed in group G3A.

Growth rate. On the basis of molecular and biochemical characteristics, all isolates except members of group G3A were found different. So, the growth rate of the molecularly and biochemically similar members of group G3A was compared to detect their distinctiveness (Table SIV). Both isolates (IUBP7 and 13) have different growth rate and, therefore, were considered to be different bacteria. Growth behavior of petrol degrading bacteria having similar molecular and biochemical profile was illustrated graphically (Fig. S2).

Petrol removal efficiency. Petrol removal efficiency for all nine bacteria was measured. Maximum degradation efficiency (69.5% ± 13.44) was observed for IUBP15, while isolate IUBP1 exhibited minimum petrol removal efficiency (41% ± 32.6) (Table SV).

Antibiotic resistance profile. All isolates tested were found sensitive to teicoplanin and linezolid and exhibited resistance to chloramphenicol and oxacillin. Zone of inhibition was recorded. Maximum zone of inhibition (37.5 mm ± 0.071) was observed for IUBP8 upon linezolid (30 μg) treatment. For linezolid (10 μg) a maximum zone of inhibition (32.5 mm ± 0.071) was recorded for IUBP14. In the case of teicoplanin, a maximum zone of inhibition (22.5 mm ± 0.2121) was shown for IUBP7.

Discussion

Screening for petrol metabolizing bacteria from contaminated soil of petrol pump resulted in the isolation of nine different bacterial species. All isolates were capable to grow in MSM and metabolizing petrol as a sole source of carbon.

Morphology. All these isolates were Gram-positive bacilli. The reason behind the dominant incidence of Gram-positive bacteria could be that in Southern Punjab day time temperatures are usually high and osmotic pressure may vary periodically over a daily cycle. A stronger cell envelope of Gram-positive bacteria enables them to proliferate more efficiently when compared to Gram-negative bacteria (Silhavy et al. 2010). This is parallel with the earliest studies in which petroleum hydrocarbons metabolizing bacteria like *Bacillus cereus*, *Proteus mirabilis*, *Bacillus subtilis*, *Enterococcus faecalis*, *Streptomyces* sp. ERI-CPDA-1, *Bacillus mojavensis* ATHE13 and *Bacillus licheniformis* ATHE9 have been reported (Balachandran et al. 2012; Eskandari et al. 2017; Ozyurek and Bilkay 2017).

Molecular characterization. Most of the petrol metabolizing bacteria (IUBP7, 8, 13, 14 and 15) isolated during the present study belonged to the genus *Burkholderia*. Our results are consistent with the earlier studies which have reported different species of *Burkholderia* capable of degrading variable aliphatic and aromatic hydrocarbons of petrol (Marin et al. 2001; Chakraborty et al. 2010; Mujahid et al. 2015). Moreover, petrol hydrocarbon metabolizing *Brevibacilli* have also been reported in the literature (Xue et al. 2006; Mnif et al. 2011; Zhan et al. 2017).

Biochemical characterization. In order to discriminate among different strains of petrol metabolizing bacteria belonging to the same species, their biochemical potential was investigated. In literature, biochemical characterization of different petrol decomposing bacteria has been reported (Lu et al. 2006b). However, this study is the first to report enzymes like arginine dehydrolase, esculinase, naphthylamidase, glucosaminidase, phosphatase enzymes and capabilities to ferment sorbitol, mannitol, and inulin.

Arginine dehydrolase (ARG) is the enzyme, which catalyzes the conversion of arginine to putrescine. ARG was detected in only two bacteria (IUBP3 and IUBP14). This enzyme has been identified as a potential anticancer agent for the treatment of hepatocellular melanomas and carcinomas. Hence, ARG positive bacteria can be further exploited for therapeutic purposes (Sharma et al. 2017).

Esculinase (ESC) test confirms the presence of esculinase, which catalyzes breakdown of esculin into esculetin and dextrose. In the present study, all the bacteria isolated were positive for esculinase and thus hold potential to be used in food industry, synthesis of *o*-alkyl glucoside, cosmetics and pesticides (Rani et al. 2014).

In our study, results of fermentation tests revealed 56% bacteria positive for mannitol, 66% positive for sorbitol and 88% positive for inulin. However, none of the bacteria was capable to ferment raffinose. Inulase-positive bacteria can be effectively used for the production of gluconic acid, mannitol, ethanol and fructose syrup (Singh et al. 2017).

Hydroxyproline β-naphthylamidase expedites catabolism of hydroxyproline β-naphthylamide and β-naphthylamine. In this study, only 11% of isolated bacteria were naphthylamidase-positive. The ρ-nitrophenyl-n-acetyl-β-D-glucosaminide (NAG) test was carried out to detect glucosaminidase enzyme, which hydrolyzes *p*-nitrophenyl substituted glycoside and releases ρ-nitrophenol. In our study, 33% of the isolates were found positive for glucosaminidase. Many studies have reported the use of glucosaminidase as biocontrol agents and in the production of important biological compounds (Scigelova and Crout 1999).

The ρ-nitrophenyl phosphate (PO_4) test is performed to detect the presence of phosphatase enzyme in bacteria. The phosphatase enzyme regulates the break-

down of ρ-nitrophenyl phosphate into ρ-nitrophenol. All isolated bacteria were positive for the phosphatase enzyme. Hence, it can be utilized for designing biosensors for environmental monitoring or as an indicator for sufficient pasteurization of milk, mineralizing organophosphates, assessment of heavy metals precipitation from effluents and in immunoassays (Nalini et al. 2015).

Growth rate. All the bacterial isolates were fast growing and exhibited exponential growth until 6 hours (IUBP14), 24 hours (IUBP5 and 13) and 30 hours (IUBP1, 2, 3, 7, 8 and 15). In our study, the maximum OD (0.27) was observed for IUBP3 while minimum OD (0.1) was observed in case of IUBP5, 7, 13 and 14. The growth rate of our bacteria is comparable with the earlier reported bacteria. Many of the isolates showed optimal growth at six hours (Table SIV). While contrary to our results, maximum OD (1.4) and minimum OD was considerably higher (0.2) in the previous reports (Vignesh et al. 2016).

Petrol degrading efficiency. All the nine bacteria incubated in the presence of petrol (0.1% v/v) for seven days at 50°C showed different petrol degrading efficiencies. The highest petrol degradation efficiency (69.5% ± 13.44 / 6 days) was observed for IUBP15. While highest petrol removal efficiency reported in the literature is 30% per seven days for *Bacillus tequilensis* grown in the presence of crude oil (1% v/v) for seven days at 30°C (Ozyurek and Bilkay 2017). In the present study, the lowest petrol degradation rate (41% ± 32.6 / 4 days) was noticed for IUBP1. However, in the literature the lowest degradation efficiency has been reported to be 80% for 21 days for HCS2 bacterial strain, incubated in MSM containing 50 mg/l petrol (0.005%) for 30 days at 30°C (Avanzi et al. 2015). The petrol degrading efficiency of other isolates IUBP2 (62% ± 19.34 / 7 days), IUBP3 (66% ± 9.90 / 6 days) and IUBP14 (63% ± 1.41 / 5 days) was somehow comparable to the reported petrol degradation rate (60% / 21 days) of HCS1 grown in the presence of 50 mg/l petrol (0.005%) for 30 days at 30°C (Avanzi et al. 2015). Based on this comparison, in this study the bacterial strains could be a better choice than many previously reported bacteria due to considerable efficiency (up to 69.5% petrol removal efficiency achieved in 4–7 days), the capability to grow in petrol saturated environment (0.1%), and at a higher temperature (50°C). Most of the previously isolated bacteria are known to grow at 30°C in the presence of lower petrol concentration (0.005%) and exhibit delayed degradation (21 days). Variations in biodegradation potential reflect the presence of different enzyme systems and metabolic pathways responsible for petrol catabolism.

In order to explore the petrol degradation capabilities and pathways existing in our isolates, we performed a GC-MS based analysis of bacterial metabolites. Our results confirmed the metabolism of multiple constituents, like alkanes, cycloalkanes, and aromatics including benzene, toluene, naphthalene, and ethylbenzene of petrol (data not shown). Hence, the ability to metabolize both, aliphatic and aromatic components of petrol, makes the isolated bacteria better choice for effective petrol remediation than earlier known petrol remediating bacteria. Moreover, multi-potential bacteria of the present study do not highlight the need to exploit the phenomenon of co-metabolism and application of bacterial consortium.

Antibiotic sensitivity profiling. The application of bacteria for eco-friendly bioremediation is restricted by their antibiotics resistance potential. The antibiotic-resistant bacteria can adversely affect the environment through their virulence and cannot be used as a whole cell preparation for effective bioremediation. The petrol metabolizing bacteria decompose petrol due to the presence of genes encoding petrol metabolizing enzymes. In order to decide whether to use a whole cell, an enzyme or a gene for bioremediation the antibiotic resistance profile of isolated bacteria was investigated. All isolates were found resistant to teicoplanin and linezolid. Hence, the whole cell uses of study bacteria cannot be recommended but their enzymes and genes can be exploited in multiple ways.

In case the desired enzymes are extracellular then their supernatant will be used for synthesizing nanoparticles, while in case of intracellular enzymes, their cell lysate can be used for purification of enzymes and for synthesizing nanoparticles. The desired genes can be cloned into any environmentally friendly bacteria for their expression.

Nanoparticles due to their high surface area to volume ratio are highly reactive and can decontaminate effluents in lesser time (Guerra et al. 2018). Bacteria due to their capability to mobilize, immobilize and reduce the metal ions, can easily precipitate metals at nanoscale (Iravani 2014). The bacterial exopolysaccharides based silver nanoparticles have been previously reported as effective, eco-friendly and cheaper tools for remediation of textile dyes (Saravanan et al. 2017). The enzymes of present study isolates can be used to synthesize nanoparticles for remediation of the petrol hydrocarbons.

Conclusion

Petrol hydrocarbons-based pollution is a real-world issue (Perera 2017). The bacteria isolated and characterized during the present study can serve as the promising tools in future for reclamation of petrol contaminated environmental resources because of their fast growth rate in the presence of petrol as an only carbon source, the capability to remove a wide range of

constituents of petrol simultaneously and without the need of growth within a consortium. The ability to produce a variety of enzymes highlights the future industrial significance of study isolates. Due to drug resistance potential a whole cell uses of the bacteria isolated cannot be recommended. However, the valuable genes and enzymes can be exploited through alternate ways like cloning of the genes into a non-virulent expression system or through the synthesis of the enzymes-based nanoparticles. Further study of factors influencing the growth and metabolism, exploitation of enzyme systems, metabolic pathways and associated genes will help to design the best system for achieving optimum removal of petrol hydrocarbons.

Acknowledgments

We are thankful to Dr. Asma Shaukat, Department of Pathology, Quaid-e-Azam Medical College, Bahawalpur, for providing us the antibiotic sensitivity discs.

Author's contributions

SE conceived the idea and designed study. FM performed all bench top work and wrote first draft of manuscript. All authors contributed to finalize the manuscript.

Conflict of interest

The authors do not report any financial or personal connections with other persons or organizations, which might negatively affect the contents of this publication and/or claim authorship rights to this publication.

Literature

Abou-Shanab RAI, Eraky M, Haddad AM, Abdel-Gaffar ARB, Salem AM. Characterization of crude oil degrading bacteria isolated from contaminated soils surrounding gas stations. Bull Environ Contam Toxicol. 2016 Nov;97(5):684–688. doi:10.1007/s00128-016-1924-2 Medline

Asiedu NY, Asiedu YA, Bediako PCK. Isolation, identification and characterization of some petroleum metabolizers from soils contaminated with petroluem oils in Kumasi Metropolis-Ghana. J Microbiol Res. 2014;4:117–124. doi:10.5923/j.microbiology.20140402.12

Avanzi IR, Gracioso LH, Baltazar MPG, Karolski B, Perpetuo EA, Nascimento CAO. Aerobic biodegradation of gasoline compounds by bacteria isolated from a hydrocarbon-contaminated soil. Environ Eng Sci. 2015 Dec;32(12):990–997. doi:10.1089/ees.2015.0122

Bacosa HP, Erdner DL, Rosenheim BE, Shetty P, Seitz KW, Baker BJ, Liu Z. Hydrocarbon degradation and response of seafloor sediment bacterial community in the northern Gulf of Mexico to light Louisiana sweet crude oil. ISME J. 2018 Oct;12(10):2532–2543. doi:10.1038/s41396-018-0190-1 Medline

Bagga J, Pandey M, Pandey V. Isolation, characterization and identification of three petroleum tolerant and degrading bacteria (*Micrococcus, Staphylococcus* and *Pseudomonas* spp.) from petroleum oil contaminated soil. Int J Innov Res Sci Eng Technol. 2015; 4(10):9993–10005. doi:10.15680/IJIRSET.2015.0410098

Balachandran C, Duraipandiyan V, Balakrishna K, Ignacimuthu S. Petroleum and polycyclic aromatic hydrocarbons (PAHs) degradation and naphthalene metabolism in *Streptomyces* sp. (ERI-CPDA-1) isolated from oil contaminated soil. Bioresour Technol. 2012 May;112:83–90. doi:10.1016/j.biortech.2012.02.059 Medline

Battikhi MN. Bioremediation of petroleum sludge. J Microbiol Exp. 2014;1:1–3. 1doi:10.15406/jmen.2014.01.00011

Bauer AW, Kirby WMM, Sherris JC, Turck M. Antibiotic susceptibility testing by a standardized single disk method. Am J Clin Pathol. 1966 Apr 01;45 4_ts:493–496. doi:10.1093/ajcp/45.4_ts.493 Medline

Chakraborty S, Mukherji S, Mukherji S. Surface hydrophobicity of petroleum hydrocarbon degrading *Burkholderia* strains and their interactions with NAPLs and surfaces. Colloids Surf B Biointerfaces. 2010 Jun;78(1):101–108. doi:10.1016/j.colsurfb.2010.02.019 Medline

Chen W, Li J, Sun X, Min J, Hu X. High efficiency degradation of alkanes and crude oil by a salt-tolerant bacterium *Dietzia* species CN-3. Int Biodeterior Biodegradation. 2017 Mar;118:110–118. doi:10.1016/j.ibiod.2017.01.029

Copley SD. Evolution of efficient pathways for degradation of anthropogenic chemicals. Nat Chem Biol. 2009 Aug;5(8):559–566. doi:10.1038/nchembio.197 Medline

Cruz LPS, Alve LP, Santos AVS, Esteves MB, Gomes ÍVS, Nunes LSS. Assessment of BTEX concentrations in air ambient of gas stations using passive sampling and the health risks for workers. J Environ Prot. 2017;08(01):12–25. doi:10.4236/jep.2017.81002

Ekpenyong C, Asuquo A. Recent advances in occupational and environmental health hazards of workers exposed to gasoline compounds. Int J Occup Med Environ Health. 2017 Feb 1;30(1):1–26. doi:10.13075/ijomeh.1896.00800 Medline

Eskandari S, Hoodaji M, Tahmourespour A, Abdollahi A, Baghi T, Eslamian S, Ostad-Ali-Askari K. Bioremediation of polycyclic aromatic hydrocarbons by *Bacillus licheniformis* ATHE9 and *Bacillus mojavensis* ATHE13 as newly strains isolated from oil-contaminated soil. J Geogr Environ Earth Sci Int. 2017 Jan 10; 11(2):1–11. doi:10.9734/JGEESI/2017/35447

Fida TT, Moreno-Forero SK, Breugelmans P, Heipieper HJ, Röling WFM, Springael D. Physiological and transcriptome response of the polycyclic aromatic hydrocarbon degrading *Novosphingobium* sp. LH128 after inoculation in soil. Environ Sci Technol. 2017 Feb 07;51(3):1570–1579. doi:10.1021/acs.est.6b03822 Medline

Guermouche M'rassi A, Bensalah F, Gury J, Duran R. Isolation and characterization of different bacterial strains for bioremediation of n-alkanes and polycyclic aromatic hydrocarbons. Environ Sci Pollut Res Int. 2015 Oct;22(20):15332–15346. doi:10.1007/s11356-015-4343-8 Medline

Guerra F, Attia M, Whitehead D, Alexis F. Nanotechnology for environmental remediation: materials and applications. Molecules. 2018 Jul 18;23(7):1760. doi:10.3390/molecules23071760 Medline

Gurav R, Lyu H, Ma J, Tang J, Liu Q, Zhang H. Degradation of n-alkanes and PAHs from the heavy crude oil using salt-tolerant bacterial consortia and analysis of their catabolic genes. Environ Sci Pollut Res Int. 2017 Apr;24(12):11392–11403. doi:10.1007/s11356-017-8446-2 Medline

Händel N, Schuurmans JM, Brul S, ter Kuile BH. Compensation of the metabolic costs of antibiotic resistance by physiological adaptation in *Escherichia coli*. Antimicrob Agents Chemother. 2013 Aug; 57(8): 3752–3762. doi:10.1128/AAC.02096-12 Medline

Iravani S. Bacteria in nanoparticle synthesis: current status and future prospects. Int Sch Res Notices. 2014;2014:1–18. doi:10.1155/2014/359316 Medline

Jain PK, Gupta VK, Gaur RK, Lowry M, Jaroli DP, Chauhan UK. Bioremediation of petroleum oil contaminated soil and water. Res J Envir Toxicol. 2011;5:1–26. doi:10.3923/rjet.2011.1.26

Lu S, Wang H, Yao Z. Isolation and characterization of gasoline-degrading bacteria from gas station leaking-contaminated soils. J Environ Sci (China). 2006a Sep;18(5):969–972. doi:10.1016/S1001-0742(06)60023-5 Medline

Lu S, Wang H, Yao Z. Isolation and characterization of gasoline-degrading bacteria from gas station leaking-contaminated soils. J Environ Sci (China). 2006b Sep;18(5):969–972. doi:10.1016/S1001-0742(06)60023-5 Medline

Maniatis T, Fritsch EF, Sambrook J. Molecular cloning: a laboratory manual. New York (USA): Cold Spring Harbor; 1982.

Marchand C, St-Arnaud M, Hogland W, Bell TH, Hijri M. Petroleum biodegradation capacity of bacteria and fungi isolated from petroleum-contaminated soil. Int Biodeterior Biodegradation. 2017 Jan;116:48–57. doi:10.1016/j.ibiod.2016.09.030

Marin MM, Smits THM, van Beilen JB, Rojo F. The alkane hydroxylase gene of *Burkholderia cepacia* RR10 is under catabolite repression control. J Bacteriol. 2001 Jul 15;183(14):4202–4209. doi:10.1128/JB.183.14.4202-4209.2001 Medline

Mnif S, Chamkha M, Labat M, Sayadi S. Simultaneous hydrocarbon biodegradation and biosurfactant production by oilfield-selected bacteria. J Appl Microbiol. 2011 Sep;111(3):525–536. doi:10.1111/j.1365-2672.2011.05071.x Medline

Morlett-Chávez JA, Ascacio-Martínez JÁ, Haskins WE, Acuña-Askar K, Barrera-Saldaña HA. Gene expression during BTEX biodegradation by a microbial consortium acclimatized to unleaded gasoline and a *Pseudomonas putida* strain (HM346961) isolated from it. Pol J Microbiol. 2017 Jun 28;66(2):189–199. doi:10.5604/01.3001.0010.7836 Medline

Mujahid TY, Wahab A, Padhiar SH, Subhan SA, Baloch MN, Pirzada ZA. Isolation and characterization of hydrocarbon degrading bacteria from petrol contaminated soil. J Basic Appl Sci. 2015 Mar 05;11:223–231. doi:10.6000/1927-5129.2015.11.32

Nalini P, Ellaiah P, Prabhakar T, Girijasankar G. Microbial alkaline phosphatases in bioprocessing. Int J Curr Microbiol Appl Sci. 2015;4:384–396.

Ozyurek SB, Bilkay IS. Determination of petroleum biodegradation by bacteria isolated from drilling fluid, waste mud pit and crude oil. Turk J Biochem. 2017;42:609–616.

Patowary K, Patowary R, Kalita MC, Deka S. Development of an efficient bacterial consortium for the potential remediation of hydrocarbons from contaminated sites. Front Microbiol. 2016 Jul 14;7:1092. doi:10.3389/fmicb.2016.01092 Medline

Perera F. Pollution from fossil-fuel combustion is the leading environmental threat to global pediatric health and equity: solutions exist. Int J Environ Res Public Health. 2017 Dec 23;15(1):16. doi:10.3390/ijerph15010016 Medline

Rani V, Mohanram S, Tiwari R, Nain L, Arora A. Beta-glucosidase: key enzyme in determining efficiency of cellulase and biomass hydrolysis. J Bioprocess Biotech. 2014;5:2.

Rappaport SM, Selvin S, Waters MA. Exposures to hydrocarbon components of gasoline in the petroleum industry. Applied Industrial Hygiene. 1987 Jul;2(4):148–154. doi:10.1080/08828032.1987.10390542

Ridgway HF, Safarik J, Phipps D, Carl P, Clark D. Identification and catabolic activity of well-derived gasoline-degrading bacteria from a contaminated aquifer. Appl Environ Microbiol. 1990 Nov; 56(11):3565–3575 Medline.

Saravanan C, Rajesh R, Kaviarasan T, Muthukumar K, Kavitake D, Shetty PH. Synthesis of silver nanoparticles using bacterial exopolysaccharide and its application for degradation of azo-dyes. Biotechnol Rep (Amst). 2017 Sep;15:33–40. doi:10.1016/j.btre.2017.02.006 Medline

Sarkar P, Roy A, Pal S, Mohapatra B, Kazy SK, Maiti MK, Sar P. Enrichment and characterization of hydrocarbon-degrading bacteria from petroleum refinery waste as potent bioaugmentation agent for in situ bioremediation. Bioresour Technol. 2017 Oct;242: 15–27. doi:10.1016/j.biortech.2017.05.010 Medline

Satyam K, Kumar D, Kumar P, Anand R, Kumar A, Roy K. Investigation of oil degrading ability of bacteria isolated from oil. Paripex - Indian J Res. 2018; 7(2):71–73.

Scigelova M, Crout DHG. Microbial β-N-acetylhexosaminidases and their biotechnological applications. Enzym Microb Technol. 1999 Jul;25(1-2):3–14. doi:10.1016/S0141-0229(98)00171-9

Sekkal S, Haddam N, Scheers H, Poels KL, Bouhacina L, Nawrot TS, Veulemans HA, Taleb A, Nemery B. Occupational exposure to petroleum products and respiratory health: a cross-sectional study from Algeria. J Occup Environ Med. 2012 Nov; 54(11):1382–1388. doi:10.1097/JOM.0b013e31825fa6c9 Medline

Sharma A, Bala K, Husain I. Optimization of arginine deaminase production from indigenous bacterium *Pseudomonas aeruginosa* PS2. Int J Curr Microbiol Appl Sci. 2017 Nov 20;6(11):3621–3632. doi:10.20546/ijcmas.2017.611.424

Silhavy TJ, Kahne D, Walker S. The bacterial cell envelope. Cold Spring Harb Perspect Biol. 2010 May 01;2(5):a000414. doi:10.1101/cshperspect.a000414 Medline

Silva TF, Rodrigues DRF, Coutinho GBF, Soares M, Almeida MS, Sarcinelli PN, Mattos RCOC, Larentis AL, Matos GGO. Ototoxicity of hydrocarbons present in gasoline: a literature review. Rev CEFAC. 2018 Feb;20(1):110–122. doi:10.1590/1982-021620182015617

Singh RS, Chauhan K, Kennedy JF. A panorama of bacterial inulinases: Production, purification, characterization and industrial applications. Int J Biol Macromol. 2017 Mar;96:312–322. doi:10.1016/j.ijbiomac.2016.12.004 Medline

Surendra SV, Mahalingam BL, Velan M. Degradation of mono-aromatics by *Bacillus pumilus* MVSV3. Braz Arch Biol Technol. 2017;60(0):60. doi:10.1590/1678-4324-2017160319

Thapa B, Kc AK, Ghimire A. A review on bioremediation of petroleum hydrocarbon contaminants in soil. Kathmandu U J Sci Eng Technol. 2012;8:164–170.

Varjani SJ. Microbial degradation of petroleum hydrocarbons. Bioresour Technol. 2017 Jan;223:277–286. doi:10.1016/j.biortech.2016.10.037 Medline

Vignesh R, Arularasan A, Gandhiraj V, Deepika RC. Isolation identification and characterization of potential oil degrading bacteria from oil contaminated sites. Int Res J Eng Technol. 2016;3(4): 2503–2508.

Xu X, Liu W, Tian S, Wang W, Qi Q, Jiang P, Gao X, Li F, Li H, Yu H. Petroleum hydrocarbon-degrading bacteria for the remediation of oil pollution under aerobic conditions: a perspective analysis. Front Microbiol. 2018 Dec 3;9:2885. doi:10.3389/fmicb.2018.02885 Medline

Xue H, Xiaolin W, Zhaowei H. Mechanism of degradation for petroleum hydrocarbon by *Brevibacillus brevis* and *Bacillus cereus*. Acta Petrol Sin. 2006;27:92.

Yuniati MD. Bioremediation of petroleum-contaminated soil: A review. IOP Conf. Ser.: Earth Environ. Sci. 2018;118:012063. doi:10.1088/1755-1315/118/1/012063

Zhan Y, Tao X, He S, Song S, Xing J, Li F, Jiang T, Ma L. Isolation, identification and degradation characteristics of oil degrading bacterial strain. OAlib. 2017;04(10):1–12. doi:10.4236/oalib.1104016

Zhao D, Kumar S, Zhou J, Wang R, Li M, Xiang H. Isolation and complete genome sequence of *Halorientalis hydrocarbonoclasticus* sp. nov., a hydrocarbon-degrading haloarchaeon. Extremophiles. 2017 Nov;21(6):1081–1090. doi:10.1007/s00792-017-0968-5 Medline

Supplementary materials are available on the journal's website.

Polish Journal of Microbiology
2019, Vol. 68, No 2, 203–209
https://doi.org/10.33073/pjm-2019-020

ORIGINAL PAPER

Prevalence and Antimicrobial Properties of Lactic Acid Bacteria in Nigerian Women During the Menstrual Cycle

FOLASHADE GRACE ADEOSHUN[1], WERNER RUPPITSCH[2], FRANZ ALLERBERGER[2] and FUNMILOLA ABIDEMI AYENI[1]*

[1] Department of Pharmaceutical Microbiology, Faculty of Pharmacy, University of Ibadan, Ibadan, Oyo State, Nigeria
[2] Austrian Agency for Health and Food Safety, Institute of Medical Microbiology and Hygiene, Vienna, Austria

Submitted 7 December 2018, revised 31 January 2019, accepted 1 February 2019

Abstract

The composition of vagina lactic acid bacteria (LAB) differs within the different ethnic group. This study is aimed at determining the prevalence of LAB with their antimicrobial properties in Nigerian women's vagina during different stages of the menstrual cycle. Microorganisms were isolated from vaginal swabs of ten Nigerian women during different stages of the menstrual cycle and identified by partial sequencing of the 16S rRNA gene. The antimicrobial properties of the LAB were tested against the multidrug-resistant uropathogens. The prevalence of LAB was higher during ovulation period while during menstruation period, it declined. Twenty-five LAB isolates were identified as three species, namely: *Lactobacillus plantarum* (15), *Lactobacillus fermentum* (9), *Lactobacillus brevis* (1) and one acetic acid bacteria – *Acetobacter pasteurianus*. The LAB had antimicrobial activities against the three uropathogens with zones of inhibition from 8 to 22 mm. The presence of LAB inhibits the growth of *Staphylococcus* sp. GF01 also in the co-culture. High LAB counts were found during ovulation period with *L. plantarum* as a dominant species while during menstruation, there was a decrease in the LAB counts. The isolated LAB has antimicrobial properties against the urogenital pathogens tested thus exhibiting their potential protective role against uropathogens.

Key words: menstrual cycle, Nigerian women, lactobacilli, uropathogens

Introduction

A healthy human vagina is primarily colonized by the genus *Lactobacillus* (Shiraishi et al. 2011) and it builds a barrier separating the pathogens from the epithelium, thereby, protecting the vagina. The pH ~4.5 also maintains the balance of the vaginal ecosystem as well as antimicrobial substances e.g. hydrogen peroxide against pathogens (Ayeni and Adeniyi 2013; Ghartey 2014). Occasional and recurrent vaginal yeast and bacterial imbalances are common among premenopausal women, which can be due to hormonal changes during menstrual cycle, antibiotic treatment, pregnancy, sexual intercourse, excessive intimate hygiene and use of tampons, which may predispose a woman to infections.

The hormonal changes occur during the reproductive stages with the resulting fluctuating levels of hormones that regulate the menstrual cycle. This is an important influence on the vaginal microbiota during human reproductive years (Farage et al. 2010). Women of different racial groups may exhibit different composition of microbial communities and, correspondingly, different susceptibility to vaginal infections. Women are more prone to urinary tract infections (UTI) than men due to the position of the urethra. The reduction in protective vaginal flora may increase the risk of these infections (Gupta et al. 2017).

Lactic acid bacteria (LAB) have been shown to inhibit the *in vitro* growth of pathogenic microorganisms, e.g. *Klebsiella* spp. *Neisseria gonorrhoeae*, *Pseudomonas aeruginosa*, *Candida albicans*, *Staphylococcus aureus*, *Escherichia coli*, etc. (Ayeni and Adeniyi 2012; Adeoshun and Ayeni 2016). This can be achieved mainly through the action of lactic acid (Graver and Wade 2011). During menstruation, the diminished population of lactobacilli and the presence of menstrual fluid make the vaginal less acidic, therefore, more prone to colonization by pathogenic microorganisms.

* Corresponding author: F.A. Ayeni, Department of Pharmaceutical Microbiology, Faculty of Pharmacy, University of Ibadan, Ibadan, Oyo State, Nigeria; **e-mail: funmiyeni@yahoo.co.uk**

Changes between different bacterial species in the vagina are associated with menses (Gajer et al. 2012).

The antimicrobial activity of the vaginal fluids correlates with an increased lactic acid content, low pH and competitive exclusion. The increased susceptibility to disease may be also related to vaginal microbiota fluctuations (Gajer et al. 2012). Ayeni and Adeniyi (2013) and Agboola et al. (2014) had reported the presence of organisms in healthy and menstruating women with their antimicrobial properties in Nigeria. However, there is no information to establish changes in vaginal microbiota at different stages of the menstrual cycle and the antimicrobial effects of the isolated LAB. Therefore, this study aimed at determining the prevalence of LAB at different stages of the menstrual cycle in Nigerian women with their potential antimicrobial properties.

Experimental

Materials and Methods

Pathogens. Ten clinical strains of uropathogens: *Klebsiella* spp., *Staphylococcus* spp. and *Pseudomonas* spp. (isolated from urine) were collected from the culture collection of the Medical Microbiological Laboratory of the University College of Medicine (UCH), Ibadan.

Sample collections, isolation, and lactic acid bacteria viability counts. Ethical approval (UI/EC/13/0258) was obtained from the Institutional Ethical Committee (IEC), Institute for Advanced Medical Research and Training (IAMRAT), College of Medicine, University of Ibadan, Ibadan, Nigeria. Ten Nigerian women volunteers aged between 20–40 years were recruited into this study. They were premenopausal, self-declared healthy, not on antibiotics or hormonal therapy for at least four months, not on contraceptives, having regular menstrual cycle, i.e. a complete menstrual cycle between 25–30 days every month, and exhibiting the three different stages within the cycle. For each volunteer, Day 1 of menstrual flow is noted as day one of the menstrual cycle. For a five-days flow, samples were taken on day 3 and for a 4-days flow, samples were taken on day 2. Safe period is between 6^{th}–12^{th} day of the menstrual cycle while the ovulation period is between 13^{th}–15^{th} day of the menstrual cycle. The safe period samples were taken on day 6 after menstrual flow stopped. The ovulation period samples were obtained midway of the menstrual cycle. The signed informed consent was obtained from each volunteer. The samples were collected from the volunteers during different stages of their menstrual cycle between August and September 2014. The volunteers used sterile swab sticks to swab the vagina according to the standard protocols. The samples were collected during the three different stages of the menstrual cycle and immediately inoculated in 10 ml MRS broth, (Oxoid, UK) adjusted to pH 5, shaken vigorously for 10 s and incubated under the microaerophilic condition using CampyGen™ at 37°C for 24 h. Serial dilutions were done using sterile normal saline and the suspension of the suitable dilution factor was plated out on MRS agar by pour plate method, then incubated under microaerophilic condition at 37°C for 48 h. The initial colony counts were noted and colonies were picked according to the differences in their colony morphology on MRS agar plates and isolated by streaking onto another MRS agar to obtain a distinct colony. Gram staining and catalase test were carried out and only the colonies that were Gram-positive and catalase-negative were picked and stored in MRS broth containing 20% w/v glycerol at –20°C for further characterization and identification.

Identification of Lactic Acid Bacteria. The DNA of the LAB isolated were extracted by QuickExtract™ DNA extraction solution (Epicentre, Wisconsin) according to the manufacturer's instructions. The PCR mixture consisted of a total volume of 20 µl (1 µl of DNA extract, 10 pmol of each primer, and 25 µl of 2-fold concentrated RedTaq Ready Mix (SigmaAldrich, Germany)). The primers used for amplification were (5'-TGTAA AACGGCCAGTAGAGTTTGATC(AC)TGGCTCAG) and (5'-CAGGAAACAGCTATGACCG(AT)ATTAC CGCGGC(GT)GCTG), containing an M13 primer sequence (Montanaro et al. 2016). PCR conditions were 95°C for 5 min; 35 cycles each of 95°C for 15 s, 58°C for 30 s, and 72°C for 45 s; and a final step at 72°C for 10 min. Ten microliters of the amplified products were analyzed on 1.5% agarose gels and subsequently sequenced using the BigDye Terminator v3.1 sequencing kit (Applied Biosystems, California). The sequence was blasted against the NCBI database for species identification. The nucleotide sequences for the 16S rRNA genes have been deposited in the GenBank database under accession numbers KX261342 to KX261366.

Antibiotic susceptibility of uropathogens. Ten uropathogenic strains were collected and screened against seven antibiotics by disk diffusion methods. A bacterial lawn was accomplished by spreading inoculum from 10^8 dilution factor of the pathogen culture which is approximately equivalent to 0.5 McFarland standards by a sterile swab stick. The antibiotic disks containing ceftazidime (30 µg), cefotaxime (30 µg), cefuroxime (30 µg), Augmentin (amoxicillin clavulanate) (10 µg), ciprofloxacin (30 µg), ofloxacin (30 µg), and gentamycin (30 µg) were placed on the surface of the solidified agar with the aid of sterile forceps and incubated aerobically at 37°C for 24 h. The susceptibility of the test organisms to the antibiotics used was documented by measuring the diameter of the clear zones of inhibition in millimeter (mm) around the antibiotics disks, and the

results were interpreted according to the guidelines of European Committee on Antimicrobial Susceptibility Testing (2015). The resistant strains were selected for LAB antimicrobial study.

Determination of LAB antimicrobial activities against bacterial uropathogens. To study the antimicrobial potential of the LAB against clinical isolates of uropathogens, three different methods were employed, which are: using the cell free supernatant *via* agar well diffusion method, using the viable LAB cells *via* agar overlay method, and co-culture of the LAB and uropathogens.

Determination of the antimicrobial activity of the cell-free supernatant. The LAB isolates were grown in MRS broth overnight under the microaerophilic condition at 37°C, centrifuged at 10 000 rpm for 10 min and the supernatant decanted. The antimicrobial activities of the cell-free supernatant were determined twice, i.e. before and after neutralization to pH of 6.5 with 1 M NaOH, using the agar well diffusion assay against *Staphylococcus* sp. GF01, *Pseudomonas aeruginosa* GF01, and *Klebsiella* sp. GF01.

Determination of the antimicrobial activity of viable lactic acid bacterial cells. The modified agar overlaid method as described by Ayeni et al. (2011) was used in this study. In summary, the LAB cells in broth were inoculated in two 2-cm-long lines on an MRS agar surface and then incubated at 37°C for 24–48 h in microaerophilic conditions. The plates were overlaid with 0.2 ml of an overnight broth culture of the test pathogen vehiculated in 10 ml soft nutrient agar and incubated at 37°C under aerobic condition. The plates were then examined for a clear zone of inhibition around the line of the LAB and the clear zones were measured in millimeters.

Coculture of lactic acid bacteria and uropathogens. The interference of the LAB strains with the growth of uropathogenic strains was evaluated by coincubating *Staphylococcus* sp. GF01 with four representative strains of LAB (*Lactobacillus brevis* GF021, obtained from the menstruation period, *Lactobacilus fermentum* GF002, *Lactobacillus plantarum* GF011, obtained from the safe period and *Lactobacillus fermentum* GF019, obtained from the ovulation period). This was done in two series of experiments.

In the first experiment, an overnight culture of *Staphylococcus* sp. GF01 was inoculated into 5 ml double strength nutrient broth and then added to 5 ml of overnight culture of the LAB and the mixture was incubated for 24 h. The monoculture of the mixture, the LAB and *Staphylococcus* sp. GF01 (control) was evaluated at time zero (t_0) and after incubation. For the second experiment, 5 ml of *Staphylococcus* sp. GF01 was incubated for 8 h, after which it was centrifuged and the supernatant discarded, 5 ml of double strength nutrient broth was added to resuspend the pellets, vortexed and added to a 5 ml of overnight culture of the LAB. *Staphylococcus* sp. GF01 monoculture and the mixture was plated out at 8 h and 24 h to evaluate the growth of *Staphylococcus* sp. GF01.

Results

The three organisms used exhibited high resistance (i.e. 0 mm zones of inhibition) towards most of the antibiotics used. The *Pseudomonas* and *Staphylococcus* strains tested were resistant to ceftazidime, cefotaxime, cefuroxime, Augmentin (amoxicillin clavulanate) but sensitive to ciprofloxacin, ofloxacin, and gentamycin, while the *Klebsiella* sp. GF01 strain was completely resistant to all the antibiotics.

Ten volunteers were assessed for a level of LAB in their vagina at different stages of the menstrual cycle. It was observed that in seven (70%) out of the ten volunteers, there was a significant shift of the LAB level from low to high (8×10^5 to 7.6×10^9) CFU/ml over the course of the menstrual cycle. In the remaining three (30%) volunteers, the presence of LAB was not observed throughout the menstrual cycle (Table I).

A total of twenty-seven (27) bacterial species were identified from the three different stages of menstrual cycle as five species (*L. plantarum* (15), *L. fermentum* (9), *Lactobacillus brevis* (1), *Bacillus safensis* (1) and *Acetobacter pasteurianus* (1)) and their percentage occurrence at different stages of the menstrual cycle was shown in Table I. Twenty-five (25) isolates (92.59%) belonging to the genus *Lactobacillus* occurred in the three stages, while one (1) isolate (3.70%) each belonged to *Bacillus* and *Acetobacter*, both noted during safe (follicular) period, only. The organism with the highest frequency of occurrence (60%) among the *Lactobacillus* species was *L. plantarum* and it constituted 55.55% among all the isolates studied, and its highest occurrence was during the ovulation period. *L. brevis* has the lowest frequency of occurrence of 4% among the *Lactobacillus* spp. and 3.7% among the total isolates, and it occurred during the menstruation period.

The cell-free supernatants and viable cells showed a clear inhibitory antimicrobial activity against *Pseudomonas aeruginosa* GF01, *Klebsiella* sp. GF01 and *Staphylococcus* sp. GF01. Out of 27 LAB isolates used against *P. aeruginosa* GF01, 20 (74.07%) of the isolates had zones of inhibition ranging from 8 to 22 mm against *Klebsiella* sp. GF01, 24 (88.89%) had zones of inhibition ranging from 10 to 20 mm, while 20 (74.07%) had inhibition zones ranging from 10 to 20 mm against *Staphylococcus* sp. GF01. *Staphylococcus* sp. GF01 was the least susceptible to the LAB isolated while *Klebsiella* sp. GF01 was the most susceptible (Table II).

Table I
Evaluation of the LAB counts at different stages of the menstrual cycle.

Week	Menstruation Period		Safe Period		Ovulation Period	
	Total CFU/ml	LAB CFU/ml	Total CFU/ml	LAB CFU/ml	Total CFU/ml	LAB CFU/ml
1	1.02×10^{8}	4.2×10^{7}	1.81×10^{10}	9.3×10^{9}	2.22×10^{10}	1.51×10^{10}
2	5.6×10^{7}	1.0×10^{6}	1.91×10^{10}	5.2×10^{9}	1.90×10^{10}	1.14×10^{10}
3	7.8×10^{7}	1.2×10^{6}	1.89×10^{10}	7.4×10^{9}	2.53×10^{10}	1.51×10^{10}
4	7.0×10^{7}	2.2×10^{6}	1.87×10^{10}	1.89×10^{10}	9.8×10^{9}	–
5	9.2×10^{7}	1.4×10^{6}	1.52×10^{10}	4.2×10^{9}	1.87×10^{10}	1.02×10^{10}
6	6.1×10^{7}	8×10^{5}	8.3×10^{9}	3.0×10^{9}	1.12×10^{10}	7.6×10^{9}
7	1.13×10^{8}	2.5×10^{6}	2.11×10^{10}	5.4×10^{9}	3.26×10^{10}	1.02×10^{10}
8	2.0×10^{3}	Nil	1.05×10^{4}	–	1.05×10^{4}	Nil
9	3.8×10^{3}	Nil	8.5×10^{3}	–	5.8×10^{3}	Nil
10	4.2×10^{3}	Nil	1.12×10^{4}	–	8.5×10^{3}	Nil

Note – Nil means no count of bacteria

Table II
Determination of the antimicrobial activity of the cell-free supernatant and viable cells.

	Cell-free supernatant			Viable Cell*		
	P. aeruginosa GF01	*Klebsiella* sp. GF01	*Staphylococcus* sp. GF01	*P. aeruginosa* GR01	*Klebsiella* sp. GR01	*Staphylococcus* sp. GF01
L. fermentum GF002	16	12	20	20	15	20
A. pasteurianus GF004	20	13	0	20	18	12
L. plantarum GF005	15	14	0	18	20	0
L. fermentum GF006	15	14	12	18	20	15
L. plantarum GF007	20	10	15	20	15	18
L. fermentum GF008	15	15	15	20	18	18
L. plantarum GF009	10	12	13	19	20	15
L. plantarum GF010	20	12	10	15	20	20
L. plantarum GF011	22	13	17	20	16	20
L. fermentum GF012	19	14	0	20	20	18
L. fermentum GF013	22	12	0	13	18	20
L. plantarum GF015	18	10	0	20	15	20
L. plantarum GF016	19	12	0	20	20	20
L. fermentum GF018	19	20	20	20	20	15
L. fermentum GF019	18	20	16	20	15	20
L. brevis GF021	19	20	15	20	20	20
L. plantarum GF022	8	10	0	0	20	15
L. plantarum GF023	10	0	0	12	15	0
L. fermentum GF024	14	13	15	12	15	15
L. plantarum GF025	10	15	0	10	18	0
L. fermentum GF026	0	18	0	0	18	0
L. plantarum GF029	0	0	0	0	0	0
L. plantarum GF030	0	0	0	10	0	0
B. safensis GF031	0	13	0	10	15	0
L. plantarum GF032	0	10	0	0	10	0
L. plantarum GF033	0	18	18	10	18	18
L. plantarum GF036	0	10	0	0	12	0

* Antimicrobial activity is expressed as diameters of inhibition zones in mm

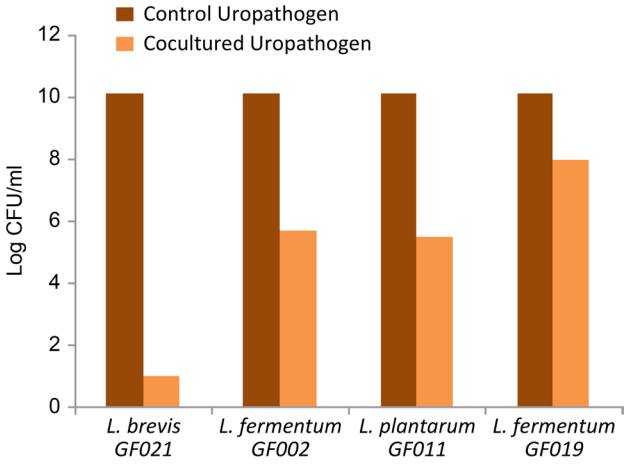

Fig 1. Inhibition of *in vitro* growth of *Staphylococcus* sp. GF01 by *L. brevis* GF021, *L. fermentum* GF002, *L. plantarum* GF011, and *L. fermentum* GF019 after 24 h – coincubation.

After the neutralization of the cell-free supernatant, no obvious antimicrobial activity was observed against the uropathogens.

The capability of the LAB strains to inhibit the *in vitro* growth of *Staphylococcus* sp. GF01 was evaluated in coculture experiment which was carried out in two parts. In the first experiment, *L. brevis* GF021 was active against *Staphylococcus* sp. GF01 with 6 $\log_{10}$ reduction after 24 h, had and 5 $\log_{10}$ reduction of *Staphylococcus* sp. GF01 after incubation with *L. fermentum* GF002 or *L. plantarum* GF011. *L. fermentum* GF019 had a low activity against *Staphylococcus* sp. GF01, which demonstrated only 3 $\log_{10}$ reduction in numbers of CFU. It was observed that *Staphylococcus* sp. GF01 did not have an effect on any of the LAB strains (Fig. 1). In the second experiment, *Lactobacillus brevis* GF021 was active against *Staphylococcus* sp. GF01 with a 6 $\log_{10}$ reduction. *L. fermentum* GF002 and *L. plantarum* GF011 were not active against *Staphylococcus* sp. GF01 while *L. fermentum* GF019 showed a low activity against *Staphylococcus* sp. GF01 with just 1 $\log_{10}$ reduction. *L. fermentum* GF019 had the least activity and *L. brevis* GF021 had the highest activity (6 $\log_{10}$ reduction) on *Staphylococcus* sp. GF01 (Fig. 2).

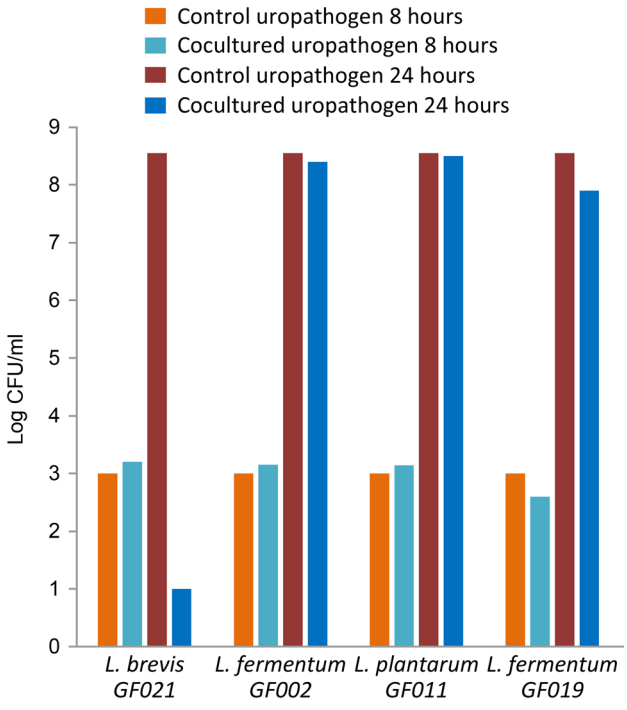

Fig 2. Inhibition of *in vitro* growth of *Staphylococcus* sp. GF01 by *L. brevis* GF021, *L. fermentum* GF002, *L. plantarum* GF011, and *L. fermentum* GF019 at 8 and 24 h of coincubation.

Discussion

The resistance to broad-spectrum antibiotics is a persistent challenge in the management of infections (Ayeni et al. 2011). In this study, *Klebsiella* sp. GF01, *P. aeruginosa* GF01 and *Staphylococcus* sp. GF01 were isolated from urogenital infections. These uropathogens were found to be multidrug resistant, especially *Klebsiella* sp. GF01, which was completely resistant to all the antibiotics tested in this study. This high phenotypic resistance is making the present antibiotic therapy for bacterial infections ineffective thereby resulting in more search for naturally occurring remedies, e.g. LAB (Ayeni et al. 2011).

The species of beneficial bacteria identified from the vaginal samples in this study were *L. fermentum, L. brevis*, *L. plantarum*, *B. safensis*, and *A. pasteurianus.* Out of 27 isolates, 25 isolates were lactobacilli where *L. plantarum* and *L. fermentum* were the most predominant species, with *L. plantarum* having the highest occurrence during the ovulation period. Dareng et al. (2016) also reported *Lactobacillus iners* and *Lactobacillus crispatus* in the vagina of Nigerian women, while a study of vaginal *Lactobacillus* strain in the pregnant Korean women reported prevalence of *L. crispatus* and *L. iners*, followed by *L. gasseri* and *L. jensenii* (Kim et al. 2017). There are versatility and species diversity in the prevalent lactobacilli present in the vagina. This can stem from different lifestyles, geographical and environmental conditions. There is usually a predominance of *Lactobacillus* in healthy women, including *L. iners* and *L. crispatus* in women in the reproductive age (Xu et al. 2013; Ghartey et al. 2014). However, there may be also a complete absence of lactobacilli in the other apparently healthy women. This is in accordance with this study, in which twenty-seven LAB were isolated from the vagina of seven healthy Nigerian women out of the ten volunteers, while no the LAB was detected in three of the women. This result of the LAB absence in women could be due to immunosuppression. Other factors could include infections, stress, nutrition intake, etc.

Many researchers have reported the prevalence of different LAB species isolated from the vagina of women from different geographical area (Gajer et al. 2012; Chaban et al. 2014; Shiraishi et al. 2011), but few have been able to report the type of LAB present or absent during the different stages of a woman's menstrual cycle in different countries and specific ethnic aspects; this could influence the structure of the microbiota in specific niches. It was observed that during the menstruating period, the LAB count was low while at the safe/follicular period, the presence of the LAB was greater, but a large amount of LAB was found at the latter part of the cycle. Thereby, there was a significant shift in the LAB level from low to high over the course of the menstrual cycle. Menstruation may enhance a distortion of the bacterial microbiota around the vulva (Shiraishi et al. 2011) and influence *Lactobacillus* spp. which were the dominant organism in most girls before the onset of menses from the early to middle stages of puberty (Hickey et al. 2015).

The absence or low the LAB count during menses may suggest the growth of yeast which can outgrow the bacteria in immunocompromised patients causing yeast and other urogenital infections. However, during safe and ovulation periods when the LAB count is increasing there is a decrease in the yeast count probably due to the antagonistic effect of these LAB on yeast or the hormonal changes taking place during these periods (Relloso et al. 2012). Women may be more susceptible to urogenital tract infections during the menstruation period compared to the ovulation period due to the high prevalence of the LAB during the ovulation period. The dynamic nature of the vaginal environment leads to changes in the microbiota of the vagina as a result of exposure to pathogens and physiologic fluctuations of the menstrual cycle (Farage et al. 2010). In the course of this study, *L. plantarum* dominated during the ovulation period, *L. brevis* was found during menstruation and *B. safensis* during the safe period. The presence of these organisms at different periods can be attributed to change in vagina pH, hormonal change and even the blood flow during menses.

Lactobacilli isolated from the vagina have a prominent role as a prophylactic aimed at improving the vaginal microbiota defense against bacterial infections. The cell-free supernatant and the viable LAB cells exhibited capabilities to inhibit the growth of the uropathogens, albeit to a different extent. The vaginal strains of *L. acidophilus* had been reported to inhibit the growth of *Klebsiella* sp. and some other uropathogenic strains (Ayeni and Adeniyi 2012; Adeoshun and Ayeni 2016). Most of the *L. plantarum* strains showed the most impressive effect. The antagonistic activity of *L. brevis* GF021 was also appreciable. It was suggested that the organic acid produced by these LAB play a major role in the antagonistic activity because after neutralization, there was no obvious effect. This result agrees with Ayeni et al. (2011) who reported that the antimicrobial properties of LAB are related to their metabolic products such as organic acids and hydrogen peroxide. Non-lactic acid bacterial strains i.e. *B. safensis* and *A. pasteurianus* also could inhibit the uropathogens growth. To the best of our knowledge, this is the first study that will report the presence of these two species in the vagina of a woman. *B. safensis* has biotechnological and industrial potentials (Larboda et al. 2014) while *A. pasteurianus* is important in vinegar production (Viana et al. 2017). The mechanism by which this organism inhibits the three uropathogens used in this study is probably due to the production of acetic acid.

The resistance of *S. aureus* strain to the cell-free supernatant from most of the LAB strains in this study prompted another mechanism of antagonism through co-culture experiment. Bamidele et al. (2013) also reported that methicillin-resistant *S. aureus* (MRSA) strains were resistant to the cell-free supernatants of the LAB but higher activities were shown when the LAB was in contact with the pathogens. Different LAB strains have different rates of the killing of *Staphylococcus* sp. GF01. In the first experiment, the growth of *Staphylococcus* sp. GF01 was not influenced by the presence of the lactobacilli while for the second experiment, the 8 h already grown *Staphylococcus* sp. GF01 overpowered the LAB activity, except for *L. brevis.* Very good activity demonstrated the strain *L. brevis* GR01. There was an inhibition ($5 \log_{10}$ reduction) observed only when the pathogen was freshly introduced but no effect was noted towards the 8 h already grown pathogen. The study of Adetoye et al. (2018) reveals a similar process where it was reported that an effective inhibition was observed when the LAB was co-cultured with the pathogens. The presence of the LAB inhibited the growth of *Staphylococcus* sp. GF01 freshly introduced, while for the already 8 h grown *Staphylococcus* sp. GF01, the effect of LAB was not obvious, except for *L. brevis.* It was suggested that *Staphylococcus* sp. GF01 was able to overpower or suppress the activity of the LAB. The decrease in the number of *Staphylococcus* sp. GF01 reveals the antimicrobial activity of the LAB cells against *Staphylococcus* sp. GF01. These data support the result obtained previously using the cell-free supernatant and the viable LAB cells confirming the high resistance of *Staphylococcus* sp. GF01 to the LAB strains.

Conclusion

The high LAB counts were found during the ovulation period while during menstruation, there was a decrease in the LAB counts. The highest occurrence

in the vagina of Nigerian women was shown for *L. plantarum* that mostly was found during the ovulation period. The LAB isolated has the antimicrobial properties against multidrug-resistant urogenital pathogens what may be applicable *in vivo*. The fermented foods such as Ogi, yogurt, etc. can be consumed during menstruation in order to replenish the beneficial bacteria. To the best of our knowledge, this is the first study in Nigeria to report a prevalence of the LAB with their protective role at different stages of a woman's menstrual cycle and also the first study to show the presence of *B. safensis* and *A. pasteurianus* in the vagina of a woman.

ORCID
Funmilola A. Ayeni 0000-0002-2379-0135

Limitation of the study

The only lactic acid bacteria mechanism of antibacterial activity investigated in this study is an organic acid. Other mechanisms might be responsible. Also, the volunteers were self-declared healthy.

Conflict of interest

The authors do not report any financial or personal connections with other persons or organizations, which might negatively affect the contents of this publication and/or claim authorship rights to this publication.

Literature

Adeoshun FG, Ayeni FA. Antagonistic effect of four *Lactobacillus* sp. on multidrug resistant *Klebsiella* sp. GF01 in coculture. African J Pharm Res Dev. 2016;8:81–87.

Adetoye A, Pinloche E, Adeniyi BA, Ayeni FA. Characterization and anti-salmonella activities of lactic acid bacteria isolated from cattle faeces. BMC Microbiol. 2018 Dec;18(1):96. doi:10.1186/s12866-018-1248-y Medline

Agboola FM, Adeniyi BA, Okolo CA, Ogunbanwo TO, Ayeni FA, Lawal TO. Probiotic potentials of Lactic Acid Bacteria isolated from vaginal swabs on selected genital pathogens. IJPSR. 2014;5(7): 2642–2650.

Ayeni FA, Adeniyi BA. Antagonistic activities of lactic acid bacteria against organisms implicated in urogenital infections. African J Pharm Res Dev. 2012;4(2):59–69.

Ayeni FA, Adeniyi BA. Antimicrobial pontentials of Lactic Acid Bacteria isolated from a Nigerian menstruating woman. Turk Silahli Kuvvetleri Koruyucu Hekim Bul. 2013;12(3):283–290. doi:10.5455/pmb.1-1339602984

Ayeni FA, Sánchez B, Adeniyi BA, de los Reyes-Gavilán CG, Margolles A, Ruas-Madiedo P. Evaluation of the functional potential of *Weissella* and *Lactobacillus* isolates obtained from Nigerian traditional fermented foods and cow's intestine. Int J Food Microbiol. 2011 May;147(2):97–104. doi:10.1016/j.ijfoodmicro.2011.03.014 Medline

Bamidele TA, Adeniyi BA, Ayeni FA, Fowora MA, Smith SI. The antagonistic activities of Lactic acid bacteria isolated from Nigerian salad vegetables against methicillin resistant *Staphylococcus aureus*. Global Res J Microbiol. 2013;3(1):18–23.

Chaban B, Links MG, Jayaprakash T, Wagner EC, Bourque DK, Lohn Z, Albert AYK, van Schalkwyk J, Reid G, Hemmingsen SM, et al. Characterization of the vaginal microbiota of healthy Canadian women through the menstrual cycle. Microbiome. 2014; 2(1):23. doi:10.1186/2049-2618-2-23 Medline

Dareng EO, Ma B, Famooto AO, Akarolo-Anthony SN, Offiong RA, Olaniyan O, Dakum PS, Wheeler CM, Fadrosh D, Yang H, et al. Prevalent high-risk HPV infection and vaginal microbiota in Nigerian women. Epidemiol Infect. 2016 Jan;144(01): 123–137. doi:10.1017/S0950268815000965 Medline

EUCAST. *Enterobacteriaceae*: Breakpoint tables for interpretation of MICs and zone diameters. Version 5.0. The European Committee on Antimicrobial Susceptibility Testing. 2015.

Farage MA, Miller KW, Sobel JD. Dynamics of the vaginal ecosystem – hormonal influences. Infec Dis Res Treat. 2010;3:1–15.

Gajer P, Brotman RM, Bai G, Sakamoto J, Schütte UME, Zhong X, Koenig SSK, Fu L, Ma Z, Zhou X, et al. Temporal dynamics of the human vaginal microbiota. Sci Transl Med. 2012 May 02;4(132):132ra52. doi:10.1126/scitranslmed.3003605 Medline

Ghartey JP, Smith BC, Chen Z, Buckley N, Lo Y, Ratner AJ, Herold BC, Burk RD. *Lactobacillus crispatus* dominant vaginal microbiome is associated with inhibitory activity of female genital tract secretions against *Escherichia coli*. PLoS One. 2014 May 7; 9(5):e96659. doi:10.1371/journal.pone.0096659 Medline

Graver MA, Wade JJ. The role of acidification in the inhibition of *Neisseria gonorrhoeae* by vaginal lactobacilli during anaerobic growth. Ann Clin Microbiol Antimicrob. 2011;10(1):8. doi:10.1186/1476-0711-10-8 Medline

Gupta K, Grigoryan L, Trautner B. Urinary tract infection. Ann Intern Med. 2017 Oct 03;167(7):ITC49–ITC64. doi:10.7326/AITC201710030 Medline

Hickey RJ, Zhou X, Settles ML, Erb J, Malone K, Hansmann MA, Shew ML, Van Der Pol B, Fortenberry JD, Forney LJ. Vaginal microbiota of adolescent girls prior to the onset of menarche resemble those of reproductive-age women. MBio. 2015 May 01; 6(2):e00097-15. doi:10.1128/mBio.00097-15 Medline

Kim JH, Yoo SM, Sohn YH, Jin CH, Yang YS, Hwang IT, Oh KY. Predominant *Lactobacillus* species types of vaginal microbiota in pregnant Korean women: quantification of the five *Lactobacillus* species and two anaerobes. J Matern Fetal Neonatal Med. 2017 Oct 02;30(19):2329–2333. doi:10.1080/14767058.2016.1247799 Medline

Montanaro L, Ravaioli S, Ruppitsch W, Campoccia D, Pietrocola G, Visai L, Speziale P, Allerberger F, Arciola CR. Molecular characterization of a prevalent ribocluster of methicillin-sensitive *Staphylococcus aureus* from orthopedic implant infections. correspondence with MLST CC30. Front Cell Infect Microbiol. 2016 Feb 16;6:8. doi:10.3389/fcimb.2016.00008 Medline

Relloso M, Aragoneses-Fenoll L, Lasarte S, Bourgeois C, Romera G, Kuchler K, Corbí AL, Muñoz-Fernández MA, Nombela C, Rodríguez-Fernández JL, et al. Estradiol impairs the Th17 immune response against *Candida albicans*. J Leukoc Biol. 2012 Jan;91(1):159–165. doi:10.1189/jlb.1110645 Medline

Shiraishi T, Fukuda K, Morotomi N, Imamura Y, Mishima J, Imai S, Miyazawa K, Taniguchi H. Influence of menstruation on the microbiota of healthy women's labia minora as analyzed using a 16S rRNA gene-based clone library method. Jpn J Infect Dis. 2011;64(1):76–80. Medline

Viana RO, Magalhães-Guedes KT, Braga RA Jr, Dias DR, Schwan RF. Fermentation process for production of apple-based kefir vinegar: microbiological, chemical and sensory analysis. Braz J Microbiol. 2017 Jul;48(3):592–601. doi:10.1016/j.bjm.2016.11.006 Medline

Xu S, Zong L, Liu M, He Y, Huang X, Zhou H. [Illumina sequencing 16S rRNA tagging reveals diverse vaginal microbiomes associated with bacterial vaginosis] (in Chinese). Nan Fang Yi Ke Da Xue Xue Bao. 2013 May;33(5):672–677 Medline

Polish Journal of Microbiology
2019, Vol. 68, No 2, 211–216
https://doi.org/10.33073/pjm-2019-021

ORIGINAL PAPER

In situ Impact of the Antagonistic Fungal Strain, *Trichoderma gamsii* T30 on the Plant Pathogenic Fungus, *Rhizoctonia solani* in Soil

MUHAMMAD ANEES[1*], MUHAMMAD ABID[2], SOBIA CHOHAN[2], MUHAMMAD JAMIL[3], NADEEM AHMED[4], LIXIN ZHANG[5] and EUI SHIK RHA[6*]

[1] Department of Microbiology, Kohat University of Science & Technology, Kohat, Pakistan
[2] Department of Plant Pathology, Baha ud Din Zakaria University, Multan, Pakistan
[3] Department of Biotechnology & Genetic Engineering, Kohat University of Science & Technology, Kohat, Pakistan
[4] Department of Botany, Mohi ud Din Islamic University AJ&K, Pakistan
[5] Northwest A & F University Yangling, China
[6] Department of Well-being Resources, Sunchon National University, South Korea

Submitted 14 October 2018, revised 12 February 2019, accepted 12 February 2019

Abstract

Rhizoctonia solani is a soil-borne fungus causing a wide range of plants diseases. *Trichoderma gamsii* strain T30 has previously been reported as antagonistic against *R. solani*. Although there are a few studies about the influence of *Trichoderma* strains on the *R. solani* density in a pathosystem in the presence of plant hosts, this report for the first time comprehensively describes *in situ* effects of a *T. gamsii* strain on the population density of *R. solani* in the soil microcosmic conditions. The population dynamics of *R. solani* were followed in the autoclaved and non-autoclaved soils in artificially prepared microcosms up to day 25 after co-inoculation with *T. gamsii* in the variable ratios (R1/T1; R1/T0.1; R1/T0.01 of *R. solani*/*T. gamsii*). The population density of *R. solani* was evaluated by qPCR. In the autoclaved soil, target DNA copies of *R. solani* increased in the control samples from 1×10^5 to 6.5×10^6. At R1/T0.01, the number of target DNA copies were not significantly changed until day 11; however, it decreased by around five times at day 25. At R1/T0.1 and R1/T1, the number of DNA copies was reduced to 2.1×10^6 and 7.6×10^5 at day 11, respectively and the reduction was as much as 17 times at day 25. In the non-autoclaved soil, the number of the fungal cells decreased at day 25 whether inoculated or not with *Trichoderma* indicating a general suppression by the soil microbiome. In brief, *T. gamsii* significantly inhibited the growth of *R. solani* in the soil *in situ* and there was a general suppressive effect of the natural microbiome.

Key words: *Rhizoctonia solani*, *in situ* study, population density, antagonism, real-time PCR

Introduction

Rhizoctonia solani is a soil-borne plant pathogenic cosmopolitan fungus. It is present in a very low density in soils, but still capable of causing considerable losses in crops of economic importance (Anees et al. 2010a). It is a fungus having a broad host spectrum, generally causing damping off and root rot diseases in a variety of crops. The diseases caused by this fungus commonly occur in patches of various sizes that are spatially mobile i.e. the patch size and location change from one season to another (Schneider et al. 1997; Anees et al. 2010a). The increased suppressiveness inside patches was hypothesized as the probable reason behind the patch mobility because of the development of the antagonistic microbiota (Anees et al. 2010b). However, because of the intrinsic complexity of the soil medium and the low density of *R. solani*, the *in situ* exposure of the pathogen towards the antagonists has not been studied in natural soils in the absence of the plant hosts although there are some reports of the *in vitro* interaction between *Rhizoctonia* and *Trichoderma* (Zhang et al. 2015).

Trichoderma species are cosmopolitan ascomycetous saprotrophic fungi present in soil and are well known for their biocontrol potential (Anees et al. 2018). *Trichoderma* species reportedly use a few different mechanisms to control the plant pathogenic fungi;

* Corresponding authors: M. Anees, Department of Microbiology, Kohat University of Science & Technology, Kohat, Pakistan; **e-mail: dr.anees@kust.edu.pk**
E.S. Rha, Department of Well-being Resources, Sunchon National University, South Korea; **e-mail: euishik@sunchon.ac.kr**

the major mechanisms may include antibiosis, production of lytic enzymes, physical intervention including mycoparasitism and the niche competition (Anees et al. 2010c). Out of the more than 100 known species of *Trichoderma*, a few have been reported as the putative biocontrol agents. For example, strains of *T. virens* and *T. harzianum* were reported as the antifungals against *Armillaria mellae* (Asef et al. 2008). The disease caused by *R. solani* was inhibited by different strains of *T. gamsii* (Anees et al. 2010c). Different strains of *T. asperellum,* and *T. pseudokoningii* were effective against foliar pathogens of agricultural crops (Prabhakaran et al. 2015), like *Alternaria solani*, *Bipolaris oryzae*, *Pyricularia oryzae* and *Sclerotinia scierotiorum*. *Trichoderma longibrachiatum* strains were reported as antagonistic against *Fusarium oxysporum* (Anees et al. 2018). Kumar et al. (2018) reported *T. viride* effective against different fungal pathogens. Here, we have used strain T30 of *T. gamsii* that has previously shown antagonistic activity against *R. solani* AG 2-2 on culture plates (Anees et al. 2010c).

The present study was designed to evaluate the *in situ* impact of the biocontrol strain on the population density of the plant pathogenic *R. solani* AG 2-2 strain G6 in the soil. For this purpose, microcosms containing the autoclaved or non-autoclaved soils were used. The microcosms were inoculated with both the pathogen (*R. solani* AG 2-2 strain G6) and the antagonist (*T. gamsii* strain T30) in different ratios. The population densities of the pathogenic fungus were followed up to day 25 using real-time polymerase chain reaction (qPCR) by the help of specific primers designed for detection of *R. solani* AG 2-2 strain G6 based on its ITS region (Edel-Harmann et al. 2009).

Experimental

Materials and Methods

The fungal inocula. Sand inocula of *R. solani* AG 2-2 strain G6 and *T. gamsii* strain T30 were prepared. Autoclaved sand (700 g; 0.5 to 1.2 mm) was mixed with a sterile malt broth (230 g/l; 91 ml). The fungi were cultured onto the malt extract agar (MEA) plates for 4 days and five culture plugs were added to the sand medium followed by incubation for two weeks at 25°C. The bottles with sand inoculum were shaken daily to break the pellets. After two weeks, each inoculum was sampled in triplicates to measure the population density of the inoculated fungi by qPCR as given below.

Soil microcosms. The soil microcosms were prepared in 100 ml cylindrical sterile aluminum boxes covered with lids. Each box contained 50 g of soil sampled from the French National Institute for Agronomic Research (INRA) experimental unit at Epoisses, Côte d'Or, from a field of sugar beet that had no recent *Rhizoctonia* disease report. The soil was a silty clay containing 6% sand, 58% silt, and 36% clay. The soil was sieved using a 4 mm sieve and dried in air at 20°C for 4 days. The microcosms were prepared with the autoclaved or non-autoclaved soils. The former was autoclaved at 105°C for 1 h each at three consecutive days. The moisture in the microcosms was adjusted to 20% (based on the dry weight) three days before inoculation using sterile water. The inoculation was performed using different ratios i.e. R1/T1, R1/T0.1, R1/T0.01, R1/T0 and R0/T0 of *R. solani*/*T. gamsii* where '1' denotes the 10^5 target DNA copies/g of soil. The ratios were found using amounts determined by qPCR assays as explained below (Edel-Harmann et al. 2009; Anees et al. 2010b). The sand inocula were evenly spread over the soil surface in the microcosms at the given ratios and incubated at 20°C. The microcosms were sampled at three different periods i.e. on days 2, 11, and 25 after inoculation in triplicate. Hence, nine independent microcosms were prepared for each experimental treatment, i.e. three microcosms per treatment for each sampling date. Both sets of microcosms (autoclaved and non-autoclaved) were inoculated on the same day.

Preparation of standard curve for the qPCR. To generate a standard curve, the internal transcribed spacer (ITS; the target DNA) region of *R. solani* strain G6 or *T. gamsii* strain T30, respectively, were cloned into the plasmid DNA (Anees et al. 2010b). The plasmid DNA was then diluted making ten-fold dilution series that contained the cloned ITS regions from 10^2 to 10^9 copies of the target DNA for each PCR reaction. The curve hence generated was then used for quantification of the target DNA in the different DNA samples (Fig. S1).

Quantification of *R. solani* by qPCR. Sand samples of 1 g were used for the extraction of genomic DNA (Edel-Harmann et al. 2004). The procedure used for the DNA extraction included chemical as well as physical processes as previously described (Anees et al. 2010b). The extracted DNA was purified using the standard procedures (Anees et al. 2010b). The extraction was done from each sample in triplicate. The extracted DNA samples were quantified by a Biophotometer (Eppendorf, Hamburg, Germany) with an optical density adjusted at 260 nm. The qPCR technique was used for quantification of *R. solani* AG 2-2 using primers G6-F2 and G6-R2 that have been specifically designed to target the ITS region rDNA gene of the pathogen (Gardes et al. 1993). The qPCR assay was performed and analyzed as previously explained (Anees et al. 2010b). The data were analyzed using analysis of variance (ANOVA) and Fisher LSD tests ($p = 0.05$) using XLSTAT – Version 2007.5 (Addinsoft).

Results

Population density of *R. solani* strain G6 in the autoclaved soil. The population density of *R. solani* strain G6 in the autoclaved soil inoculated only with *R. solani* increased significantly from 1×10^5 to 6.5×10^6 copies/g of soil at day 25 after inoculation (Fig. 1). The different doses of *T. gamsii* strain T30 affected the population densities of *R. solani* as given in Fig. 1.

At a ratio of R1/T0.01 of *R. solani* G6 and *T. gamsii* T30, the number of copies of target DNA increased in a similar way as in the absence of *Trichoderma* at day 11 after inoculation; however, the population density decreased significantly by five times at day 25 as compared to the control (1/0). The higher doses (R1/T0.1 and R1/T1 of *R. solani* G6/*T. gamsii* T30), significantly reduced the number of target DNA copies to 2.1×10^6 and 7.55×10^5/g of soil, respectively at day 11 after inoculation. Whatever the inoculated dose of *T. gamsii* was in the microcosm, the target DNA copies of *R. solani* G6 decreased to similar levels that were significantly lower than in the absence of *T. gamsii.* When the two fungi were introduced in the microcosms at the same dose (R1/T1), the population density was 17 times lower than in the control samples, not treated with *Trichoderma.*

Population density of *R. solani* strain G6 in the non-autoclaved soil. The effect of the different ratios of T30 on the population densities of *R. solani* G6 in the non-autoclaved soil is given in Fig. 2. In the control samples, not treated with *Trichoderma*, the number of target DNA copies/g of soil was determined to be equal to 1.2×10^5 at day 11 after inoculation, which was not significantly different from the initial density, and then the density decreased significantly contrary to what was observed in the autoclaved soil.

On the other hand, for the ratios (R1/T0.1 and R1/T1), the number of target DNA copies of *R. solani* was significantly lower than in the control (R1/T0) at day 2 after inoculation. At the ratios R1/T0.1 and R1/T1, the number of target DNA copies had increased at day 11 and then decreased significantly at day 25. However, there was no effect of the ratio R1/T0.01 on the population densities of the pathogen. Overall, the population densities of *R. solani* were lower than those observed in the autoclaved soil.

The DNA copies of *R. solani* remained undetected in the non-inoculated (0/0) autoclaved or non-autoclaved soils.

Discussion

The soil is a complex medium, which makes studies of the fungal growth and interactions between different fungi difficult (Schmidt et al. 2015). This is especially true for fungi that occur in low densities such

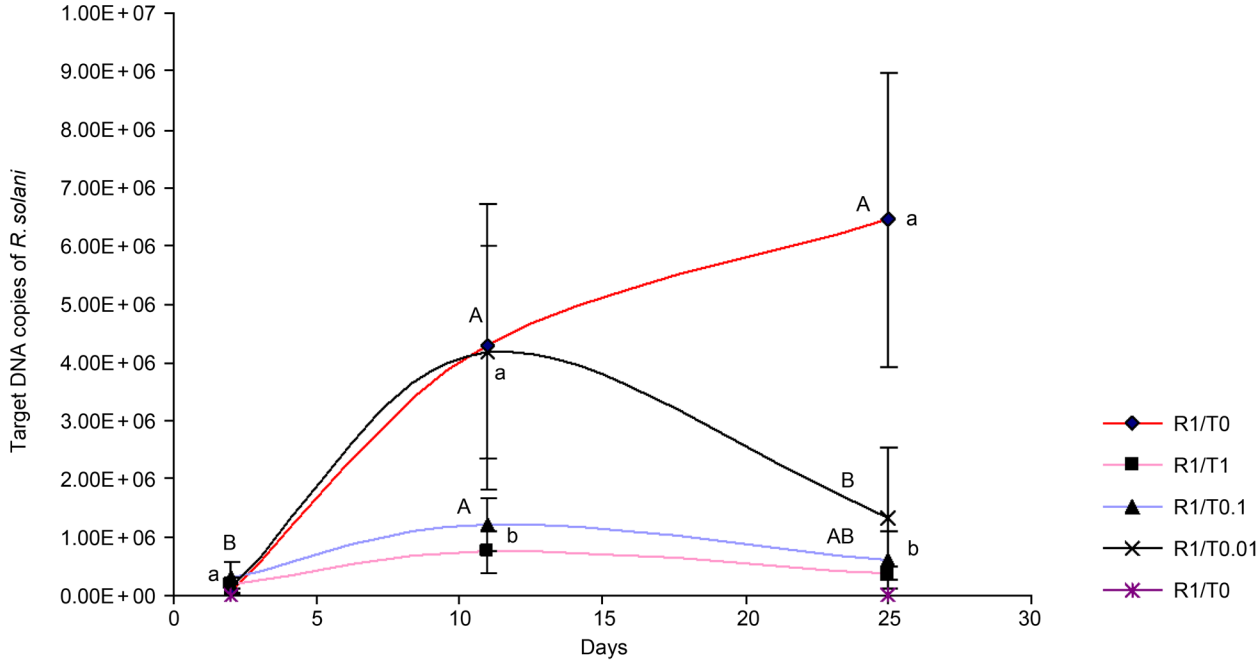

Fig. 1. The influence of different doses of *T. gamsii* T30 on the *R. solani* G6 growth in the autoclaved soil (R1/T0 represents the *R. solani* G6/*T. gamsii* T30 in the ratios 1/0 and similarly R1/T0.01 = 1/0.01 ratio, R1/T0.1 = 1/0.1 ratio, and R1/T1 = 1/1 ratio; with $1 = 10^5$ copies of the targeted DNA per g of soil). The significant differences in the number of DNA copies are shown using different letters ($p \leq 0.05$). Different small letters show the significant differences among different treatments for a given sampling time. Different capital letters indicate significant differences among different sampling times for a given treatment. If the letters happen to be identical at a given data point (either small or capital), they are written only once for the sake of clarity.

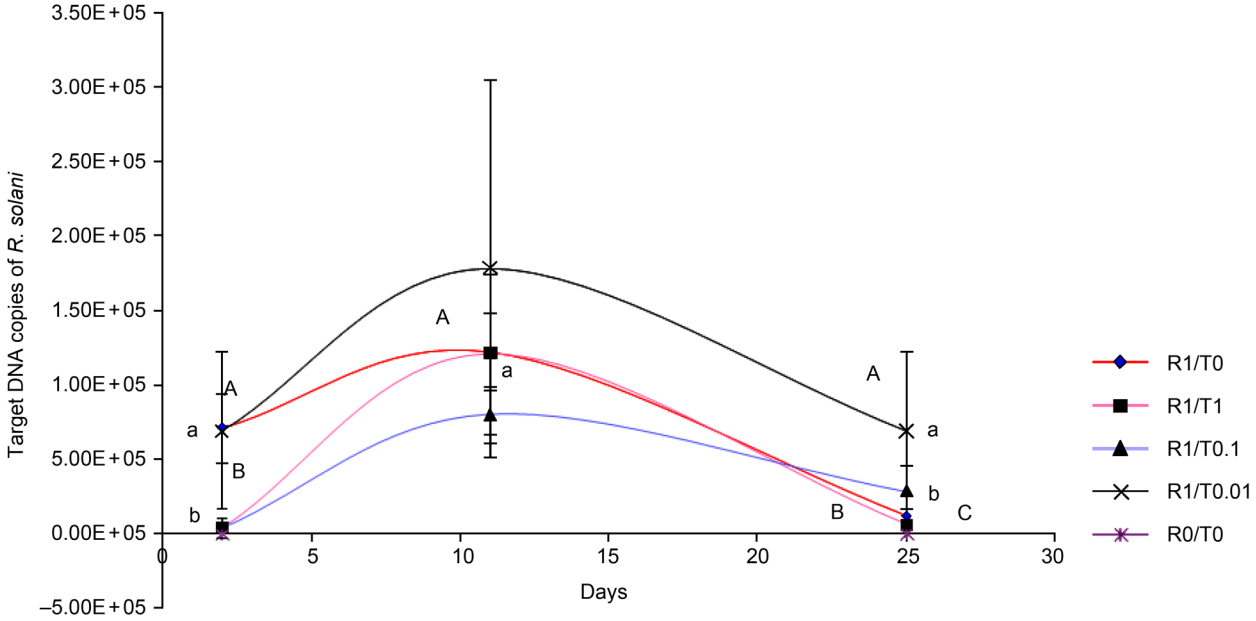

Fig. 2. The influence of different doses of *T. gamsii* T30 on the *R. solani* G6 growth in the non-autoclaved soil (R1/T0 represents *R. solani* G6/*T. gamsii* T30 in the ratio 1/0 and similarly R1/T0.01 = 1/0.01 ratio, R1/T0.1 = 1/0.1 ratio, R1/T1 = 1/1 ratio; with $1 = 10^5$ copies of the target DNA per g of soil). The significant differences in the number of DNA copies are shown using different letters ($p \leq 0.05$). Different small letters show significant differences among different treatments for a given sampling time. Different capital letters indicate the significant differences among different sampling times for a given treatment. If the letters happen to be identical at a given data point (either small or capital), they are written only once for the sake of clarity.

as *R. solani* (Ogoshi et al. 1996). In such cases, qPCR offers a viable and feasible way to explore and follow the pathogens and their antagonists quantitatively (Edel-Harmann et al. 2004; Gerin et al. 2019). However, most of the previous reports used either plant tissues or other derived media for assessment of the fungal interactions. For instance, the interaction of endophytic fungi and the pathogen has recently been reported inside plant tissues using the qPCR technique (Chow et al. 2018). The interaction of *T. gamsii* and *Fusarium* spp. in the plant-based substrata such as rice kernels and wheat haulms was studied in the artificial conditions using the same technique (Matarese et al. 2012). The interaction of two pathogens, *Aphanomyces euteiche*s and *Fusarium* spp. causing root rot disease in field pea was also recently investigated in plant tissues using multiplex qPCR (Willsey et al. 2018). Hypothetically, the antagonistic fungi are supposed to control the pathogenic fungi in soil, however, the interaction is further complicated by the presence of the general microbiome that may entail several antagonistic microorganisms (Steinberg et al. 2007). *Trichoderma* spp. are known for their antagonistic effects using multiple mechanisms. Here, we reported the impact of *T. gamsii* strain T30, a biocontrol strain, on the population density of *R. solani* G6 in different ratios in soil under *in situ* conditions in the absence of a plant host. The assays were conducted in the artificially prepared microcosms containing the autoclaved or non-autoclaved soils, respectively.

The present study demonstrated that *T. gamsii* T30 inhibited the growth of the pathogenic fungus in the autoclaved soil *in situ*. In addition to this, the present study showed the direct control of the pathogen by T30 and, moreover, a dose-dependent response was also observed i.e. with the increase in T30 inoculum, the inhibition of G6 was also stronger. The inhibition of *R. solani* by T30 in the present study may have been due to the water-soluble metabolites produced by the antagonist, as reported previously (Anees et al. 2010b). The same strain inhibited the disease caused by *R. solani* in carrots in the bioassays performed in the controlled climatic chambers, which may further reinforce the present results (Anees et al. 2010c).

In the autoclaved soil, the population density of *R. solani* increased significantly when it was alone until day 25 with a linear growth showing its saprophytic ability in the absence of competitors. This fact is consistent with earlier reports of the higher intrinsic saprophytic ability of the fungus (Ogoshi et al. 1996). However, the presence of the natural microbiome significantly reduced the growth of fungus in the presence or absence of *T. gamsii* T30. The highest number of target DNA copies detected in the non-autoclaved soil was 100 times lower than the highest number in the autoclaved soil at day 25 after inoculation. This shows the poor competitiveness of *R. solani* strain G6 as compared to the general microbiome in the natural soils. That may be why the naturally occurring soil inoculum of

R. solani is too small to be detected and often occurs as sclerotia (1 sclerotium/10 g of soil; Rodríguez-Molina et al. 2000). The situation varies in case of ascomycetous pathogens such as *F. oxysporum* which occurs generally as 100–1000 propagules/g of soil (Neate and Schneider 1996). With the small density in soil, *R. solani* faces a severe competitive pressure of the general microbiome in the soil, as depicted in the present study which is generally referred to as a general microbial suppression (Weller et al. 2002). The competition for nutrients or niches can be the reason for the general microbial suppression because a robust increase in density was observed upon amendment with the buckwheat meal (Steinberg et al. 2007). *R. solani*, therefore, needs a host plant or a source of nutrients for growth and further dispersal (Steinberg et al. 2007).

In conclusion, the present study for the first time gave an insight into the *in situ* control of *R. solani* G6 by *T. gamsii* T30 in the soil in absence of the plant host in the artificially prepared microcosms. However, future studies of the interaction of the two fungi in the presence of host would also be interesting. The present study also explained the poor competitiveness of *R. solani*, which may be the reason for the generally low densities of *R. solani* in the soil.

ORCID
Muhammad Anees 0000-0001-7886-195X

Acknowledgments
The present work was conducted under the kind supervision of Christian Steinberg and Veronique Edel-Hermann in INRA, UMR1347 Agroécologie, BP 86510, F-21000 Dijon, France.

Conflict of interest
The authors do not report any financial or personal connections with other persons or organizations, which might negatively affect the contents of this publication and/or claim authorship rights to this publication.

Literature

Anees M, Edel-Hermann V, Steinberg C. Build up of patches caused by *Rhizoctonia solani.* Soil Biol Biochem. 2010a Oct;42(10): 1661–1672. doi:10.1016/j.soilbio.2010.05.013

Anees M, Tronsmo A, Edel-Hermann V, Gautheron N, Faloya V, Steinberg C. Biotic changes in relation to local decrease in soil conduciveness to disease caused by *Rhizoctonia solani.* Eur J Plant Pathol. 2010b Jan;126(1):29–41. doi:10.1007/s10658-009-9517-0

Anees M, Tronsmo A, Edel-Hermann V, Hjeljord LG, Héraud C, Steinberg C. Characterization of field isolates of *Trichoderma* antagonistic against *Rhizoctonia solani.* Fungal Biol. 2010c Sep;114(9): 691–701. doi:10.1016/j.funbio.2010.05.007 Medline

Asef M, Goltapeh E, Danesh Y. Antagonistic effects of *Trichoderma* species in biocontrol of *Armillaria mellea* in fruit trees in Iran. J Plant Prot Res. 2008 Jun 1;48(2):213–222. doi:10.2478/v10045-008-0025-6

Chow YY, Rahman S, Ting ASY. Interaction dynamics between endophytic biocontrol agents and pathogen in the host plant studied via quantitative real-time polymerase chain reaction (qPCR) approach. Biol Control. 2018 Oct;125:44–49. doi:10.1016/j.biocontrol.2018.06.010

Edel-Hermann V, Dreumont C, Pérez-Piqueres A, Steinberg C. Terminal restriction fragment length polymorphism analysis of ribosomal RNA genes to assess changes in fungal community structure in soils. FEMS Microbiol Ecol. 2004;47(3):397–404. doi:10.1016/S0168-6496(04)00002-9 Medline

Edel-Hermann V, Jobard M, Gautheron N, Friberg H, Steinberg C. A real-time PCR assay for the identification and the quantification of *Rhizoctonia solani* AG-2-2 in soil. Multitrophic Interactions in Soil. Bulletin IOBC/WPRS. 2009;42:41–46.

Gardes M, Bruns TD. ITS primers with enhanced specificity for basidiomycetes – application to the identification of mycorrhizae and rusts. Mol Ecol. 1993 Apr;2(2):113–118. doi:10.1111/j.1365-294X.1993.tb00005.x Medline

Gerin D, Pollastro S, Raguseo C, De Miccolis Angelini RM, Faretra F. A ready-to-use single-and duplex-TaqMan-qPCR assay to detect and quantify the biocontrol agents *Trichoderma asperellum* and *Trichoderma gamsii.* Front Microbiol. 2018 Aug 31;9:2073. doi:10.3389/fmicb.2018.02073 Medline

Kumar V, Kumar Dubedi Anal A, Nath V. Biocontrol fitness of an indigenous *Trichoderma viride*, isolate NRCL T-01 against *Fusarium solani* and *Alternaria alternata* causing diseases in litchi (*Litchi chinensis*). Int J Curr Microbiol Appl Sci. 2018 Mar 20;7(03):2647–2662. doi:10.20546/ijcmas.2018.703.306

Matarese F, Sarrocco S, Gruber S, Seidl-Seiboth V, Vannacci G. Biocontrol of Fusarium head blight: interactions between *Trichoderma* and mycotoxigenic *Fusarium.* Microbiology. 2012 Jan 01; 158(1):98–106. doi:10.1099/mic.0.052639-0 Medline

Neate SM, Schneider HM. Sampling and quantification of *Rhizoctonia solani* in soil. In: Sneh B, Jabaji-Hare S, Neate S, Dijst D, editors. *Rhizoctonia* species: taxonomy, molecular biology, ecology, pathology and disease control. Dordrecht (Netherlands): Kluwer Academic Publishers; 1996. p. 185–195.

Ogoshi A. Introduction – the genus *Rhizoctonia*. In: Sneh B, Jabaji-Hare S, Neate S, Dijst G, editors. *Rhizoctonia* species: taxonomy, molecular biology, ecology, pathology and disease control. Dordrecht (Netherlands): Kluwer Academic Publishers; 1996. p. 1–9.

Prabhakaran N, Prameeladevi T, Sathiyabama M, Kamil D. Screening of different *Trichoderma* species against agriculturally important foliar plant pathogens. J Environ Biol. 2015 Jan;36(1): 191–198. Medline

Rodríguez-Molina MC, Tello-Marquina JC, Torres-Vila LM, Bielza-Lino P. Micro-scale systematic sampling of soil: heterogeneity in populations of *Fusarium oxysporum*, *F. solani*, *F. roseum* and *F. moniliforme.* J Phytopathol. 2000 Dec;148(11-12):609–614. doi:10.1046/j.1439-0434.2000.00575.x

Schmidt R, Cordovez V, de Boer W, Raaijmakers J, Garbeva P. Volatile affairs in microbial interactions. ISME J. 2015 Nov;9(11): 2329–2335. doi:10.1038/ismej.2015.42 Medline

Schneider JHM, Schilder MT, Dijst G. Characterization of *Rhizoctonia solani* AG 2 isolates causing bare patch in field grown tulips in the Netherlands. Eur J Plant Pathol. 1997;103(3):265–279. doi:10.1023/A:1008643311984

Steinberg C, Edel-Hermann V, Alabouvette C, Lemanceau P. Soil suppressiveness to plant diseases. In: Van Elsas JD, Jansson J, Trevors JT, editors. Modern soil microbiology. New York (USA): CRC Press; 2007. p. 455–478.

Weller DM, Raaijmakers JM, Gardener BBM, Thomashow LS. Microbial populations responsible for specific soil suppressiveness to plant pathogens. Annu Rev Phytopathol. 2002 Sep;40(1):309–348. doi:10.1146/annurev.phyto.40.030402.110010 Medline

Willsey TL, Chatterton S, Heynen M, Erickson A. Detection of interactions between the pea root rot pathogens *Aphanomyces euteiches* and *Fusarium* spp. using a multiplex qPCR assay. Plant Pathol. 2018 Dec;67(9):1912–1923. doi:10.1111/ppa.12895

Zhang X, Harvey PR, Stummer BE, Warren RA, Zhang G, Guo K, Li J, Yang H. Antibiosis functions during interactions of *Trichoderma afroharzianum* and *Trichoderma gamsii* with plant pathogenic *Rhizoctonia* and *Pythium*. Funct Integr Genomics. 2015 Sep;15(5):599–610. doi:10.1007/s10142-015-0456-x Medline

Supplementary materials are available on the journal's website.

Polish Journal of Microbiology
2019, Vol. 68, No 2, 217–224
https://doi.org/10.33073/pjm-2019-022

ORIGINAL PAPER

Campylobacter fetus is Internalized by Bovine Endometrial Epithelial Cells

LIZETH GUADALUPE CAMPOS-MÚZQUIZ[1], ESTELA TERESITA MÉNDEZ-OLVERA[1], BEATRIZ ARELLANO-REYNOSO[2] and DANIEL MARTÍNEZ-GÓMEZ[1]*

[1] Doctorado en Ciencias Agropecuarias, Universidad Autónoma Metropolitana Xochimilco, México
[2] Facultad de Medicina Veterinaria y Zootecnia, Universidad Nacional Autónoma de México, Ciudad Universitaria, Ciudad de México, México

Submitted 5 December 2018, revised 13 February 2019, accepted 14 February 2019

Abstract

Campylobacter fetus is an important venereal pathogen of cattle that causes infertility and abortions. It is transmitted during mating, and it travels from the vagina to the uterus; therefore, an important cell type that interacts with *C. fetus* are endometrial epithelial cells. Several virulence factors have been identified in the genome of *C. fetus*, such as adhesins, secretion systems, and antiphagocytic layers, but their expression is unknown. The ability of *C. fetus* to invade human epithelial cells has been demonstrated, but the ability of this microorganism to infect bovine endometrial epithelial cells has not been demonstrated. Bovine endometrial epithelial cells were isolated and challenged with *C. fetus*. The presence of *C. fetus* inside the endometrial epithelial cells was confirmed by the confocal immunofluorescence. *C. fetus* was not internalized when actin polymerization was disturbed, suggesting cytoskeleton participation in an internalization mechanism. To evaluate the intracellular survival of *C. fetus*, a gentamicin protection assay was performed. Although *C. fetus* was able to invade epithelial cells, the results showed that it did not have the capacity to survive in the intracellular environment. This study reports for the first time, the ability of *C. fetus* to invade bovine endometrial epithelial cells, and actin participation in this phenomenon.

Key words: Bacterial infection, pathogenicity, virulence, pathogen-host interaction, infectivity

Introduction

Campylobacter fetus is a microaerophilic, Gram-negative bacterium that causes embryonic mortality, abnormal estrus cycles, reduced fertility and abortions in 5–10% of cases in cattle and sheep. *C. fetus* is divided into three subspecies: *C. fetus* subsp. *fetus*, *C. fetus* subsp. *venerealis*, and *C. fetus* subsp. *testudinum*. *C. fetus* subsp. *venerealis* is the etiologic agent of bovine genital campylobacteriosis, which causes infertility, abortions and embryonic death, and is mainly isolated from the genital tract (Nachamkin et al. 2008). *C. fetus* subsp. *venerealis* resides in the epithelial crypts of the prepuce and is transmitted to the cow by copulation or artificial insemination with the contaminated semen. On the other hand, *C. fetus* subsp. *fetus* is a commensal bacterium of the gastrointestinal tract of cattle and sheep. It can be associated with an infertility syndrome in cattle and abortions in sheep (Irons et al. 2004).

Although *C. fetus* is an animal health problem, little has been studied regarding its pathogenicity mechanisms. However, considering the pathogenesis of infection by this organism, it must possess characteristics that allow it to colonize or invade tissues and evade the immune system response. Several virulence factors, such as adhesins, secretion systems, and antiphagocytic layers, have been identified in the genome of *C. fetus* (Kienesberger et al. 2014). Nonetheless, it is still necessary to investigate *C. fetus* interactions with animal hosts.

When *C. fetus* reaches the genital tract of the cow, epithelial cells are the first cell type that it interacts with. These epithelial cells play important roles in innate immunity, such as acting as physical and immunological barriers, signaling the activation of the immune system through the production of cytokines and chemokines and inducing death in the infected cells (Farage et al. 2011).

* Corresponding author: D. Martínez-Gómez, Laboratorio de Biología Molecular, Departamento de Producción Agrícola y Animal, Universidad Autónoma Metropolitana Xochimilco, México; **e-mail: dmartinez@correo.xoc.uam.mx**

In previous works, it has been shown that *C. fetus* is able to adhere to and invade human epithelial cells; for example, Graham (2002) determined that different strains of *C. fetus* subsp. *fetus* isolated from human, and the *C. fetus* ATCC 27374 strain isolated from cattle, adhered to 41.3–87.3% and were internalized within 25.2–34.6% of INT 407 cells. Additionally, Baker and Graham (2010) demonstrated that *C. fetus* subsp. *fetus* can invade and translocate into Caco-2 cells. Chiapparrone et al. (2014; 2016) demonstrated the adhesion mediated by flagella to MDBK cells and adhesion to different parts of the sperm cells in *C. fetus* subsp. *venerealis*. Even though it has been described the ability of *C. fetus* to adhere to bovine cells, the ability of invasion to bovine endometrial epithelial cells of the bovine-adapted *C. fetus* strains has not yet been described. In this work, the ability of *C. fetus* to adhere and invade into bovine endometrial epithelial cells is evaluated.

Experimental

Materials and Methods

Bacterial strains and culture conditions. *C. fetus* ATCC 27374 has been described previously (Salama et al. 1995). *C. fetus* was grown on the *Campylobacter* selective agar supplemented with 5% sheep blood at 37°C for 48 h in an anaerobic chamber under the microaerophilic conditions. *Salmonella enterica* subsp. *enterica* serovar Typhimurium ATCC 14028 has been previously described (Trüper et al. 2005). *S. enterica* Typhimurium was grown on the Luria Bertani agar and later inoculated in the hyperosmolar Luria Bertani Broth at 37°C for 12 h. *Escherichia coli* EPEC was donated by Dr. Jose Luis Puente from the Instituto de Biotecnología, Universidad Nacional Autónoma de México.

Primary endometrium epithelial cell cultures. Epithelial cells from the endometrium were recovered using the protocol by Skarzynski et al. (2000) with some modifications. The uterus was removed from five sacrificed cows 15 min after exsanguination. A piece of the uterus, 5 cm^2, was removed and washed three times in Hank's solution supplemented with 1.6 mg/ml gentamicin and transported to the laboratory in the same solution on ice. Serosa was removed from the tissue, and the rest was cut into small pieces (approximately 3 mm^2) and washed 3 times with pH 7.2 phosphate buffered saline (PBS) (NaH_2PO_4 1.9 mM, Na_2HPO_4 8.1 mM, NaCl 154 mM). Then, digestion solution (0.5 mg/ml collagenase Type I from *Clostridium histolyticum* (Sigma-Aldrich); 0.1 mg/ml DNAse (Thermo Fisher); 100 µg/ml gentamycin (Sigma Aldrich); in Dulbecco's modified Eagle's medium (DMEM) supplemented with 10% fetal bovine serum (DMEM-S) was added and incubated at 37°C with oscillation for 2 h. The supernatant was recovered and centrifuged at 4000 × g for 10 min. The pellet was washed three times with DMEM:PBS (1:1). The pellets were resuspended in 5 ml of DMEM-S and filtered with a 40 µm strainer. The recovered cells were placed on the cell culture dishes with DMEM-S with 50 mM HEPES (4-(2-hydroxyethyl)-1-piperazineethanesulfonic acid) and an antibiotic/antifungal (penicillin G 10 000 U, streptomycin 5 000 µg, and amphotericin B 12.5 µg). For fibroblast depuration, one-minute trypsinisation was performed every day for three days (Munson et al. 1988). The cell cultures were evaluated by RT-PCR and immunofluorescence to confirm that they were endometrial epithelial cells. First, the total RNA was extracted from cells using TRIzol following the manufacturer's methodology. Then, cDNA was synthesized using an AMV First Strand cDNA Synthesis Kit (New England Biolabs Inc.) following the manufacturer's instructions. The primers for Keratin 8 were as follows: forward 5'-CGTGTCAGAAATCTGAGACTGC-3' and reverse 5'-TGGTGGAGGACTTYAAGACC-3'. The PCR mixture was prepared with primers (40 nM), Master Mix (Fermentas) and 100 ng cDNA. The PCR conditions were as follows: pre-heat at 95°C for 5 min; 30 cycles of denaturalization at 94°C for 30 s, annealing at 60°C for 30 s and extension at 72°C for 20 s. The PCR products were evaluated by electrophoresis in 2% agarose gels stained with ethidium bromide. For immunofluorescence, a polyclonal antibody against bovine cytokeratin 18 (Santa Cruz Biotechnology) was used in the cell cultures fixed in plates.

C. fetus PCR confirmation. Three pairs of primers for the *asp*A, *gln*A, *glt*A and 16sRNA genes were designed. Before each assay, PCR was performed to confirm the purity of *C. fetus* cultures. The primer sequences and product sizes were as follows: *aspA*: F-5'-CCTATGACTTTAGGTCAAGAG-3', R-5'-TGTAG CTAGAGTACGGCAAG-3' (575 bp); *gltA*: F-5'-CGA-TATAGCGTGGCTAGCTG-3', F-5'-AGCGTGAGTAG ATCCTACG-3' (520 bp); *glnA*: F-5'-CTTCCGTTATC TCCATAAAGC-3', R-5'-GATGGTAGTTCTATAGA GGC-3' (649 bp); 16sRNA: F-5'-GAGATCACCAGGA ATACCC-3', R-5'-CACCTGTCTCAACTTTCTAGC-3' (351 bp). For these primers, the PCR conditions were a pre-heat of 95°C for 1 min, then 30 cycles denaturation at 94°C for 30 s, annealing at 50°C for 30 s and extension at 72°C for 30 s.

Cell adhesion assays. The adherence was evaluated by quantitative and qualitative methods. For quantitative evaluation, three independent adherence assays with three replicates were performed following the method described by Bacon et al. (2001). First, *C. fetus* was grown on the *Campylobacter* selective agar supplemented with 5% sheep blood for 48 h and harvested in PBS. *Escherichia coli* EPEC was used as an adhesion

control and was grown in hyperosmolar LB for 12 h. The bacterial inoculum was determined by spectrophotometry and plating. The multiplicity of infection (MOI) was 1000:1. The infected cell cultures were centrifuged at 165 × g for 3 min to maximize bacteria-cell contact and incubated for 1 h at 37°C. The percentage of adhered bacteria was calculated by the formula [(CFU intracellular / CFU inoculum) × 100]. For visual interpretation, cells were fixed with methanol and stained with 100% Giemsa for 40 min.

Intracellular survival assays. Three independent assays with three replicates per time were performed as described by Elsinghorst (1994) with some modifications. First, *C. fetus* was grown on the *Campylobacter* selective agar supplemented with 5% sheep blood for 48 h and harvested in PBS. To prepare the inoculum, bacteria were quantified by spectrophotometry and diluted in DMEM to an adjusted MOI of 1000:1. Epithelial cells of the endometrium were seeded at 40 000 cells per well in a 48-well dish. After washing three times with PBS, the epithelial cells were infected. The plates were centrifuged at 165 × g for 3 min to maximize bacterial-cell contact and incubated for 2 h at 37°C. Following incubation, the monolayers were washed three times with PBS and incubated with DMEM supplemented with 10% fetal bovine serum, 50 mM HEPES and 30 µg/ml gentamicin. The plating of the samples of the medium confirmed the complete killing of the extracellular *C. fetus.* Bacteria were recovered at 0, 2, 4, 10 and 24 h post-infection (p.i.); supernatant medium was removed, and the intracellular bacteria were recovered by adding 1 ml of Triton X100 1% for 5 min, and the solution was homogenized and added to a microcentrifuge tube. Fifty microliters of each well were plated on the *Campylobacter* selective agar supplemented with 5% sheep blood at 37°C for 72 h in an anaerobic chamber under low oxygen conditions (Oxoid Campy Gen, catalogue number CN0025A). *S. enterica* Typhimurium was used as a positive control of infection because they can invade the bovine reproductive tract (Hall and Jones 1977).

Cytoskeleton inhibition assays. To establish the possible mechanism involved in *C. fetus* invasion in these epithelial cells, cytoskeleton inhibition assays were performed. Cytochalasin D (Sigma-Aldrich) was prepared as a 1 mM stock in dimethyl sulfoxide, and nocodazole was prepared as a 10 mM stock in dimethyl sulfoxide. Gentamicin protection assays were performed as described above, with some modifications. Forty thousand cells per well were plated in a 48-well dish. After washing three times with PBS, DMEM with cytochalasin D (3 mM) or nocodazole (30 mM) was added to the wells, and the cells were incubated for 30 min at 37°C. Then, bacteria were added, and the inhibitor concentration was kept at the half during the infection. The plates were centrifuged at 165 × g for 3 min to maximize the bacteria-cell contact and incubated at 37°C. *C. fetus* infection lasted for 2 h with an MOI of 1000:1 and *Salmonella* infection for 15 min with an MOI of 50:1. After infection, the inoculum was removed, and cells were washed three times with PBS and DMEM supplemented with 10% fetal bovine serum, Hepes 50 mM, and 30 µg/ml gentamicin. Cells were lysed with 50 µl of Triton X100 1% in each well and plated on the *Campylobacter* selective agar supplemented with 5% sheep blood at 37°C for 72 h in an anaerobic chamber under low oxygen conditions (Oxoid Campy Gen, catalogue number CN0025A).

Immunofluorescence Microscopy. Epithelial cells from bovine endometrium were infected as described above. At 0 and 2 h p.i., cells were washed three times with PBS and fixed with methanol for 4 min at 4°C. The fixed cells were washed three times with PBS and permeabilized by incubation in PBS containing 0.1% saponin for one min. Then, coverslips were incubated with 50 µg/ml phalloidin-FITC diluted with 1% dimethyl sulfoxide (DMSO) for 1 h at room temperature. The coverslips were washed three times with saponin 0.05% and PBS. After that, coverslips were incubated with primary antibodies (rabbit anti-*C. fetus*) diluted 1:1000 (saponin 0.05%, 5% horse serum, PBS) for an hour at 37°C. Afterward, the coverslips were washed three times with saponin 0.05% and incubated with secondary antibodies (goat anti-rabbit (US Biological) and diluted with Alexa Fluor 594 to 1:1000 for 30 min at room temperature. After three washes with 0.05% saponin, coverslips were mounted onto glass slides. Images were acquired with a Zen Zeiss LSM800 fluorescence microscope.

Statistical analysis. Each assay was subjected to a Shapiro-Wilks test and a Welch's test. Then, to determine the time at which the intracellular bacterial count was different in each treatment, Student's T-test was used.

Results

***C. fetus* adheres to epithelial cells of bovine endometrium.** To confirm that *C. fetus* could adhere to epithelial cells from the endometrium, an adherence assay was performed. First, endometrial epithelial cell cultures were established from cells isolated from uterus tissue obtained from slaughtered cows. The cells established a monolayer until the second week of incubation when these cells presented a polygonal epithelial-like form (Fig. 1A). These cells were used until the seventh passage since later splits presented different morphologies and diminished cell proliferation rates. For cell type confirmation, cytokeratin 18 from epithelial cells was immunostained with Alexa 488 (Fig. 1B), and RT-PCR for keratin 8 was performed (Fig. 1C). The results obtained

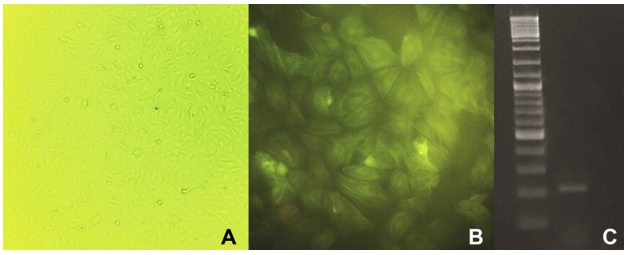

Fig. 1. Epithelial cells from bovine endometrium maintained in DMEM supplemented with 10% fetal bovine serum.

A) Normal appearance of the epithelial-like cells (20×). B) Immunofluorescence. Cytokeratin 18 of epithelial cells of bovine endometrium stained with Alexa 488 (green) (40×). C) The results of RT-PCR for keratin 8 on 2% agarose gel after staining with ethidium bromide. In left lane: DNA ladder (Thermo Fisher Scientific); right lane: the amplicon of keratin 8 (215 pb).

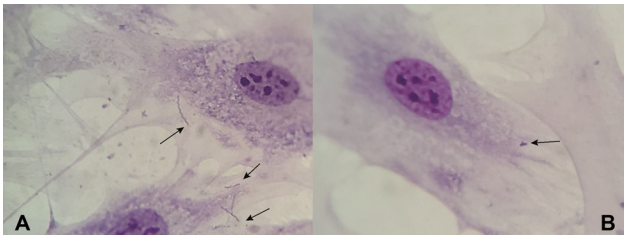

Fig. 2. The adherence assay. Epithelial cells from bovine endometrium were challenged with *C. fetus* (A) or *E. coli* (B) for 1 h, fixed with methanol and stained with Giemsa (100×). The arrows show the adhered bacteria.

show that cells in culture corresponded to endometrial epithelial cells. In the adherence assays, the average percentage of epithelial cell-adhered bacteria was 0.13%. Adhered *C. fetus* was observed by microscopy (Fig. 2A). *E. coli* EPEC showed a typically localized adherence pattern (Fig. 2B). These results confirm that *C. fetus* can adhere to endometrial epithelial cells.

***C. fetus* invades bovine endometrial epithelial cells.** After the adherence capacity of *C. fetus* was confirmed, a gentamicin protection assay was carried out to determine the intracellular survival of *C. fetus* in epithelial cells from bovine endometrium. The results obtained with MOI of 1000:1 showed a decrease in the number of *C. fetus* viable cells. At 0 h p.i there were an average (~) of 3795 CFU, at 2 h p.i they decreased to ~ 163 CFU, at 4 h there were ~ 36 CFU and 10 h p.i the organisms didn't grow. No viable cells were recovered at 24 h p.i., suggesting that the bacteria have the capacity to enter the cells, but it might not survive inside epithelial cells of the endometrium (Fig. 3). *Salmonella* invaded the bovine endometrial epithelial cells used in this study. At 0 h, the bacteria were present inside the cells ~ 8430 CFU, and at 4 h they started to replicate, increasing to ~ 14 585 CFU showing normal intracellular infection behavior in bovine epithelial cells (data not show). The presence of *C. fetus* inside the cells was confirmed by confocal microscopy. Before immuno-

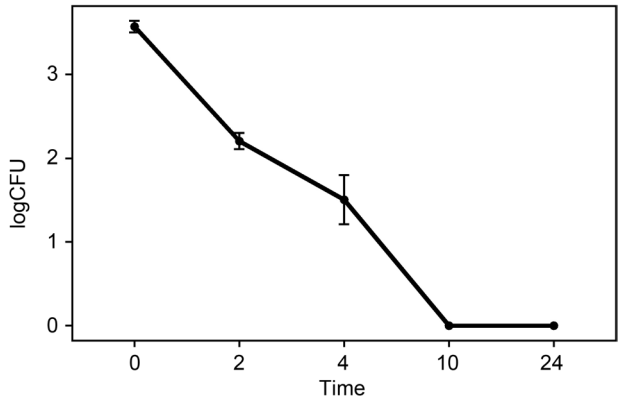

Fig. 3. The intracellular survival assay. Epithelial cells of endometrium of bovine were infected with *C. fetus* ATCC 27374 (a MOI of 1000:1). The intracellular bacteria were recovered and plated on the Campylobacter selective agar supplemented with 5% of blood. Average log CFU are shown at 0, 2, 4, 10 and 24 h p.i.

fluorescence, rabbit anti-*C. fetus* serum was adsorbed to avoid unspecific labeling and tested by Western blotting (Fig. S1, supplemental material). Additionally, the secondary antibody specificity and anti-rabbit HRP antibodies were tested by Western blotting. The results obtained in the Western blots, with a total bacterial protein extract and total cell protein extract, showed that adsorbed anti-*C. fetus* antisera recognized only antigens in *C. fetus* and not in epithelial cells, and the anti-rabbit antibodies did not recognize antigens in bacteria or epithelial cells (Fig. S1, supplemental material). The confocal fluorescence at 2 h p.i. showed the

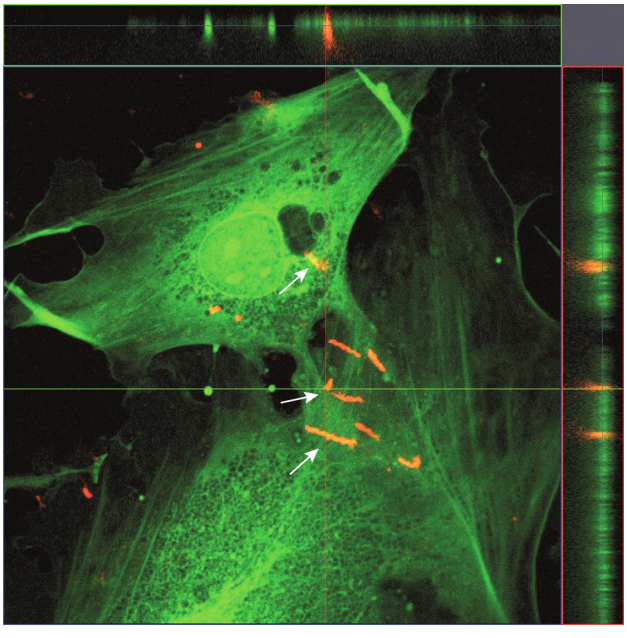

Fig. 4. Confocal differential fluorescent staining of internal *C. fetus* ATCC 27374 on the infected epithelial cells of bovine endometrium. Epithelial cells were grown on coverslips and infected with *C. fetus* ATCC 27374 at a MOI of 1000:1. Cytoskeleton was stained with phalloidin-FITC (green), and the bacteria with Alexa 594 (red) 2 h p.i. White arrows show intracellular *C. fetus* (70×).

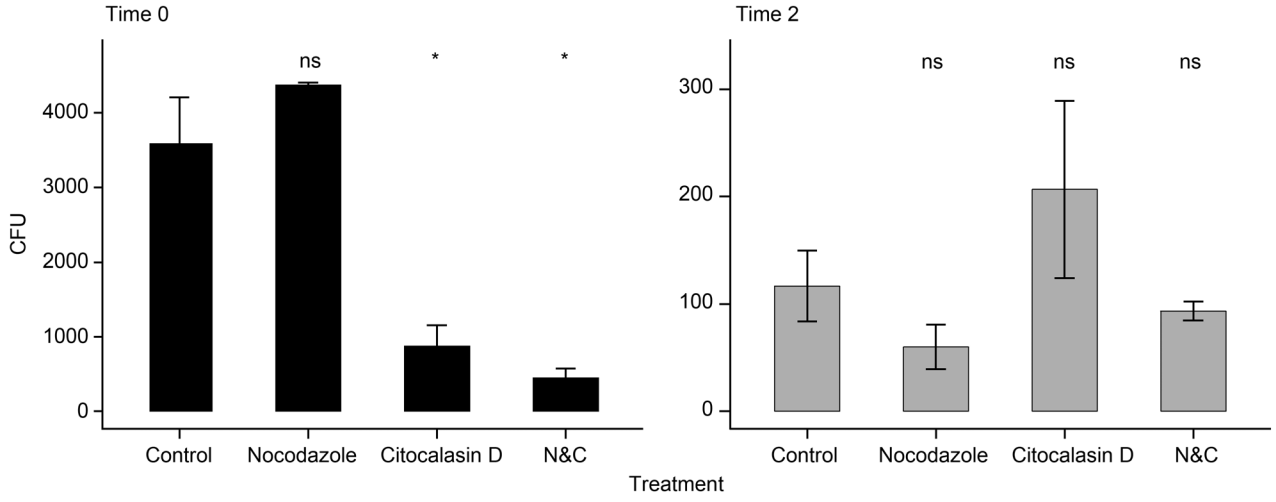

Fig. 5. The cytoskeleton inhibition assay. Epithelial cells of endometrium of bovine were treated with cytocalasin D or nocodazole before and during infection. The cells were infected with *C. fetus* ATCC 27374 (a MOI of 1000:1). The intracellular bacteria were recovered and plated on the Campylobacter selective agar supplemented with 5% of blood. Average log CFU are shown at 0 and 2 p.i. T-test was performed. All treatments were compared to the not-treatment control, *($p < 0.001$).

intracellular bacteria, demonstrating that *C. fetus* can invade epithelial cells from bovine endometrium but is not able to proliferate inside of them (Fig. 4).

***C. fetus* uses actin to invade bovine endometrial epithelial cells.** Internalization of *C. fetus* was modified when the cytoskeleton of the endometrium epithelial cells was altered. Treatment with cytochalasin D decreased the capability of internalization of *C. fetus* (~ 873 CFU). There was no change in *C. fetus* internalization when using nocodazole (~ 4330 CFU) suggesting that actin plays an important role in this process (Fig. 5).

Discussion

The invasion of *C. fetus* in some human cell lines, such as Hep-2 and Caco-2 has already been described (Konkel and Joens 1989; Baker and Graham 2010). Although these results suggest the ability of this microorganism to invade cells, the interaction with endometrial epithelial cells, the first type of cell that interacts with *C. fetus*, has not been described. In this work, an intracellular survival assay including gentamicin protection and immunofluorescence showed that *C. fetus* can invade the bovine endometrial epithelial cells, this result relates with the ones reported in the literature, which shows that *Campylobacter* spp. is able to invade cells (Konkel and Joens 1989; Graham 2002; Baker and Graham 2010).

The use of primary cultures for the evaluation of virulence of different pathogens has been widely reported. Most studies investigating the relationship between the host and bacteria, tend to focus on the cell types that comprise the biological barriers, signaling events within the host and the virulence factors of the pathogen, which are involved in the initial phase of the disease (Benjamin et al. 2011). In this work, a primary culture of bovine endometrial epithelial cells was established, considering that these cells could be the first in contact with *C. fetus*. The primary cultures showed a positive reaction against cytokeratin 18. The expression of this protein has been described in bovine endometrial epithelial cells (Haeger et al. 2015).

Cell culture models can compartmentalize and define the broad range of molecular mechanisms that underlie strategies of microbial virulence such as host receptor ligand binding and invasion mechanism. These mechanisms have not been identified in *C. fetus*; however, in this work, its ability to adhere to bovine cells was shown. The pathogenicity factors that could mediate this adhesion could be diverse. McSweegan and Walker (1986) described the role of lipopolysaccharide as a molecule that allows the adhesion of *C. jejuni* to INT407 cells. Monteville et al. (2003) identified a *C. jejuni cad*F homologous gene in *C. fetus*, which encodes for an outer membrane fibronectin binding protein (Accession No. Nz_CP00880). This protein in *C. jejuni* binds to fibronectin (Konkel et al. 1997), which is expressed on the epithelial cells of the endometrium (Mularoni et al. 1992). In *C. fetus* Moolhuijzen et al. (2009) have identified the *PEB1* gene, which participates in adhesion in *C. jejuni*. It has been described that *C. fetus* has a protein coat that may interfere in the contact with other cells (Yang et al. 1992). However, in this study, *C. fetus* was able to invade epithelial cells, so it is possible that the protein layer does not interfere, or it may exist some other mechanism, not yet described, for this bacterium that allows it to adhere the epithelial cells.

Intact epithelial surfaces are a highly effective barrier to evade invasion by pathogens. A capability to

disrupt intact epithelial surfaces is an important characteristic for many specialized bacterial pathogens. In this work *C. fetus* showed the capability to invade cells; however, internalization mechanisms have not been described for these species. *C. fetus* possesses a type IV secretion system (Kienesberger et al. 2014), which is used by many pathogens for substrate translocation, for example in *Bartonella henselae* this system translocates BepC and BepF, the proteins factors that trigger invasome-mediated internalization (Truttmann et al. 2011). In *C. fetus,* Ali et al. (2012) identified a CiaB homologous, which in *C. jejuni* is translocated through flagellum and is required for internalization (Konkel et al. 1999). More research is required in order to identify the virulence mechanisms that mediate cellular invasion.

The previous reports have demonstrated that *C. jejuni* make use of microtubules to invade epithelial cells (Oelschlaeger et al. 1993; Hu and Kopecko 1999). In this work, it was observed that when actin polymerization was inhibited, *C. fetus* could not be internalized in the same way as the control, suggesting that actin plays an important role in the internalization mechanism, too. Moreover, Baker and Graham (2010) showed that cytochalasin D treatment on Caco-2 epithelial cells was not able to inhibit *C. fetus* internalization. Those results differ from the ones obtained in this work, the treatment with cytochalasin D of our primary culture did not inhibit totally the invasion of *C. fetus*, it only reduced it. This difference could be explained by the treatment conditions with cytochalasin D or by the incubation time of the bacteria in the cellular infection assays.

Although in this work was shown that *C. fetus* had the ability to invade cells, its intracellular survival was minimal (at 10 hours post infection the number of the intracellular bacteria had decreased significantly). Treatment of the cells with nocodazole, a drug that inhibits endosome-lysosome fusion (Funato et al. 1997), did not help *C. fetus* to survive inside the cell. This suggests that their inability to persist within cells could be explained by metabolic adaptations for the intracellular environment and not necessarily by lysosomal degradation. The intracellular bacteria require the metabolic adaptations to remain alive in the harsh intracellular environment. For example, *S. enetrica subsp.* Typhimurium shows upregulation of glycolysis and the Entner-Doudoroff pathway during the vacuolar stage (Eisenreich et al. 2015). *Campylobacter* spp. does not ferment carbohydrates because it lacks phosphofructokinase and essential enzymes for the Entner-Doudoroff pathway, and its principal source of carbon are amino acids (Kelly 2008). *Legionella pneumophila* also lacks the glycolysis pathway and uses amino acids as a carbon source, but unlike *Campylobacter*, it uses the Entner-Doudoroff pathways as an important carbon source (Eisenreich et al. 2015).

Another explanation that could help understanding why in the intracellular survival assay *C. fetus* was internalized and eliminated from the cells, is the metabolic reprogramming, which does not allow *C. fetus* to grow on agar plates after having gone through the intracellular stage. In *C. jejuni*, during its intracellular stay, the respiration is reprogrammed, favoring the use of fumarate and reducing the expression of enzymes of aerobic respiration (Liu et al. 2012). In this way, when bacteria are recovered in artificial media, their growth is reduced. This explanation could be the least likely, however, in the work done by Watson and Galán (2008) this phenomenon was found.

The invasive nature of *C. fetus* has been well established *in vivo* in clinical veterinary situations and *in vitro* with human intestinal epithelial cells assays. Baker and Graham (2010) showed the translocation of *C. fetus* through the barriers of intestinal epithelial cells with the culture of Caco-2 cells. Louwen et al. (2012) also showed a similar phenomenon with *C. jejuni* in Caco-2 cells. Therefore, the short permanence of viable *C. fetus* in the endometrial culture cells could be interpreted as normal, considering that the only objective of *C. fetus* is to be translocated.

There are many studies on *Campylobacter* spp. invasion capability (Mooney et al. 2003; Watson and Galán 2008), however, this report presents the ability of *C. fetus* to invade bovine endometrium epithelial cells. This could be used in future work as a bovine infection model and be an important element for understanding the pathogenicity mechanisms of *C. fetus*.

C. fetus could have been originated as a pathobiont in humans and jump to bovine as their host, generating adapted strains. The bovine strains contain in their genome the unique accessory genes (virulence factors) not seen in human strains (Iraola et al. 2017). This would explain why *C. fetus* can persist in the intestine of humans (Lastovica and Skirrow 2000) and may be associated with infertility and sporadic abortions in cattle and sheep (Irons et al. 2004). The *C. fetus* strain used in this work was isolated from a clinical case of an aborted calve, and it is known to cause abortions in cattle (Smith and Taylor 1919; Véron and Chatelain 1973). Graham et al. (2002; 2010) used this strain in some invasion assays using human cell cultures.

In conclusion, this work showed that *C. fetus* adheres and invades bovine endometrial epithelial cells. Gentamicin protection assays and fluorescence microscopy suggest that *C. fetus* can survive inside cells for only a few hours (4 h). Additionally, *C. fetus* is internalized using an actin-dependent mechanism in this cell type. All knowledge generated in this area will serve to propose and develop new strategies for the control of pathogens.

ORCID
Daniel Martínez-Gómez 0000-0001-8051-8210

Acknowledgments

We are grateful with Doctorado en Ciencias Agropecuarias and Temamatla slaughterhouse for providing facilities. This work was supported by Universidad Autónoma Metropolitana, Unidad Xochimilco and by Consejo Nacional de Ciencia y Tecnología, México (CONACYT- becario 469811).

Conflict of interest

The authors do not report any financial or personal connections with other persons or organizations, which might negatively affect the contents of this publication and/or claim authorship rights to this publication.

Literature

Ali A, Soares SC, Santos AR, Guimarães LC, Barbosa E, Almeida SS, Abreu VAC, Carneiro AR, Ramos RTJ, Bakhtiar SM, et al. *Campylobacter fetus* subspecies: comparative genomics and prediction of potential virulence targets. Gene. 2012 Oct;508(2): 145–156. doi:10.1016/j.gene.2012.07.070 Medline

Bacon DJ, Szymanski CM, Burr DH, Silver RP, Alm RA, Guerry P. A phase-variable capsule is involved in virulence of *Campylobacter jejuni* 81-176. Mol Microbiol. 2001 May;40(3):769–777. doi:10.1046/j.1365-2958.2001.02431.x Medline

Baker NT, Graham LL. *Campylobacter fetus* translocation across Caco-2 cell monolayers. Microb Pathog. 2010 Nov;49(5):260–272. doi:10.1016/j.micpath.2010.06.008 Medline

Chiapparrone ML, Morán PE, Echevarría HM, Soto P, Paolicchi FA, Catena M. *Campylobacter fetus* subsp. *venerealis* adhesion to MDBK cells. Rev Argent Microbiol. 2014;46(3):269–270. doi:10.1016/S0325-7541(14)70081-1 Medline

Chiapparrone ML, Soto P, Catena M. Characterization of the *Campylobacter fetus* subsp. *venerealis* adhesion to bovine sperm cells. Int. J. Morphol. 2016;34(4):1419–1423. doi:10.4067/S0717-95022016000400040

Duell BL, Cripps AW, Schembri MA, Ulett GC. Epithelial cell coculture models for studying infectious diseases: Benefits and limitations. J Biomed Biotechnol. 2011;2011:852419. doi:10.1155/2011/852419 Medline

Eisenreich W, Heesemann J, Rudel T, Goebel W. Metabolic adaptations of intracellular bacterial pathogens and their mammalian host cells during infection ("Pathometabolism"). Microbiol Spectr. 2015 Jun 25;3(3). doi:10.1128/microbiolspec.MBP-0002-2014 Medline

Elsinghorst EA. Measurement of invasion by gentamicin resistance. In: Clark VL, Bavoil PM, editors. Bacterial Pathogenesis Part B: Interaction of Pathogenic Bacteria with Host Cells. San Diego (USA): Academic Press; 1994. p. 405–420. doi:10.1016/0076-6879(94)36030-8

Farage MA, Miller KW, Gerberick GF, Saito FH, Ledger WJ, Witkin SS. Innate immunity in the lower female mucosal tract. J Steroids Horm Sci. 2011;02(02):106. doi:10.4172/2157-7536.1000106

Funato K, Beron W, Yang CZ, Mukhopadhyay A, Stahl PD. Reconstitution of phagosome-lysosome fusion in streptolysin *O*-permeabilized cells. J Biol Chem. 1997 Jun 27;272(26):16147–16151. doi:10.1074/jbc.272.26.16147 Medline

Graham LL. *Campylobacter fetus* adheres to and enters INT 407 cells. Can J Microbiol. 2002 Nov;48(11):995–1007. doi:10.1139/w02-096 Medline

Haeger JD, Hambruch N, Dantzer V, Hoelker M, Schellander K, Klisch K, Pfarrer C. Changes in endometrial ezrin and cytokeratin 18 expression during bovine implantation and in caruncular endometrial spheroids in vitro. Placenta. 2015 Aug;36(8):821–831. doi:10.1016/j.placenta.2015.06.001 Medline

Hall GA, Jones PW. A study of the pathogenesis of experimental *Salmonella dublin* abortion in cattle. J Comp Pathol. 1977 Jan;87(1): 53–65. doi:10.1016/0021-9975(77)90079-2 Medline

Hu L, Kopecko DJ. *Campylobacter jejuni* 81-176 associates with microtubules and dynein during invasion of human intestinal cells. Infect Immun. 1999 Aug;67(8):4171–4182. Medline

Iraola G, Forster SC, Kumar N, Lehours P, Bekal S, García-Peña FJ, Paolicchi F, Morsella C, Hotzel H, Hsueh PR, et al. Distinct *Campylobacter fetus* lineages adapted as livestock pathogens and human pathobionts in the intestinal microbiota. Nat Commun. 2017 Dec;8(1):1367. doi:10.1038/s41467-017-01449-9 Medline

Irons PC, Schutte AP, van der Walt ML, Bishop GC. Genital campylobacteriosis in cattle. In: Coetzer JAW, Tustin RC, editors. Infectious diseases of livestock with special reference to southern Africa. Cape Town (South Africa): Oxford University Press; 2004. p. 159–1468.

Kelly DJ. Complexity and versatility in the physiology and metabolism of *Campylobacter jejuni*. In: Nachamkin I, Szymanski CM, editors. *Campylobacter*. Washington, DC (USA): ASM Press; 2008. p. 41–62.

Kienesberger S, Sprenger H, Wolfgruber S, Halwachs B, Thallinger GG, Perez-Perez GI, Blaser MJ, Zechner EL, Gorkiewicz G. Comparative genome analysis of *Campylobacter fetus* subspecies revealed horizontally acquired genetic elements important for virulence and niche specificity. PLoS One. 2014 Jan 9;9(1):e85491. doi:10.1371/journal.pone.0085491 Medline

Konkel ME, Garvis SG, Tipton SL, Anderson DE Jr, Cieplak W Jr. Identification and molecular cloning of a gene encoding a fibronectin-binding protein (CadF) from *Campylobacter jejuni*. Mol Microbiol. 1997 Jun;24(5):953–963. doi:10.1046/j.1365-2958.1997.4031771.x Medline

Konkel ME, Joens LA. Adhesion to and invasion of HEp-2 cells by *Campylobacter* spp. Infect Immun. 1989 Oct;57(10):2984–2990. Medline

Konkel ME, Kim BJ, Rivera-Amill V, Garvis SG. Bacterial secreted proteins are required for the internalization of *Campylobacter jejuni* into cultured mammalian cells. Mol Microbiol. 1999 May; 32(4):691–701. doi:10.1046/j.1365-2958.1999.01376.x Medline

Lastovica AJ, Skirrow MB. Clinical significance of *Campylobacter* and related species other than *Campylobacter jejuni* and *C. coli*. In: Nachamkin I, Blaser MJ, editors. *Campylobacter*. Washington, DC (USA): ASM Press; 2000. p. 89–120.

Liu X, Gao B, Novik V, Galán JE. Quantitative proteomics of intracellular *Campylobacter jejuni* reveals metabolic reprogramming. PLoS Pathog. 2012 Mar 8;8(3):e1002562. doi:10.1371/journal.ppat.1002562 Medline

Louwen R, Nieuwenhuis EES, van Marrewijk L, Horst-Kreft D, de Ruiter L, Heikema AP, van Wamel WJB, Wagenaar JA, Endtz HP, Samsom J, et al. *Campylobacter jejuni* translocation across intestinal epithelial cells is facilitated by ganglioside-like lipooligosaccharide structures. Infect Immun. 2012 Sep;80(9): 3307–3318. doi:10.1128/IAI.06270-11 Medline

McSweegan E, Walker RI. Identification and characterization of two *Campylobacter jejuni* adhesins for cellular and mucous substrates. Infect Immun. 1986 Jul;53(1):141–148 Medline.

Monteville MR, Yoon JE, Konkel ME. Maximal adherence and invasion of INT 407 cells by *Campylobacter jejuni* requires the CadF outer-membrane protein and microfilament reorganization. Microbiology. 2003 Jan 01;149(1):153–165. doi:10.1099/mic.0.25820-0 Medline

Moolhuijzen PM, Lew-Tabor AE, Wlodek BM, Agüero FG, Comerci DJ, Ugalde RA, Sanchez DO, Appels R, Bellgard M. Genomic analysis of *Campylobacter fetus* subspecies: identification of candidate virulence determinants and diagnostic assay targets. BMC Microbiol. 2009;9(1):86. doi:10.1186/1471-2180-9-86 Medline

Mooney A, Byrne C, Clyne M, Johnson-Henry K, Sherman P, Bourke B. Invasion of human epithelial cells by *Campylobacter upsaliensis*. Cell Microbiol. 2003 Nov;5(11):835–847. doi:10.1046/j.1462-5822.2003.00325.x Medline

Mularoni A, Mahfoudi A, Beck L, Coosemans V, Bride J, Nicollier M, Adessi GL. Progesterone control of fibronectin secretion in guinea pig endometrium. Endocrinology. 1992 Nov;131(5): 2127–2132. doi:10.1210/endo.131.5.1425413 Medline

Munson L, Chandler SK, Schlafer DH. Cultivation of bovine fetal and adult endometrial epithelial cells. J Tiss Cult Met. 1988.11(3): 129–133. doi:10.1007/BF01404265

Nachamkin I, Szymanski C, Blaser MJ. *Campylobacter*. Washington, DC (USA): ASM Press; 2008. 749 p.

Oelschlaeger TA, Guerry P, Kopecko DJ. Unusual microtubule-dependent endocytosis mechanisms triggered by *Campylobacter jejuni* and *Citrobacter freundii*. Proc Natl Acad Sci USA. 1993 Jul 15;90(14):6884–6888. doi:10.1073/pnas.90.14.6884 Medline

Salama SM, Newnham E, Chang N, Taylor DE. Genome map of *Campylobacter fetus* subsp. *fetus* ATCC 27374. FEMS Microbiol Lett. 1995 Oct;132(3):239–245. doi:10.1111/j.1574-6968.1995.tb07840.x Medline

Skarzynski DJ, Miyamoto Y, Okuda K. Production of prostaglandin F(2alpha) by cultured bovine endometrial cells in response to tumor necrosis factor alpha: cell type specificity and intracellular mechanisms. Biol Reprod. 2000 May 01;62(5):1116–1120. doi:10.1095/biolreprod62.5.1116 Medline

Smith T, Taylor MS. Some morphological and biological characters of the spirilla (*Vibrio fetus*, n. sp.) associated with disease of the fetal membranes in cattle. J Exp Med. 1919 Oct 1;30(4):299-311. doi:10.1084/jem.30.4.299

Trüper HG; Judicial Commission of the International Committee on Systematics of Prokaryotes. The type species of the genus *Salmonella* Lignieres 1900 is *Salmonella enterica* (ex Kauffmann and Edwards 1952) Le Minor and Popoff 1987, with the type strain LT2T, and conservation of the epithet enterica in Salmonella enterica over all earlier epithets that may be applied to this species. Opinion 80. Int J Syst Evol Microbiol. 2005 Jan 01;55(1):519–520. doi:10.1099/ijs.0.63579-0 Medline

Truttmann MC, Rhomberg TA, Dehio C. Combined action of the type IV secretion effector proteins BepC and BepF promotes invasome formation of *Bartonella henselae* on endothelial and epithelial cells. Cell Microbiol. 2011 Feb;13(2):284–299. doi:10.1111/j.1462-5822.2010.01535.x Medline

Véron M, Chatelain R. Taxonomic study of the genus *Campylobacter* Sebald and Véron and the designation of the neotype strain for the type species, *Campylobacter fetus* (Smith and Taylor) Sebald and Véron. Int J Syst Bacteriol. 1973 Apr 01;23(2):122–134. doi:10.1099/00207713-23-2-122

Watson RO, Galán JE. *Campylobacter jejuni* survives within epithelial cells by avoiding delivery to lysosomes. PLoS Pathog. 2008;4(1):e14. doi:10.1371/journal.ppat.0040014 Medline

Yang LY, Pei ZH, Fujimoto S, Blaser MJ. Reattachment of surface array proteins to *Campylobacter fetus* cells. J Bacteriol. 1992 Feb; 174(4):1258–1267. doi:10.1128/jb.174.4.1258-1267.1992 Medline

Supplementary materials are available on the journal's website.

Polish Journal of Microbiology
2019, Vol. 68, No 2, 225–232
https://doi.org/10.33073/pjm-2019-024

ORIGINAL PAPER

Patterns of Drug-Resistant Bacteria in a General Hospital, China, 2011–2016

TINGTING MAO, HUIJUAN ZHAI, GUANGCAI DUAN and HAIYAN YANG*

Department of Epidemiology, College of Public Health of Zhengzhou University, Zhengzhou, Henan, China

Submitted 28 November 2018, revised 19 February 2019, accepted 6 March 2019

Abstract

Drug-resistant bacteria has been a threat to public life and property. We described the trends and changes in antibiotic resistance of important pathogens in a general hospital in Zhengzhou, China from 2011 to 2016, to control antimicrobial-resistant bacteria in hospital and provide support to clinicians and decision-making departments.

Five dominant bacteria were enrolled based on the data from the general hospital during 6 years. The results of antimicrobial susceptibility testing were interpreted according to Clinical and Laboratory Standards Institute (CLSI). From 2011 to 2016, a total of 19,260 strains of bacteria were isolated, of which *Klebsiella pneumoniae*, *Escherichia coli*, *Staphylococcus aureus*, *Pseudomonas aeruginosa* and *Acinetobacter baumannii* accounted for 51.98%. The resistance rate of *K. pneumoniae* and *E. coli* to carbapenem was less than 15%, but resistance of *K. pneumoniae* to carbapenems increased with time and resistance of *E. coli* to meropenem increased. The rate of extended-spectrum beta-lactamase (ESBL) production among *K. pneumoniae* and *E. coli* was decreasing. For most antibiotics, the resistance rate of ESBL-positive isolates was higher than that of ESBL-negative isolates, excluding carbapenems and cefoxitin. For *S. aureus*, the rate of methicillin-resistant *S. aureus* (MRSA) was stable. Resistance of *S. aureus* to mostly antibiotics decreased with time. Besides polymyxin B, *P. aeruginosa* and *A. baumannii* showed high resistance to other antibiotics. For *A. baumannii*, the resistance rate to mostly antibiotics was increasing. The bacteria showed high levels of resistance and multiple drug resistance. Continuous surveillance and optimizing the use of antibiotics are essential.

Key words: antimicrobial resistance, Gram-negative bacteria, ESBL, MRSA, surveillance

Introduction

The emergence and spread of drug-resistant bacteria have always been a public concern. With the increase of resistance to available antimicrobial agents and the emergence of multi-drug resistant bacteria, antimicrobial resistance has caused serious threats to public health in the world (Livermore 2012; Rossolini et al. 2014; Yang et al. 2017). It can cause damage to human health and, at the same time, it can lead to a situation where there is no cure. The research reported that antimicrobial resistance causes about 700 000 deaths worldwide each year, and if no effective action is taken, it is expected to cause 10 million deaths a year by 2050 (Hoffman et al. 2015).

Simultaneously, antibiotics that become ineffective against bacteria have been reported (Liu et al. 2016). The bacterial resistance crisis has been greatly attributed to the overuse and misuse of these antibiotics (Pathak et al. 2013; Michael et al. 2014; Tang et al. 2018). Monitoring of the epidemiology of resistance provides useful information for prevention and helps clinicians prescribe the effective antibiotic therapy (Ventola 2015), as well as optimize the use of antibiotics, which has become one of the most important parts of drug resistance control (Lafaurie et al. 2012; Wang et al. 2018). In this study, the significant changes and trends in antibiotic resistance of clinically important pathogens isolated from a general hospital in Zhengzhou, Henan Province, China, from 2011 to 2016 were described to provide a more complete picture of bacterial infections and to help clinicians and decision-making departments undertake the proper decisions for patients and antibiotic use.

* Corresponding author: H. Yang, Department of Epidemiology, College of Public Health of Zhengzhou University, Zhengzhou, Henan, China; **e-mail: yhy@zzu.edu.cn**

Experimental

Materials and Methods

Based on the data from a general hospital in Zhengzhou, Henan province, China from 2011 to 2016, five dominant bacteria (*Klebsiella pneumoniae*, *Escherichia coli*, *Staphylococcus aureus*, *Pseudomonas aeruginosa*, and *Acinetobacter baumannii*) were investigated in this study. The antibiotic susceptibilities of the isolates were determined using the broth dilution method according to Clinical and Laboratory Standards Institute (CLSI 2017). In this study, the intermediate was attributed as the resistant. The differences in proportions were compared using the chi-squared test and the variation tendency was compared using the chi-squared for trend. Two-sided test with $p < 0.05$ were taken as statistically significant, with the use of SAS 9.1.

Results

From 2011 to 2016, a total of 19 260 bacterial isolates were obtained, with five dominant bacteria being *K. pneumoniae* (17.71%), *E. coli* (14.45%), *S. aureus* (7.42%), *P. aeruginosa* (6.64%), and *A. baumannii* (5.75%). Overall, these isolates accounted for 51.98% of all reported isolates. Also, a wavy increase was observed in the detection rates of these isolates (Table I).

During the study period, the detection rate of *K. pneumoniae* isolates was stable, meanwhile, the rate of extended-spectrum beta-lactamase (ESBL)-producing *K. pneumoniae* (ESBL-*K. pneumoniae*) showed a downward trend ($\chi^2 = -4.6619$, $p < 0.0001$). A significant increase of resistance was observed for cefotaxime, meropenem, and imipenem to *K. pneumoniae* and ESBL-*K. pneumoniae*. But a significant decrease of resistance was seen for nitrofurantoin. Beyond that, the resistance rates of ampicillin, levofloxacin, cefepime, and piperacillin-tazobactam against *K. pneumoniae* increased from 97.1% to 100%, from 34.42% to 35.05%, from 23.91% to 34.91%, and from 21.74% to 30.58%, respectively. In addition, the rate of trimethoprim-sulfamethoxazole decreased from 71.38% to 55.07%. These results are shown in Table II and Table S-I. The resistance rates of ESBL-*K. pneumoniae* isolates to cefuroxime, ceftriaxone, ampicillin-sulbactam, trimethoprim-sulfamethoxazole, gentamicin, cefotaxime, cefepime, nitrofurantoin, levofloxacin were higher than the rates displayed by ESBL-negative *K. pneumoniae* isolates ($p < 0.05$) (Table S-II).

During the study period, the detection rates of *E. coli* and ESBL-producing *E. coli* (ESBL-*E. coli*) showed a declining trend ($\chi^2 = -4.7904$, $p < 0.0001$ and $\chi^2 = -2.1785$, $p = 0.0294$, respectively). A significant increase of resistance against *E. coli* and ESBL-*E. coli* was observed for cefotaxime, ceftazidime, and meropenem. But a significant decrease of resistance was seen for trimethoprim-

Table I
Distribution of bacterial isolates in relation to years and type of samples.

Category	No. isolates	*Klebsiella pneumoniae*		*Escherichia coli*		*Staphylococcus aureus*		*Pseudomonas aeruginosa*		*Acinetobacter baumannii*		Total	
		n	%	n	%	n	%	n	%	n	%	n	%
Year													
2011	1429	276	19.31	213	14.91	96	6.72	108	7.56	68	4.76	761	53.25
2012	3350	524	15.64	531	15.85	248	7.40	236	7.04	114	3.40	1653	49.34
2013	3143	486	15.46	493	15.89	219	6.98	168	5.35	114	3.63	1480	47.09
2014	3073	605	19.69	477	15.52	213	6.93	248	8.07	224	7.29	1767	57.50
2015	3750	781	20.83	522	13.92	254	6.77	259	6.91	292	7.89	2108	56.21
2016	4515	739	16.37	548	12.18	400	8.86	259	5.74	296	6.56	2242	49.66
Total	19260	3411	17.71	2784	14.45	1430	7.42	1278	6.64	1108	5.75	10011	51.98
χ^2			1.5767		−4.7904		2.5513		−1.7311		7.8954		1.9893
p			0.1149		< 0.0001		0.0107		0.0834		< 0.0001		0.0467
Samples													
Sputum		2741	80.36	493	17.71	81	5.66	1023	80.05	910	82.13	5248	27.25
Urine		382	11.2	1565	56.21	249	17.41	110	8.61	87	7.85	2393	12.42
Blood		104	3.05	265	9.52	275	19.23	30	2.35	24	2.17	698	3.62
Secretion		92	2.7	217	7.79	620	43.36	65	5.09	41	3.70	1035	5.37
Throat swabs		27	0.79	8	0.29	6	0.42	3	0.23	3	0.27	47	0.24
Others		65	1.91	236	8.48	199	13.92	47	3.68	43	3.88	590	3.06

Table II
The resistance rates of *K. pneumoniae* to 15 antimicrobial agents in the years 2011 to 2016.

Antimicrobial agent	MIC breakpoints	2011	2012	2013	2014	2015	2016	Total	χ^2	*p*
	I (μg/ml)	n = 276	n = 524	n = 486	n = 605	n = 781	n = 739	n = 3411		
Ampicillin	16	97.1	99.05	98.97	99.5	100	100	99.38	5.2285	< 0.0001
Cefotaxime	2	52.17	54.39	45.27	56.86	100	100	73.67	26.9374	< 0.0001
Nitrofurantoin	64	76.81	65.84	49.59	56.36	54.16	58.59	58.49	–4.711	< 0.0001
Trimethoprim--sulfamethoxazole	4/76	71.38	70.61	52.06	35.7	37	55.07	50.78	–9.1411	< 0.0001
Ampicillin-sulbactam	16/8	52.54	49.81	46.09	40.17	47.25	47.9	46.79	–1.1923	0.2332
Cefuroxime	16	50.72	49.81	43.21	42.64	47.76	51.01	47.46	0.51	0.6101
Ceftriaxone	2	48.91	53.24	43.21	37.52	46.09	48.71	46.06	–0.9744	0.3299
Gentamicin	8	44.93	43.7	33.74	31.74	40.46	40.46	38.82	–0.8754	0.3813
Cefoxitin	16	40.58	43.51	34.77	31.9	39.44	39.51	38.17	–0.6514	0.5148
Levofloxacin	4	34.42	33.21	22.02	26.12	37.26	35.05	31.78	2.3291	0.0199
Cefepime	16	23.91	33.59	22.84	26.28	35.47	34.91	30.69	3.7816	0.0002
Piperacillin-tazobactam	32/4–64/4	21.74	24.81	18.93	23.64	32.01	30.58	26.41	4.7683	< 0.0001
Amikacin	32	26.09	26.53	16.05	18.02	28.55	23	23.19	0.376	0.7069
Meropenem	2	0	0	0	0.99	10.12	11.37	4.95	12.3843	< 0.0001
Imipenem	2	0	0	0	1.49	9.22	7.98	4.1	10.4364	< 0.0001

Table III
The resistance rates of *E. coli* to 16 antimicrobial agents in the years 2011 to 2016.

Antimicrobial agent	MIC breakpoints	2011	2012	2013	2014	2015	2016	Total	χ^2	*p*
	I (μg/ml)	n = 213	n = 531	n = 493	n = 477	n = 522	n = 548	n = 2784		
Ampicillin	16	92.49	93.03	90.06	86.37	87.16	88.87	89.4	–3.0413	0.0024
Cefotaxime	2	69.01	72.88	71.4	73.17	100	100	82.79	16.5655	< 0.0001
Trimethoprim--sulfamethoxazole	4/76	93.9	93.03	81.74	77.99	70.69	69.16	79.63	–11.9199	< 0.0001
Ampicillin-sulbactam	16/8	76.06	73.63	80.53	67.92	60.15	62.96	69.43	–6.7117	< 0.0001
Cefuroxime	16	70.42	73.45	71.81	67.51	60.92	62.59	67.42	–4.8433	< 0.0001
Levofloxacin	4	73.71	71.56	67.95	65.62	66.67	61.13	67.1	–4.0714	< 0.0001
Ceftriaxone	2	69.01	72.5	68.97	64.36	60.15	62.23	65.88	–4.3853	< 0.0001
Gentamicin	8	74.18	65.73	60.45	59.75	51.34	52.92	59.2	–6.7725	< 0.0001
Cefepime	16	49.77	54.24	46.25	38.36	30.65	38.32	42.21	–7.1678	< 0.0001
Ceftazidime	8	17.84	1.32	48.48	43.61	34.29	36.31	31.25	9.9654	< 0.0001
Cefoxitin	16	30.52	29.57	29.41	21.17	12.07	10.77	21.19	–10.1704	< 0.0001
Nitrofurantoin	64	28.17	27.31	16.02	14.47	10.73	11.13	16.88	–8.6556	< 0.0001
Piperacillin-tazobactam	32/4–64/4	14.55	18.64	13.18	13.63	6.7	10.77	12.72	–4.6131	< 0.0001
Amikacin	32	18.31	15.25	10.75	8.39	8.24	8.03	10.78	–5.3067	< 0.0001
Imipenem	2	0.94	1.51	2.43	1.26	1.15	1.64	1.54	–0.1060	0.9156
Meropenem	2	0	0.56	0.2	1.05	0.96	2.01	0.9	3.1604	0.0016

sulfamethoxazole, ampicillin-sulbactam, gentamicin, cefepime, cefoxitin, nitrofurantoin, and amikacin. A marked decrease of resistance against *E. coli* was observed for cefuroxime and ceftriaxone, i.e., from 70.42% to 62.59%, and from 69.01% to 62.23%, respectively. However, the resistance rates of these two antimicrobial agents to ESBL-*E. coli* showed an increasing trend (both from 95.6% to 100%). All the ESBL-*E. coli* isolates were resistant to ampicillin. These data are presented in Table III and Table S-III. The resistance

rates of ESBL-*E. coli* isolates to ceftriaxone, cefuroxime, ampicillin-sulbactam, cefepime, ampicillin, cefotaxime, levofloxacin, ceftazidime, gentamicin, and trimethoprim-sulfamethoxazole were higher than the rates of the ESBL-negative *E. coli* isolates ($p < 0.05$) (Table S-IV).

During the study period, the detection rate of *S. aureus* showed an upward trend ($\chi^2 = 2.5513$, $p = 0.0107$), meanwhile, the rate of methicillin-resistant *S. aureus* (MRSA) was stable. A significant decrease of resistance of isolates of *S. aureus* (including MRSA) was observed for erythromycin, azithromycin, clarithromycin, trimethoprim-sulfamethoxazole, clindamycin, cefoxitin, norfloxacin, moxifloxacin, gentamicin, tetracycline, rifampicin, nitrofurantoin, and teicoplanin. No *S. aureus* isolate was found to be resistant to linezolid and vancomycin. All MRSA isolates were resistant to oxacillin. These results are depicted in Table IV and Table S-V. The resistance rates of MRSA to 15 antimicrobial agents were higher than that of methicillin-susceptible *S. aureus* (MSSA) ($p < 0.05$) (Table S-VI).

During the study period, the detection rate of *P. aeruginosa* was stable. A significant decrease of resistance was observed for gentamicin, tobramycin, and polymyxin B from 52.78% to 50.58%, from 53.7% to 44.4%, and from 20.37% to 6.56%, respectively. In addition, a marked increase was seen for meropenem from 44.44% in 2011 to 49.81% in 2016 (Table V).

During the study period, the detection rate of *A. baumannii* showed an increasing tendency ($\chi^2 = 7.8954$, $p < 0.0001$). A significant increase of resistance of the isolates was observed for ceftriaxone, gentamicin, ciprofloxacin, ceftazidime, trimethoprim-sulfamethoxazole, cefepime, levofloxacin, piperacillin-tazobactam, and amikacin (Table VI).

Discussion

This study provided data about detection rates and resistance patterns of five dominant bacteria isolated in a general hospital in Zhengzhou, Henan province, China, between 2011 and 2016. Overall, the detection rates of these bacteria showed a slowly increasing trend. In addition, Gram-negative bacteria seemed to be the main cause of infection. The possible explanation of these phenomena could be the overrepresentation of some types of the samples (sputum and urine), or a double-membrane structure and the occurrence of efficient efflux pumps in Gram-negative bacteria (Blair et al. 2014). Several studies have reported similar findings. The data from CHINET surveillance between 2005 and 2014 showed that the five selected species, including *E. coli*, *K. pneumoniae*, *P. aeruginosa*, *A. baumannii*, and *S. aureus* accounted for 51.9 to 60.3%

Table IV
The resistance rates of *S. aureus* to 18 antimicrobial agents in the years 2011 to 2016.

Antimicrobial agent	MIC breakpoints	2011	2012	2013	2014	2015	2016	Total	χ^2	*p*
	I (μg/ml)	n = 96	n = 248	n = 219	n = 213	n = 254	n = 400	n = 1430		
Penicillin	0.25	92.71	93.55	94.06	95.77	88.19	89.00	91.68	–2.759	0.0058
Erythromycin	1–4	95.83	87.10	80.82	80.28	82.28	81.00	83.15	–3.0012	0.0027
Azithromycin	4	90.63	86.29	80.37	81.22	77.95	76.50	80.70	–3.8879	0.0001
Clarithromycin	4	90.63	83.87	79.45	79.81	70.08	69.00	76.43	–6.0151	< 0.0001
Trimethoprim--sulfamethoxazole	4/76	85.42	91.13	62.56	69.95	73.62	51.25	68.95	–9.9209	< 0.0001
Clindamycin	1–2	67.71	65.73	59.36	56.34	55.12	58.25	59.51	–2.4495	0.0143
Cefoxitin	8	69.79	72.18	71.23	58.69	44.49	41.50	56.36	–9.6125	< 0.0001
Norfloxacin	8	70.83	64.11	63.01	59.62	52.36	43.75	55.94	–6.6063	< 0.0001
Levofloxacin	2	67.71	61.29	57.99	56.34	48.43	36.25	51.19	–7.6331	< 0.0001
Moxifloxacin	1	63.54	56.45	52.51	53.99	48.03	34.50	48.32	–6.5328	< 0.0001
Gentamicin	8	64.58	64.11	46.12	45.54	35.83	35.00	45.45	–8.242	< 0.0001
Tetracycline	8	58.33	57.26	47.49	47.42	38.98	37.00	45.45	–5.9025	< 0.0001
Oxacillin	4	53.13	42.74	33.79	43.66	45.67	42.25	42.59	–0.6128	0.8283
Rifampicin	2	40.63	30.65	25.57	21.60	17.32	10.00	21.19	–8.1147	< 0.0001
Nitrofurantoin	64	26.04	15.73	16.44	9.86	5.91	8.00	11.75	–5.7483	< 0.0001
Teicoplanin	16	11.46	12.10	5.02	4.23	0.79	1.75	4.90	–6.6928	< 0.0001
Linezolid	8	0	0	0	0	0	0	0		
Vancomycin	4–8	0	0	0	0	0	0	0		

Table V
The resistance rates of *P. aeruginosa* to 13 antimicrobial agents in the years 2011 to 2016.

Antimicrobial agent	MIC breakpoints	2011	2012	2013	2014	2015	2016	Total	χ^2	*p*
	I (μg/ml)	n = 108	n = 236	n = 168	n = 248	n = 259	n = 259	n = 1278		
Ticarcillin	32–64	70.37	74.58	76.79	76.21	75.29	76.45	75.35	0.9182	0.3585
Piperacillin	32–64	57.41	63.14	54.76	56.45	61.00	61.39	59.47	0.3942	0.6934
Imipenem	4	50.00	52.97	60.71	53.63	62.16	57.92	56.73	1.8507	0.0642
Aztreonam	16	50.93	48.31	54.76	50.00	52.90	54.83	51.96	1.1464	0.2516
Gentamicin	8	52.78	61.02	55.36	43.95	49.42	50.58	51.80	–2.2516	0.0243
Ceftazidime	16	43.52	52.54	54.76	49.19	51.74	53.28	51.41	0.8686	0.3851
Tobramycin	8	53.70	58.90	52.38	39.11	49.81	44.40	48.98	–3.0892	0.0020
Piperacillin-tazobactam	32/4–64/4	43.52	51.27	42.86	41.94	52.90	53.28	48.44	1.6789	0.0932
Norfloxacin	8	50.93	54.24	47.02	39.92	48.26	48.26	47.81	–1.2309	0.2183
Meropenem	4	44.44	41.95	45.24	45.16	54.44	49.81	47.34	2.4052	0.0162
Cefepime	16	42.59	46.19	50.60	37.90	49.81	51.74	46.71	1.5010	0.1334
Ciprofloxacin	2	48.15	52.97	45.83	41.53	45.56	44.02	46.09	–1.7609	0.0783
Levofloxacin	4	45.37	47.88	40.48	37.90	45.95	45.95	43.97	–0.0615	0.9510
Amikacin	32	36.11	40.68	37.50	29.03	35.52	36.29	35.68	–0.9114	0.3621
Polymyxin B	4	20.37	19.49	14.29	9.68	13.51	6.56	13.15	–4.5199	< 0.0001

Table VI
The resistance rates of *A. baumannii* to 13 antimicrobial agents in the years 2011 to 2016.

Antimicrobial agent	MIC breakpoints	2011	2012	2013	2014	2015	2016	Total	χ^2	*p*
	I (μg/ml)	n = 68	n = 114	n = 114	n = 224	n = 292	n = 296	n = 1108		
Ceftriaxone	16–32	32.35	64.04	72.81	72.77	79.11	80.74	73.19	7.4412	< 0.0001
Ampicillin-sulbactam	16/8	41.18	64.91	81.58	76.79	73.63	64.53	69.77	1.5591	0.1190
Gentamicin	8	44.12	67.54	64.04	74.55	68.15	75.68	69.49	4.0867	< 0.0001
Ciprofloxacin	2	39.71	57.89	64.04	73.66	69.52	75.34	68.32	5.6165	< 0.0001
Ceftazidime	16	39.71	52.63	64.04	66.07	62.67	72.64	63.72	5.0871	< 0.0001
Trimethoprim--sulfamethoxazole	4/76	39.71	63.16	60.53	60.27	66.78	64.86	62.27	3.0414	0.0024
Cefepime	16	35.29	50.00	56.14	62.05	61.99	70.95	60.92	5.8829	< 0.0001
Levofloxacin	4	41.18	53.51	64.04	65.18	59.93	64.53	60.83	2.9341	0.0033
Piperacillin-tazobactam	32/4–64/4	29.41	50.00	57.02	58.04	64.38	68.24	59.75	6.0938	< 0.0001
Amikacin	32	33.82	60.53	56.14	62.50	57.53	62.84	58.66	2.8410	0.0045
Meropenem	4	19.12	46.49	57.89	54.02	47.95	47.64	48.19	1.9045	0.0568
Imipenem	4	20.59	48.25	61.40	59.38	45.55	37.16	46.48	–1.0354	0.3005
Polymyxin B	4	10.29	21.93	15.79	19.64	13.63	18.24	16.88	0.0504	0.9598

of all isolates (Hu et al. 2016). In a four-year study in Italy, researchers found that Gram-negative bacteria appeared to be the major causes of infection (Reale et al. 2017). Thus, in terms of quantity and proportion, Gram-negative bacteria have become a major threat in nosocomial infections.

During the study period, the situation with these multi-resistant isolates was complicated. For *K. pneumoniae* and *A. baumannii*, the rates of multi-resistant isolates were increasing. For *E. coli*, *P. aeruginosa*, and *S. aureus*, the rates were decreasing. From these results, one can get directions for making recommendations by some government policies, such as separation the clinic from the pharmacy, hospital surveillance and preventive measures. All these recommendations may have played a role in combating antibiotic resistance. But more importantly, a problem demanding prompt solution is how to prevent the spread of multi-drug

resistant isolates and how to optimize the use of the existing antibiotics.

Overall, among the Enterobacteriaceae, 14.34% of *K. pneumoniae* isolates and 50.18% of *E. coli* isolates were ESBL producers. A marked decrease in the detection rates was seen for ESBL-*K. pneumoniae* and ESBL-*E. coli*. In addition, the resistance rates of ESBL-positive isolates to multiple antibiotics (mainly cephalosporin antibiotics) were higher than that of ESBL-negative isolates. This might be related to the extensive use of cephalosporin in clinical practice, especially the third generation cephalosporin (Pathak et al. 2013; Tang et al. 2018). But the resistance rate of ESBL-positive isolates to cefoxitin was lower than that of ESBL-negative isolates. Also, the resistance rate of these isolates to cefoxitin was lower than that to the third generation cephalosporin. In the absence of details about the resistance genes of these isolates, we could not infer that this was related to *AmpC*. Moreover, the ESBL-positive isolates were not only resistant to cephalosporin antibiotics, but also resistant to fluoroquinolones. As observed in this study, the resistance rate of ESBL-*K. pneumoniae* and ESBL-*E. coli* to levofloxacin was 37.22% and 79.10%, with a marked increase, respectively. This has led to growing utilization of carbapenems. Fortunately, the majority of *K. pneumoniae* and *E. coli* were sensitive to carbapenems (Hu et al. 2016; Khan et al. 2017; Yang et al. 2017).

Although the resistance rate of *S. aureus* to most antibiotics was declining, the resistance rate of the isolates was still above 40%. This indicated the severity of multidrug resistance in *S. aureus*. This phenomenon was more pronounced in MRSA. During the study period, the detection rate of MRSA was 42.38%. The data from CHINET surveillance showed a marked decrease of MRSA from 69% in 2005 to 44.6% in 2014 (Hu et al. 2016). The resistance rate of MRSA to antibiotics was apparently higher than that of MSSA, except linezolid and vancomycin. This was associated with SCC*mec* elements. The SCC*mec* element is a mobile genetic element that carries a variety of antibiotic resistance genes, such as drug-resistance genes against mercury, cadmium, kanamycin, bleomycin, erythromycin, spectinomycin, and fusidic acid (Ito et al. 2001; Holden et al. 2004). Currently, vancomycin is still an ideal antibiotic to treat *S. aureus*-related infections, but vancomycin-resistant *S. aureus* has been reported (Panesso et al. 2015; Walters et al. 2015; Olufunmiso et al. 2017).

In this study, besides polymyxin B, *P. aeruginosa* showed high resistance to other antibiotics. The emergence of multidrug-resistant *P. aeruginosa* posed a difficult problem for clinical treatment (Vincent 2003). Compared with the data from CHINET, the resistance rate of *P. aeruginosa* to nine antibiotics (imipenem, meropenem, gentamicin, ceftazidime, tobramycin, piperacillin-tazobactam, cefepime, ciprofloxacin, levofloxacin, and amikacin) in this study were higher than in the surveillance data, which might be related to differences among the surveillance area (Hu et al. 2016). Aminoglycosides are recognized for their efficacy against *P. aeruginosa* (Holbrook and Garneau-Tsodikova, 2018). Although the resistance rate of *P. aeruginosa* to aminoglycoside antibiotics was decreasing, the strains showed high levels of resistance. For example, the antibiotic with the lowest resistance rate was amikacin, which resistance rate was 35.68%. Meanwhile, *P. aeruginosa* also showed high resistance to carbapenems, which might be related to the high use of these antibiotics in clinics.

A similar trend was observed for *A. baumannii*, and more seriously, the detection rate of isolates and the resistance rate of isolates to the majority of antibiotics were increasing. These were consistent with other studies (Peneș et al. 2017). This was mainly due to the membrane impermeability of *A. baumannii*, which leads to difficulty in traversing the membrane and reaching their targets by antibiotics (Sugawara and Nikaido 2012; Zgurskaya et al. 2015). Carbapenem antibiotics are important for the treatment the *A. baumannii* infection, but reports have shown that the rate of carbapenems-resistant *A. baumannii* was increasing (Agodi et al. 2015; Hu et al. 2016). Research had shown that the increasing use of carbapenems was associated with the increasing rate of carbapenem-resistant *A. baumannii* (Tan et al. 2015). This showed the importance of rational use of antibiotics. Rigatto et al. (2015) had shown a benefit of combination monotherapy with polymyxin B for severe extensively drug-resistant *A. baumannii* or *P. aeruginosa* infections. Resistance to polymyxin B would increase the difficulty of treating multi-drug resistant *A. baumannii* and *P. aeruginosa*. Chung et al. (2016) have developed a new combination therapy using minimal concentrations of polymyxin B.

Conclusions

In conclusion, Gram-negative bacteria appeared to be the main cause of infection in this study. The resistance rates of five species of the bacteria to most antibiotics were decreasing, but the isolates showed high levels of resistance and multiple-drug resistance, especially *P. aeruginosa* and *A. baumannii*. Methods such as the combination of antibiotics to optimize the use of antibiotics may help to solve the problem. Simultaneously, this study showed that some antibiotics continue to be active against these isolates, such as meropenem and imipenem for ESBL-*K. pneumoniae* and ESBL-*E. coli*, linezolid and vancomycin for MRSA and polymyxin B for *P. aeruginosa,* and *A. baumannii*. The mobility of modern society is unprecedented. Geographical boundaries cannot stop the spread of drug-resistant bacteria.

ORCID
Haiyan Yang 0000-0002-1797-304X

Limitation

Our study has several limitations. First, we do not know the use of antibiotics in patients from whom the bacteria were isolated, nor their outcomes. Second, we did not track the changes of these strains at the genetic level in the laboratory.

Acknowledgments

This study received financial support from the Henan Province University Science and Technology Innovation Talent Projects (17HASTIT045).

Conflict of interest

The authors do not report any financial or personal connections with other persons or organizations, which might negatively affect the contents of this publication and/or claim authorship rights to this publication.

Literature

Agodi A, Barchitta M, Quattrocchi A, Maugeri A, Aldisio E, Marchese AE, Mattaliano AR, Tsakris A. Antibiotic trends of *Klebsiella pneumoniae* and *Acinetobacter baumannii* resistance indicators in an intensive care unit of Southern Italy, 2008–2013. Antimicrob Resist Infect Control. 2015 Dec;4(1):43. doi:10.1186/s13756-015-0087-y Medline

Blair JMA, Richmond GE, Piddock LJV. Multidrug efflux pumps in Gram-negative bacteria and their role in antibiotic resistance. Future Microbiol. 2014 Oct;9(10):1165–1177. doi:10.2217/fmb.14.66 Medline

Chung J, Bhat A, Kim C, Yong D, Ryu C. Combination therapy with polymyxin B and netropsin against clinical isolates of multidrug-resistant *Acinetobacter baumannii*. Sci. Rep.-UK. 2016;6:28168.

CLSI. Performance Standards for Antimicrobial Susceptibility Testing. Wayne (USA): Clinical Laboratory Standards Institute; 2017.

Hoffman SJ, Outterson K, Røttingen JA, Cars O, Clift C, Rizvi Z, Rotberg F, Tomson G, Zorzet A. An international legal framework to address antimicrobial resistance. Bull World Health Organ. 2015 Feb 01;93(2):66–66. doi:10.2471/BLT.15.152710 Medline

Holbrook SYL, Garneau-Tsodikova S. Evaluation of aminoglycoside and carbapenem resistance in a collection of drug-resistant *Pseudomonas aeruginosa* clinical isolates. Microb Drug Resist. 2018 Sep;24(7):1020–1030. doi:10.1089/mdr.2017.0101 Medline

Holden MTG, Feil EJ, Lindsay JA, Peacock SJ, Day NPJ, Enright MC, Foster TJ, Moore CE, Hurst L, Atkin R, et al. Complete genomes of two clinical *Staphylococcus aureus* strains: evidence for the rapid evolution of virulence and drug resistance. Proc Natl Acad Sci USA. 2004 Jun 29;101(26):9786–9791. doi:10.1073/pnas.0402521101 Medline

Hu FP, Guo Y, Zhu DM, Wang F, Jiang XF, Xu YC, Zhang XJ, Zhang CX, Ji P, Xie Y. Resistance trends among clinical isolates in China reported from CHINET surveillance of bacterial resistance, 2005–2014. Clin. Microbiol. Infec. 2016;22:S9–S14.

Ito T, Katayama Y, Asada K, Mori N, Tsutsumimoto K, Tiensasitorn C, Hiramatsu K. Structural comparison of three types of staphylococcal cassette chromosome mec integrated in the chromosome in methicillin-resistant *Staphylococcus aureus*. Antimicrob Agents Chemother. 2001 May 01;45(5):1323–1336. doi:10.1128/AAC.45.5.1323-1336.2001 Medline

Khan ER, Aung MS, Paul SK, Ahmed S, Haque N, Ahamed F, Sarkar SR, Roy S, Rahman MM, Mahmud MC, et al. Prevalence and molecular epidemiology of clinical isolates of *Escherichia coli* and *Klebsiella pneumoniae* harboring Extended-Spectrum Beta-Lactamase and carbapenemase genes in Bangladesh. Microb Drug Resist. 2018 Dec;24(10):1568–1579. doi:10.1089/mdr.2018.0063 Medline

Lafaurie M, Porcher R, Donay JL, Touratier S, Molina JM. Reduction of fluoroquinolone use is associated with a decrease in methicillin-resistant *Staphylococcus aureus* and fluoroquinolone-resistant *Pseudomonas aeruginosa* isolation rates: a 10 year study. J Antimicrob Chemother. 2012 Apr 01;67(4):1010–1015. doi:10.1093/jac/dkr555 Medline

Liu YY, Wang Y, Walsh TR, Yi LX, Zhang R, Spencer J, Doi Y, Tian G, Dong B, Huang X, et al. Emergence of plasmid-mediated colistin resistance mechanism MCR-1 in animals and human beings in China: a microbiological and molecular biological study. Lancet Infect Dis. 2016 Feb;16(2):161–168. doi:10.1016/S1473-3099(15)00424-7 Medline

Livermore DM. Fourteen years in resistance. Int J Antimicrob Agents. 2012 Apr;39(4):283–294. doi:10.1016/j.ijantimicag.2011.12.012 Medline

Michael CA, Dominey-Howes D, Labbate M. The antimicrobial resistance crisis: causes, consequences, and management. Front Public Health. 2014 Sep 16;2:145. doi:10.3389/fpubh.2014.00145 Medline

Olufunmiso O, Tolulope I, Roger C. Multidrug and vancomycin resistance among clinical isolates of *Staphylococcus aureus* from different teaching hospitals in Nigeria. Afr Health Sci. 2017 Sep 18;17(3):797–807. doi:10.4314/ahs.v17i3.23 Medline

Panesso D, Planet PJ, Diaz L, Hugonnet JE, Tran TT, Narechania A, Munita JM, Rincon S, Carvajal LP, Reyes J, et al. Methicillin-Susceptible, Vancomycin-Resistant *Staphylococcus aureus*, Brazil. Emerg Infect Dis. 2015 Oct;21(10):1844–1848. doi:10.3201/eid2110.141914 Medline

Pathak A, Chandran SP, Mahadik K, Macaden R, Lundborg CS. Frequency and factors associated with carriage of multi-drug resistant commensal *Escherichia coli*among women attending antenatal clinics in Central India. BMC Infect Dis. 2013 Dec;13(1):199. doi:10.1186/1471-2334-13-199 Medline

Peneș NO, Muntean AA, Moisoiu A, Muntean MM, Chirca A, Bogdan MA, Popa MI. An overview of resistance profiles ESKAPE pathogens from 2010–2015 in a tertiary respiratory center in Romania. Rom J Morphol Embryol. 2017;58(3):909–922. Medline

Reale M, Strazzulla A, Quirino A, Rizzo C, Marano V, Postorino MC, Mazzitelli M, Greco G, Pisani V, Costa C, et al. Patterns of multi-drug resistant bacteria at first culture from patients admitted to a third level University hospital in Calabria from 2011 to 2014: implications for empirical therapy and infection control. Infez Med. 2017 Jun 1;25(2):98–107. Medline

Rigatto MH, Vieira FJ, Antochevis LC, Behle TF, Lopes NT, Zavascki AP. Polymyxin B in Combination with Antimicrobials Lacking *In Vitro* Activity versus Polymyxin B in Monotherapy in Critically Ill Patients with *Acinetobacter baumannii* or *Pseudomonas aeruginosa* Infections. Antimicrob Agents Chemother. 2015 Oct;59(10):6575–6580. doi:10.1128/AAC.00494-15 Medline

Rossolini GM, Arena F, Pecile P, Pollini S. Update on the antibiotic resistance crisis. Curr Opin Pharmacol. 2014 Oct;18:56–60. doi:10.1016/j.coph.2014.09.006 Medline

Sugawara E, Nikaido H. OmpA is the principal nonspecific slow porin of *Acinetobacter baumannii*. J Bacteriol. 2012 Aug 01;194(15):4089–4096. doi:10.1128/JB.00435-12 Medline

Tan CK, Tang HJ, Lai CC, Chen YY, Chang PC, Liu WL. Correlation between antibiotic consumption and carbapenem-resistant *Acinetobacter baumannii* causing health care-associated infections at a hospital from 2005 to 2010. J Microbiol Immunol Infect. 2015 Oct;48(5):540–544. doi:10.1016/j.jmii.2014.02.004 Medline

Tang X, Xiao M, Zhuo C, Xu Y, Zhong N. Multi-level analysis of bacteria isolated from inpatients in respiratory departments in China. J Thorac Dis. 2018 May;10(5):2666–2675. doi:10.21037/jtd.2018.04.46 Medline

Ventola CL. The antibiotic resistance crisis: part 2: management strategies and new agents. P T. 2015 May;40(5):344–352. Medline

Vincent JL. Nosocomial infections in adult intensive-care units. Lancet. 2003 Jun;361(9374):2068–2077. doi:10.1016/S0140-6736(03)13644-6 Medline

Walters MS, Eggers P, Albrecht V, Travis T, Lonsway D, Hovan G, Taylor D, Rasheed K, Limbago B, Kallen A. Vancomycin-Resistant *Staphylococcus aureus* – Delaware, 2015. MMWR Morb Mortal Wkly Rep. 2015 Sep 25;64(37):1056. doi:10.15585/mmwr.mm6437a6 Medline

Wang S, Han LZ, Ni YX, Zhang YB, Wang Q, Shi DK, Li WH, Wang YC, Mi CR. Changes in antimicrobial susceptibility of commonly clinically significant isolates before and after the interventions on surgical prophylactic antibiotics (SPAs) in Shanghai. Braz J Microbiol. 2018 Jul;49(3):552–558. doi:10.1016/j.bjm.2017.12.004 Medline

Yang Q, Xu YC, Kiratisin P, Dowzicky MJ. Antimicrobial activity among gram-positive and gram-negative organisms collected from the Asia-Pacific region as part of the Tigecycline Evaluation and Surveillance Trial: comparison of 2015 results with previous years. Diagn Microbiol Infect Dis. 2017 Dec;89(4):314–323. doi:10.1016/j.diagmicrobio.2017.08.014 Medline

Zgurskaya HI, López CA, Gnanakaran S. Permeability Barrier of Gram-Negative Cell Envelopes and Approaches To Bypass It. ACS Infect Dis. 2015 Nov 13;1(11):512–522. doi:10.1021/acsinfecdis.5b00097 Medline

Supplementary materials are available on the journal's website.

Polish Journal of Microbiology
2019, Vol. 68, No 2, 233–246
https://doi.org/10.33073/pjm-2019-025

ORIGINAL PAPER

Analysis of the Amino Acid Sequence Variation of the 67–72p Protein and the Structural Pili Proteins of *Corynebacterium diphtheriae* for their Suitability as Potential Vaccine Antigens

KLAUDIA BRODZIK[1], KATARZYNA KRYSZTOPA-GRZYBOWSKA[1], MACIEJ POLAK[1], JAKUB LACH[2], DOMINIK STRAPAGIEL[2, 3] and ALEKSANDRA ANNA ZASADA[1]

[1] Department of Sera and Vaccines Evaluation, National Institute of Public Health – National Institute of Hygiene, Warsaw, Poland
[2] Biobank Lab, Department of Molecular Biophysics, Faculty of Biology and Environmental Protection, University of Lodz, Lodz, Poland
[3] BBMRI.pl Consortium, Wroclaw Research Center EIT+, Wroclaw, Poland

Submitted 4 December 2018, revised 8 March 2019, accepted 9 March 2019

Abstract

The aim of this study was to identify the potential vaccine antigens in *Corynebacterium diphtheriae* strains by *in silico* analysis of the amino acid variation in the 67–72p surface protein that is involved in the colonization and induction of epithelial cell apoptosis in the early stages of infection. The analysis of pili structural proteins involved in bacterial adherence to host cells and related to various types of infections was also performed. A polymerase chain reaction (PCR) was carried out to amplify the genes encoding the 67–72p protein and three pili structural proteins (SpaC, SpaI, SapD) and the products obtained were sequenced. The nucleotide sequences of the particular genes were translated into amino acid sequences, which were then matched among all the tested strains using bioinformatics tools. In the last step, the affinity of the tested proteins to major histocompatibility complex (MHC) classes I and II, and linear B-cell epitopes was analyzed. The variations in the nucleotide sequence of the 67–72p protein and pili structural proteins among *C. diphtheriae* strains isolated from various infections were noted. A transposition of the insertion sequence within the gene encoding the SpaC pili structural proteins was also detected. In addition, the bioinformatics analyses enabled the identification of epitopes for B-cells and T-cells in the conserved regions of the proteins, thus, demonstrating that these proteins could be used as antigens in the potential vaccine development. The results identified the most conserved regions in all tested proteins that are exposed on the surface of *C. diphtheriae* cells.

Key words: *Corynebacterium diphtheriae*, non-toxigenic, pili, 67–72p protein, vaccine

Introduction

Corynebacterium diphtheriae is the etiological agent of a serious infectious disease – diphtheria. The diphtheria vaccine is highly effective but is directed only against the diphtheria toxin. The non-toxigenic *C. diphtheriae* strains may cause many severe invasive diseases, e.g., endocarditis, septic arthritis, bacteremia, and noninvasive wound infections. The notified increasing number of non-toxigenic *C. diphtheriae* infections indicates that infections are a growing problem in Europe (Belko et al. 2000; Zasada et al. 2010; Zasada 2013; Fricchione et al. 2014; Dangel et al. 2018). It is hypothesized that high vaccination coverage has resulted in the emergence of non-toxin-producing (non-toxigenic) *C. diphtheriae* strains, which acquired new virulence factors.

The diphtheria toxoid vaccination protects against the action of the toxin but does not protect against colonization and invasion by *C. diphtheriae*. Little is known about *C. diphtheriae* virulence factors other than the diphtheria toxin. The degree of adhesion of microorganisms to host cells has been shown to be an important pathogenicity factor for both toxigenic and non-toxigenic strains (Colombo et al. 2001). The virulence factors that facilitate bacterial colonization to specific host tissues and are related to pathogenesis include pili and fimbriae (Reardon-Robinson and Ton-That 2014). These structures are covalently attached to

* Corresponding author: K. Brodzik, Department of Sera and Vaccines Evaluation, National Institute of Public Health National Institute of Hygiene, Warsaw, Poland; **e-mail: kbrodzik@pzh.gov.pl**

the bacterial cell wall and are recognized by the related host receptors (Sauer et al. 2000; Rogers et al. 2011). The surface structures are potential candidates for the development of new vaccines and antimicrobial therapies, due to their significant role in pathogenesis (Maione et al. 2005; Soriani and Telford 2010). Pili are found in both Gram-positive and Gram-negative bacteria, albeit with different folding mechanisms (Thanassi et al. 1998; Ton-That and Schneewind 2004). The function of pili is not only the involvement in adhesion, but they also act as bacteriophage receptors and participate in DNA transfer, biofilm formation, cell aggregation, host cell penetration, and motility (Proft and Baker 2009).

There are three types of pili in *C. diphtheriae* strains (SpaA, SapD, and SpaH), each containing the LPXTG motif (Ton-That and Schneewind 2003; Gaspar and Ton-That 2006; Swierczynski and Ton-That 2006). The genes involved in the production of pili encode nine pili proteins, defined in the successive letters from SpaA to SpaI, and five sortases defined from SrtA to SrtE, which are organized in three separate clusters. The sixth sortase SrtF (class-D homolog) is now referred to as the housekeeping sortase, located in a different region of the chromosome (Ton-That and Schneewind 2003). *C. diphtheriae*, like other Gram-positive bacteria (e.g. *Streptococcus pneumoniae*, group A and B streptococci or *Actinomycetes*), have the gene encoding cysteine transpeptidase (sortase) conserved in the genome, which is necessary for the assembly of pili (Ton-That and Schneewind 2004; Marraffini et al. 2006).

Pili are composed of three proteins: the main subunit forming the stem of pili, and two smaller subunits located at the base and at the end of the pili, e.g., SpaA-type pili is structured in such way that the SpaA pili protein creates a stem, SpaC is located at the end of pili, while SpaB is located along the stem and at the base (Ton-That and Schneewind 2003; Mandlik et al. 2008; Rogers et al. 2011). SpaA is important for the formation of the pile structure (Ton-That and Schneewind 2004). It has been proven that in the absence of SpaA protein, SpaB and SpaC are anchored in the cell wall as monomers (Mandlik et al. 2007).

The adhesion process of *C. diphtheriae* strains to the surface of human cells is multifactorial. Functions and mechanisms of action of fimbriae (Mandlik et al. 2007), non-fimbrial 67–72p adhesin (Colombo et al. 2001), trans-sialidase (Mattos-Guaraldi et al. 1998), hydrophobins, and sugar residues (Mattos-Guaraldi et al. 1999a; 2000; Moreira et al. 2003) are poorly understood, especially how they jointly participate in the adherence to the host cells and in the colonization of these cells during bacterial infection.

Initially, the 67–72p adhesive protein was described as a ligand responsible for the adherence of *C. diphtheriae* to human erythrocytes (Colombo et al. 2001). Later, the participation of this protein in the adherence of bacteria to HEp-2 cells was described (Hirata et al. 2004). The presence of the 67–72p protein has been confirmed in *C. diphtheriae* strains isolated from various sources, e.g., on the surface of the cells of invasive HC01 strain isolated from the blood of a patient with endocarditis (Sabbadini et al. 2012).

C. diphtheriae strains exhibit cell surface hydrophobicity and autoaggregation. Thanks to these features, microorganisms avoid immune defenses and are able to survive on the surface of the skin and mucosal membranes (Mattos-Guaraldi et al. 1999b). In addition, it has been proven that the 67–72p protein has the ability to induce host cell death, giving a signal for apoptosis in the early stages of infection. The occurrence of 67–72p hemagglutinin is one of the characteristics of the potentially invasive strains because it can contribute to the cytotoxicity and apoptosis of the infected cells (Sabbadini et al. 2012).

In our study, we analyzed the nucleotide and amino acid sequences of the genes encoding pili proteins which contribute to bacterial adherence to host cells, and also the gene encoding 67–72p protein involved in adhesion, colonization, and induction of the cell apoptosis in the early stage of infection, which should be used in a preliminary research for the finding of new vaccine antigens.

Experimental

Materials and Methods

Bacterial strains. In total, 10 *C. diphtheriae* nontoxigenic isolates were used in this study (Table I). Strains were isolated in Poland in 2010–2017 from patients with bacteremia, wound infection, septic arthritis, endocarditis, and serous cyst contents. The strain NCTC 13129 was used as the control strain.

Table I
C. diphtheriae strains used in this study.

Strain	Biotype	Site of isolation	Year of isolation
27/E	*mitis*	Serous cyst contents	2010
40/E	*gravis*	Blood	2014
68/E	*gravis*	Endocarditis	2015
71/E	*gravis*	Wound	2015
73/E	*gravis*	Blood	2016
77/E	*gravis*	Wound	2016
78/E	*gravis*	Blood	2016
79/E	*gravis*	Blood and joint fluid	2016
86/E	*gravis*	Blood	2017
89/E	*gravis*	Wound	2017

DNA isolation. *C. diphtheriae* strains were grown on Columbia agar with 5% sheep blood (BioMerieux) for 24 h at 37°C under aerobic conditions. Genomic DNA was isolated using a Wizard Genomic DNA Purification Kit (Promega) according to the Gram-positive bacteria procedure provided by the manufacturer.

Polymerase Chain Reaction (PCR). The oligonucleotide primers for amplification of the genes coding 67–72p protein and structural pili proteins (SpaC, SpaI, SapD) were designed based on the nucleotide sequence of the *C. diphtheriae* NCTC 13129 whole genome, available from GenBank under the number BX248353 (Table II).

The PCR reaction was conducted in a total volume of 25 µl and the reaction mixture contained 0.5 µl genomic DNA, 12.5 µl HotStarTaq Master Mix (Qiagen), and 1 µl of 10 µM solution of each primer (Table II). The cycling conditions were as follows: initial denaturation at 95°C/10 min and 29 cycles of denaturation at 94°C/1 min, primer annealing at 52°C/45 s, primer extension at 72°C/1 min and a final elongation at 72°C/10 min.

The PCR products were enzymatically cleaned using an Exo-BAP Mix kit (EURx), according to the manufacturer's procedure and then sent for sequencing.

Sequencing of fragment 4 of the gene encoding SpaC protein in strain 89/E. Based on the result of the

Table II
Primers used in this study.

Gene	Primer	Sequence	Length of the amplified fragment
67–72p	6772p1L	TGAAAAATAATTTAAGGAGTTCCAA	695 bp
	6772p1R	CAACCCACCAGTAACAGCAA	
	6772p2L	CTGTTTTGCTGGTCGTAGCA	841 bp
	6772p2R	ACCTCATCAACCTGGTTTGC	
	6772p3L	GAATCGTTGCAGCCCAAG	699 bp
	6772p3R	CCTTAAGCACTGGGTCGTTT	
	6772p4L	CACCGACAACGTTGGTTACA	844 bp
	6772p4R	TTCTGGCTTGTCCCTGTTCT	
	6772p5L	TCAAGCCGGAGTCCCAGA	692 bp
	6772p5R	TCAGTTGTGTCTGGTGAAAGG	
spaI	SpaI1L	GCGGAATCAACACCAACAC	600 bp
	SpaI1R	AAGCGCTTACGATCCAAGAA	
	SpaI2L	ACACGGCCTTCCAAACTTC	482 bp
	SpaI2R	TGATATTGAGGCGTCGCTAA	
sapD	SapD1L	TCGCGAAGGTAAGAAATACTCA	698 bp
	SapD1R	CGTTTGTATCCGAGCCACTT	
	SapD2L	GTCCAAAACAAGAGCGGAAA	814 bp
	SapD2R	GGTTCAGTGAAAACCCAGTTG	
spaC	SpaC1L	GCCTACTCTCACTGGCAAGG	824 bp
	SpaC1R	ACATGGCGATCTCCTGAAGT	
	SpaC2L	TCGTGCAGGACGTACCAATA	838 bp
	SpaC2R	AACTGCACTGTGACCGAAAA	
	SpaC3L	GGCATCATAAAGTGCAATCG	808 bp
	SpaC3R	TCACGTTGAGTTCTTCGTTCA	
	SpaC4L	CATTCGTTTTTGTTCCGTGA	850 bp
	SpaC4R	GGTGTAGAAACGCCTCGAAA	
	SpaC5L	CCAAATTCAACAGTTTGATTATCACT	850 bp
	SpaC5R	TTCCTGTCACTTACACCTGTCG	
	SpaC6L	CAAAATACGGATTGGTTTCTGG	845 bp
	SpaC6R	AGCTGGCTGGAATTTCGAT	
	SpaC7L	CAAAGGTGTCTTGGCCATTT	687 bp
	SpaC7R	TCACGCCAGTAAGTCTTGCTAA	
	SpaC8L	CTGGCATCTGGATGTCATTG	578 bp
	SpaC8R	ACCGAACGTGCCTAGCGTA	

first round of sequencing, new primers were designed to completely sequence a fragment of approximately 2000 bp, as follows: SpaC4L 5'-CATTCGTTTTTGTTCCGTGA-3' and SC1pR 5'-GAGCTGCTTGAAGTTGCAGA-3' (391 bp), SC2pL 5'-CCCGAACACGTTTGGTAAGT-3' and SC2pR 5'-GGGTAGTGGGTCAGGGTTTT-3' (687 bp), SC3pL 5'-CGCACACAATCAGTGACTAAAA-3' and SC3pR 5'-ACAACGTATTCGCAGCAGTG-3' (850 bp), SC4pL 5'-ATGGTTATCGCCGTATCTGG-3' and SpaC4R 5'-GGTGTAGAAACGCCTCGAAA-3' (764 bp). The PCR reaction was carried out according to the above conditions, the PCR products were then enzymatically purified and sent for sequencing.

Comparing the sequenced fragments and the translated nucleotide sequences for proteins. The sequences of the particular gene fragments were obtained as fluorograms. The BioEdit program was used for the gene assembly, alignment of sequences and comparative calculations. The translation of DNA into protein sequences was performed using the BLASTx program.

Analysis of 67–72p, SpaC, SpaI and SapD protein affinity to MHC classes I and II and linear epitopes. Amino acid sequences of *C. diphtheriae* NCTC 13129 reference strain available from the National Center for Biotechnology Information (NCBI) were used for analysis. To predict the cellular localization of the proteins, the software packages CELLO v.2.5 (Yu et al. 2006) and PSORTb version 3.0.2 (Yu et al. 2010) were used. The analysis for the transmembrane domains was performed using TMHMM Server v. 2.0. The MHC classes I and II binding prediction was performed using the immune epitope database (IEDB) (Kim et al. 2012) for the recommended human leukocyte antigen (HLA) allele set (Bui et al. 2005; Nielsen et al. 2003). Analysis has also been carried out using Propred-I (for MHC class I) and Propred (for MHC class II) regarding the number of alleles for which epitopes were found in the proteins analyzed (Singh and Raghava 2001; 2003). The prediction of linear B-cell epitopes has been carried out using the Bepipred Linear Epitope Prediction 2.0 (Jespersen et al. 2017). VaxiJen 2.0 was used for prediction of the protective antigens. The results page on VaxiJen server creates lists of the selected target, the protein sequence, its prediction probability, and a statement of protective antigen or non-antigen, according to a predefined cut-off. Since more of the models had their highest accuracy at a threshold of 0.5, this threshold value was chosen for all bacterial models types (Doytchinova and Flower 2007).

Results

The isolates from invasive diseases and wound infections were included in the study because a wound can be a portal of entry for invasive infections. Moreover, future vaccines against non-toxigenic *C. diphtheriae* should protect against all kinds of infections. The analyses conducted in this study showed the variability of *C. diphtheriae* strains in terms of the nucleotide sequence of the genes encoding the 67–72p protein (99.37–100% average similarity) and structural proteins of pili SpaC (38.94–99.97% average similarity), SpaI (81.39–100% average similarity), and SapD (63.78–100% average similarity). The 27/E strain, the only representative of the *mitis* biotype, was the most different from the other strains tested. This strain did not have the gene coding for the SpaI protein, while the average similarities of the nucleotide sequence of genes encoding the 67–72p, SapD, and SpaC proteins were 99.37%, 98.64%, and 38.94%, respectively when compared to the reference strain. Despite the significant variation, we managed to locate two fragments of the 67–72p protein (fragments No. 3 and 5), where the nucleotide sequences were 100% identical for all *C. diphtheriae* strains tested (the most conserved in the genome). In contrast, for *C. diphtheriae* biotype *gravis* we found as many as nine fragments located in the sequence of the gene encoding 67–72p protein (fragment No. 1, 3, 5) and the genes coding for the pili SapD (fragment No. 1), SpaI (fragment No. 2), and SpaC (fragment No. 2, 3, 7, 8), which were 100% identical in all nine strains tested (Table III).

The nucleotide sequences of the genes investigated were translated into the amino acid sequences. We revealed that the identified mutations resulted in a reading frame shift or were synonymous and nonsynonymous substitutions (Table IV).

In addition, we observed that a fragment of 1380 bp was inserted in the place of the gene encoding the SpaC protein in the 89/E strain (Table III). After sequencing the fragment No. 4 of *spaC*, we obtained the exact nucleotide sequence, which we compared to the available sequences in the GeneBank using the Nucleotide Basic Local Alignment Search Tool (BLASTn). In this way, we proved that the 1380 bp insertion sequence (IS) was transposed, which interrupted the continuity of the tested gene between 3072 bp and 3073 bp of the reference sequence of the NCTC 13129 strain. The result from the BLAST search revealed that the insertion fragment we detected was similar to the sequence of IS3 family transposase also identified in other *C. diphtheriae* strains but in different locations.

Analysis of the 67–72p, SpaC, SpaI and SapD protein affinity to MHC classes I and II, and linear B-cell epitopes in the first stage relied on the determination of the position of the proteins tested in the cell membrane and confirmation that all selected proteins were at least partially membranous or extracellular (Table V). Then, using the IEDB platform, it was observed that all proteins have high-affinity areas for MHC receptors of both classes and the fragments, which can be recog-

Table III
Comparison of the nucleotide sequences of all strains tested against the reference strain, given in percent (%).
The sequences are presented according to the analysed fragments.

Target protein	Fragment	27E	40E	68E	71E	73E	77E	78E	79E	86E	89E
67–72p	1	98.35	100	100	100	100	100	100	100	100	100
	2	99.5	100	100	100	100	100	100	100	100	99.87
	3	100	100	100	100	100	100	100	100	100	100
	4	99.01	100	100	100	100	100	100	100	97.90	97.90
	5	100	100	100	100	100	100	100	100	100	100
SapD	1	98.91	100	100	100	100	100	100	100	100	100
	2	98.37	27.52	100	100	100	100	100	100	99.86	99.86
SpaI	1	–	100	100	100	100	100	100	62.77	100	100
	2	–	100	100	100	100	100	100	100	100	100
SpaC	1	72.78	99.87	99.87	99.87	99.87	99.87	99.87	99.87	99.87	99.87
	2	97.11	100	100	100	100	100	100	100	100	100
	3	–	100	100	100	100	100	100	100	100	100
	4	–	100	100	100	100	100	100	100	99.75	IS*
	5	91.47	99.21	100	100	99.87	100	100	100	100	100
	6	–	100	100	100	100	100	99.87	99.87	100	100
	7	50.16	100	100	100	100	100	100	100	100	100
	8	–	100	100	100	100	100	100	100	100	100

* – In the fragment 4 of the gene encoding SpaC protein, the insertion sequence has been transposed

Table IV
Comparison of amino acid sequences of all strains tested against the reference strain, given in percent (%).

Target protein	27E	40E	68E	71E	73E	77E	78E	79E	86E	89E
67–72p	99	100	100	100	100	100	100	98	98	100
SapD	97	99	100	100	100	100	100	100	99	99
SpaI	–	100	100	100	100	100	100	84	100	100
SpaC	48	99	99	99	69	99	69	69	69	51

nized by antibodies. The output for the prediction of the high- affinity MHC binding peptides is typically given either in the units of a predicted affinity (IC_{50} nanomolar) or as a percentile score reflecting the relative affinity of a selected peptide compared with a universe of random sequences. According to Paul et al. (2013), there are four categories of percentile ranks: 1) 0–0.30; 2) 0.30–1.25; 3) 1.25–5.0; and 4) 5.0–15.0. Their study proved that four pools of predicted peptides derived from the first two categories (0–0.30; 0.30–1.25) were immunogenic but finally, the transgenic mice in their study recognized only one peptide pool from the first category (0–0.30) (Paul et al. 2013). We can say that the smaller the percentile rank value, the higher the affinity. As for the IC_{50} value, according to the IEDB Solutions Centre guidelines, $IC_{50} < 50$ designs very high affinity, $IC_{50} < 500$ – high affinity, and $IC_{50} < 5000$ means low affinity (Fleri 2013). Accepting even the threshold of cutting off the percentile rank below 1 or IC_{50} below 50, we still could have at least 100 to several hundred regions with high affinity for each of the proteins (Table VI, Table VII).

Table V
Extracellular regions of individual proteins.

Region*	67–72p				SpaC	SpaI	SapD
Start	44	138	235	310	36	1	1
Stop	57	169	257	987	1845	236	631

*Amino acid positions

Table VIII contains data on the number of alleles for which epitope that was found in the proteins analyzed. Overall, 40 HLA alleles of human origin encoded by HLA-A and HLA-B were selected for ProPred1. The HLA 7 from mouse s-derived (MHC-Db, MHC-Db revised, MHC-Dd, MHC-Kb, MHC-Kd, MHC-Kk,

Table VI
MHC class I epitopes predicted from the target proteins.

MHC I					
Target protein	Alleles	Start	End	Peptide	Percentile rank
67–72p	HLA-A*02:06	6	14	FTNDRFWSV	0.06
67–72p	HLA-B*44:02	34	42	SENDSSVEY	0.06
67–72p	HLA-A*30:02	68	77	RMASYWLDRY	0.06
67–72p	HLA-B*44:02	9	17	AEALSQVGI	0.07
67–72p	HLA-A*02:06	27	36	MILGALVPTV	0.07
67–72p	HLA-A*68:01	1	9	YAFTLPALR	0.11
67–72p	HLA-A*01:01	43	51	DTDSSTYTY	0.11
67–72p	HLA-A*01:01	48	56	YTTLTSLPY	0.11
67–72p	HLA-B*44:03	34	42	SENDSSVEY	0.11
67–72p	HLA-B*57:01	58	66	SSLAIGNAW	0.12
SapD	HLA-B*44:03	65	74	AEWQELDTWW	0.06
SapD	HLA-B*07:02	4	13	RPIWAGIGAF	0.11
SapD	HLA-B*44:03	28	36	KEGAYGLEY	0.11
SapD	HLA-A*68:01	47	55	NVFFKNNSR	0.12
SapD	HLA-B*40:01	10	18	IEAQISGSL	0.17
SapD	HLA-A*24:02	70	79	VWYAPQNIPF	0.18
SapD	HLA-A*68:01	24	32	DTVGSESAR	0.2
SapD	HLA-B*51:01	50	58	YPLHISYLV	0.2
SapD	HLA-A*68:01	41	50	EPAFGVTIPK	0.22
SapD	HLA-A*68:01	17	26	EAYVKNGAFK	0.26
SpaC	HLA-A*11:01	658	666	STNSVWIPK	0.06
SpaC	HLA-A*01:01	220	229	LSDDKPFDLY	0.07
SpaC	HLA-B*53:01	233	241	LPSEDDYYW	0.1
SpaC	HLA-A*68:02	191	199	EVVELENAV	0.1
SpaC	HLA-A*02:06	1859	1867	LVAAALWLV	0.11
SpaC	HLA-A*23:01	88	96	PYRFGIYTF	0.11
SpaC	HLA-A*68:01	1436	1444	NTTYSITYK	0.11
SpaC	HLA-A*31:01	363	371	RFKNARCQR	0.11
SpaC	HLA-B*44:02	1054	1063	AENTLSADAI	0.11
SpaC	HLA-A*23:01	1578	1587	SYTCTMPHLF	0.12
SpaI	HLA-A*30:01	2	11	KKTHLFRIPA	0.08
SpaI	HLA-B*07:02	9	17	IPAATTAAV	0.1
SpaI	HLA-B*07:02	147	155	RPAEYRRTL	0.1
SpaI	HLA-B*57:01	109	117	RSRLSDEVW	0.12
SpaI	HLA-A*30:02	129	137	VTGLPMGVY	0.18
SpaI	HLA-A*02:01	137	145	YLVSETPPA	0.2
SpaI	HLA-A*02:03	20	29	LLASGPIASA	0.2
SpaI	HLA-A*02:06	153	161	RTLDFLITV	0.21
SpaI	HLA-B*51:01	196	205	FPPVESSVTL	0.24
SpaI	HLA-A*68:01	252	261	LAIAGFLVQR	0.32

and MHC-Ld) was omitted. The Proteasome Filter and Immunoproteasome filters were included in the analysis and for both, the threshold score of 4% was used. The ProPred1 cut-off threshold was also set at 4%. At the ProPred, 51 alleles related to MHC class II were considered. These were HLA-DR alleles. These molecules were encoded by DRB1 and DRB5 genes containing HLA DR1 (2 alleles), DR3 (7 alleles), DR4 (9 alleles),

Table VII
MHC class II epitopes predicted from the target proteins.

MHC II					
Target protein	Alleles	Start	End	Peptide	Percentile rank
67–72p	HLA-DRB3*01:01	660	674	DGSVDLYEFDENDPV	0.01
67–72p	HLA-DRB3*01:01	713	727	MLARYHVDDARDFFT	0.01
67–72p	HLA-DPA1*03:01/DPB1*04:02	15	29	PQRRLTWLIPLLMIL	0.01
67–72p	HLA-DPA1*03:01/DPB1*04:02	173	187	STFSVLLVVAFLIAL	0.01
67–72p	HLA-DRB1*07:01	49	63	VDFRGVFNKVIATRI	0.01
67–72p	HLA-DPA1*01/DPB1*04:01	165	179	LPALRLVVSTFSVLL	0.01
67–72p	HLA-DPA1*01/DPB1*04:01	267	281	VISAVVAISFFSVIV	0.01
67–72p	HLA-DRB1*09:01	100	114	PVVQYRAAVEKGVHR	0.02
67–72p	HLA-DRB3*01:01	712	726	KMLARYHVDDARDFF	0.02
67–72p	HLA-DPA1*01:03/DPB1*02:01	172	186	VSTFSVLLVVAFLIA	0.02
SapD	HLA-DRB3*01:01	181	195	GKDSIPEHLDKNMYF	0.01
SapD	HLA-DRB1*03:01	531	545	PLHISYLVGDATIAR	0.03
SapD	HLA-DQA1*04:01/DQB1*04:02	535	549	SYLVGDATIARAKEI	0.09
SapD	HLA-DRB1*03:01	444	458	PSDALLPDSKMTVSL	0.12
SapD	HLA-DQA1*03:01/DQB1*03:02	616	630	VQDEAVTTAAEWQEL	0.13
SapD	HLA-DRB1*03:01	442	456	DLPSDALLPDSKMTV	0.13
SapD	HLA-DQA1*03:01/DQB1*03:02	615	629	DVQDEAVTTAAEWQE	0.16
SapD	HLA-DRB5*01:01	640	654	LLGILGIVGAFVLFR	0.24
SapD	HLA-DQA1*04:01/DQB1*04:02	537	551	LVGDATIARAKEILA	0.27
SapD	HLA-DRB1*03:01	346	360	TGTPKTIINDGHMDL	0.29
SpaC	HLA-DRB3*01:01	157	171	NDIDRGIKYDAVYFI	0.01
SpaC	HLA-DRB3*01:01	505	519	DNGTYRFKADTDAFK	0.01
SpaC	HLA-DRB3*01:01	1427	1441	EHSVDPWLLNTTYSI	0.01
SpaC	HLA-DRB3*01:01	1699	1713	VVINNVYTTDAEINI	0.01
SpaC	HLA-DRB3*01:01	1804	1818	EVTLDNYDADSGLIT	0.01
SpaC	HLA-DRB3*01:01	1450	1464	IKDRSYSNDVDIQAD	0.02
SpaC	HLA-DRB1*03:01	769	783	AGDIVKVVVDNTAKR	0.03
SpaC	HLA-DRB1*09:01	1845	1859	NGYLRWLLAGAAGLL	0.04
SpaC	HLA-DPA1*03:01/DPB1*04:02	21	35	LAMVMSIVLVPLIAA	0.05
SpaC	HLA-DRB3*01:01	1432	1446	PWLLNTTYSITYKCD	0.07
SpaI	HLA-DRB3*01:01	147	161	RPAEYRRTLDFLITV	0.07
SpaI	HLA-DRB1*08:02	3	17	KTHLFRIPAATTAAV	0.18
SpaI	HLA-DRB3*01:01	151	165	YRRTLDFLITVPAGM	0.19
SpaI	HLA-DPA1*01/DPB1*04:01	248	262	LGIALAIAGFLVQRR	0.28
SpaI	HLA-DRB3*01:01	43	57	ISDIRCDTGSLTLIK	0.29
SpaI	HLA-DRB5*01:01	155	169	LDFLITVPAGMRTAD	0.42
SpaI	HLA-DRB1*09:01	95	109	AGWDAAKALTIQEAR	0.44
SpaI	HLA-DRB1*11:01	50	64	TGSLTLIKRPPAAFE	0.44
SpaI	HLA-DQA1*01:02/DQB1*06:02	242	256	VLGIAALGIALAIAG	0.48
SpaI	HLA-DPA1*02:01/DPB1*05:01	150	164	EYRRTLDFLITVPAG	0.6

DR7 (2 alleles), DR8 (6 alleles), DR11 (9 alleles), DR13 (11 alleles), DR15 (3 alleles), and DR51 (2 alleles). The cut-off threshold was set at 3%.

The target protein sequences were scanned for B-cell epitopes using the Bepipred Linear Epitope Prediction 2.0. The selected B-cell linear epitopes of the proteins analyzed are shown in Table IX.

The results obtained with the VaxiJen server also confirmed the possibility of using the proteins as antigens in vaccines (Table X).

Table VIII
Number of alleles for which epitopes were found in the proteins tested.

Target protein	Number of MHC alleles of class I (per 40)	% Bound alleles MHC class I	Number of MHC alleles of class II (per 51)	% Bound alleles MHC class II
67–72p	40	100	51	100
SpaC	37	92.5	51	100
SpaI	34	85	50	98
SapD	33	82.5	51	100

Table IX
B-cell epitopes predicted from the target proteins.

Target protein	No.	Start	End	Peptide	Length
6772p	1	4	20	GFTRPAAAPKRPQRRLT	17
6772p	2	48	53	EVDFRG	6
6772p	3	87	111	GRPDELEFFDPDSPVVQYRAAVEKG	25
6772p	4	143	156	NRQDFGVSDQQFGM	14
6772p	5	194	211	GGIRAGNQAAGVKGSITN	18
6772p	6	281	287	VTKDLRI	7
6772p	7	316	329	SPNRAEKESEYISR	14
6772p	8	337	369	AYGITDDAVTYKDNWGAKGASSEKVASDSATVS	33
6772p	9	381	410	PTFTQQQQLRNFYGFPKSLAMDRYVIDGEL	30
6772p	10	421	434	DPNALKENQRDWIN	14
6772p	11	452	467	QVDEVARDVGSARGGY	16
6772p	12	474	490	DLQTTDKEAQELGIVVK	17
6772p	13	498	507	PVIASATDGA	10
6772p	14	514	541	SENDSSVEYDTDSSTYTYQGKGGVNIGN	28
6772p	15	562	566	RVNGN	5
6772p	16	573	581	RDPRERVHN	9
6772p	17	612	645	TSLPYAERTSLSEATNDTTAQVGNSAQRLVTDNV	34
6772p	18	680	705	GVFPGTVKAKSEISEELMNHLRYPED	26
6772p	19	714	749	LARYHVDDARDFFTNDRFWSVPSDPSATEGQKDVAQ	36
6772p	20	760	763	DTGK	4
6772p	21	773	777	RGLQR	5
6772p	22	803	837	TDTLTQGPKQAQDTMMSSDQIASDRTLWKDTNDLF	35
6772p	23	861	868	RKNQASAF	8
6772p	24	896	944	GIDPKEAQDLGEAKGLKPESQNRDKPEDKEGKAPSTPSAPASGSGTTGE	49
6772p	25	956	976	LQSAKNGSNEEYGRALDELDK	21
SpaC	1	38	49	ANAEPLPKKEFE	12
SpaC	2	64	69	SLSASD	6
SpaC	3	100	113	SPAAGNKNFTPVSL	14
SpaC	4	131	146	MPAIRENKKGSPNGGT	16
SpaC	5	176	184	PTWDNNGRN	9
SpaC	6	225	228	PFDL	4
SpaC	7	231	234	PILP	4
SpaC	8	246	254	WKIDRSLTG	9
SpaC	9	324	332	PSIETDKNG	9
SpaC	10	355	358	TGDQ	4
SpaC	11	371	387	RYSYGQAPTDIPIKTSD	17
SpaC	12	417	432	KVNVNTPQLLEELNNQ	16

Table IX. Continued.

Target protein	No.	Start	End	Peptide	Length
SpaC	13	455	468	GVHNGESKEIGKVA	14
SpaC	14	478	507	VTPKVDDSRMKLSTTWSSENTTADANQDNG	30
SpaC	15	512	522	KADTDAFKNKK	11
SpaC	16	531	537	NYEAQTA	7
SpaC	17	545	561	IINRDKIPATKLPEKFP	17
SpaC	18	569	591	VPHPNARPEHGGLPETNPYFVDS	23
SpaC	19	601	610	SIEIGPFPVG	10
SpaC	20	619	659	ARLDPNVQADAKIPGFSLKTEWNSNICFGNTIDNNSQDCST	41
SpaC	21	664	672	IPKPGQYSL	9
SpaC	22	676	684	NTYTRELAS	9
SpaC	23	690	702	TVSGDASDLTNSH	13
SpaC	24	712	731	DSGVEVYSQDNIVVKKDGRQ	20
SpaC	25	746	754	EKQPEQKGV	9
SpaC	26	761	769	PFHLRASTA	9
SpaC	27	779	786	NTAKRQVA	8
SpaC	28	792	812	KKVHKKDTFSPEISASIDALT	21
SpaC	29	819	846	CTVPGVETPRKVLKTVSDNQTVEFGNFP	28
SpaC	30	857	861	TEAPA	5
SpaC	31	881	885	TPINK	5
SpaC	32	891	895	FENAR	5
SpaC	33	904	948	VLDGDMPQALVDQIPSSFTVNVACSITGNHSITLQKDEQKAVPGV	45
SpaC	34	957	968	SEEVTPITGATH	12
SpaC	35	971	991	HWIKGELLEVADSTDITINPN	21
SpaC	36	1001	1007	HYETDAV	7
SpaC	37	1012	1037	TKRVRVIDQVGNDVNSELKNAVVRPE	26
SpaC	38	1043	1052	RYRCEINGQV	10
SpaC	39	1059	1073	SADAINTGATKVPRG	15
SpaC	40	1079	1131	EEDSSSVELSNATLSHVEFFVHGTKTNDKASVAINSDHNRLDATNTFTLKTGS	53
SpaC	41	1135	1146	KKKVDGEGVSTI	12
SpaC	42	1157	1164	RCTLGDWK	8
SpaC	43	1174	1188	FDSAESHSVKDIPVG	15
SpaC	44	1195	1204	EDSEKAQEPN	10
SpaC	45	1210	1240	RWTHTDSTNGWGDTEAACENHAACEVDPKNE	31
SpaC	46	1250	1255	NEKENF	6
SpaC	47	1276	1288	KVLTNDGPELAGK	13
SpaC	48	1298	1346	TDPRFAGSDLADKHSIPDPTITVALNAKGQSRASYQVADERHDSVEVPV	49
SpaC	49	1357	1360	IALY	4
SpaC	50	1378	1401	AVQRTSSNSASARFVTEKQENNGT	24
SpaC	51	1409	1413	DYIRP	5
SpaC	52	1424	1437	AKPEHSVDPWLLNT	14
SpaC	53	1443	1483	YKCDDPYIKDRSYSNDVDIQADAEKPTPIFADPTAHVKIPA	41
SpaC	54	1492	1498	NTEGHLP	7
SpaC	55	1506	1555	DETNKVAEFAGEHEKRSYFTPEIKDVVLSESEPTRIEFTNSYVMPQRILS	50
SpaC	56	1560	1569	VEGDPGHAVI	10
SpaC	57	1582	1605	TMPHLFPNQPNPMSQEVGNKVARG	24
SpaC	58	1614	1622	TWRSPEVPI	9
SpaC	59	1630	1643	EEDDPALRTKLENN	14
SpaC	60	1645	1687	LRMVPTYLFPTERAGAASAPVIPPLTDRPIYNGTEPRLQMPES	43

Table IX. Continued.

Target protein	No.	Start	End	Peptide	Length
SpaC	61	1718	1723	ADNSPL	6
SpaC	62	1734	1755	GENGQRKELPEVADAPAKSAKS	22
SpaC	63	1808	1825	DNYDADSGLITVEHPQGK	18
SpaC	64	1837	1842	STLPLT	6
SapD	1	23	72	PVSASEDAALDATGHKKGEPAFGVTIPKGTTYRDSDGKEVPHPCVDRKIG	50
SapD	2	86	96	YSVKEPATDLP	11
SapD	3	104	113	DGQQVVPQES	10
SapD	4	122	145	AGEDGEELSRIRIPDDEEFSFLGK	24
SapD	5	157	162	IPFANG	6
SapD	6	174	190	DPHHEPKGKDSIPEHLD	17
SapD	7	224	234	SNDEELKTIEY	11
SapD	8	264	269	AFKVKT	6
SapD	9	281	350	DEEVGLPEGTTTNLNKITKPLDKDATNEPPTDPSEKKKPPRPEKGHSETSSPSA LDDSIERAWKLTGTPK	70
SapD	10	371	380	TVINREGKKY	10
SapD	11	392	418	SGGDQGGPLVKTDSWKDRIEAQISGSL	27
SapD	12	441	451	EDLPSDALLPD	11
SapD	13	525	529	GKQES	5
SapD	14	542	606	TIARAKEILAGEKLGGSLKKKPQEKETKKPASVQNKSGKHNKDTVGSESARK RQQLAATSGSDTN	65
SapD	15	624	632	AAEWQELDT	9
SpaI	1	22	50	ASGPIASADSRTITGATDGLNISDIRCDT	29
SpaI	2	55	75	LIKRPPAAFEGVDKADLPAGT	21
SpaI	3	86	124	IEGIDLTKQAGWDAAKALTIQEARSRLSDEVWKAVSGRD	39
SpaI	4	144	153	PAKRPAEYRR	10
SpaI	5	166	174	RTADGNVAS	9
SpaI	6	186	242	TDDLPPTVPVFPPVESSVTLTPSSPVPGTPKTPGKPDLPEKFRKEVTDRLGNT GANV	57
SpaI	7	263	266	KKNE	4

Table X
Prediction of the protective antigens from the VaxiJen server.

Protein	Overall Prediction for the Antigen
6772p	0.5123
SpaC	0.6757
SpaI	0.5504
SapD	0.5544

Discussion

The huge success of vaccination against diphtheria almost enabled the elimination of the disease in Europe and other developed countries. However, in many countries with high vaccination coverage, i.e. France, Italy, Switzerland, Germany, and Canada an increase in non-toxigenic *C. diphtheriae* infections has been observed. For example, Poland is a country where the last case of diphtheria was recorded in the year 2000 and where the vaccination level of over 95% is achieved (Zasada et al. 2010). The first case of non-toxigenic infection with *C. diphtheriae* biotype *gravis* was recorded in Poland in 2004, where this bacterium induced sepsis and endocarditis in a patient (Zasada et al. 2005) and since then, practically every year, several cases of invasive *C. diphtheriae* infections have been diagnosed. In northern Germany, the number of non-toxigenic *C. diphtheriae* infections increased from five in 2013 to 23 in 2016, and 24 in only the first half of 2017 (Dangel et al. 2018). In England and Wales, a dramatic increase in infections was recorded since 1986, peaking at almost 300 cases in the year 2000 (Edwards et al. 2011). These examples indicate that the development of a new vaccine against non-toxigenic *C. diphtheriae* infection is of very important and necessary demand.

In vaccine development, the potential virulence factors exposed on the surface of a pathogen are considered

as suitable antigens for an effective acellular vaccine. It has been shown that pili of Gram-positive bacteria play a direct role in the pathogenesis. For example, studies on *S. pneumoniae* have proved that those strains, which have a pili island, adhere better to lung epithelial cells than do the strains that lack this island. In the invasive disease model, the piliated strain is more virulent and has a competitive advantage over the pili-negative strain after the mixed intranasal infection. Infection with the piliated strain induces a stronger inflammatory response and a higher level of the tumor necrosis factor in the bloodstream of mice, which may be due to the higher adhesion of the piliated bacteria to the cells involved in the innate immune response and their detection by host cell pattern-recognition receptors (Barocchi et al. 2006). The pili proteins are used as antigens in vaccines, for example in some acellular pertussis vaccines (Mosley et al. 2016).

The adhesion of *Corynebacterium* to host cells was observed for the first time for *C. renale* pili, which caused agglutination of trypsinized sheep red blood cells (Honda and Yanagawa 1974). It was not until more than thirty years later that Mandlik and colleagues identified adhesins, which were involved in adherence to pharyngeal host cells – the minor pilins SpaB and SpaC of *C. diphtheriae* (Mandlik et al. 2007). Subsequent studies showed that wild type *C. diphtheriae* cells bind to human lung epithelial, laryngeal, and pharyngeal cells, whereas mutants that lacked SrtA (i.e. they did not polymerize the SpaA-type pili) showed more than a 90% lower ability to adhere to human pharyngeal cells. Moreover, mutants that lacked only the major pili subunit, SpaA, showed a 10% reduction in adherence to these cells. In contrast, mutants that lacked either of the minor pilin subunits, SpaB or SpaC, showed a 70–75% reduction in adhesion. In addition, the latex beads coated only with SpaB or SpaC were sufficient to adhere to the host pharyngeal cells, while the SpaA-coated beads did not bind. SpaB and SpaC are anchored in the cell wall as monomers independent of the pilus structures. It is likely that the long pili mediate the initial attachment, while the monomeric pilins on the surface of the bacteria participate in the formation of an adhesion zone allowing the delivery of toxins and other virulence factors and may even play a significant role in host cell signaling (Rogers et al. 2011).

In addition to pili, *C. diphtheriae* produces the 67–72p protein located on its surface, which is involved in colonization, induction of apoptosis, and epithelial cell necrosis that were once attributed exclusively to the action of the diphtheria toxin (Sabbadini et al. 2012). This finding was also confirmed by Cerdeño-Tárraga et al. (2003) who sequenced the genome of the British clinical isolate (strain NCTC13129 biotype *gravis* – used in our study as the reference strain) and proved that the recent acquisition of pathogenicity factors went beyond the toxin itself and included the fimbrial proteins and adhesins. The 67–72p can act as an invasive and apoptotic protein for *C. diphtheriae* strains. The ability to penetrate, survive and induce apoptosis in epithelial cells may explain the endurance and dissemination of *C. diphtheriae* (Sabbadini et al. 2012). Proteins, which act as adhesins were also detected among other bacteria, e.g., the occurrence of the extracellular Eap protein was confirmed to be involved in colonization of eukaryotic cells by *S. aureus* strains (Haggar et al. 2003).

Our research is based on reverse vaccination. This method relies on the sequencing of pathogen genomes and determination *in silico* the most likely protective antigens prior to conducting experiments to prove this. Originally, this method was used to identify antigens as probable candidate vaccines against serogroup B meningococci (Christensen et al. 2013). In another study, Droppa-Almeida et al. (2018) used several available bioinformatics tools to design the efficient immunodominant epitopes for the development of the peptide vaccine against *C. pseudotuberculosis* for sheep and goats. Thanks to this research, it was possible to highlight the importance of bioinformatics software in the design of vaccines, especially in the identification of appropriate vaccine candidates, immune-informatics analysis and design of peptide vaccine from multi-epitopes (Droppa-Almeida et al. 2018). Bioinformatics tools present a lot of advantages, such as speed and low cost, so we used them at particular stages of the research.

First, we selected the gene encoding the 67–72p protein and the three pili genes *spaC*, *sapD* and *spaI* as the genes most frequently detected in various *C. diphtheriae* isolates as it was reported in our previous study (Zasada et al. 2012). In the present study, we found two fragments of 594 bp and 215 bp in the nucleotide sequence of the gene coding for the 67–72p surface protein, which were identical in all analyzed strains of *C. diphtheriae,* and in total, nine identical in *C. diphtheriae* biotype *gravis* strains sequences of the genes encoding 67–72p protein and structural proteins pili SpaI, SpaC and SapD (Table III). The sequence stability of these fragments represents a first step toward being the potential vaccine candidates. The analysis of amino acid sequences of these fragments confirmed that the proteins tested are located in the membrane or cell wall and have a large extracellular part (Table V).

An effective vaccine should induce a protective and long-lasting immune response. Therefore, we carried out analyses of the affinity of the tested proteins to MHC classes I and II and linear B-cell epitopes. MHC class I presents antigens to CD8+ T-cells and MHC class II presents antigens to CD4+ T-cells. The antigens, which are recognized by CD4+ and/or CD8+ T-cell receptors,

have the potential to stimulate a long-lasting and cytotoxic immune response. B-cell epitopes can induce both primary and secondary immunity. We showed that, in each of the proteins, areas with high affinity to MHC receptors can be distinguished (Table VI, Table VII, Table VIII) and we localized B-cell epitopes from target proteins (Table IX). In addition, the VaxiJen server was used that is a reliable and consistent tool for predicting protective antigens of bacterial, viral and cancer origin. The results obtained also confirmed that the proteins tested by us could be interesting to use as antigens in vaccines (Table X).

Our studies have shown that in the genome of the 89/E strain, the insertion element of 1380 bp was transposed and attached to fragment 4 of the gene encoding the SpaC pili protein. The process of transposition of ISs can inactivate genes (Trost et al. 2012). Mandlik et al. (2007) confirmed the reduced *C. diphtheriae* adhesive activity as the result of mutations at the base pili protein SpaB and at the tip pili protein SpaC of the SpaA-type pili. Premature stop codons in the continuity of the genes encoding the proteins responsible for the adhesion of bacteria to host cells inactivate them and limit the colonization process. We did not investigate the adhesive activity of the strain 89/E and, therefore, we can only posit the influence of the insertion on the adhesive properties of the strain based on the data published by other researchers.

Due to the fact that in many European countries the number of infections with non-toxigenic *C. diphtheriae* strains has recently increased, a key aspect of our research was the understanding of virulence factors other than the diphtheria toxin and identification of new vaccine targets. An important problem is also the understanding of the colonization process and in particular the mechanism of adhesion and structure of the proteins, which participate in this process. Blocking the 67–72p surface protein or pili structural proteins could effectively prevent the adhesion of *C. diphtheriae* bacteria to host tissues, colonization, and infection development. Due to the comparison of the nucleotide sequences of the *C. diphtheriae* strains identification of the most conserved sequences in the genome and determination of the variability between strains was achieved. The conserved sequences identified in 67–72p, SpaC, SapD and SpaI in our study are identical for all *C. diphtheriae* strains tested and contain the epitopes for B-cells and T-cells and will be used in further research on the construction of a new vaccine. The main limitation of this study is the small number of isolates investigated. However, the results obtained here support further studies with a larger number of isolates from different countries. Moreover, the results of *in silico* analysis should be confirmed by *in vivo* studies on an animal model. The new vaccine will act to inactivate the antigens responsible for the host cell colonization by *C. diphtheriae* strains and inhibit the development of infection.

ORCID
Klaudia Brodzik 0000-0002-6875-2570
Maciej Polak 0000-0002-2288-5650
Aleksandra A. Zasada 0000-0003-2774-0941

Acknowledgments
The authors wish to thank the Laboratory of Bacteriological Diagnostics, Department of Bacteriology and Biocontamination Control NIPH-NIH for providing us with several *C. diphtheriae* isolates.

Funding
This study was supported by the National Institute of Public Health – National Institute of Hygiene internal-grant for young researchers (No. 1/EMMŁ/2017). Dominik Strapagiel and Jakub Lach were supported by the Polish Ministry of Science and Higher Education, grant DIR/WK/2017/01.

Conflicts of Interest
The authors do not report any financial or personal connections with other persons or organizations, which might negatively affect the contents of this publication and/or claim authorship rights to this publication.

Literature

Barocchi MA, Ries J, Zogaj X, Hemsley C, Albiger B, Kanth A, Dahlberg S, Fernebro J, Moschioni M, Masignani V, et al. A pneumococcal pilus influences virulence and host inflammatory responses. Proc Natl Acad Sci USA. 2006 Feb 21;103(8):2857–2862. doi:10.1073/pnas.0511017103 Medline

Belko J, Wessel DL, Malley R. Endocarditis caused by *Corynebacterium diphtheriae* : case report and review of the literature. Pediatr Infect Dis J. 2000 Feb;19(2):159–163. doi:10.1097/00006454-200002000-00015 Medline

Bui HH, Sidney J, Peters B, Sathiamurthy M, Sinichi A, Purton KA, Mothé BR, Chisari FV, Watkins DI, Sette A. Automated generation and evaluation of specific MHC binding predictive tools: ARB matrix applications. Immunogenetics. 2005 Jun; 57(5):304–314. doi:10.1007/s00251-005-0798-y Medline

Cerdeño-Tárraga AM, Efstratiou A, Dover LG, Holden MT, Pallen M, Bentley SD, Besra GS, Churcher C, James KD, De Zoysa A, et al. The complete genome sequence and analysis of *Corynebacterium diphtheriae* NCTC13129. Nucleic Acids Res. 2003 Nov15; 31(22):6516–6523. doi:10.1093/nar/gkg874 Medline

Christensen H, Hickman M, Edmunds WJ, Trotter CL. Introducing vaccination against serogroup B meningococcal disease: an economic and mathematical modelling study of potential impact. Vaccine. 2013 May;31(23):2638–2646. doi:10.1016/j.vaccine.2013.03.034 Medline

Colombo AV, Hirata R Jr, Souza CÃMR, Monteiro-Leal LH, Previato JO, Formiga LCD, Andrade AFB, Mattos-Guaraldi ALÌ. *Corynebacterium diphtheriae* surface proteins as adhesins to human erythrocytes. FEMS Microbiol Lett. 2001 Apr;197(2):235–239. doi:10.1111/j.1574-6968.2001.tb10609.x Medline

Dangel A, Berger A, Konrad R, Bischoff H, Sing A. Geographically Diverse Clusters of Nontoxigenic *Corynebacterium diphtheriae* Infection, Germany, 2016–2017. Emerg Infect Dis. 2018 Jul;24(7): 1239–1245. doi:10.3201/eid2407.172026 Medline

Doytchinova IA, Flower DR. VaxiJen: a server for prediction of protective antigens, tumour antigens and subunit vaccines. BMC Bioinformatics. 2007 Dec;8(1):4.
doi:10.1186/1471-2105-8-4 Medline

Droppa-Almeida D, Franceschi E, Padilha FF. Immune-informatic analysis and design of peptide vaccine from multi-epitopes against *Corynebacterium pseudotuberculosis*. Bioinform Biol Insights. 2018 Jan;12:1–9. doi:10.1177/1177932218755337 Medline

Edwards B, Hunt AC, Hoskisson PA. Recent cases of non-toxigenic *Corynebacterium diphtheriae* in Scotland: justification for continued surveillance. J Med Microbiol. 2011 Apr 01;60(4):561–562. doi:10.1099/jmm.0.025643-0 Medline

Fleri W. Selecting thresholds (cut-offs) for MHC class I and II binding predictions [Internet]. IEDB Solutions Center; 2014 [cited 2019 January 22]. Available from https://help.iedb.org/hc/en-us/articles/114094151811-Selecting-thresholds-cut-offs-forMHC-class-I-and-II-bind-ing-predictions

Fricchione MJ, Deyro HJ, Jensen CY, Hoffman JF, Singh K, Logan LK. Non-toxigenic penicillin and cephalosporin-resistant *Corynebacterium diphtheriae* endocarditis in a child: a case report and review of the literature. J Pediatric Infect Dis Soc. 2014 Sep 01;3(3):251–254. doi:10.1093/jpids/pit022 Medline

Gaspar AH, Ton-That H. Assembly of distinct pilus structures on the surface of *Corynebacterium diphtheriae*. J Bacteriol. 2006 Feb 15;188(4):1526–1533.
doi:10.1128/JB.188.4.1526-1533.2006 Medline

Haggar A, Hussain M, Lönnies H, Herrmann M, Norrby-Teglund A, Flock JI. Extracellular adherence protein from *Staphylococcus aureus* enhances internalization into eukaryotic cells. Infect Immun. 2003 May 01;71(5):2310–2317.
doi:10.1128/IAI.71.5.2310-2317.2003 Medline

Hirata R Jr, Souza SMS, Rocha-de-Souza CM, Andrade AFB, Monteiro-Leal LH, Formiga LCD, Mattos-Guaraldi AL. Patterns of adherence to HEp-2 cells and actin polymerisation by toxigenic *Corynebacterium diphtheriae* strains. Microb Pathog. 2004 Mar;36(3):125–130. doi:10.1016/j.micpath.2003.10.002 Medline

Honda E, Yanagawa R. Attachment of *Corynebacterium renale* to tissue culture cells by the pili. Am J Vet Res. 1975 Nov;36(11):1663–1666. Medline

Jespersen MC, Peters B, Nielsen M, Marcatili P. BepiPred-2.0: improving sequence-based B-cell epitope prediction using conformational epitopes. Nucleic Acids Res. 2017 Jul 03;45(W1):W24–W29. doi:10.1093/nar/gkx346

Kim Y, Ponomarenko J, Zhu Z, Tamang D, Wang P, Greenbaum J, et al. Immune epitope database analysis resource. Nucleic Acids Res. 2012 Jul 01;40(W1):W525–W530. doi:10.1093/nar/gks438

Maione D, Margarit I, Rinaudo CD, Masignani V, Mora M, Scarselli M, Tettelin H, Brettoni C, Iacobini ET, Rosini R, et al. Identification of a universal Group B *streptococcus* vaccine by multiple genome screen. Science. 2005 Jul 01;309(5731):148–150.
doi:10.1126/science.1109869 Medline

Mandlik A, Das A, Ton-That H. The molecular switch that activates the cell wall anchoring step of pilus assembly in gram-positive bacteria. Proc Natl Acad Sci USA. 2008 Sep 16;105(37):14147–14152.
doi:10.1073/pnas.0806350105 Medline

Mandlik A, Swierczynski A, Das A, Ton-That H. *Corynebacterium diphtheriae* employs specific minor pilins to target human pharyngeal epithelial cells. Mol Microbiol. 2007 Apr;64(1):111–124.
doi:10.1111/j.1365-2958.2007.05630.x Medline

Marraffini LA, DeDent AC, Schneewind O. Sortases and the art of anchoring proteins to the envelopes of gram-positive bacteria. Microbiol Mol Biol Rev. 2006 Mar 01;70(1):192–221.
doi:10.1128/MMBR.70.1.192-221.2006 Medline

Mattos-Guaraldi AL, Cappelli EA, Previato JO, Formiga LCD, Andrade AFB. Characterization of surface saccharides in two *Corynebacterium diphtheriae* strains. FEMS Microbiol Lett. 1999a Jan;170(1):159–166.
doi:10.1111/j.1574-6968.1999.tb13369.x Medline

Mattos-Guaraldi AL, Duarte Formiga LC, Pereira GA. Cell surface components and adhesionin *Corynebacterium diphtheriae*. Microbes Infect. 2000 Oct;2(12):1507–1512.
doi:10.1016/S1286-4579(00)01305-8 Medline

Mattos-Guaraldi AL, Formiga LCD, Andrade AFB. Cell surface hydrophobicity of sucrose fermenting and nonfermenting *Corynebacterium diphtheriae* strains evaluated by different methods. Curr Microbiol. 1999b Jan;38(1):37–42.
doi:10.1007/PL00006769 Medline

Mattos-Guaraldi AL, Formiga LCD, Andrade AFB. *Trans*-Sialidase activity for sialic acid incorporation on *Corynebacterium diphtheriae*. FEMS Microbiol Lett. 1998 Nov;168(2):167–172.
doi:10.1111/j.1574-6968.1998.tb13269.x Medline

Moreira LO, Andrade AFB, Vale MD, Souza SMS, Hirata R Jr, Asad LMOB, Asad NR, Monteiro-Leal LH, Previato JO, Mattos-Guaraldi AL. Effects of iron limitation on adherence and cell surface carbohydrates of *Corynebacterium diphtheriae* strains. Appl Environ Microbiol. 2003 Oct 01;69(10):5907–5913.
doi:10.1128/AEM.69.10.5907-5913.2003 Medline

Mosley JF 2nd, Smith LL, Parke CK, Brown JA, LaFrance JM, Clark PK. Quadracel: vaccination against diphtheria, tetanus, pertussis, and poliomyelitis in children. P T. 2016 Apr;41(4):238–253.
Medline

Nielsen M, Lundegaard C, Worning P, Lauemøller SL, Lamberth K, Buus S, Brunak S, Lund O. Reliable prediction of T-cell epitopes using neural networks with novel sequence representations. Protein Sci. 2003 May;12(5):1007–1017. doi:10.1110/ps.0239403 Medline

Paul S, Weiskopf D, Angelo MA, Sidney J, Peters B, Sette A. HLA class I alleles are associated with peptide-binding repertoires of different size, affinity, and immunogenicity. J Immunol. 2013 Dec 15;191(12):5831–5839.
doi:10.4049/jimmunol.1302101 Medline

Proft T, Baker EN. Pili in Gram-negative and Gram-positive bacteria – structure, assembly and their role in disease. Cell Mol Life Sci. 2009 Feb;66(4):613–635.
doi:10.1007/s00018-008-8477-4 Medline

Reardon-Robinson ME, Ton-That H. Assembly and function of *Corynebacterium diphtheriae* pili. In: Burkovski A, editor. *Corynebacterium diphtheriae* and related toxigenic species. Dordrecht (Netherlands): Springer; 2014. p. 123–141.

Rogers EA, Das A, Ton-That H. Adhesion by pathogenic corynebacteria. Adv Exp Med Biol. 2011;715:91–103.
doi:10.1007/978-94-007-0940-9_6 Medline

Sabbadini PS, Assis MC, Trost E, Gomes DLR, Moreira LO, dos Santos CS, Pereira GA, Nagao PE, Azevedo VAC, Hirata Júnior R, et al. *Corynebacterium diphtheriae* 67-72p hemagglutinin, characterized as the protein DIP0733, contributes to invasion and induction of apoptosis in HEp-2 cells. Microb Pathog. 2012 Mar;52(3):165–176. doi:10.1016/j.micpath.2011.12.003 Medline

Sauer F, Mulvey MA, Schilling JD, Martinez JJ, Hultgren SJ. Bacterial pili: molecular mechanisms of pathogenesis. Curr Opin Microbiol. 2000 Feb 1;3(1):65–72.
doi:10.1016/S1369-5274(99)00053-3 Medline

Singh H and Raghava GPS. ProPred1: Prediction of promiscuous MHC class-I binding sites. Bioinformatics. 2003 May 22;19(8):1009–1014. Medline

Singh H, Raghava GPS. ProPred: prediction of HLA-DR binding sites. Bioinformatics. 2001 Dec 01;17(12):1236–1237.
doi:10.1093/bioinformatics/17.12.1236 Medline

Soriani M, Telford JL. Relevance of pili in pathogenic streptococci pathogenesis and vaccine development. Future Microbiol. 2010 May;5(5):735–747. doi:10.2217/fmb.10.37 Medline

Swierczynski A, Ton-That H. Type III pilus of corynebacteria: pilus length is determined by the level of its major pilin subunit. J Bacteriol. 2006 Sep 01;188(17):6318–6325. doi:10.1128/JB.00606-06 Medline

Thanassi DG, Saulino ET, Hultgren SJ. The chaperone/usher pathway: a major terminal branch of the general secretory pathway. Curr Opin Microbiol. 1998 Apr;1(2):223–231. doi:10.1016/S1369-5274(98)80015-5 Medline

Ton-That H, Schneewind O. Assembly of pili in Gram-positive bacteria. Trends Microbiol. 2004 May;12(5):228–234. doi:10.1016/j.tim.2004.03.004 Medline

Ton-That H, Schneewind O. Assembly of pili on the surface of *Corynebacterium diphtheriae.* Mol Microbiol. 2003 Nov;50(4): 1429–1438. doi:10.1046/j.1365-2958.2003.03782.x Medline

Trost E, Blom J, de Castro Soares S, Huang IH, Al-Dilaimi A, Schröder J, Jaenicke S, Dorella FA, Rocha FS, Miyoshi A, et al. Pangenomic study of *Corynebacterium diphtheriae* that provides insights into the genomic diversity of pathogenic isolates from cases of classical diphtheria, endocarditis, and pneumonia. J Bacteriol. 2012 Jun 15;194(12):3199–3215. doi:10.1128/JB.00183-12 Medline

Yu CS, Chen YC, Lu CH, Hwang JK. Prediction of protein subcellular localization. Proteins. 2006 Aug 15;64(3):643–651. doi:10.1002/prot.21018 Medline

Yu NY, Wagner JR, Laird MR, Melli G, Rey S, Lo R, Dao P, Sahinalp SC, Ester M, Foster LJ, et al. PSORTb 3.0: improved protein subcellular localization prediction with refined localization subcategories and predictive capabilities for all prokaryotes. Bioinformatics. 2010 Jul 1;26(13):1608–1615. doi:10.1093/bioinformatics/btq249 Medline

Zasada A, Zaleska M, Podlasin R, Seferyńska I. The first case of septicemia due to nontoxigenic *Corynebacterium diphtheriae* in Poland: case report. Ann Clin Microbiol Antimicrob. 2005;4(1):8. doi:10.1186/1476-0711-4-8 Medline

Zasada AA, Baczewska-Rej M, Wardak S. An increase in nontoxigenic *Corynebacterium diphtheriae* infections in Poland – molecular epidemiology and antimicrobial susceptibility of strains isolated from past outbreaks and those currently circulating in Poland. Int J Infect Dis. 2010 Oct;14(10):e907–e912. doi:10.1016/j.ijid.2010.05.013 Medline

Zasada AA, Formińska K, Rzeczkowska M. [Occurence of pili genes in *Corynebacterium diphtheriae* strains] (in Polish). Med Dosw Mikrobiol. 2012;64(1):19–27. Medline

Zasada AA. Nontoxigenic highly pathogenic clone of *Corynebacterium diphtheriae*, Poland, 2004–2012. Emerg Infect Dis. 2013 Nov;19(11):1870–1872. doi:10.3201/eid1911.130297 Medline

Polish Journal of Microbiology
2019, Vol. 68, No 2, 247–254
https://doi.org/10.33073/pjm-2019-026

ORIGINAL PAPER

Gastric Microbiota Alteration in *Klebsiella pneumoniae*-Caused Liver Abscesses Mice

NAN CHEN[1, 2], TONG-TONG JIN[2, 1], WEN-NING LIU[2, 1], DONG-QING ZHU[2, 1], YING-YING CHEN[3], YUE-LIANG SHEN[3], ZONG-XIN LING[4]*, HONG-JIE WANG[1, 2]* and LI-PING ZHANG[5, 6]*

[1] Central Laboratory, Affiliated Hospital of Hebei University and
[2] Department of Medical Microbiology, Medicine College, Hebei University, Baoding, China
[3] Department of Pharmacology, Zhejiang Medical College, Zhejiang University, Hangzhou, China
[4] Collaborative Innovation Center for Diagnosis and Treatment of Infectious Diseases, State Key Laboratory for Diagnosis and Treatment of Infectious Diseases, the First Affiliated Hospital, College of Medicine, Zhejiang University, Hangzhou, China
[5] Key Laboratory of Medicinal Chemistry and Molecular Diagnosis of Ministry of Education, Hebei University, Baoding, China
[6] College of Life Sciences, Hebei University, Baoding, China

Submitted 16 January 2019, revised 14 March 2019, accepted 24 March 2019

Abstract

Gastric microbiota provides a biological barrier against the invasion of foreign pathogens from the oral cavity, playing a vital role in maintaining gastrointestinal health. *Klebsiella* spp. of oral origin causes various infections not only in gastrointestinal tract but also in other organs, with *Klebsiella pneumoniae* serotype K1 resulting in a liver abscess (KLA) through oral inoculation in mice. However, the relationship between gastric microbiota and the extra-gastrointestinal KLA infection is not clear. In our study, a 454 pyrosequencing analysis of the bacterial 16S rRNA gene shows that the composition of gastric mucosal microbiota in mice with or without KLA infection varies greatly after oral inoculation with *K. pneumoniae* serotype K1 isolate. Interestingly, only several bacteria taxa show a significant change in gastric mucosal microbiota of KLA mice, including the decreased abundance of *Bacteroides*, *Alisptipes* and increased abundance of *Streptococcus*. It is worth noting that the abundance of *Klebsiella* exhibits an obvious increase in KLA mice, which might be closely related to KLA infection. At the same time, the endogenous antibiotics, defensins, involved in the regulation of the bacterial microbiota also show an increase in stomach and intestine. All these findings indicate that liver abscess caused by *K. pneumoniae* oral inoculation has a close relationship with gastric microbiota, which might provide important information for future clinical treatment.

Key words: *Klebsiella pneumoniae* serotype K1, defensins, gastric mucosal microbiota, High-throughput pyrosequencing, liver abscess

Introduction

Klebsiella pneumoniae as one of the most important pathogens leads to many infections including nosocomial and community-acquired infections. K1 or K2 serotype *K. pneumoniae*-caused pyogenic liver abscess (KLA) is a highly invasive community-acquired infection and often develops serious complications (Siu et al. 2012). Previous studies show that liver abscess infection can be caused by many pathogens and that *K. pneumoniae* causes less than 10% liver infection (Lee et al. 1991; Zibari et al. 2000). Recently the rate of KLA infection has increased greatly even up to 70% in some regions (Kuo et al. 2013). And drug-resistant *K. pneumoniae* isolated from KLA infection has been reported to be increased in Beijing (Li et al. 2014).

It is well known that oral-gastrointestinal tract is one of the main pathways for the foreign pathogen, which

* Corresponding authors: L.-P. Zhang, Key Laboratory of Medicinal Chemistry and Molecular Diagnosis of Ministry of Education, Hebei University and College of Life Sciences, Hebei University, Baoding, China; **e-mail: zhlping201@163.com**
H.-J. Wang, Central Laboratory, Affiliated Hospital of Hebei University and Medicine College, Hebei University, Baoding, China; **e-mail: hongjiew68@163.com**
Z.-X. Ling, Collaborative Innovation Center for Diagnosis and Treatment of Infectious Diseases, State Key Laboratory for Diagnosis and Treatment of Infectious Diseases, The First Affiliated Hospital, College of Medicine, Zhejiang University, Hangzhou, China; **e-mail: lingzongxin@zju.edu.cn**

causes human infection. *Klebsiella* spp. of oral origin causes various diseases not only in the gastrointestinal tract but also in other organs. Atarashi et al. (2017) hold that oral *Klebsiella* spp. colonizing the intestines causes inflammatory bowel disease (IBD). It has also been identified that oral inoculation of *K. pneumoniae* K1 or K2 serotype isolates causes liver abscess infections in mice (Tu et al. 2009; Chen et al. 2014).

Gastric microbiota provides a biological barrier against the invasion of foreign pathogens entering the oral pathway, playing a vital role in maintaining gastrointestinal health. (Bik et al. 2006). For example, *Helicobacter pylori* can successfully colonize stomach tissues via the oral pathway what results in infection. It has been identified that *H. pylori* infections can change the overall composition of stomach microbiota (Lofgren et al. 2011). Probiotics have been used for clinical treatment of gastritis caused by *H. pylori* (Sheu et al. 2002; Lesbros-Pantoflickova et al. 2007). But the relationship between the microbiota in gastric mucosal and extra-gastrointestinal liver abscess infection caused by *K. pneumoniae* through the oral pathway is not clear.

Experimental

Materials and Methods

Mouse model of KLA infection. In our previous study, *K. pneumoniae* K1 serotype clinical isolate Kp1002 was identified to cause KLA infection in C57BL/6 mice by oral inoculation (Chen et al. 2014). In the present study, six-week-old male C57BL/6 mice were orally inoculated with 10^6 CFU of Kp1002 using a 21-gauge feeding needle as previously described, with the phosphate buffered saline (PBS) given to the healthy control. All the mice were killed 48 h after oral inoculation. The serum, stomachs and cecum samples were retrieved for the following analysis. Mice with Kp1002 inoculation were divided into two groups: mice with KLA infection (KLA group) and mice without KLA infection (NKLA group) according to the criterion in our previous study (Chen et al. 2014). Five mice were randomly selected from each group and their samples were prepared for the following analysis. Mice in this study were raised in the Specific Pathogen Free (SPF) animal house. All the animal experiments in this study were conducted in accordance with the National Research Council Guide for Care and Use of Laboratory Animals and were approved by the Institutional Animal Care and Use Committee of the First Affiliated Hospital of Zhejiang Medical University (2013–012) and the Animal Welfare and Ethical Committee of Hebei University (2018026).

DNA extraction and high-throughput sequencing analysis. After mice sacrificed, the stomachs of the mice were isolated, with the corpus tissues divided and used in DNA extraction. DNA was extracted from 25 mg corpus tissue using a PureLink™ Genomic DNA Mini Kit (Invitrogen, USA) according to the manufacturer's instructions, with addition of lysozyme at the concentration of 20 mg/ml (Sigma-Aldrich, USA) at the beginning of cell lysis. DNA concentrations were tested by NanoDrop ND-1000 spectrophotometer (Thermo Electron Corporation). DNA integrity and size were checked by agarose gel electrophoresis. The DNA was stored at –80°C for the 16S rRNA gene sequencing analysis. 16S rRNA gene was amplified by PCR with primers 27F (5'-AGAGTTTGATCCTGGCTCAG-3') and 533R (5'-TTACCGCGGCTGCTGGCAC-3') (Ling et al. 2015, Chen et al. 2018). The 16S rRNA gene amplification products were sequenced by the 454 Life Sciences genome sequencer FLX system (Roche, Switzerland). The metagenomic sequence data were deposited in the NCBI Sequence Read Archive under Accession number SRP111617. The sequencing data processing methods were described in our previous study (Ling et al. 2015, Chen et al. 2018).

Biosample collection and analysis of defensins and cytokines. After mice sacrificed, the stomachs and cecum of the mice were isolated. The contents of the stomachs or cecum were collected as previously described (Li et al. 2015). The contents were removed and washed off with an isopycnic 0.09% NaCl solution. The washout material was centrifuged at 10 000 rpm for 20 min at 4°C. Then, the supernatant was harvested for the defensins analysis using an ELISA test kit (Mlbio, Shanghai, China). Serum samples were separated and stored at –80°C for the analysis of the cytokines using an ELISA test kit (Mlbio, Shanghai, China).

Data processing and statistical analysis. Mothur (http://www.mothur.org) was used for diversity and taxonomy-based analyses at a 97% similarity level as previously described (Ling et al. 2015, Chen et al. 2018). The Mann-Whitney U test was performed with the SPSS 16.0 software, and the ELISA analysis data statistical analyses were performed using One-way ANOVA analysis as implemented in the SPSS 16.0 software.

Results

The overall structure of the gastric mucosal microbiota alteration after oral inoculation with *K. pneumoniae* K1 serotype isolate. Gastric mucus samples were obtained from KLA, NKLA, and Kp1002-untreated healthy control groups and the 16S rRNA gene was sequenced. Totally 153 397 high-quality reads were obtained after sequencing analysis, including 46 329 sequences from a healthy group, 53 863 sequences from NKLA group and 53 205 sequences from KLA

group. These sequences had an average length of 477 bp (range from 400 bp to 521 bp). Operational taxonomic unit (OTU) was identified at the 97% similarity level. The coverage percentage was calculated by Good's method (Ling et al. 2015, Chen et al. 2018) and the coverage percentage values of healthy, NKLA and KLA groups were 98.27%, 98.54%, and 98.40%, respectively. These values showed sufficient sequencing depth in this study. The richness estimators (ACE and Chao1 value) and diversity indices (Shannon and Simpson indices) displayed no obvious difference between healthy and Kp1002-treated groups ($p > 0.05$) (Fig. S1). Rarefaction analysis estimates showed that species richness differed between the healthy and Kp1002-treated groups (Fig. 1A). The rank-abundance curves generated from OTU analysis also revealed differences between the healthy and Kp1002-treated groups (Fig. 1B). Beta-diversity indices analysis was performed by the unweighted UniFrac method and principal coordinate analysis (PCoA). Unweighted PCoA revealed obvious differences among the three groups, indicating variations in microbial communities (Fig. 1C). At the same time, PCoA of weighted UniFrac analysis also showed the different trends among the three groups (Fig. S2). A Venn diagram showed different OTU data in three groups and that the overlapping OTU data. Totally 3890 OTUs were obtained from three groups. In addition, 624 common OTUs were shared by the KLA and NKLA groups, which was higher than that shared by the healthy group and any of the other groups (Fig. 1D). These results suggested that the overall structure of gastric mucosal microbiota was obviously altered in Kp1002-treated mice in comparison with that in healthy mice, whereas it did not show a great difference between KLA group and NKLA group.

Major alterations in the composition of gastric mucosal microbiota in KLA mice. The sequences obtained in this study belonged to twelve bacterial phyla, with eleven of them found in healthy mice, including the most abundant phyla Bacteroidetes and Firmicutes. At the genus level, 93 genera were obtained. The healthy group consists of 46 genera with four abundant genera (> 1% of the total DNA sequences), including *Lactobacillus*, *Bacteroides*, *Alistipes*, and *Clostridium*

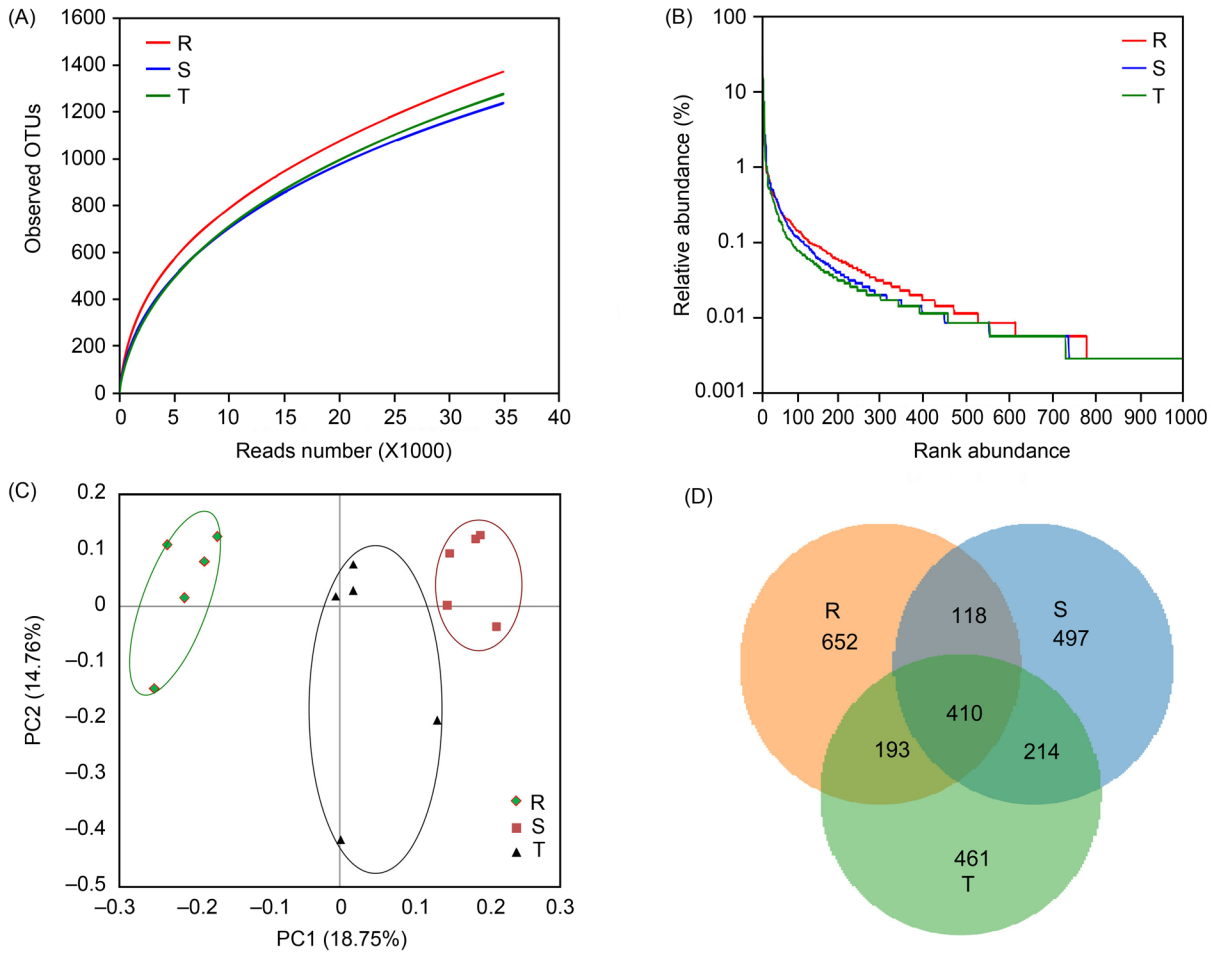

Fig. 1. Overall structure alteration in gastric microbiota.
The species richness (A) and Rank abundance curve (B) were based on OTUs analysis of the three groups. (C) PCoA of weighted UniFrac analysis plot of gastric microbiota of three groups. (D) Venn diagram showed the OTUs overlaps among the three groups. (R, healthy group; S, NKLA group; T, KLA group).

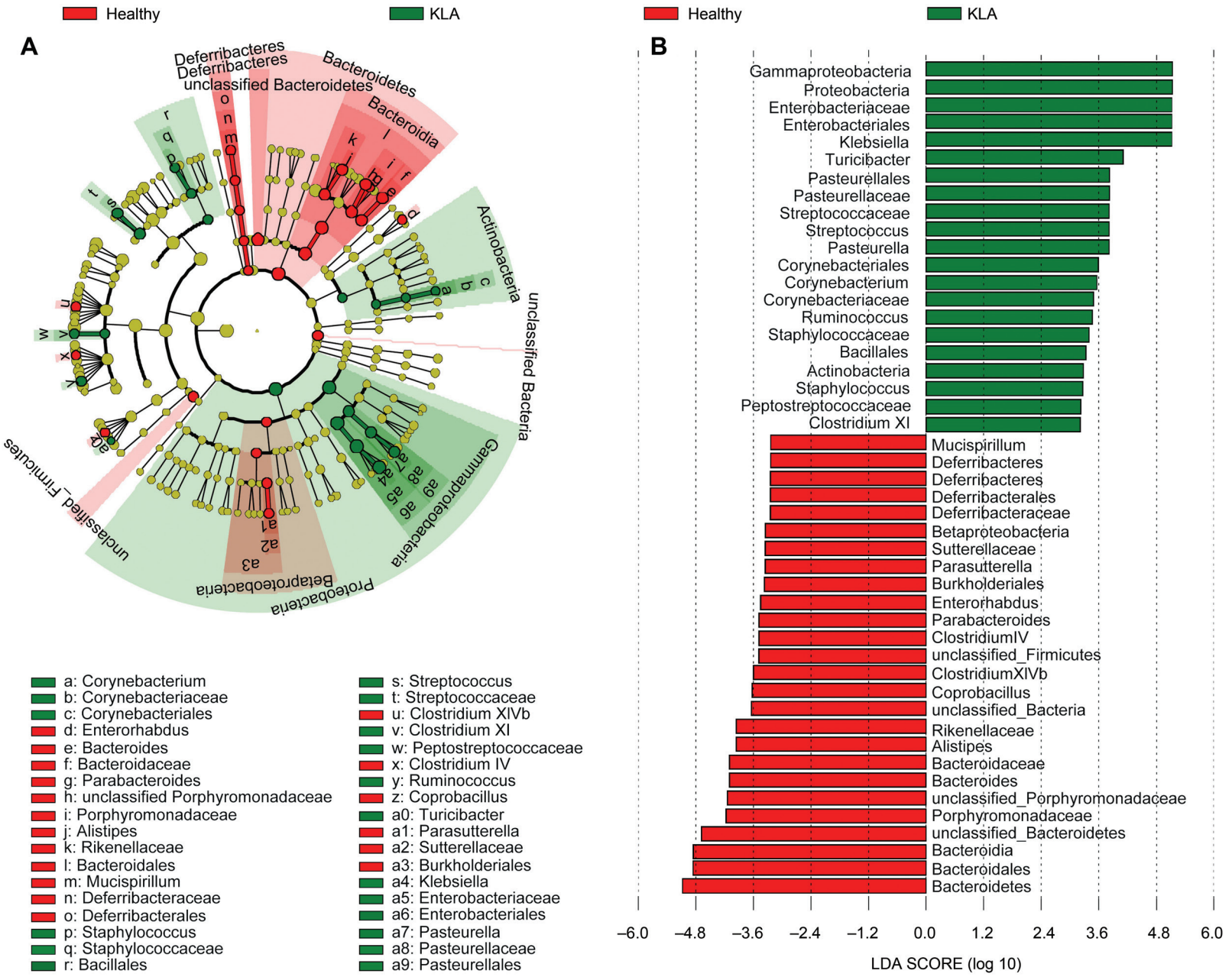

Fig. 2. The differences in gastric microbiota composition between healthy and KLA groups by LEfSe analysis.

Taxonomic cladogram (A) and Linear discriminative analysis (LDA) scores (B) exhibited the different enriched bacteria taxa between healthy group (Red) and KLA group (Green). All of the taxa showed in the figure with LDA threshold value > 2.

sensu stricto. There were 47 genera in the NKLA group with six abundant genera, and 59 genera in the KLA group with six abundant genera.

The linear discriminant analysis effect size (LEfSe) method was employed in this study to assess alterations in the composition of gastric mucosal microbiota in KLA mice. The gastric mucosal microbiota composition was significantly altered in KLA-infected mice when compared to that in healthy mice (Fig. 2). At the same time since the overall structure of gastric mucous microbiota showed differences between healthy mice and Kp1002-treated mice in Fig. 1, and for better understanding of the special changes in gastric microbiota from KLA infection mice, the significant differences in microbiota composition between NKLA and KLA mice were also explored. The specific changes of gastric mucosal microbiota in KLA mice were summarized in Fig. 3.

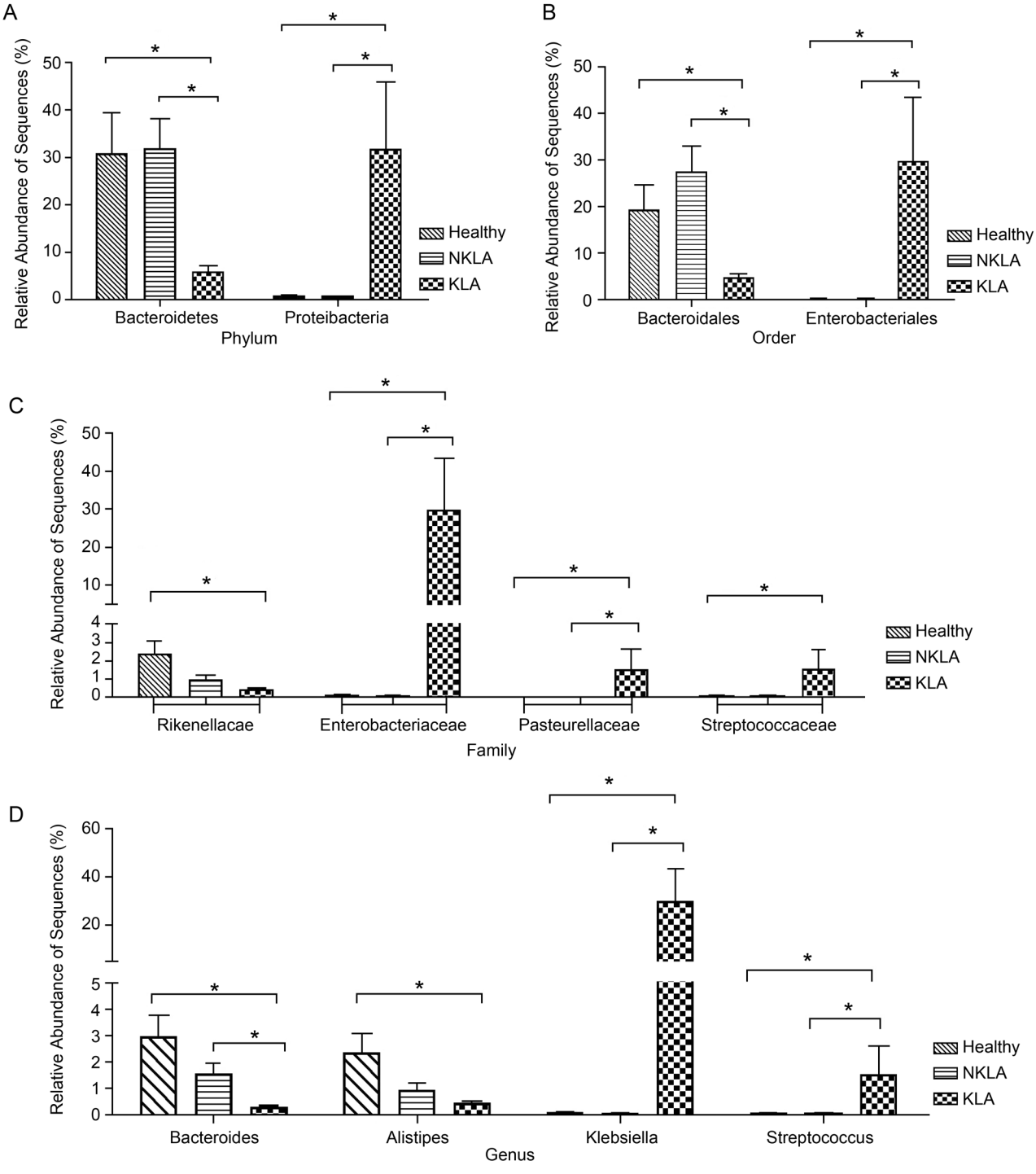

Fig. 3. Comparing the differences at the relative abundance of bacterial sequences at the different levels including phylum, order, family and genus level among three groups. (Mann-Whitney U test, *: $p < 0.05$).

The KLA and healthy mice showed significant differences in the abundance of phylum Bacteroidetes, a marked decrease in the KLA group compared with that in the healthy group ($p < 0.05$). In addition, the abundance of the non-predominant phylum Proteobacteria in the KLA group significantly increased ($p < 0.05$) (Fig. 3A). At the order level analyses, the great changes were observed in KLA infection mice. Compared with the healthy mice, the KLA infection mice showed an obvious decrease in the abundance of *Bacteroidales* and a significant increase in *Enterobacteriales* ($p < 0.05$) (Fig. 3B). At the family level, the data showed that the KLA infection mice exhibited a great decrease in the abundance of *Rikenellaceae* and a marked increase in the

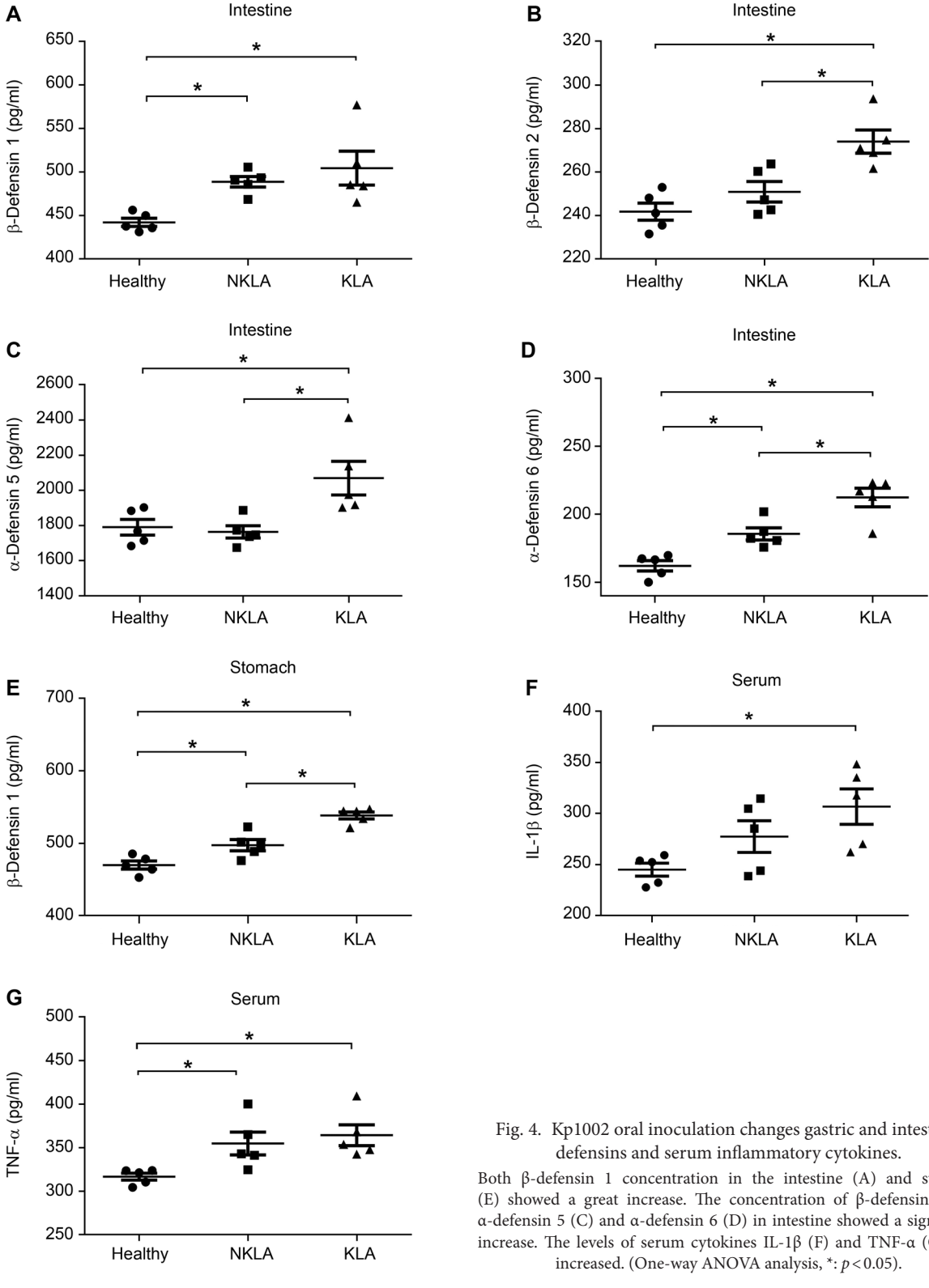

Fig. 4. Kp1002 oral inoculation changes gastric and intestinal defensins and serum inflammatory cytokines.

Both β-defensin 1 concentration in the intestine (A) and stomach (E) showed a great increase. The concentration of β-defensin 2 (B), α-defensin 5 (C) and α-defensin 6 (D) in intestine showed a significant increase. The levels of serum cytokines IL-1β (F) and TNF-α (G) also increased. (One-way ANOVA analysis, *: $p < 0.05$).

abundance of *Enterobacteriaceae*, *Pasteurellaceae*, and *Streptococcaceae* compared to the healthy mice ($p < 0.05$) (Fig. 3C). Further detailed analyses at the genus level showed that a great decrease in the abundance of *Bacteroides* and *Alistipes* and an obvious increase in *Klebsiella* and *Streptococcus* in the KLA group compared to the healthy group ($p < 0.05$) (Fig. 3D). The differences between the KLA and NKLA groups displayed trends in gastric mucosal microbiota composition at the phylum, order, family and genus level similar to that between the healthy and KLA groups (Fig. 3).

***K. pneumoniae* oral inoculation changes immune barrier.** In our previous study, we found that cecal contents microbiota significant changes in KLA mice (Chen et al. 2018). Herein, we examined the immune barrier in the stomach and intestine. Fig. 4 shows alterations in defensins and cytokines in KLA mice. Compared with healthy mice, KLA infection mice showed significant increases in β-defensin 1, β-defensin 2, α-defensin 5, α-defensin 6 in the cecum, and β-defensin 1 in the stomach ($p < 0.05$). The levels of serum cytokines interleukin 1 beta (IL-1β) and tumor necrosis factor alpha (TNF-α) also significantly increased in the KLA mice compared to that of healthy mice ($p < 0.05$). On the other hand, compared with healthy mice, NKLA mice also showed a great increase in β-defensin 1 and α-defensin 6 in the cecum, and β-defensin 1 in the stomach when compared to that of healthy mice ($p < 0.05$).

Discussion

Our previous study indicates that KLA infections are accompanied by changes in intestinal microbiota composition (Chen et al. 2018). The intestinal microbiota has been widely accepted to be an important biological barrier against foreign pathogens. The stomach has long been considered to be sterile due to the low pH of the gastric acid secreted by goblet cells. However, stomach actually consists of a microbial community, which provides a biological barrier against the invasion of foreign pathogens, especially pathogens of oral origin such as *H. pylori,* and maintains the gastrointestinal health (Bik et al. 2006; Andersson et al. 2008; Lofgren et al. 2011). To better understand the relationship between gastric microbiota and extra-gastrointestinal KLA infections, this study analyzes changes in gastric microbiota composition in KLA mice.

The present study observes great alterations in gastric mucosal microbiota composition in KLA mice. KLA mice show a significant reduction in Bacteroidetes in the gastric microbiota, with a great reduction in the abundance of Bacteroidetes in the gastric microbiota of *H. pylori*-infected mice (Lofgren et al. 2011). In human, positive *H. pylori* status is also associated with decreased abundance of Bacteroidetes (Maldonado-Contreras et al. 2011). Gastritis in male mice is accompanied by decreased *Bacteroides species* ASF519 colonization, indicating that inflammation-driven atrophy alters the gastric niche for the gastrointestinal commensal bacteria colonization (Lertpiriyapong et al. 2014). It seems that the decrease in the abundance of phylum Bacteroidetes or genus *Bacteroides* might be closely related to the gastrointestinal and extra-gastrointestinal infections caused by foreign pathogen through an oral pathway.

At the same time, the abundance of *Klebsiella* significantly increased in gastric mucosa of KLA infection mice. Sung et al. (2016) used 454-pyrosequencing to compare the microbiota composition between gastric fluid and gastric mucosa samples and found that using gastric mucosa samples was more effective in detecting meaningful bacteria, such as *H. pylori,* nitrosating or nitrate-reducing bacteria. In our study, the increase in the abundance of *Klebsiella* in gastric mucosa might be an effective bioindicator for KLA infection.

On the other hand, in the gastrointestinal tract, the constitutive expression of defensins imparts the regulation of the bacterial microbiota and immunomodulatory activity and is involved in the pathogenesis of various intestinal infection diseases (Wehkamp et al. 2005). α-defensin 5 has been reported to have microbicidal activity against various bacteria, including *Escherichia coli* and *Staphylococcus aureus* (Ouellette et al. 1994). The production of β-defensins 2, 3, and 4 is significantly higher in ulcerative colitis (Rahman et al. 2011). The present study also finds out that the defensin expression levels in the stomach or cecum are higher in KLA mice. Simultaneously, the elevated proinflammatory cytokines IL-1β and TNF-α could be induced by β-defensins (Ghosh et al. 2011). These findings show the changes in the gastrointestinal microbiota in response to *K. pneumoniae*, as well as an increase of the expression of defensins and cytokines.

It should not be ignored that Kp1002-treated mice without KLA infection also exhibited changes in the gastrointestinal microbiota and increased expression levels of defensins relative to that in healthy mice. We also find that after oral inoculation with the *K. pneumoniae* isolate, mouse infection rates continuously increase after 48 h (data not shown). These changes in gastrointestinal microbiota and defensins expression levels may be related to the infection process, thereby providing new insight into KLA treatment.

Acknowledgements

This study was supported by Natural Science Foundation of Hebei Province (No. H2015201076), Preferential funding for postdoctoral research projects of Hebei Province (No. B2017003032), and Graduate students' innovative funding projects of Hebei University (No. hbu2018ss75).

We thank the support from the Affiliated Hospital of Hebei University Postdoctoral workstation and Hebei University Biology Postdoctoral research station. We also thank the support from Key Bioengineering Discipline of Hebei Province, Engineering Laboratory of Microbial Breeding and Preservation of Hebei Province.

Conflict of interest

The authors do not report any financial or personal connections with other persons or organizations, which might negatively affect the contents of this publication and/or claim authorship rights to this publication.

Literature

Andersson AF, Lindberg M, Jakobsson H, Bäckhed F, Nyrén P, Engstrand L. Comparative analysis of human gut microbiota by barcoded pyrosequencing. PLoS One. 2008 Jul 30;3(7):e2836. doi:10.1371/journal.pone.0002836 Medline

Atarashi K, Suda W, Luo C, Kawaguchi T, Motoo I, Narushima S, Kiguchi Y, Yasuma K, Watanabe E, Tanoue T, et al. Ectopic colonization of oral bacteria in the intestine drives T_H1 cell induction and inflammation. Science. 2017 Oct 20;358(6361):359–365. doi:10.1126/science.aan4526 Medline

Bik EM, Eckburg PB, Gill SR, Nelson KE, Purdom EA, Francois F, Perez-Perez G, Blaser MJ, Relman DA. Molecular analysis of the bacterial microbiota in the human stomach. Proc Natl Acad Sci USA. 2006 Jan 17;103(3):732–737. doi:10.1073/pnas.0506655103 Medline

Chen N, Ling ZX, Jin TT, Li M, Zhao S, Zheng LS, Xi X, Wang LL, Chen YY, Shen YL, et al. Altered profiles of gut microbiota in *Klebsiella pneumoniae*-induced pyogenic liver abscess. Curr Microbiol. 2018 Jul;75(7):952–959. doi:10.1007/s00284-018-1471-7 Medline

Chen N, Wang L, Xue J, Ma X, Zhao S, Rong R, Li H, Ding L, Zheng M, Chen Y, et al. Different metabolic profiles of K1 serotype and non-serotype K1 and K2 *Klebsiella pneumoniae* isolates in oral infection mice model. Microb Pathog. 2014 Oct;75:41–48. doi:10.1016/j.micpath.2014.08.006 Medline

Ghosh SK, Gupta S, Jiang B, Weinberg A. *Fusobacterium nucleatum* and human beta-defensins modulate the release of antimicrobial chemokine CCL20/macrophage inflammatory protein 3α. Infect Immun. 2011 Nov;79(11):4578–4587. doi:10.1128/IAI.05586-11 Medline

Kuo SH, Lee YT, Li CR, Tseng CJ, Chao WN, Wang PH, Wong RH, Chen CC, Chen SC, Lee MC. Mortality in Emergency Department Sepsis score as a prognostic indicator in patients with pyogenic liver abscess. Am J Emerg Med. 2013 Jun;31(6):916–921. doi:10.1016/j.ajem.2013.02.045 Medline

Lee KT, Sheen PC, Chen JS, Ker CG. Pyogenic liver abscess: multivariate analysis of risk factors. World J Surg. 1991 May;15(3): 372–376, discussion 376–377. doi:10.1007/BF01658732 Medline

Lertpiriyapong K, Whary MT, Muthupalani S, Lofgren JL, Gamazon ER, Feng Y, Ge Z, Wang TC, Fox JG. Gastric colonisation with a restricted commensal microbiota replicates the promotion of neoplastic lesions by diverse intestinal microbiota in the *Helicobacter pylori* INS-GAS mouse model of gastric carcinogenesis. Gut. 2014 Jan;63(1):54–63. doi:10.1136/gutjnl-2013-305178 Medline

Lesbros-Pantoflickova D, Corthésy-Theulaz I, Blum AL. *Helicobacter pylori* and probiotics. J Nutr. 2007 Mar 01;137(3) Suppl 2: 812S–818S. doi:10.1093/jn/137.3.812S Medline

Li M, Liang P, Li Z, Wang Y, Zhang G, Gao H, Wen S, Tang L. Fecal microbiota transplantation and bacterial consortium transplantation have comparable effects on the re-establishment of mucosal barrier function in mice with intestinal dysbiosis. Front Microbiol. 2015 Jul 07;6:692. doi:10.3389/fmicb.2015.00692 Medline

Li W, Sun G, Yu Y, Li N, Chen M, Jin R, Jiao Y, Wu H. Increasing occurrence of antimicrobial-resistant hypervirulent (hypermucoviscous) *Klebsiella pneumoniae* isolates in China. Clin Infect Dis. 2014 Jan 15;58(2):225–232. doi:10.1093/cid/cit675 Medline

Ling Z, Liu X, Cheng Y, Jiang X, Jiang H, Wang Y, Li L. Decreased diversity of the oral microbiota of patients with hepatitis B virus-induced chronic liver disease: a pilot project. Sci Rep. 2015 Dec; 5(1):17098. doi:10.1038/srep17098 Medline

Lofgren JL, Whary MT, Ge Z, Muthupalani S, Taylor NS, Mobley M, Potter A, Varro A, Eibach D, Suerbaum S, et al. Lack of commensal flora in *Helicobacter pylori*-infected INS-GAS mice reduces gastritis and delays intraepithelial neoplasia. Gastroenterology. 2011 Jan;140(1):210–220.e4. doi:10.1053/j.gastro.2010.09.048 Medline

Maldonado-Contreras A, Goldfarb KC, Godoy-Vitorino F, Karaoz U, Contreras M, Blaser MJ, Brodie EL, Dominguez-Bello MG. Structure of the human gastric bacterial community in relation to *Helicobacter pylori* status. ISME J. 2011 Apr;5(4):574–579. doi:10.1038/ismej.2010.149 Medline

Ouellette AJ, Hsieh MM, Nosek MT, Cano-Gauci DF, Huttner KM, Buick RN, Selsted ME. Mouse Paneth cell defensins: primary structures and antibacterial activities of numerous cryptdin isoforms. Infect Immun. 1994 Nov;62(11):5040–5047. Medline

Rahman A, Fahlgren A, Sundstedt C, Hammarström S, Danielsson Å, Hammarström ML. Chronic colitis induces expression of β-defensins in murine intestinal epithelial cells. Clin Exp Immunol. 2011 Jan;163(1):123–130. doi:10.1111/j.1365-2249.2010.04282.x Medline

Sheu BS, Wu JJ, Lo CY, Wu HW, Chen JH, Lin YS, Lin MD. Impact of supplement with *Lactobacillus*- and *Bifidobacterium*-containing yogurt on triple therapy for *Helicobacter pylori* eradication. Aliment Pharmacol Ther. 2002 Sep;16(9):1669–1675. doi:10.1046/j.1365-2036.2002.01335.x Medline

Siu LK, Yeh KM, Lin JC, Fung CP, Chang FY. *Klebsiella pneumoniae* liver abscess: a new invasive syndrome. Lancet Infect Dis. 2012 Nov;12(11):881–887. doi:10.1016/S1473-3099(12)70205-0 Medline

Sung J, Kim N, Kim J, Jo HJ, Park JH, Nam RH, Seok YJ, Kim YR, Lee DH, Jung HC. Comparison of gastric microbiota between gastric juice and mucosa by next generation sequencing method. J Cancer Prev. 2016 Mar 30;21(1):60–65. doi:10.15430/JCP.2016.21.1.60 Medline

Tu YC, Lu MC, Chiang MK, Huang SP, Peng HL, Chang HY, Jan MS, Lai YC. Genetic requirements for *Klebsiella pneumoniae*-induced liver abscess in an oral infection model. Infect Immun. 2009 Jul 01;77(7):2657–2671. doi:10.1128/IAI.01523-08 Medline

Wehkamp J, Fellermann K, Herrlinger KR, Bevins CL, Stange EF. Mechanisms of Disease: defensins in gastrointestinal diseases. Nat Clin Pract Gastroenterol Hepatol. 2005 Sep;2(9):406–415. doi:10.1038/ncpgasthep0265 Medline

Zibari GB, Maguire S, Aultman DF, McMillan RW, McDonald JC. Pyogenic liver abscess. Surg Infect (Larchmt). 2000 Apr;1(1):15–21. doi:10.1089/109629600321254 Medline

Supplementary materials are available on the journal's website.

Polish Journal of Microbiology
2019, Vol. 68, No 2, 255–261
https://doi.org/10.33073/pjm-2019-027

ORIGINAL PAPER

Influence of Environmental and Genetic Factors on Proteomic Profiling of Outer Membrane Vesicles from *Campylobacter jejuni*

RENATA GODLEWSKA[1]*, JOANNA KLIM[1], JANUSZ DĘBSKI[2], AGNIESZKA WYSZYŃSKA[1] and ANNA ŁASICA[1]

[1] Department of Bacterial Genetics, Institute of Microbiology, Faculty of Biology, University of Warsaw, Warsaw, Poland
[2] Mass Spectrometry Laboratory, Institute of Biochemistry and Biophysics, Polish Academy of Sciences, Warsaw, Poland

Submitted 30 January 2019, revised 5 April 2019, accepted 12 April 2019

Abstract

The proteomes of outer membrane vesicles (OMVs) secreted by *C. jejuni* 81–176 strain, which was exposed to oxygen or antibiotic stress (polymyxin B), were characterized. We also assessed the OMVs production and their content in two mutated strains – Δ*dsbI* and Δ*htrA*. OMVs production was significantly increased under the polymyxin B stress and remained unaltered in all other variants. Interestingly, the qualitative load of OMVs was constant regardless of the stress conditions or genetic background. However, certain proteins exhibited notable quantitative changes, ranging from 4-fold decrease to 10-fold increase. Up- or downregulated proteins (e.g. major outer membrane protein *porA*, iron ABC transporter, serine protease- *htrA*, 60 kDa chaperonin-*groL*, enolase) represented various cell compartments (cytoplasm, periplasm, and membrane) and exhibited various functions; nevertheless, one common group was noted that consisted of components of flagellar apparatus, i.e., FlaA/B, FlgC/E, which were mostly upregulated. Some of these proteins are the putative substrates of DsbI protein. Further investigation of the regulation of *C. jejuni* OMVs composition and their role in virulence will allow a better understanding of the infectious process of *C. jejuni*.

Key words: *Campylobacter jejuni,* outer membrane vesicles (OMVs), proteomics

Introduction

The outer membrane (OM) of Gram-negative bacteria can naturally bulge out, entraps periplasmic content and pinches off to form spheres of 50–250 nm in diameter called outer membrane vesicles (OMVs). OMVs contain mostly outer membrane-associated and periplasmic proteins, but also cytoplasm-located molecules, quorum-signaling molecules, DNA and RNA and, thus, provide bacteria with means to interact adaptively with their environment, host and other microorganisms (Schwechheimer and Kuehn 2015). Alterations in size, number, and content of OMVs are frequently regarded as bacterial responses to changes in the environment (such as pH, temperature, ionic strength, and antibiotic pressure), including endogenous stress (Mcbroom et al. 2007, Schwechheimer and Kuehn 2015). This notion is supported by a number of observations. A treatment with polymyxin B (a cyclic cationic antimicrobial peptide that alters the membrane permeability) or with ciprofloxacin (an antibiotic that damages DNA and activates the SOS system) increased OMVs formation by *Pseudomonas aeruginosa* PA14 strain (MacDonald and Kuehn 2013). The hyper-vesiculating *yieM* mutant (ΔyieM) of *Escherichia* coli grew faster in the presence of polymyxin B than the nonmutated strain (Manning and Kuehn 2013). *P. aeruginosa* cells could respond with increased OMVs production to hydrogen peroxide treatment and temperature change (MacDonald and Kuehn 2013). Overexpression of a periplasmic fusion protein to imitate misfolded OM protein in *E. coli* resulted in hypervesiculation and tenfold increase of its concentration in OMVs; moreover, increased OMV production accompanied mutations in the σ^E heat shock response in *E. coli* (Mcbroom et al. 2007). Furthermore, the genes participating in cellular

* Corresponding author: R. Godlewska, Department of Bacterial Genetics, Institute of Microbiology, Faculty of Biology, University of Warsaw, Warsaw, Poland; **e-mail: renatag@biol.uw.edu.pl**

stress response (*degS*, *depP*, *rseA*) are engaged in the vesicle formation (Mcbroom et al. 2006). Mutations of *degP,* encoding periplasmic serine protease-chaperone responsible for the degradation of misfolded proteins in *E. coli,* as well as mutations of *mucD*, its homolog in *P. aeruginosa*, increase OMVs production (MacDonald and Kuehn 2013). Thus, bacteria may use OMVs to selectively dispose of misfolded proteins, particularly large aggregates, which are resistant to proteolytic cleavage and are too big to be discarded through OM pores (Mcbroom et al. 2007). OMVs may, therefore, help bacteria to survive under harsh conditions and establish a lasting resistance.

In this study, we investigated whether the production of *C. jejuni* OMVs and their protein composition correlates to environmental stress conditions. We also examined the influence of mutations in the *htrA* and *dsbI* genes on the level of OMVs production. The *C. jejuni htrA* gene is the *E. coli degP* gene homolog, while the *dsbI* gene is a disulfide oxidoreductase – a component of the Dsb system in *C. jejuni*, involved in the introduction of disulfide bonds into periplasmic proteins for securing their proper fold and function.

Experimental

Materials and Methods

Bacterial strains, media, and culture conditions. Bacterial strains and plasmids used are listed in Table I. *C. jejuni* strains were grown on Blood Agar No. 2 (BA, Oxoid) plates supplemented with 5% horse blood, Campylobacter Selective Supplement (Blaser-Wang) (Oxoid), and tetracycline (10 μg/ml) at 37°C or 42°C for 16–24 h under microaerobic conditions in a Mart anaerobic jar (flushed with 6% O_2, 10% CO_2, 85% N_2 gas mixture using an Anoxomat Mart II system).

If necessary, plates were also supplemented with chloramphenicol (20 μg/ml) and/or kanamycin (25 μg/ml). *Campylobacter* strains used for isolation of OMVs were grown in Mueller-Hinton broth for ~16 hours with shaking under microaerobic conditions at 37°C.

Stress was induced by either addition of polymyxin B to a final concentration of 5.5 μg/ml (~15× higher than in Campylobacter Selective Supplement, minding an intrinsic resistance of *C. jejuni* to this compound (Iovine 2013)) or by incubation in the atmosphere of 15% O_2 and 6% CO_2. Higher oxygen atmosphere was generated by CO_2 Gen sachets (Thermo Scientific Oxoid Microbiology Products) in the 2.5-litre gas jar. Cultures in optimal and stress conditions were conducted parallel. Overnight culture of *C. jejuni* was diluted 1:100. The same number of bacterial cells was used as inoculum for fresh media and grown in optimal and stress conditions in 37°C with shaking. After ~16 h optical density of each culture was measured, and bacteria were plated on BA medium to assess the number of bacteria cells (CFU/ml). The bacterial concentration ranged between $8\times10^6 - 1\times10^7$ CFU/ml in the presence of polymyxin B while in 15% O_2 atmosphere was between $1.5\times10^7 - 5.5\times10^7$ CFU/ml. In optimal growth conditions, the concentration of bacteria was in the range from 1×10^8 to 5×10^8 CFU/ml.

Construction of *C. jejuni* mutants. The *C. jejuni htrA* mutant was obtained following the approach of Brøndsted et al. (2005). Mutagenesis was performed with a gene replacement method. A suicide mutagenesis plasmid was constructed in 2-step PCR. First, the upstream and downstream fragments of 5' and 3' end of the *htrA* gene were amplified with use of *C. jejuni* 81–176 chromosomal DNA as a template. For the fragment containing 3' end of the *htrA* gene (421 bp), primers UW564 (5'-CGAGCTC**AAATGCAGTGCTTTCTTATC**-3') and UW565 (5'-CTCGAGCTGCAGTCTAGA**CAACATCTCCTTCCATTAAATC**-3') were used, while primers UW566 (5'-CCGGTACC**CAAATCGCTTTGTACGCCTTTAG**-3') and UW567 5'-TCTAGACTGCAGCTCGAG**TTTCTCGTGGTGGTGGAAATAAC**-3') were used for amplification of the fragment containing 5' end of the gene (428 bp). In the sequences of the primers above, the restriction enzyme sites are underlined, and bases complementary to the htrA gene are indicated in bold.

In the second round of PCR, the amplified *htrA* fragments were joined, creating PCR fragments containing a deletion of 186 bp in *htrA* and introducing a XhoI-PstI-XbaI restriction sites instead. The final PCR product was cloned into the *C. jejuni* nonreplicable pBluescript II SK cloning vector with the use of SacI-KpnI enzymes, resulting in plasmid pUWM1321. Finally, the *cat* gene encoding for chloramphenicol

Table I
Strains used in this study.

Strain or plasmid	Genotype / resistance / description	Reference
Campylobacter jejuni		
81–176 (ATCC BAA-, 2151)	pVir, Tc^R (Wild type, human isolate)	
81–176 *htrA*$^-$	pVir, *htrA*::*aphA3*, Tc^R, Km^R	This study
81–176 *dsbI*$^-$	pVir, *dsbI*::*cat* Tc^R, Cm^R	(Raczko et al. 2005)

resistance in *C. jejuni* cells (obtained from pRY109) was cloned into the PstI site of pUWM1321, resulting in the final mutagenesis plasmid denoted pUWM1329. The *cat* gene in this construct is transcribed in the same direction as the *htrA* gene.

C. jejuni 81–176 was electroporated with pUWM1329, and several chloramphenicol-resistant colonies were isolated. The disruption of the *htrA* gene as a result of double cross-over recombination and lack of wild-type *htrA* allele in the genome of the strain obtained was verified by PCR.

C. jejuni dsbI mutant was obtained in our lab and described earlier (Raczko et al. 2005).

OMV purification and quantification. OMVs were isolated from *C. jejuni* strain 81–176 by the method we used before (Godlewska et al. 2016) and described by Elmi et al. (2012) and Chutkan et al. (2013). Briefly, *C. jejuni* 81–176 strain was grown in the Mueller-Hinton broth under microaerobic conditions at 37°C. An overnight culture was diluted 1:100 into 330 ml of fresh growth media and grown 16–18 h to a mid-log phase. The cells were pelleted twice using centrifugation at 6000 × g for 2 × 20 min at 4°C. Supernatants were filtered through a 0.22 μm filter device to remove the remaining cells. The filtrate was ultracentrifuged in a Beckman L7-55 Ultracentrifuge at 150 000 × g for 3 h at 4°C using a 50.2 Ti rotor. OMVs preparations were plated on BA plates and incubated under microaerobic conditions to confirm the absence of viable bacteria.

OMVs production was quantified by determining protein concentration (BCA assay) and normalized to CFU at the time of harvest. This method allows indirect estimate the concentration of OMV based on total protein content but does not provide additional information about the size or quantity of OMV. Relative OMVs production levels were determined by comparison to the wild-type cell results in the control samples. Means of three independent experiments with standard deviations (error bars) were calculated.

Sample preparation for MS analysis. Membrane proteins were extracted by suspending OMVs in 1.5% sodium deoxycholate and 0.1% SDS in 25 mM ammonium bicarbonate, followed by sonication for 10 minutes (50% cycle). Protein concentration was estimated with Direct Detect (Milipore) and equalized to 40 μg per sample. Proteins were subsequently reduced with *tris*(2-carboxyethyl)phosphine for 30 min at 60°C, alkylated with methyl methanethiosulfonate and digested with 0.5 μg of trypsin at 37°C overnight. The reaction was quenched with trifluoroacetic acid (TFA).

LC-MS-MS/MS analysis. The resulting peptide mixtures were analyzed by LC-MS-MS/MS (liquid chromatography coupled to tandem mass spectrometry) using a Nano-Acquity (Waters) LC system and an Orbitrap Velos mass spectrometer (Thermo Electron Corp). Peptides were applied to RP-18 precolumn (nanoACQUITY Symmetry® C18) using water containing 0.1% TFA as a mobile phase and then transferred to nano-HPLC RP-18 column (nanoACQUITY BEH C18) using an acetonitrile gradient 5–35% in 180 minutes in the presence of 0.05% formic acid with the flow rate of 250 ml/min. Column outlet was directly coupled to the ion source of the spectrometer working in the regime of data dependent MS to MS/MS switch. To ensure reproducibility, sample preparations and MS analysis were repeated four times.

Database searching. The data acquired were processed by a Mascot Distiller followed by Mascot Search (Matrix Science, on-site license) against the UniProt database restricted to *Campylobacter jejuni* 81–176 and NCTC11168 sequences. The search parameters for precursor and product ions mass tolerance were 20 ppm and 0.1 Da, respectively, enzyme specificity: trypsin, missed cleavage sites allowed: 1, fixed modification of cysteine methylation and variable modification of methionine oxidation. To estimate the false-positive discovery rate (FDR), the decoy search option was enabled. The label-free quantitation was performed as described previously (Bakun et al. 2009) using in-house MScan software to select the proteins with an FDR < 1% and identified by at least two peptides.

LC-MS data were converted by an in-house MsConvert tool into 2D heat maps recognized by MSparky – an in-house modification of the Sparky NMR (http://www.cgl.ucsf.edu/home/ sparky) – and the qualitative information from MScan was correlated with quantitative data from MSparky on the basis of m/z, retention time and isotopic profile fitting, generating a list of identified peptides with signal intensity values, subsequently subjected to statistical analysis using in-house Diffprot software (Malinowska et al. 2012). All software used is accessible at http://proteom.ibb.waw.pl.

Results and Discussion

Alterations in OMVs production. In our experiments, the presence of polymyxin B significantly increased OMVs production by *C. jejuni* 81–176 strain, based on total OMVs' protein content corrected for CFU measurement (Fig. 1). We did not assess the size and shape of OMVs. Polymyxin B is a cyclic cationic antimicrobial peptide (AMPs), which penetrates into the bacterial cell, integrates into the outer leaflet of the outer membrane and impairs the structure of OM forming pores, altering the membrane permeability. Our results are consistent with the previous observations.

Many studies have revealed that the levels of OMVs production depend largely on the growth conditions of bacteria (oxygen stress, antibiotic pressure, and envelope stress) (Mcbroom et al. 2007; Kulp et al. 2015).

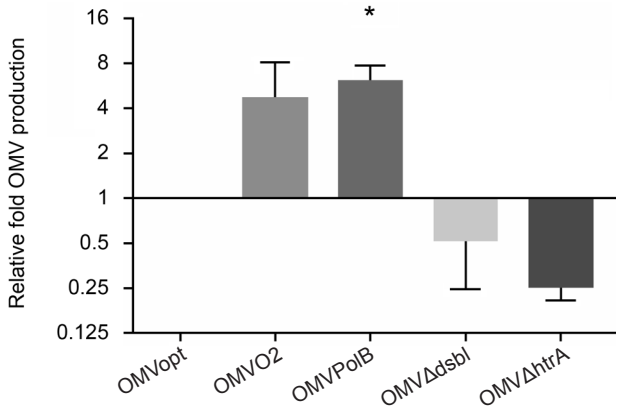

Fig. 1. Comparison of the OMVs production.

The concentration of OMVs, isolated from *C. jejuni* 81–176 grown under optimal and stress conditions (15% O_2 and polymyxin B) and from *C. jejuni* 81–176 *dsbI* and *htrA* mutants, was measured by BCA assay. The concentration of OMVs produced by the strain grown under optimal conditions was marked as 1. A statistical analysis was performed using GraphPad Prism 6 (GraphPad Software). Statistical analysis was carried out using multifactorial (one-way) ANOVA followed by Tukey's multiple comparisons test. An asterisk indicates significant differences ($p < 0.05$) between analyzed groups and the control group.

It was observed that stress (physical and chemical) increases the number of secreted OMVs. The *E. coli* hyper-vesiculating *yieM* mutant (Δ*yieM*) grown on the medium containing polymyxin B exhibited survival rate higher than the wild type strain, (Manning and Kuehn 2011, Manning and Kuehn 2013). MacDonald and Kuehn also concluded that polymyxin B treatments increased OMVs formation by *P. aeruginosa* PA14 strain (MacDonald and Kuehn 2013).

OMVs release was also increased under oxygen stress (15% O_2 instead of a physiological level of 6% O_2), albeit nonsignificantly. Our results are consistent with the data obtained for other bacterial species. *P. aeruginosa* cells, treated with ciprofloxacin (an antibiotic that leads to DNA damage and, as a consequence, to activation of the of SOS system), responded with increased production of OMVs. Moreover, MacDonald and Kuehn (2013) found that OMVs production significantly increased after hydrogen peroxide treatment. Also, physiological stress increased OMVs production. The same authors have also shown that temperature change and oxidative stress-stimulated OMVs production by *P. aeruginosa* (MacDonald and Kuehn 2013).

We further explored the relationship between OMVs production level and mutations in the *htrA* and *dsbI* genes of *C. jejuni*. Surprisingly, we haven't noticed any significant changes (Fig. 1).

Qualitative content of OMV proteome. We have made the identification and quantitative analysis of the protein contents of *C. jejuni* OMVs using the LC-MS-MS/MS analysis. OMVs were isolated from the wild-type strain 81–176 grown in optimal and under the stress conditions (increased oxygen content, presence of polymyxin B). We also analyzed the OMVs from *C. jejuni* strains with mutations in the *htrA* and *dsbI* genes. To ensure reproducibility, each analysis was repeated four times.

Irrespectively of the factors used (polymyxin B, oxygen content, *ΔhtrA* and *ΔdsbI* mutations), the qualitative protein composition of the OMVs in our study matched the previously presented for the unstressed wt strain (Elmi et al. 2012). However, we discovered numerous quantitative differences described and discussed below.

Polymyxin B influence on the quantitative composition of OMVs. *C. jejuni* exhibits intrinsic resistance to polymyxin B, presumably due to the absence of the appropriate targets and/or low-affinity binding to targets (Iovine 2013). We used a relatively high concentration of antibiotic to induce the stress (~15 times higher concentration than in Campylobacter Selective Supplement). We noticed that four proteins exhibited increased level within OMVs and one showed a decrease (Table II). The highest, nine-fold increase was noted for the major outer membrane protein (MOMP) encoded by the *porA* gene. Overexpression of MOMP alters membrane permeability and plays a role in *Campylobacter* resistance against antibiotics, probably also against polymyxin B. MOMP elevation in OMVs was observed also under aerobic stress, consistent with the study demonstrating upregulation of MOMP expression in *Campylobacter* subjected to low and high oxygen level (1.88% and > 15%, respectively) (Guccione et al. 2017).

Another highly upregulated protein (over 6-fold) was a putative pyridoxamine 5'-phosphate oxidase (Cj1613c), predicted to catalyze the terminal step in *de novo* vitamin B_6 synthesis: oxidation of pyridoxamine-5-P (PMP) and pyridoxine-5-P (PNP) to pyridoxal-5-P (https://www.ebi.ac.uk/interpro/entry/IPR024029, InterPro, Protein sequence analysis & classification). PMP is a coenzyme required for the biosynthesis of deoxysugars, which attach to lipopolysaccharides (LPS), the major integral components of the outer membrane of Gram-negative bacteria (Romo and Liu 2011). Thus, the overexpression of Cj1613c may be linked to the destabilization of the bacterial envelope. Also, vitamin B6 itself was implicated in oxidative stress responses (Bilski et al. 2000).

Additionally, two flagellar proteins (FlaB and FlgE) were overrepresented. The destabilization of bacterial envelope may affect the integrity of flagella and result in an elevation of flagellar proteins in OMV. Of note, synthesis of flagella proteins and the ability to form flagella affects the production of OMVs by *E. coli* W3110 (Manabe et al. 2013).

The underrepresented protein was identified as HtrA, which is surprising and resonates with the observed lack of effect of *htrA* mutation on the OMVs production and composition (*see 'Genetic factors...' for a joint discussion*).

Table II
Up- and downregulated proteins under the polymyxin B and oxidative stress
and in the *ΔdsbI* mutant background (the protein numeration of *C. jejuni* NCTC11168 strain).

Protein / Gene	Number of peptides	*q*-value	Fold*
Strain 81–176 wt vs. strain 81–176 grown under oxidative stress conditions			
Major outer membrane protein (*porA*, Cj1259)	56	0.00038	+1.96
Flagellin A (*flaA*, Cj1339c)	25	0.00494	+2.18
Iron ABC transporter, periplasmic iron-binding protein (Cj0175c)	29	0.00507	+1.83
Putative lipoprotein (Cj1090c)	7	0.00627	–4.07
Strain 81–176 wt vs. strain 81–176 grown under the polymyxin B stress			
Flagellin B (*flaB*, Cj1338c)	83	0.00021	+4.57
Major outer membrane protein (*porA*, Cj1259)	60	0.00021	+9.09
Serine protease, protease DO (*htrA*, Cj1228c)	55	0.01684	–3.14
Flagellar hook protein (*flgE*, Cj1729c)	34	0.019	+4.67
Putative pyridoxamine 5-phosphate oxidase (Cj1613c)	7	0.08	+6.16
Strain 81–176 wt vs. strain 81–176 *dsbI*$^-$			
60 kDa chaperonin (*groL*, Cj1221)	95	0.00040	–4.45
Fagellar hook-associated protein (*flgL*, Cj0887c)	20	0.003	+8.81
Enolase (Cj1672c)	27	0.02	–2.16
Coproporphyrinogen-III oxidase (*hemN*, Cj0992c)	10	0.038	+10.68
Flagellar basal body rod protein (*flgC*, Cj0527c)	18	0.042	–2,49
Flagellar hook protein (*flgE*, Cj1729c)	33	0.059	+2.7
Anthranilate synthase subunit I (*trpE*, Cj0345)	18	0.06	–2.7
Fumarate hydratase class II (*fumC,* Cj1364c)	34	0.09	–2.3
Strain 81–176 wt vs. strain 81–176 *htrA*$^-$			
No significant changes noted			

* Positive values correspond to the fold of higher abundance in the stress conditions and negative values correspond to the fold of lower abundance in the stress conditions for each spot.

Oxygen influence on the quantitative composition of OMVs. Oxidative stress resulted in an elevation of the level of three proteins and a decrease of the level of one within *Campylobacter* OMVs (Table II). MOMP and flagellar proteins were again among overrepresented, perhaps embodying a general response to the environmental stress. The third upregulated protein was the periplasmic iron-binding protein (Cjj81176_0211). While the iron uptake should be tightly controlled to avoid the iron-associated oxidative-stress-mediated damage to the cell, the changes in the Cjj81176_0211 expression were subtle and more studies are needed to unequivocally claim their impact (Holmes et al. 2005).

Genetic factors and the quantitative composition of OMVs. The mechanism of OMVs biogenesis remains unclear, but many studies suggest that the vesiculation has a genetic basis. Recently nearly 150 genes were implicated in the *E. coli* OMVs production, leading to the conclusion that the surface-exposed oligosaccharides negatively affect the vesiculation and an intact oxidative stress response is required for the wild type vesiculation (Kulp et al. 2015). Roier et al. (2016) have recently shown the role of the *vacJ*/*yrb* genes in the OMVs biogenesis. They found that mutations within these genes that make up ABC (ATP-binding cassette) transport system increase the OMVs production in *Haemophilus influenzae* and *Vibrio cholerae*. The disruption of both or one of these genes entails phospholipid accumulation in the outer leaflet of OM which initiates an outward bulging of OM. Further accumulation supports the budding of the OM, which leads to the formation and release of OMVs (Roier et al. 2016).

One of the first identified over-vesiculating mutants was the *E. coli degP* mutant. The *degP* homolog of *C. jejuni*, *htrA*, is vital for heat tolerance, bacterial invasion, and transmigration (Backert et al. 2018). It encodes a protein with proteolytic and chaperone activity, known to participate in periplasmic protein quality control in stress response (Boehm et al. 2018) (*see also 'Introduction'*). Unexpectedly, HtrA was underrepresented in OMVs from *Campylobacter* upon the polymyxin B stress (Table II). It thus seems that HtrA is not involved in the envelope stress response, warranting further investigations. Moreover, the *htrA* mutation neither significantly increased the OMVs production (Fig. 1) nor altered the OMV composition (Table II). In

contrast, DegP in *Vibrio cholerae* was shown to affect the level of nine proteins in OMVs (Altindis et al. 2014). However, most of these proteins were involved in biofilm formation, a phenomenon not observed in the present study due to the culture conditions.

Interestingly, *C. jejuni* and *Helicobacter pylori* have recently been shown to actively secrete HtrA to cleave host cell junctional proteins such as E-cadherin (Hoy et al. 2010; Boehm et al. 2018). Others and we (Elmi et al. 2012) identified HtrA protein inside OMVs and the 11168H *htrA* mutant exhibited reduced proteolytic activity of OMVs (Elmi et al. 2018). In light of the current study, the latter may be largely due to the lack of HtrA protein itself.

The second gene we analyzed was *dsbI*, a rare variant of the DsbB paralog identified by our group (Raczko et al. 2005) and absent in *E. coli*. It belongs to *C. jejuni* Dsb (disulfide bond) system, which catalyzes the formation of disulfide bridges in extracytoplasmic proteins, stabilizing their tertiary and quaternary structures. Disturbances of Dsb cause protein misfolding and formation of insoluble aggregates accumulating in the periplasm. Under such circumstances, cells may increase the formation of vesicles as a protective mechanism. We observed that DsbI activity in *C. jejuni* manifests only if DsbB is inactivated, but still none of the DsbI substrates or redox partners are known. We hypothesized that DsbI is more specific than DsbB and acts only on a subset of DsbB substrates (Raczko et al. 2005). So, we were looking for substrates, which are affected by DsbI itself. We showed that mutation of *dsbI* (as well as *htrA*) of *C. jejuni* does not alter the amount of OMVs produced (Fig. 1), but our study revealed eight proteins, whose content in OMVs is significantly altered by *dsbI* mutation (Table II). Most of them possess one or more cysteine residues and may be able to form intra- or intermolecular bridges. Particularly noteworthy is the increase in the level of flagellar proteins (FlgC, FlgE and FlgL), observed also in response to the environmental stress. Our previous data revealed that double *ΔdsbIΔdsbB* mutant was completely nonmotile, whereas motility of a *ΔdsbI* mutant was comparable to the wild strain (Raczko et al. 2005).

Further two alterations comprised decreased content of 60 kDa GroL chaperonin and enolase, two of 12 most immunoreactive proteins possibly involved in the development of Guillain-Barré syndrome (GBS) (Loshaj-Shala et al. 2018). GroL and enolase reside in the cytoplasm, therefore OMVs may provide for their export. Further, we saw an overrepresentation of coproporphyrinogen-III oxidase, which catalyzes the conversion of coproporphyrinogen-III to protoporphyrinogen-IX during the heme biosynthesis. These three changes remain completely unclear.

Further studies are required to fully explain the production and function of OMVs and to provide us with new methods to control bacterial growth and host invasion.

Summarizing, we characterized how the proteome of secreted OMVs changed when the *C. jejuni* 81–176 strain was exposed to stress induced by the antibiotic polymyxin B or by increased oxygen levels. Our study is one of the few presenting such a comprehensive approach to the problem. Other studies in this field focused on particular genes and proteins, showing the interdependence of their levels, the total OMVs production and stress conditions. Thanks to our complete methodology, we identified all proteins, whose level in OMVs is altered by the conditions applied.

Several of the proteins identified, mostly upregulated ones, were components of the flagella apparatus. Presence of flagella protein in OMVs is not extraordinary. Manabe et al. (2013) reported that both the synthesis of flagella proteins and the ability to form flagella affects the production of OMVs by *E. coli* W3110.

In the study similar and somewhat complementary to ours, Chan et al. analyzed the OMV proteome of two clinical extraintestinal pathogenic *E. coli* (ExPEC) isolates under the stress conditions of the limited iron availability and the presence of the antibiotic gentamicin. Low iron environment resulted in major changes in the OMV proteome, including the upregulation of several stress response proteins (Hsp100/Clp proteins, ClpX and ClpA, the AAA+ protease, ClpP, which they interact with, and also ClpB) (Chan et al. 2017).

At present, we can propose neither causes nor consequences of up- or downregulation of certain proteins (coproporphyrinogen-III oxidase (*hemN* Cj0992c) or unknown putative lipoprotein), indicating that further research in this field is needed.

Further investigation of the regulation of *C. jejuni* OMVs' composition combined with their role in virulence will allow us to better understand the pathomechanisms of the infection.

ORCID
Renata Godlewska 0000-0001-7810-8482

Acknowledgements
We thank Dr. L. Trzeciak for his critical reading of the manuscript.

Funding
This work was supported by the PARENT BRIDGE programme of the Foundation for Polish Science, co-financed from the European Union under the European Regional Development Fund [project POMOST/2012-6/4].

Conflict of interest
The authors do not report any financial or personal connections with other persons or organizations, which might negatively affect the contents of this publication and/or claim authorship rights to this publication.

Literature

Altindis E, Fu Y, Mekalanos JJ. Proteomic analysis of *Vibrio cholerae* outer membrane vesicles. Proc Natl Acad Sci USA. 2014 Apr 15;111(15):E1548–E1556. doi:10.1073/pnas.1403683111 Medline

Backert S, Bernegger S, Skórko-Glonek J, Wessler S. Extracellular HtrA serine proteases: an emerging new strategy in bacterial pathogenesis. Cell Microbiol. 2018 Jun;20(6):e12845. doi:10.1111/cmi.12845 Medline

Bakun M, Karczmarski J, Poznanski J, Rubel T, Rozga M, Malinowska A, Sands D, Hennig E, Oledzki J, Ostrowski J, et al. An integrated LC-ESI-MS platform for quantitation of serum peptide ladders. Application for colon carcinoma study. Proteomics Clin Appl. 2009 Aug;3(8):932–946. doi:10.1002/prca.200800111 Medline

Bilski P, Li MY, Ehrenshaft M, Daub ME, Chignell CF. Vitamin B6 (pyridoxine) and its derivatives are efficient singlet oxygen quenchers and potential fungal antioxidants. Photochem Photobiol. 2000;71(2):129–134. doi:10.1562/0031-8655(2000)071<0129:SIPVBP>2.0.CO;2 Medline

Boehm M, Simson S, Escher U, Schmidt A-M, Bereswill S, Tegtmeyer N, Backert S, Heimesaat MM. Function of serine protease HtrA in the lifecycle of the foodborne pathogen *Campylobacter jejuni*. Eur J Microbiol Immunol. 2018 Jul 17;8(3):70–77. doi:10.1556/1886.2018.00011 Medline

Brøndsted L, Andersen MT, Parker M, Jørgensen K, Ingmer H. The HtrA protease of *Campylobacter jejuni* is required for heat and oxygen tolerance and for optimal interaction with human epithelial cells. Appl Environ Microbiol. 2005 Jun 01;71(6):3205–3212. doi:10.1128/AEM.71.6.3205-3212.2005 Medline

Chan KW, Shone C, Hesp JR. Antibiotics and iron-limiting conditions and their effect on the production and composition of outer membrane vesicles secreted from clinical isolates of extraintestinal pathogenic *E. coli*. Proteomics Clin Appl. 2017 Jan;11(1-2):1600091. doi:10.1002/prca.201600091 Medline

Chutkan H, MacDonald I, Manning A, Kuehn MJ. Quantitative and qualitative preparations of bacterial outer membrane vesicles. Methods Mol Biol. 2013;966:259–272. doi:10.1007/978-1-62703-245-2_16 Medline

Elmi A, Dorey A, Watson E, Jagatia H, Inglis NF, Gundogdu O, Bajaj-Elliott M, Wren BW, Smith DGE, Dorrell N. The bile salt sodium taurocholate induces *Campylobacter jejuni* outer membrane vesicle production and increases OMV-associated proteolytic activity. Cell Microbiol. 2018 Mar;20(3):e12814. doi:10.1111/cmi.12814 Medline

Elmi A, Watson E, Sandu P, Gundogdu O, Mills DC, Inglis NF, Manson E, Imrie L, Bajaj-Elliott M, Wren BW, et al. *Campylobacter jejuni* outer membrane vesicles play an important role in bacterial interactions with human intestinal epithelial cells. Infect Immun. 2012 Dec;80(12):4089–4098. doi:10.1128/IAI.00161-12 Medline

Godlewska R, Kuczkowski M, Wyszyńska A, Klim J, Derlatka K, Woźniak-Biel A, Jagusztyn-Krynicka EK. Evaluation of a protective effect of in ovo delivered *Campylobacter jejuni* OMVs. Appl Microbiol Biotechnol. 2016 Oct;100(20):8855–8864. doi:10.1007/s00253-016-7699-x Medline

Guccione EJ, Kendall JJ, Hitchcock A, Garg N, White MA, Mulholland F, Poole RK, Kelly DJ. Transcriptome and proteome dynamics in chemostat culture reveal how *Campylobacter jejuni* modulates metabolism, stress responses and virulence factors upon changes in oxygen availability. Environ Microbiol. 2017 Oct;19(10):4326–4348. doi:10.1111/1462-2920.13930 Medline

Holmes K, Mulholland F, Pearson BM, Pin C, McNicholl-Kennedy J, Ketley JM, Wells JM. *Campylobacter jejuni* gene expression in response to iron limitation and the role of Fur. Microbiology. 2005 Jan 01;151(1):243–257. doi:10.1099/mic.0.27412-0 Medline

Hoy B, Löwer M, Weydig C, Carra G, Tegtmeyer N, Geppert T, Schröder P, Sewald N, Backert S, Schneider G, et al. *Helicobacter pylori* HtrA is a new secreted virulence factor that cleaves E-cadherin to disrupt intercellular adhesion. EMBO Rep. 2010 Oct;11(10):798–804. doi:10.1038/embor.2010.114 Medline

Iovine NM. Resistance mechanisms in *Campylobacter jejuni*. Virulence. 2013 Apr;4(3):230–240. doi:10.4161/viru.23753 Medline

Kulp AJ, Sun B, Ai T, Manning AJ, Orench-Rivera N, Schmid AK, Kuehn MJ. Genome-wide assessment of outer membrane vesicle production in *Escherichia coli*. PLoS One. 2015 Sep 25;10(9): e0139200. doi:10.1371/journal.pone.0139200 Medline

Loshaj-Shala A, Colzani M, Brezovska K, Poceva Panovska A, Suturkova L, Beretta G. Immunoproteomic identification of antigenic candidate *Campylobacter jejuni* and human peripheral nerve proteins involved in Guillain-Barré syndrome. J Neuroimmunol. 2018 Apr;317:77–83. doi:10.1016/j.jneuroim.2018.01.006 Medline

MacDonald IA, Kuehn MJ. Stress-induced outer membrane vesicle production by *Pseudomonas aeruginosa.* J Bacteriol. 2013 Jul 01; 195(13): 2971–2981. doi:10.1128/JB.02267-12 Medline

Malinowska A, Kistowski M, Bakun M, Rubel T, Tkaczyk M, Mierzejewska J, Dadlez M. Diffprot – software for non-parametric statistical analysis of differential proteomics data. J Proteomics. 2012 Jul; 75(13):4062–4073. doi:10.1016/j.jprot.2012.05.030 Medline

Manabe T, Kato M, Ueno T, Kawasaki K. Flagella proteins contribute to the production of outer membrane vesicles from *Escherichia coli* W3110. Biochem Biophys Res Commun. 2013 Nov;441(1):151–156. doi:10.1016/j.bbrc.2013.10.022 Medline

Manning AJ, Kuehn MJ. Contribution of bacterial outer membrane vesicles to innate bacterial defense. BMC Microbiol. 2011; 11(1):258. doi:10.1186/1471-2180-11-258 Medline

Manning AJ, Kuehn MJ. Functional advantages conferred by extracellular prokaryotic membrane vesicles. J Mol Microbiol Biotechnol. 2013;23(1-2):131–141. doi:10.1159/000346548 Medline

McBroom AJ, Johnson AP, Vemulapalli S, Kuehn MJ. Outer membrane vesicle production by *Escherichia coli* is independent of membrane instability. J Bacteriol. 2006 Aug 01;188(15):5385–5392. doi:10.1128/JB.00498-06 Medline

McBroom AJ, Kuehn MJ. Release of outer membrane vesicles by Gram-negative bacteria is a novel envelope stress response. Mol Microbiol. 2007 Jan;63(2):545–558. doi:10.1111/j.1365-2958.2006.05522.x Medline

Raczko AM, Bujnicki JM, Pawlowski M, Godlewska R, Lewandowska M, Jagusztyn-Krynicka EK. Characterization of new DsbB-like thiol-oxidoreductases of *Campylobacter jejuni* and *Helicobacter pylori* and classification of the DsbB family based on phylogenomic, structural and functional criteria. Microbiology. 2005 Jan 01;151(1):219–231. doi:10.1099/mic.0.27483-0 Medline

Roier S, Zingl FG, Cakar F, Durakovic S, Kohl P, Eichmann TO, Klug L, Gadermaier B, Weinzerl K, Prassl R, et al. A novel mechanism for the biogenesis of outer membrane vesicles in Gram-negative bacteria. Nat Commun. 2016 Dec;7(1):10515. doi:10.1038/ncomms10515 Medline

Romo AJ, Liu H. Mechanisms and structures of vitamin B6-dependent enzymes involved in deoxy sugar biosynthesis. Biochimica et Biophysica Acta (BBA) - Proteins and Proteomics. 2011 Nov; 1814(11):1534–1547. doi:10.1016/j.bbapap.2011.02.003 Medline

Schwechheimer C, Kuehn MJ. Outer-membrane vesicles from Gram-negative bacteria: biogenesis and functions. Nat Rev Microbiol. 2015 Oct;13(10):605–619. doi:10.1038/nrmicro3525 Medline

Polish Journal of Microbiology
2019, Vol. 68, No 2, 263–268
https://doi.org/10.33073/pjm-2019-029

ORIGINAL PAPER

Effects of Sodium Tripolyphosphate on Oral Commensal and Pathogenic Bacteria

JI-HOI MOON[1, 2*], MI HEE NOH[1], EUN-YOUNG JANG[3], SEOK BIN YANG[1], SANG WOOK KANG[4], KYU HWAN KWACK[5], JAE-IN RYU[6] and JIN-YONG LEE[1*]

[1] Department of Maxillofacial Biomedical Engineering, School of Dentistry, Kyung Hee University, Seoul, Republic of Korea
[2] Department of Life and Nanopharmaceutical Sciences, Kyung Hee University, Seoul, Republic of Korea
[3] Department of Dentistry, Graduate School, Kyung Hee University, Seoul, Republic of Korea
[4] Department of Oral and Maxillofacial Pathology, School of Dentistry, Kyung Hee University, Seoul, Republic of Korea
[5] Institute of Oral Biology, School of Dentistry, Graduate school, Kyung Hee University, Seoul, Republic of Korea
[6] Department of Preventive Dentistry, School of Dentistry, Kyung Hee University, Seoul, Republic of Korea

Submitted 10 January 2019, revised 20 April 2019, accepted 22 April 2019

Abstract

Polyphosphate (polyP) is a food additive with antimicrobial activity. Here we evaluated the effects of sodium tripolyphosphate (polyP3, $Na_5P_3O_{10}$) on four major oral bacterial species, in both single- and mixed-culture. PolyP3 inhibited three opportunistic pathogenic species: *Fusobacterium nucleatum*, *Prevotella intermedia*, and *Porphyromonas gingivalis*. On the contrary, a commensal bacterium *Streptococcus gordonii* was relatively less susceptible to polyP3 than the pathogens. When all bacterial species were co-cultured, polyP3 (≥ 0.09%) significantly reduced their total growth and biofilm formation, among which the three pathogenic bacteria were selectively inhibited. Collectively, polyP3 may be an alternative antibacterial agent to control oral pathogenic bacteria.

Key words: polyphosphate, antibacterial, oral bacteria, commensal, pathogenic

Introduction

Periodontitis is a polymicrobial biofilm-mediated disease of the oral cavity and is a chronic inflammatory condition of the periodontium, leading to the damage of structural tooth support, resorption of bone, and eventually tooth loss (Schaudinn et al. 2009). The microbial etiology of periodontitis is defined by oral biofilm, also called dental plaque, in which resides an interdependent microbial community containing numerous bacterial species (Sundus et al. 2016). A typical dental biofilm begins with the formation of the salivary acquired pellicle, which is a result of the selective adsorption of salivary components, such as statherin, histatin, acidic proline-rich proteins, albumin, mucins, and α-amylase onto the tooth surface (Kreth et al. 2009; Willems et al. 2016). Early colonizers then directly attach to various molecules of the acquired pellicle *via* the selective adhesin-receptor binding and form an initial dental plaque (Kreth et al. 2009). Representative bacteria that constitute the initial biofilm are streptococci, which are mostly commensal/non-periodontopathogenic bacteria and makeup over 80% of the early biofilm inhabitants (Kreth et al. 2009), quickly followed by *Actinomyces*, *Gemella*, *Neisseria*, and *Veillonella*. As plaque matures, the composition of the biofilm changes. With the introduction and an increasing number of anaerobic bacteria such as *Porphyromonas*, *Fusobacterium*, *Prevotella*, *Veillonella*, and *Capnocytophaga*, the diversity of the species constituting the plaque increases (Willems et al. 2016). Several experimental studies suggested that periodontal diseases are generally associated with Gram-negative anaerobic bacteria, such as *Aggregatibacter actinomycetemcomitans*, *Tannerella forsythia*, *Prevotella* spp., *Fusobacterium* spp. and *Porphyromonas gingivalis* (Torkko and Asikainen 1993; Tanner and Izard 2006; Han 2015; How et al. 2016;

* Corresponding authors: J.-Y. Lee, Department of Maxillofacial Biomedical Engineering, School of Dentistry, Kyung Hee University, Seoul, Republic of Korea; **e-mail: ljinyong@khu.ac.kr**
J.-H. Moon, Department of Maxillofacial Biomedical Engineering, School of Dentistry, Kyung Hee University, Seoul, Republic of Korea; **e-mail: prudence75@khu.ac.kr**

Suprith et al. 2018). However, it is now widely accepted that not any one of these bacterial species alone, but a concerted interaction of these members can cause the destructive events involved in the periodontal disease progression (Liu et al. 2012; Hajishengallis 2015; Khan et al. 2015; Patini et al. 2018).

Polyphosphate (polyP) is an inorganic polymer composed of three to several hundred orthophosphate residues linked by phosphoanhydride bonds (Kornberg et al. 1999). The type of polyP varies depending on the length of the phosphate chain constituting it, for example, polyP3, polyP5, polyP15, polyP45, and so on, even up to polyP chains of many hundreds of phosphate residues. The Food and Drug Administration (FDA) has listed sodium pyro-, tri-, and hexametaphosphates as the Generally Recognized as Safe (GRAS) food additives. PolyP is often added to dairy and meat products for water binding, ion exchange, emulsification, and antioxidation (Ellinger 1972). In addition, due to the antimicrobial effects against various Gram-positive bacteria and fungi (Knabel et al. 1991), thereby suppressing food spoilage, polyP has drawn the attention of food industry.

Recently, it was reported that some Gram-negative anaerobic periodontal pathogens were highly sensitive to polyP. The minimum inhibitory concentrations (MICs) of polyP against *P. gingivalis* W83 and *P. intermedia* ATCC 49046 ranged from 0.06 to 0.075%, which were much lower than those previously reported for Gram-positive bacteria (Moon et al. 2011; Jang et al. 2016). Bacterial species rarely inhabit infection sites alone instead reside in diverse, multispecies communities (Stacy et al. 2016). Hence, to adequately assess the potential of polyP as a controlling agent against oral pathogenic bacteria, it is necessary to ascertain the effect of polyP not only on an individual microbial species but also on the consortium of mixed-species. In the present study, we investigated the effects of sodium tripolyphosphate (polyP3, $Na_5P_3O_{10}$), listed as a GRAS, on four major oral bacterial species, including commensal and pathogenic bacteria. We also evaluated the antimicrobial effect of polyP3 against the mixed-species consortium consisting of the four bacterial species.

Experimental

Materials and Methods

Bacterial strains and culture condition. We used *S. gordonii* G9B, *F. nucleatum* ATCC 23726, *P. gingivalis* ATCC 53977 (previously designated A7A1-28), and *P. intermedia* ATCC 49046. Each bacterial strain was grown either in Brucella agar (Becton, Dickinson and Company, Sparks, MD, USA) supplemented with 5% sheep blood, 5 μg/ml hemin (Sigma Chemical Co., St. Louis, MO, USA) and 1 μg/ml vitamin K_1 (Sigma), or in Brucella broth (Becton, Dickinson and Company) supplemented with 5 μg/ml hemin and 1 μg/ml vitamin K_1 (B-HK). The bacterial culture was incubated at 37°C under anaerobic conditions (85% N_2, 10% H_2 and 5% CO_2).

MIC determination and individual bacterial growth. PolyP with chain length 3 (polyP3, $Na_5P_3O_{10}$, Sigma) was dissolved in distilled water to 10% (wt/vol) and sterilized using a 0.22-μm filter. The MIC of polyP3 against the individual bacterial species was determined by agar dilution method according to CLSI guidelines (CLSI 2007). Briefly, optical density at 600 nm (OD_{600}) of each bacterial suspension was adjusted, then the suspension was inoculated at a cell density of approximately 10^5 to 10^6 cells/spot on Brucella blood agar plates containing polyP3 (final concentrations of 0.015–0.2%). The number of the inoculated bacterial cells was confirmed by serial dilution and colony forming unit (CFU) count. All inoculated plates were incubated at 37°C for 72 h. The MIC was defined as the lowest concentration that inhibited the bacterial growth on the plate. To evaluate the effect of polyP3 on the growth of the bacteria at a high inoculum density, each bacterial strain cultured to exponential phase was adjusted to approximately 10^8 cells/ml in B-HK, then exposed to polyP3 at various concentrations. The bacterial growth was measured by reading OD_{600} after 24 hours.

Total growth and biofilm formation of mixed bacterial culture. We also investigated the effect of polyP3 on the total growth and biofilm formation of the four bacterial species in a mixed culture. In preliminary studies, we observed that a mixed-species biofilm with relatively uniform distribution of four strains can be developed by inoculating *S. gordonii*, *F. nucleatum*, *P. gingivalis* and *P. intermedia* cells at a ratio of 1 : 1 : 100 : 100. We estimated the number of individual bacterial cells by measuring and adjusting of OD_{600} of each culture, then mixed so that the cell number ratio was as above. The mixed bacterial suspension was dispensed in triplicate into wells (500 μl/well) of a 24-well plate containing B-HK (500 μl) supplemented with polyP3 at various concentrations. The final bacterial suspension was approximately 10^8 to 10^9 cells/ml. Two identical 24-well plates were prepared for each of three independent experiments and cultured for 72 h under the same environment as the culture condition for single bacterial species, without agitation and media replenishment. To assess the total growth (planktonic and biofilm bacterial growth), the biofilm bacterial cells were dispersed and mixed thoroughly with planktonic bacterial cells, and OD_{600} of the suspension was measured (Moon et al. 2013, 2015). The suspension was diluted 2 to 10 times, and OD_{600} of the diluted suspension was also measured. The amount of biofilm formed by the mixed bacterial species was measured using the other plate. The plank-

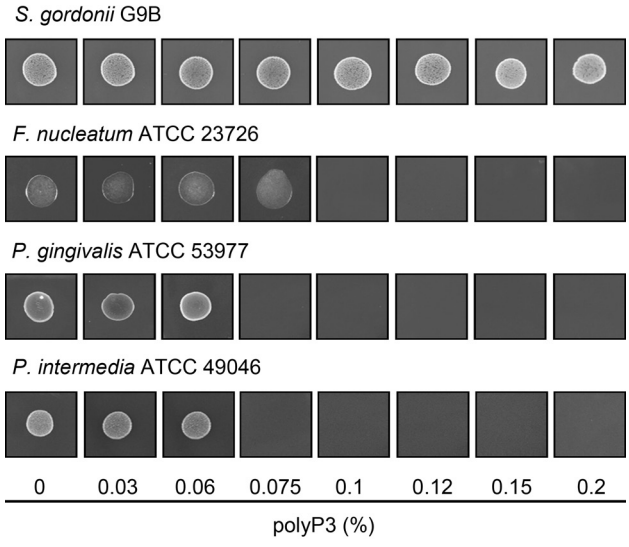

Fig. 1. MIC determination of polyP3 by the agar dilution method. The bacterial cells were spot-inoculated (approximately 10^5 to 10^6 cells/spot) onto Brucella blood agar plates containing polyP3 at various concentrations and incubated at 37°C for 3 days anaerobically. The MIC was defined as the lowest concentration that inhibited the bacterial growth on the plate. The results for *P. intermedia* ATCC 49046 are the same as those reported in our previous study (Jang et al. 2016).

tonic bacterial cells and the spent media were removed, and the biofilm formed in the wells was washed twice with physiological saline, then stained with 0.1% crystal violet for 10 min. The plate was washed three times with physiological saline and air dried. Then, 500 µl of 95% ethanol was added to release the crystal violet from the biofilm, and the OD_{600} was recorded.

Scanning electron microscopy (SEM). Mixed species biofilms were developed as described above, then washed, dried, fixed in ethanol and dried again, as described previously (Jang et al. 2016). The biofilm samples were coated with gold using a sputter-coater (IB-3, Eiko, Tokyo, Japan) and then observed at 10 kV under a scanning electron microscope (Model S-4700; Hitachi High Technologies America. Inc., Pleasanton, CA, USA).

Results and Discussion

PolyP3 effectively inhibits the major oral pathogenic bacteria. It has been reported that polyP has antibacterial activity against various Gram-positive bacteria (such as *Staphylococcus aureus*, *Bacillus cereus*, *Listeria monocytogenes*, and mutans streptococci) at the concentrations between 0.1 and 0.5%, although it varies depending on the bacterial strain, inoculum density and culture medium (Post et al. 1963; Shibata and Morioka 1982; Zaika and Kim 1993; Lee et al. 1994). In the present study, the growth of a Gram-positive bacterium *S. gordonii* was not inhibited by polyP3 (up to 0.2%) on an agar plate (Fig. 1). Meanwhile, in liquid medium, the bacterial growth was slightly but significantly reduced by polyP3 in the range of 0.01–0.1%, and almost completely inhibited at concentrations ≥ 0.2% (Fig. 2). Compared to

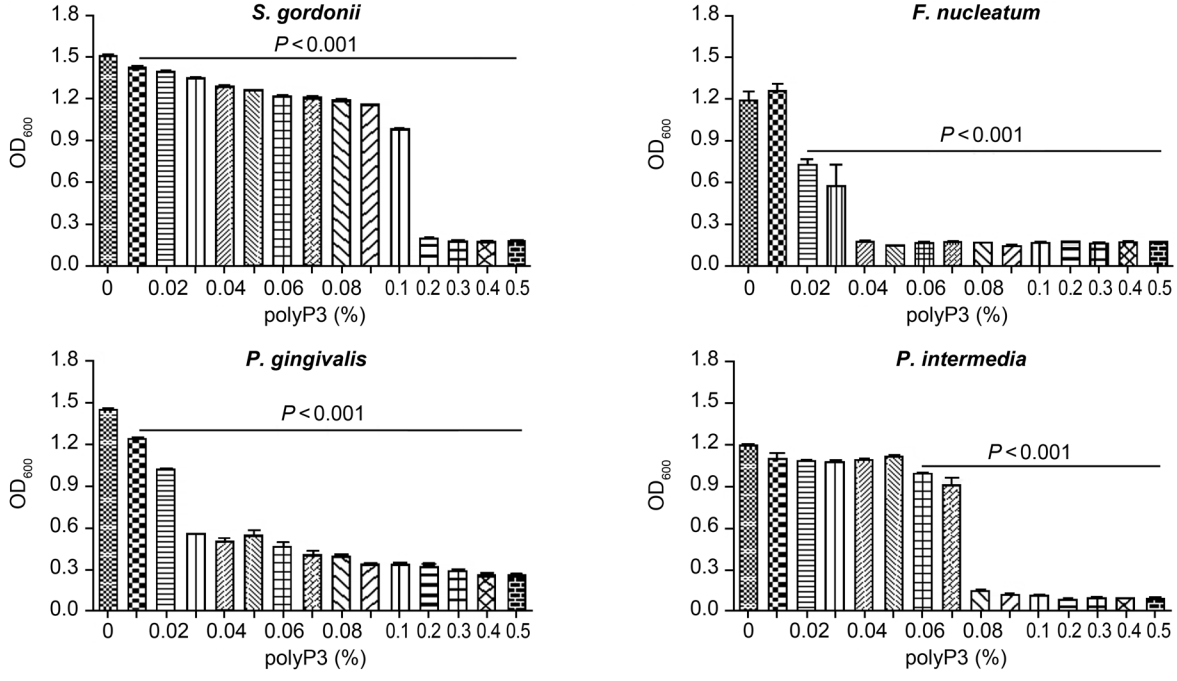

Fig. 2. Effect of polyP3 on the growth of the bacteria at a high inoculum density. Each bacterial strain cultured to exponential phase was adjusted to approximately 10^8 cells/ml in B-HK, then exposed to polyP3 at various concentrations. The bacterial growth was measured by reading optical density at 600 nm (OD_{600}) after the 24-hour incubation. Data are means ± SDs from two independent experiments performed in triplicate. One-way ANOVA with Tukey's post-hoc tests $p < 0.001$, versus control (0% polyP3).

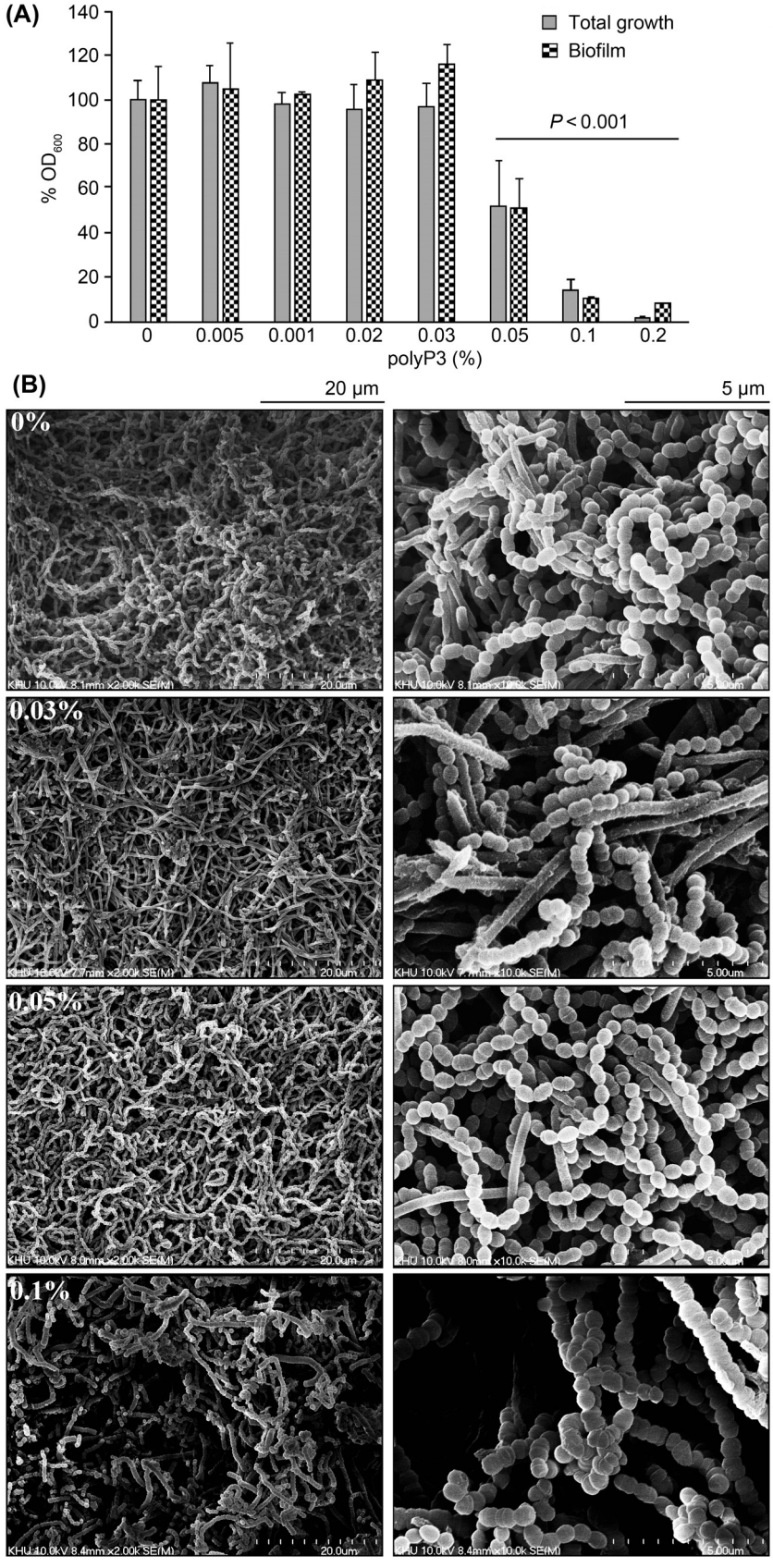

Fig. 3. Effect of polyP3 on the growth and biofilm formation of the four bacterial species in a mixed culture.

(A) To assess the total growth (planktonic and biofilm bacterial growth), the biofilm bacterial cells were dispersed, mixed thoroughly with planktonic bacterial cells, and OD_{600} of the suspension was measured. The suspension was diluted 2 to 10 times, and OD_{600} of the diluted suspension was also measured. The amount of biofilm formed by the mixed bacterial species was quantitated by crystal violet staining. Readings were expressed as mean $\%OD_{600}$ ($\%OD_{600} = OD_{600}/\text{mean } OD_{600}$ of control $\times 100$). One-way ANOVA with Tukey's post-hoc tests $p < 0.001$, versus control (0% polyP3). (B) SEM images of the biofilms at a magnification of 20 000 × (left) and 100 000 × (right).

S. gordonii, the three pathogenic bacteria: *F. nucleatum* ATCC 23726, *P. gingivalis* ATCC 53977, and *P. intermedia* ATCC49046 were more susceptible to polyP3. As shown in Fig. 1, the MICs of polyP3 against the bacteria were 0.1, 0.075 and 0.075 %, respectively, as determined by the agar dilution method. Notably, despite the bacterial inoculum concentration approximately 1000-fold higher than that used for the MIC determination, polyP3 still exerted a strong antibacterial activity in liquid medium (BH-K) (Fig. 2). The difference between the antibacterial effects of polyP3 observed in the agar and broth dilution methods is likely due to the fact that the MIC determined by the agar dilution method was the concentration at which the bacterial growth was completely inhibited bacteriostatically and/or bactericidally. MIC determined by agar dilution method is not affected by whether an antibacterial agent is bactericidal or bacteriostatic. In contrast, if the bacterial cells were killed by polyP3 in the liquid medium, they may have been lysed, lowering the OD_{600} values. It is also possible that the liquid medium enhanced the contact of polyP3 with individual bacterial cells, resulting in an excellent antimicrobial effect of polyP3 in the liquid medium.

PolyP3 selectively inhibits the major oral pathogenic bacteria in the mixed-culture. When the four bacterial species were co-cultured, the total growth, as well as the biofilm formation, was enhanced, probably due to their symbiotic relationship. As shown in Fig. 3A, the total growth and biofilm formation of the mixed species were significantly inhibited by polyP3 (≥0.05%). In the morphological analysis by SEM (Fig. 3B), the control biofilm (not exposed to polyP3) showed a multilayered structure consisting of spherical-shaped *S. gordonii*, spindle-shaped *F. nucleatum*, along with rod-shaped bacterial cells presumed to be *P. gingivalis* and *P. intermedia*. On the other hand, in the biofilms exposed to polyP3 (≥0.05%), spindle- and rod-shaped cells decreased. The biofilm exposed to 0.1% polyP3 was a simple structure composed of only streptococci, indicating that polyP3 still exerts stronger antimicrobial effects against the three Gram-negative pathogenic bacteria than *S. gordonii* in the mixed culture.

There are a vast number of U.S. patents for the use of polyP3 in oral care preparations. Although STPP has been included in oral care products for stain removal and brightening of the enamel, antibacterial effect of polyP3 apparently has not drawn the attention of the dentistry academy and the oral health industry. Here, we are inclined to emphasize the powerful potential of polyP3 with antibacterial activity, which is required for an ideal oral hygiene product. PolyP3 can be an effective antibacterial agent to control the major oral pathogenic bacteria *P. intermedia*, *P. gingivalis*, and *F. nucleatum*. The ability of polyP3 to selectively inhibit pathogens and maintain the proportion of commensal bacteria may be effective in preventing oral diseases caused by these pathogenic bacteria.

ORCID
Ji-Hoi Moon 0000-0003-0286-5297

Acknowledgements
This research was supported by the National Research Foundation of Korea (NRF) funded by the Ministry of Science & ICT (NRF-2016R1D1A1B03932450 and NRF-2018R1A2B6002173).

Conflict of interest
The authors do not report any financial or personal connections with other persons or organizations, which might negatively affect the contents of this publication and/or claim authorship rights to this publication.

Literature

CLSI. Methods for antimicrobial susceptibility testing of anaerobic bacteria approved standard. 7th ed. Document M11-A7. Wayne (PA): Clinical and Laboratory Standards Institute; 2007.

Ellinger RH. Phosphates as food ingredients. Cleveland (OH): CRC Press; 1972. p. 3–14.

Hajishengallis G. Periodontitis: from microbial immune subversion to systemic inflammation. Nat Rev Immunol. 2015 Jan;15(1): 30–44. doi:10.1038/nri3785 Medline

Han YW. *Fusobacterium nucleatum*: a commensal-turned pathogen. Curr Opin Microbiol. 2015 Feb;23:141–147. doi:10.1016/j.mib.2014.11.013 Medline

How KY, Song KP, Chan KG. *Porphyromonas gingivalis*: an overview of periodontopathic pathogen below the gum line. Front Microbiol. 2016 Feb 09;7:53. doi:10.3389/fmicb.2016.00053 Medline

Jang EY, Kim M, Noh MH, Moon JH, Lee JY. *In vitro* effects of polyphosphate against *Prevotella intermedia* in planktonic phase and biofilm. Antimicrob Agents Chemother. 2016 Feb;60(2):818–826. doi:10.1128/AAC.01861-15 Medline

Khan SA, Kong EF, Meiller TF, Jabra-Rizk MA. Periodontal diseases: bug induced, host promoted. PLoS Pathog. 2015 Jul 30; 11(7):e1004952. doi:10.1371/journal.ppat.1004952 Medline

Knabel SJ, Walker HW, Hartman PA. Inhibition of *Aspergillus flavus* and selected gram-positive bacteria by chelation of essential metal cations by polyphosphates. J Food Prot. 1991 May;54(5):360–365. doi:10.4315/0362-028X-54.5.360

Kornberg A, Rao NN, Ault-Riché D. Inorganic polyphosphate: a molecule of many functions. Annu Rev Biochem. 1999 Jun;68(1): 89–125. doi:10.1146/annurev.biochem.68.1.89 Medline

Kreth J, Merritt J, Qi F. Bacterial and host interactions of oral streptococci. DNA Cell Biol. 2009 Aug;28(8):397–403. doi:10.1089/dna.2009.0868 Medline

Lee RM, Hartman PA, Olson DG, Williams FD. Bactericidal and bacteriolytic effects of selected food-grade phosphates, using *Staphylococcus aureus* as a model system. J Food Prot. 1994 Apr; 57(4):276–283. doi:10.4315/0362-028X-57.4.276

Liu B, Faller LL, Klitgord N, Mazumdar V, Ghodsi M, Sommer DD, Gibbons TR, Treangen TJ, Chang YC, Li S, et al. Deep sequencing of the oral microbiome reveals signatures of periodontal disease. PLoS One. 2012 Jun 4;7(6):e37919. doi:10.1371/journal.pone.0037919 Medline

Moon JH, Jang EY, Shim KS, Lee JY. *In vitro* effects of *N*-acetyl cysteine alone and in combination with antibiotics on *Prevotella intermedia.* J Microbiol. 2015 May;53(5):321–329. doi:10.1007/s12275-015-4500-2 Medline

Moon JH, Kim C, Lee HS, Kim SW, Lee JY. Antibacterial and antibiofilm effects of iron chelators against *Prevotella intermedia.* J Med Microbiol. 2013 Sep 01;62(Pt_9):1307–1316. doi:10.1099/jmm.0.053553-0 Medline

Moon JH, Park JH, Lee JY. Antibacterial action of polyphosphate on *Porphyromonas gingivalis.* Antimicrob Agents Chemother. 2011 Feb;55(2):806–812. doi:10.1128/AAC.01014-10 Medline

Patini R, Staderini E, Lajolo C, Lopetuso L, Mohammed H, Rimondini L, Rocchetti V, Franceschi F, Cordaro M, Gallenzi P. Relationship between oral microbiota and periodontal disease: a systematic review. Eur Rev Med Pharmacol Sci. 2018 Sep;22(18): 5775–5788. Medline

Post FJ, Krishnamurty GB, Flanagan MD. Influence of sodium hexametaphosphate on selected bacteria. Appl Microbiol. 1963 Sep; 11: 430–435. Medline

Schaudinn C, Gorur A, Keller D, Sedghizadeh PP, Costerton JW. Periodontitis: an archetypical biofilm disease. J Am Dent Assoc. 2009 Aug;140(8):978–986. doi:10.14219/jada.archive.2009.0307 Medline

Shibata H, Morioka T. Antibacterial action of condensed phosphates on the bacterium *Streptococcus mutans* and experimental caries in the hamster. Arch Oral Biol. 1982;27(10):809–816. doi:10.1016/0003-9969(82)90034-6 Medline

Stacy A, Fleming D, Lamont RJ, Rumbaugh KP, Whiteley M. A commensal bacterium promotes virulence of an opportunistic pathogen *via* cross-respiration. MBio. 2016 Jul 06;7(3):e00782-16. doi:10.1128/mBio.00782-16 Medline

Sundus H, Mukhtar H, Nawaz A. Industrial applications and production sources of serine alkaline proteases: A review. J Bacteriol Mycol Open Acces. 2016;3:191–194.

Suprith S, Setty S, Bhat K, Thakur S. Serotypes of *Aggregatibacter actinomycetemcomitans* in relation to periodontal status and assessment of leukotoxin in periodontal disease: A clinico-microbiological study. J Indian Soc Periodontol. 2018;22(3):201–208. doi:10.4103/jisp.jisp_36_18 Medline

Tanner ACR, Izard J. *Tannerella forsythia*, a periodontal pathogen entering the genomic era. Periodontol 2000. 2006 Oct;42(1):88–113. doi:10.1111/j.1600-0757.2006.00184.x Medline

Torkko H, Asikainen S. Occurrence of *Porphyromonas gingivalis* with *Prevotella intermedia* in periodontal samples. FEMS Immunol Med Microbiol. 1993 Mar;6(2-3):195–198. doi:10.1111/j.1574-695X.1993.tb00325.x Medline

Willems HME, Xu Z, Peters BM. Polymicrobial biofilm studies: from basic science to biofilm control. Curr Oral Health Rep. 2016 Mar;3(1):36–44. doi:10.1007/s40496-016-0078-y Medline

Zaika LL, Kim AH. Effect of sodium polyphosphates on growth of *Listeria monocytogenes.* J Food Prot. 1993 Jul;56(7):577–580. doi:10.4315/0362-028X-56.7.577

Polish Journal of Microbiology
2019, Vol. 68, No 2, 269–280
https://doi.org/10.33073/pjm-2019-030

ORIGINAL PAPER

The Joint Effect of pH Gradient and Glucose Feeding on the Growth Kinetics of *Lactococcus lactis* CECT 539 in Glucose-Limited Fed-Batch Cultures

MÓNICA COSTAS MALVIDO[1], ELISA ALONSO GONZÁLEZ[1], RICARDO J. BENDAÑA JÁCOME[2] and NELSON PÉREZ GUERRA[1*]

[1] Department of Analytical and Food Chemistry. Food Science and Technology Faculty, University of Vigo, Ourense Campus, Ourense, Spain
[2] Department of Engineering, Materials, Structural Mechanics and Construction, Food Science and Technology Faculty, University of Vigo, Ourense Campus, Ourense, Spain

Submitted 24 February 2019, revised 10 April 2019, accepted 25 April 2019

Abstract

Two glucose-limited realkalized fed-batch cultures of *Lactococcus lactis* CECT 539 were carried out in a diluted whey medium (DW) using two different feeding media. The cultures were fed a mixture of a 400 g/l concentrated lactose and a concentrated mussel processing waste (CMPW, 101.72 g glucose/l) medium (fermentation I) or a CMPW medium supplemented with glucose and KH_2PO_4 up to concentrations of 400 g glucose/l and 3.21 g total phosphorus/l, respectively (fermentation II). For an accurate description and a better understanding of the kinetics of both cultures, the growth and product formation by *L. lactis* CECT 539 were both modelled, for the first time, as a function of the amounts of glucose (*G*) added and the pH gradient (*VpH*) generated in every realkalization and feeding cycle, by using an empirical polynomial model. With this modeling procedure, the kinetics of biomass, viable cell counts, nisin, lactic acid, acetic acid and butane-2,3-diol production in both cultures were successfully described (R^2 values >0.970) and interpreted for the first time. In addition, the optimum *VpH* and *G* values for each product were accurately calculated in the two realkalized fed-batch cultures. This approach appears to be useful for designing feeding strategies to enhance the productions of biomass, bacteriocin, and metabolites by the nisin-producing strain in wastes from the food industry.

Key words: fed-batch fermentation, empirical modeling, probiotic biomass, nisin, glucose-limited cultures

Introduction

In recent years, there has been an increasing interest in using probiotic cultures from lactic acid bacteria (LAB) as additives in animal feed to prevent or treat diseases (Alvarez-Olmos and Oberhelman 2001) and enhance the production results, e.g. weight gain and feed conversion efficiency (Guerra et al. 2007a).

For a successful application in animal feed, the probiotic cultures should contain a high concentration of viable cells, bacteriocins and fermentation metabolites to control the growth of pathogenic bacteria in both the animal feed and gut of the animals (Guerra et al. 2007a; Costas et al. 2018). Three alternatives for this purpose are: i) the use of cheaper fermentation and feeding media (like wastes from the food industry), ii) the selection of an appropriate strain, and iii) the design of an adequate fermentation procedure.

Whey (a waste from the cheese-making process) and mussel processing wastes (MPW) contain lactose in the relatively high concentration (~ 50 g/l in case of whey), glycogen (~ 10 g/l in case of MPW), proteins (~ 5.0 g/l in case of whey and 3.5 g/l in case of MPW), as well as micronutrients, including amino acids, vitamins and minerals (Murado et al. 1994; Costas et al. 2018). For these reasons, both substrates have been used for productions of probiotic biomass (Costas et al. 2018) and bacteriocins (Garsa et al. 2014; Costas et al. 2018) by different LAB.

The comparison of the antibacterial activity of 38 bacteriocin-producing LAB (including *Lactococcus*, *Pediococcus*, *Lactobacillus*, and *Leuconostoc* strains)

* Corresponding author: N. Pérez Guerra, Department of Analytical and Food Chemistry, Food Science and Technology Faculty, University of Vigo. Ourense Campus, Ourense. Spain; **e-mail: nelsonpg@uvigo.es**

against a set of 19 indicator bacteria (including *Listeria*, *Enterococcus*, *Carnobacterium*, *Lactococcus*, *Lactobacillus*, and *Leuconostoc* strains) showed that the nisin produced by *L. lactis* CECT 539 was the most potent bacteriocin with the broadest antibacterial spectrum (Guerra and Pastrana 2002). In addition, previous studies showed that the strain CECT 539 has potential as a probiotic additive for animal feed (Guerra et al. 2007a), or as a food products' preservative to extend their shelf life (Guerra et al. 2005).

Considering that fed-batch fermentation allows obtaining cultures with a high concentration of viable cells (Cho et al. 2010; Costas et al. 2018), the use of this fermentation technique for production of highly concentrated probiotic cultures on whey and MPW could be very advantageous. With this approach, the high mean chemical oxygen demand of these wastes, about 70 g/l in case of whey (Slavov 2017) and 25 g/l in case of MPW (Murado et al. 1994), and consequently their contamination effects could be considerably reduced.

Previous studies showed that the growth and nisin synthesis by LAB in realkalized fed-batch cultures depend on the stepwise pH profiles generated in the cultures, due to i) the effect of pH on nutrient uptake, ii) the inhibitory effect of low pH values on biomass and product formation, and iii) the specific effect of pH on bacteriocin synthesis (Cabo et al. 2001; Costas et al. 2018). Then, the use of an adequate mathematical model describing the joint effect of the culture pH and nutrient (glucose) addition on the productions of biomass, nisin and fermentation products could provide a better understanding for controlling and optimizing the fermentation process.

However, to our knowledge, no information is available on the quantification of the joint effect of glucose addition with the feeding media and the pH gradients (*VpH*) generated in the cultures on the synthesis of biomass, nisin, lactic acid, acetic acid and butane-2,3-diol by *L. lactis* strains.

For these reasons, in the present study, a first glucose-limited realkalized fed-batch culture in DW medium was designed by using a medium prepared with mussel processing wastes (CMPW) and a 400 g/l concentrated lactose (CL) as feeding media. From the results obtained in this culture, the effects of glucose addition and *VpH* on biomass and product synthesis by *L. lactis* CECT 539 were quantified, for the first time, by using empirical modeling. To validate the effectiveness of this modeling procedure, a second glucose-limited realkalized fed-batch culture in DW medium was carried out by using the CMPW medium supplemented with glucose and KH_2PO_4 up to concentrations of 400 g glucose/l and 3.21 g total phosphorus/l as feeding medium.

Experimental

Materials and Methods

Bacterial strains and culture media. The LAB strains used in this study were selected as the best nisin producer (*Lactococcus lactis* CECT 539) and the most nisin-sensitive bacterium (*Carnobacterium piscicola* CECT 4020) in a previous study (Guerra and Pastrana 2002). Both strains were obtained from the Spanish Type Culture Collection (CECT, Valencia, Spain). Working cultures of both strains were grown on MRS as agar slants.

The culture media used in this study (Table I) were prepared with diluted whey (DW) and a concentrated mussel processing waste (CMPW) obtained from local dairy and mussel processing plants, respectively. The pretreatment of both substrates was described by Costas et al. (2018).

Inoculum preparation and fermentation conditions. A loop of cells of *L. lactis* CECT 539 from a 1-day old MRS slant was used to inoculate 10 ml of MRS broth, which was incubated at 30°C and 200 rpm for 12 h. Subsequently, 1 ml of this pre-inoculum was transferred aseptically to a 250 ml Erlenmeyer flask containing 50 ml of DW medium and incubated at 30°C/12 h (200 rpm). An aliquot of this culture (containing 7.4×10^9 CFU/ml) was used as the inoculum for the realkalized fed-batch fermentations to obtain an initial viable cell count of 1.5×10^9 CFU/ml (0.03 g of cell dry weight/ml) in the fermentation medium (Costas et al. 2018).

The two fixed-volume realkalized fed-batch fermentations (cultures I and II) were carried out in duplicate in a 6-l bench-top fermenter (New Brunswick Scientific, Edison, NJ, USA) containing 4 l of sterilized DW medium (pH 7.0), at 30°C, 200 rpm and with an aera-

Table I
Mean composition (g/l) of the substrates used as culture media.

Nutrient	DW medium	CMPW medium	CMPWGP medium
Lactose	22.62±0.05	–	–
Glucose	–	101.72±0.17	400.00±0.01
Total nitrogen	0.433±0.02	0.540±0.01	0.431±0.02
Total phosphorus	0.227±0.02	0.060±0.00	3.210±0.06
Proteins	2.07±0.01	3.47±0.03	2.75±0.02

tion level of 0.5 l/h. The first culture was fed a mixture of CMPW medium and 400 g/l concentrated lactose (CL), and the second fermentation was fed a CMPW medium supplemented with glucose and KH_2PO_4 up to concentrations of 400 g glucose/l and 3.21 g total phosphorus/l (CMPWGP medium) and sterile distilled water (if needed). In the two realkalized fed-batch cultures the feeding media were used to bring the cultures up to the initial total sugars (TS) concentration (22.62 g/l) in the fermentation medium in every realkalization and feeding cycle.

However, the CMPW medium has a mean total sugars concentration (101.72 g/l) considerably lower than that (400 g/l) of the CL substrate and a total phosphorus (TP) concentration (0.060 g/l) lower than that (0.227 g/l) of the fermentation medium (Table I). Therefore, the use of the unsupplemented CMPW medium as the unique substrate to feed the growing culture has two drawbacks. First, high volumes of the feeding substrate could be necessary to replenish the initial TS levels in the culture medium in every realkalization and feeding cycle, increasing considerably the volume of fermentation medium and provoking the dilution of the culture. Second, the use of CMPW medium jointly with the sample extraction every 12 h, could lead to the exhaustion of the phosphorus source in the fermentation medium, thus limiting the growth of *L. lactis* CECT 539 (Costas et al. 2018).

For these reasons, the CMPW medium was firstly supplemented with KH_2PO_4 up to 3.21 g TP/l to obtain the same C/TP relationship (31.7) as in the MRS medium, because this salt was found to be the best TP source for nisin synthesis (De Vuyst and Vandamme 1993). Then, the medium was supplemented with glucose up to a concentration of 400 g/l.

Samples were taken from the culture medium in the corresponding fermenter every 12 h and divided into three aliquots to measure the viable cell counts (first aliquot), the culture pH and concentrations of biomass, nutrients and fermentation products (second aliquot), and also the nisin activity (third aliquot).

Realkalization and feeding procedure. After determining the TS concentration in the samples withdrawn at every sampling time (12 h), the fermentation medium was realkalized up to the initial pH of 7.0 with a volume of 5 N NaOH (V_{NaOH}) to generate different pH gradients. Then, the volumes of feeding substrates (*VFS*) needed to bring the culture up to the initial TS concentration (22.62 g/l) in each culture were calculated by developing the corresponding mass balance equations, as indicated below.

The volume of fermentation medium (*VFM*) in the two fed-batch fermentations was kept constant ($(dVFM/dt) = 0$) by matching the volumes added to the fermenter ($VFS_{tn} + VNaOH_{tn}$) with the sampling volume (VS_{tn}):

$$VS_{tn} = VFS_{tn} + VNaOH_{tn} = (VCMPW_{tn} + VCL_{tn}) + \\ + VNaOH_{tn} \quad \text{(for fermentation I)} \qquad [1.1]$$

$$VS_{tn} = VFS_{tn} + VNaOH_{tn} = (VCMPWGPt_{n} + VdW_{tn}) + \\ + VNaOH_{tn} \quad \text{(for fermentation II)} \qquad [1.2]$$

Where $VNaOH_{tn}$, $VCMPW_{tn}$, VCL_{tn}, $VCMPWGP_{tn}$ and VdW_{tn} are respectively, the volumes (in l) of 5 N NaOH, CMPW medium, concentrated lactose (CL), CMPWGP medium and distilled water added to the fermenter at the beginning of every realkalization and feeding cycle.

From equations [1.1] and [1.2] it follows that:

$$VCMPW_{tn} = VS_{tn} - VNaOH_{tn} - VCL_{tn} \\ \text{(for fermentation I)} \qquad [2.1]$$

$$VCMPWGP_{tn} = VS_{tn} - VNaOH_{tn} - VdW_{tn} \\ \text{for fermentation II)} \qquad [2.2]$$

The reduction in the mass (in grams) of TS in the medium due to the joint effect of the extraction of samples and TS consumption by the growing strain (TS_{E+C}) was calculated by applying a mass balance equation for the total sugars in the fermenter:

$$TS_{E+C} = V \cdot [TS]_{tn} - (V - VS_{tn}) \cdot [TS]_{tn+1} \qquad [3]$$

Where $[TS]_{tn}$ and $[TS]_{tn+1}$ are the total sugars concentration (in g/l) at the beginning and at the end of every feeding cycle. The difference ($V–VS_{tn}$) represents the remaining volume (l) in the fermenter after the extraction of samples.

Therefore, the mass of TS (in grams) that must be added to the fermenter to restore the initial TS concentration in the DW medium was calculated by the following expressions:

$$VCMPW \cdot [TS_{CMPW}] + VCL \cdot [TS_{CL}] = TS_{E+C} \\ \text{(for fermentation I)} \qquad [4.1]$$

$$VCMPWGP \cdot [TS_{CMPWGP}] = TS_{E+C} \\ \text{(for fermentation II)} \qquad [4.2]$$

Where $[TS_{CMPW}]$, $[TS_{CL}]$ and $[TS_{CMPWGP}]$ are the total sugars concentration in the CMPW, CL and CMPWGP media, respectively.

Substituting Eq. [2.1] into Eq. [4.1] gives:

$$(VS_{tn} + VNaOH_{tn} - VCL_{tn}) \cdot [TS_{CMPW}] + \\ + VCL_{tn} \cdot [TS_{CL}] = TS_{E+C} \\ \text{(for fermentation I)} \qquad [5.1]$$

Thus, the V_{CL} was calculated as:

$$VCL_{tn} = \frac{(TS_{E+C} - VS_{tn} \cdot [TS_{CMPW}] + VNaOH_{tn} \cdot [TS_{CMPW}])}{([TS_{CL}] - [TS_{CMPW}])} \qquad [6.1]$$

The *VCMPW* was obtained by introducing the values of *VCL* and *VNaOH* into Eq. [2.1].

The $VCMPWGP_{tn}$ in fermentation II was obtained by rearranging Eq. [4.2]:

$$VCMPWGP_{tn} = \frac{TS_{E+C}}{[TS_{CMPWGP}]} \quad [6.2]$$

The *VdW* was obtained by introducing the values of *VCMPWGP* and *VNaOH* into Eq. [2.2].

These sampling, feeding, and realkalization procedures were repeated every 12 h in all the cultures.

Viable cell counts. The first aliquot of culture medium was used to count the total viable cells [VCC, as colony forming units (CFU)/ml] by plating serial dilutions of this aliquot (in triplicate) onto MRS agar and incubation at 30°C for 48 h (Costas et al. 2018).

Biomass, nutrients and fermentation products. Triplicate equivolume subaliquots from the second aliquot of the culture medium were centrifuged (12 000 × g for 15 min at 4°C) and after separation of the supernatants, the sedimented cells were washed with saline (0.8% (w/v) NaCl) and centrifuged (12 000 × g for 15 min at 4°C) two times. The rinsed cells were again resuspended in saline to measure the optical density at 700 nm of the three subaliquots using the sterile saline as a blank. Then, the biomass concentration (X, as g dry cell weight/l) was determined from a standard curve (Costas et al. 2018). The supernatants were used to measure the culture pH and the concentrations of nutrients (total sugars, nitrogen, phosphorus, protein, glucose and lactose) and fermentation products (lactic acid, acetic acid and butane-2,3-diol).

The concentration of total sugars was measured using the phenol/sulfuric acid method (Dubois et al. 1956) according to Strickland and Parsons (1968a), with glucose (at concentrations between 12.5–125.0 µg/ml) as standard. Total nitrogen was quantified by the micro-Kjeldahl method, replacing distillation by the spectrophotometric method of Havilah et al. (1977), with ammonium sulfate (at concentrations between 12.5–500.0 mg/l) as standard. Total phosphorus was determined by the molybdate reaction (Murphy and Riley 1962) according to Strickland and Parsons (1968b), with KH_2PO_4 (at concentrations between 0.2–2.0 mg/l) as standard. Protein was measured by the method of Lowry et al. (1951), with bovine serum albumin (at concentrations between 0.05–0.50 g/l) as standard.

Concentrations of glucose (G), lactose (L), lactic acid (LA), acetic acid (AA) and butane-2,3-diol (B) were quantified by a high-performance liquid chromatography (HPLC) system equipped with an ION-300 Organic Acids column (length 300 mm, internal diameter 7.8 mm) with a precolumn IONGUARD™ (polymeric guard column), both obtained from Tecknokroma S. Coop. C. Ltda, Barcelona, Spain. Sugars and fermentation products were separated at 60–65°C using a 0.012 N sulfuric acid aqueous mobile phase flowing at 0.4 ml/min and detected using a refractometer with a refractive index detector. Solutions of glucose, lactose, lactic acid, acetic acid and butane-2,3-diol at a concentration between 0.5 and 10.0 g/l were used as standards. Prior to HPLC analysis, all samples and standards were filtered using syringe filters (0.22-µm pore size, 25-mm diameter disk filters, Membrane Solutions, Dallas, TX, USA) (Costas et al. 2018). All the analytical determinations were performed in triplicate.

Nisin. Triplicate samples of the third aliquot of the culture samples were adjusted to pH 3.5 with 5 N HCl to prevent the adsorption of molecules of bacteriocin onto the producer cell surfaces, heat-treated in a boiler water bath for 3 min to kill the cells and centrifuged (27 200 × g for 15 min at 4°C). The antibacterial activity of the cell-free supernatants (CFS) adjusted at pH 6.0 was determined by a photometric bioassay method (Cabo et al. 2001) using *C. piscicola* CECT 4020 as indicator strain (Costas et al. 2018). Nisin activity (Nis) was expressed as bacteriocin units (BU) per ml CFS, being one BU/ml defined as the inverse of the dilution of CFS causing 50% growth inhibition of the target strain compared with control tubes (Murado et al. 2002).

Statistical analyses. The effects of the pH gradients (*VpH*) generated in the culture and the addition of glucose (*G*) with the feeding with CMPW or CMPWGP media on the synthesis of biomass, viable cells and products (Nis, LA, AA and B) in every realkalization and feeding cycle in the two realkalized fed-batch cultures were described with a second-order polynomial model [7]:

$$Ps = A_1 + A_2 \cdot VpH + A_3 \cdot VpH^2 + A_4 \cdot G + A_5 \cdot G^2 + \\ + A_6 \cdot VpH \cdot G \quad [7]$$

Where *Ps* represents the levels of X, VCC, Nis, LA, AA or B synthesized in every realkalization and feeding cycle. A_1, A_2, A_3, A_4, A_5, and A_6 are constants.

The corresponding values for the constants and their standard errors were obtained by using the nonlinear curve-fitting software of the SigmaPlot program, version 12.0 (Systat Software Inc., 2012). The coefficients of the models were considered statistically significant if their *p* values were lower than 0.05.

The goodness-of-fit of model [7] for each product was evaluated by analyzing the determination coefficient (R^2) and the mean relative percentage deviation modulus (*RPDM*) (Guerra et al. 2007b):

$$RPDM = \frac{100}{n} \sum_{i=1}^{n} \frac{|P_t - cP_t|}{P_t} \quad [8]$$

Where P_t and cP_t are respectively, the experimental and calculated X, VCC, Nis, LA, AA or B concentrations (with model [7]) and *n* is the number of experimental data points. *RPDM* values < 10% and R^2 values

> 0.95 indicate a good fit for practical purposes (Guerra et al. 2007b).

The experimental concentrations of X, VCC, Nis, LA, AA or B synthesized (Ps_t) in every realkalization and feeding cycle were calculated as follows:

$$Ps_t = P_t - P_{t-12\text{h}} \cdot \frac{(VFM - VS_{t-12\text{h}})}{VFM} \quad [9]$$

Where $P_{t\text{-}12\text{h}}$ and P_t are the experimental concentrations of biomass or products at the beginning and at the end of every realkalization and feeding cycle, respectively.

Subsequently, the calculated X, VCC, Nis, LA, AA or B concentrations at the end of every realkalization and feeding cycle (cP_t) were obtained as:

$$cP_t = cPs_t + cPs_{t-12\text{h}} \cdot \frac{(VFM - VS_{t-12\text{h}})}{VFM} \quad [10]$$

Where $cPs_{t\text{-}12\text{h}}$ and cPs_t are respectively, the X, VCC, Nis, LA, AA or B concentrations at the beginning and at the end of every realkalization and feeding cycle calculated with model [7].

The differences between the predictions of model [7] and experimental data were minimized according to the sum of squares of errors (*SSE*) of the model fit:

$$SSE = \sum_{i=1}^{n} \sum_{j=1}^{m} \left(P_t - cP_t\right)^2 \quad [11]$$

Where *m* represents the number of variables. Other terms are as previously described.

Results and Discussion

Growth kinetics of *L. lactis* CECT 539 in the realkalized fed-batch cultures. The evolution of the culture variables (pH and concentrations of nutrients: glucose, lactose, proteins, total nitrogen, and phosphorus) in the cultures I and II are shown in Figures 1 and 2, respectively. Although the pH gradients decreased progressively in both cultures, *L. lactis* CECT 539 did not lose completely its capacity to recover the acidic pH at the end of fermentation. In both cultures, glucose was completely consumed in every realkalization and feeding cycle, but relatively high concentrations of lactose remained in the media (Figs. 1 and 2). The proteins and total nitrogen and phosphorus were consumed in parallel with the production of biomass, but the complete exhaustion of these nutrients was not observed in the cultures (Figs. 1, 2 and 3).

The nisin-producing strain was grown in two growth cycles (Fig. 3) composed of two exponential growth phases, separated by an intermediate lag phase, as observed before in previously realkalized fed-batch cultures in DW medium (Guerra et al. 2007b; Costas et al. 2016, 2018).

Since *L. lactis* CECT 539 exhibited a diauxic growth in a batch culture in DW medium supplemented with glucose (Costas et al. 2016), it could be logical to suppose that the nisin-producing strain presented two growth phases within every realkalization and feeding cycle of 12 h in the realkalized fed-batch cultures I and II. However, the diauxic growth pattern observed in both cultures would not be related with the use of glucose- and lactose-containing substrates (culture I) or with a glucose-containing substrate (culture II), as feeding media. This is mainly because the feeding media were added at the beginning of every realkalization and feeding cycle to bring the culture up to the initial total sugars concentration (22.62 g/l) of the fermentation (DW) medium (Guerra et al. 2007b; Costas et al. 2016, 2018), and the experimental X concentrations were obtained at the end of every cycle (Figs. 1, 2 and 3).

The TN and TP concentrations decreased progressively in the first culture as a consequence of their consumption by the nisin-producing strain and the sample collection every 12 h. However, in the second fermentation, the growth slowed down at 144 h of incubation, even though the culture was fed with a substrate (CMPWGP) containing a relatively high TP concentration (3.21 g/l) that produced an increase in the concentration of this nutrient in the fermentation medium (Fig. 2).

Thus, culture II was stopped at 168 h because the cells entered in the second stationary phase of growth after 144 h of incubation and, taking into account the profiles described by the variables X and Nis in fermentation I (left side of Fig. 3), it is logical to consider that the extension of the fermentation would not produce significant increases in the concentration of both variables.

In addition, the TN source could be considered as a limiting substrate for the growth of *L. lactis* CECT 539 in fermentations I and II, rather than the two carbon (glucose and lactose) or TP sources. Thus, the nisin-producing strain probably grown first consuming the free amino acids and utilizable oligopeptides (Letort et al. 2002) present in the DW medium and/or the inorganic nitrogen (Guerra et al. 2007b) added with the feeding media (CMPW or CMPWGP). In the second exponential growth phase, the strain CECT 539 probably utilized the less preferred nitrogen sources, for example, the proteins present in both the DW and CMPW media (Murado et al. 1994; Letort et al. 2002).

Nisin production paralleled both the biomass production and pH gradients generated in the two cultures (Figs. 1, 2 and 3), because this metabolite was produced as a pH-dependent primary product in this kind of realkalized fed-batch fermentations (Cabo et al. 2001; Guerra et al. 2007b; Costas et al. 2016; 2018). Lactic acid

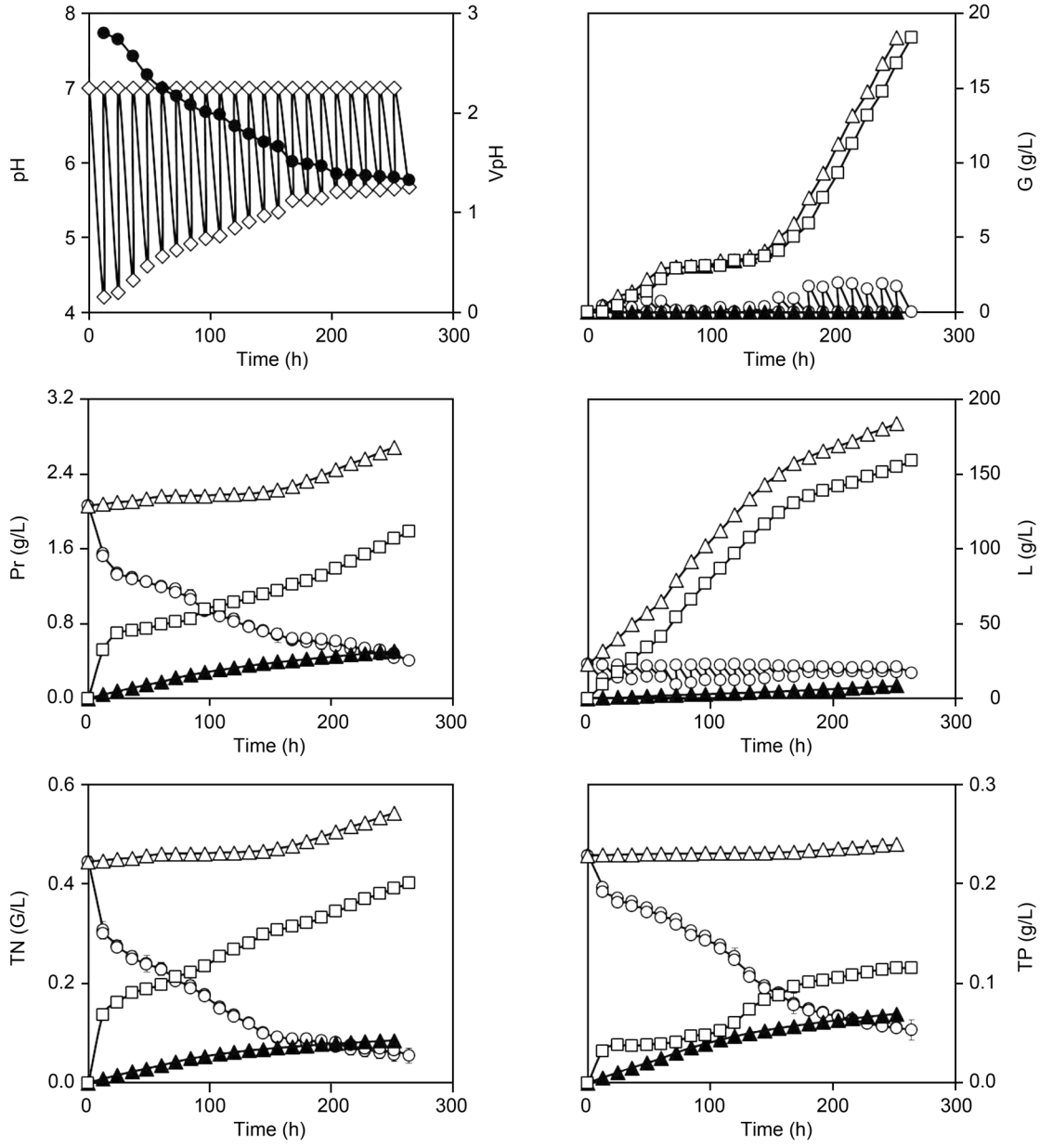

Fig. 1. Time course of the culture pH (◇), pH gradient (VpH, ●), and remaining (○), consumed (⊠), added (Δ) and extracted (▲) concentrations of glucose (G), lactose (L), proteins (Pr), total nitrogen (TN), and phosphorus (TP) in the realkalized fed-batch culture I. The data reported are means ± standard deviations of two repeated experiments and three replicate measurements.

was also synthesized in parallel with biomass synthesis in both cultures, but the productions of acetic acid and butane-2,3-diol triggered after 84 h of fermentation (left and right sides of Fig. 3).

Although the incubation times in fermentation I (264 h) and fermentation II (168 h) were different, the final levels of X, VCC, Nis and AA synthesized in the first culture (3.07 g/l, 1.75×10^{10} CFU/ml, 105.61 BU/ml, and 1.78 g/l, respectively) were almost similar ($p > 0.05$) to those (3.08 g/l, 1.75×10^{10} CFU/ml, 103.68 BU/ml, and 1.66 g/l, respectively) obtained in fermentation II. Only the LA and B concentrations in the first culture (16.98 and 4.96 g/l) were higher ($p < 0.05$) than those (13.62 and 2.24 g/l) obtained in fermentation II (Fig. 3).

This observation indicates that the CMPWGP medium can be used as an appropriate feeding substrate for the production of probiotic biomass and nisin. However, further studies based on optimizing its TP concentration are required to avoid the accumulation of this nutrient in the fermentation medium.

Empirical models obtained for biomass and product synthesis in the first fed-batch culture. Table II shows the statistically significant values obtained for the constants of model [7] for the dependent variables (X, VCC, Nis, LA, AA and B) in fermentation I. In all cases, *RPDM* values < 6 % and R^2 values > 0.994 were obtained, indicating that the fitted models described appropriately the trend observed for all the dependent variables in

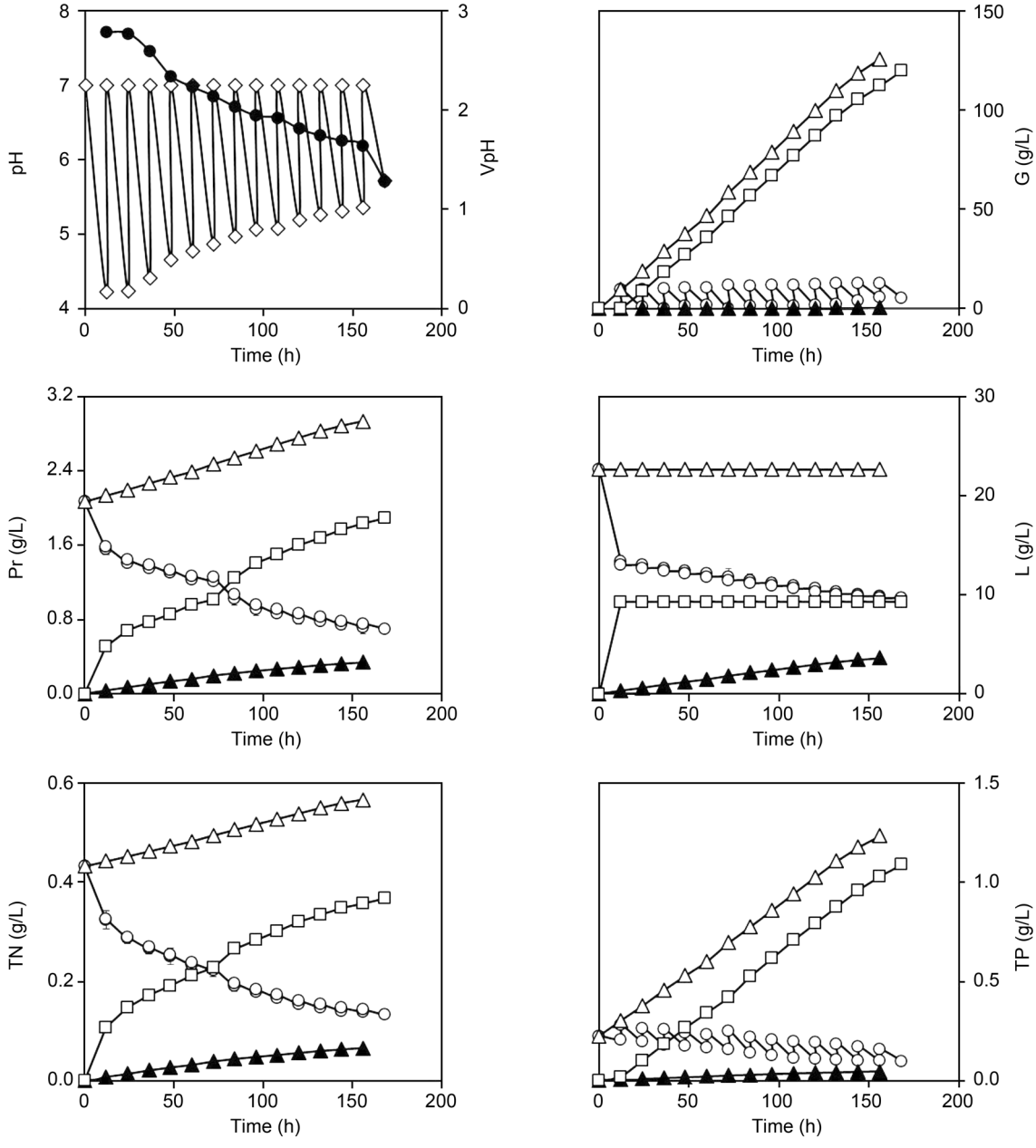

Fig. 2. Time course of the culture pH (◇), pH gradient (VpH, ●), and remaining (○), consumed (⊠), added (Δ) and extracted (▲) concentrations of glucose (G), lactose (L), proteins (Pr), total nitrogen (TN), and phosphorus (TP) in the realkalized fed-batch culture II. The data reported are means ± standard deviations of two repeated experiments and three replicate measurements.

response to the addition of glucose and the pH gradients generated in the culture. The fitted models obtained for each dependent variable are discussed below:

Biomass and viable cell counts. For both dependent variables (X and VCC), the values of the coefficients for the lineal (*VpH* and *G*) and quadratic (VpH^2 and G^2) terms had a negative and positive sign, respectively (Table II). However, while the coefficient of the binary interaction between *VpH* and *G* had a positive sign for X, it was not statistically significant for VCC.

From a mathematical point of view, these results indicate that X and VCC increased for *VpH* and *G* values lower and higher than the corresponding optimum values (*VpHopt* and *Gopt*) for both independent variables. However, from the results obtained in previous works (Cabo et al. 2001; Guerra et al. 2007b), it could be reasonable to consider the obtained optimum *VpH* values (1.81 for X and 1.92 for VCC) as the minimum pH gradient that allows the growth of *L. lactis* CECT 539 in the first culture. In fact, the corresponding maximum final pH values, 5.19 for X and 5.08 for VCC (*pHopt* = 7.0 – *VpHopt*), were slightly higher than that (pH = 4.86) observed in the previous batch cultures of the nisin-producing strain in DW medium (Guerra et al. 2007b). These maximum final pH values for the growth of *L. lactis* CECT 539 are lower than that (5.50)

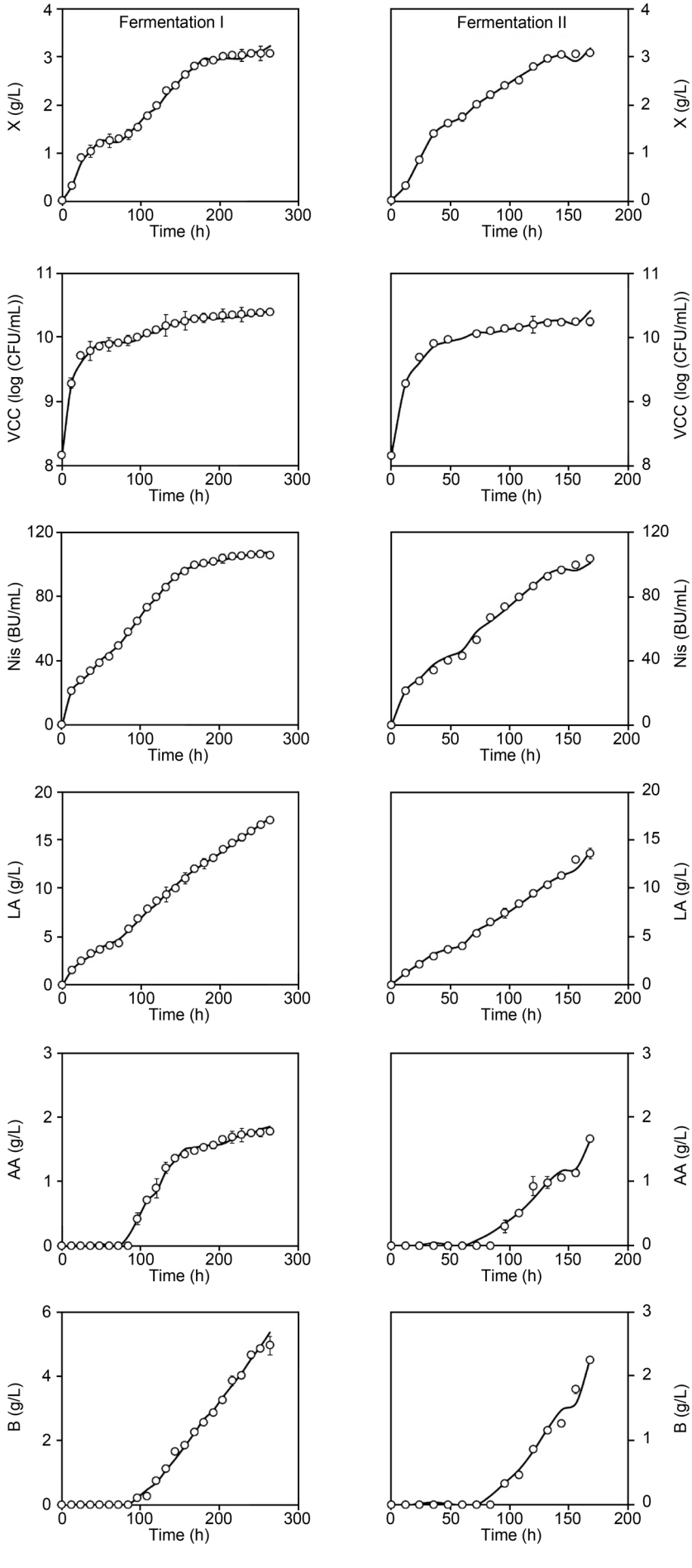

Fig. 3. Time course of the biomass (X), viable cell counts (VCC), nisin (Nis), lactic acid (LA), acetic acid (AA), and butane-2,3-diol (B) in the realkalized fed-batch cultures I (left side), and II (right side). The data reported are means ± standard deviations of two repeated experiments and three replicate measurements. The solid lines drawn through the experimental data for each variable were obtained according to the empirical model [7].

Table II
Significant values ($p < 0.05$) for the constants in model [7] for the different dependent variables in the first fed-batch culture.

Parameter	Biomass	Viable cell counts	Nisin	Lactic acid	Acetic acid	Butane-2,3-diol
A_1	4.12 ± 0.631	1.86 ± 0.084	1.13 ± 0.113	5.71 ± 0.235	1.16 ± 0.003	2.75 ± 0.277
A_2	−3.60 ± 0.545	−1.56 ± 0.072	8.67 ± 0.4244	−4.04 ± 0.225	−0.70 ± 0.012	−2.00 ± 0.265
A_3	0.83 ± 0.116	0.41 ± 0.015	−2.07 ± 0.206	0.88 ± 0.054	0.12 ± 0.005	0.37 ± 0.064
A_4	−1.09 ± 0.383	−0.15 ± 0.051	−9.25 ± 1.547	−0.92 ± 0.040	−0.46 ± 0.021	−0.19 ± 0.021
A_5	0.14 ± 0.062	0.03 ± 0.008	2.93 ± 0.314	0.26 ± 0.019	0.15 ± 0.011	0.03 ± 0.003
A_6	0.35 ± 0.168	NS	0.74 ± 0.203	NS	NS	NS
R^2	0.9950	0.9948	0.9993	0.9986	0.9949	0.9954
RPDM (%)	3.335	0.228	1.121	3.760	1.701	5.809
VpHopt	1.81	1.92	2.32	2.30	2.83	2.40
pHopt = 7.0 − *VpHopt*	5.19	5.08	4.68	4.70	4.17	4.60
Gopt (g/l)	1.64	2.72	1.29	1.76	1.41	2.80

observed for *L. lactis* ATCC 11454 in MRS broth (Penna and Moraes 2002).

The decrease in the bacterial growth at pH values lower than 5.19 or 5.08 could be related to a reduction in the metabolic activity of *L. lactis* CECT 539 probably caused by a limitation in micronutrients or nutrient transport (Poolman and Konings 1988).

Using the same argument as that used for the *VpHopt*, it can be also reasonable to consider the values of *Gopt* (1.59 g/l for X and 1.63 g/l for VCC) as the minimum concentrations of glucose that should be in the culture medium to stimulate the growth of *L. lactis* CECT 539.

Nisin. The statistically significant coefficient for the quadratic term VpH^2 with a negative sign indicates that the optimum *VpH* value (2.32) for maximum nisin production (Table II) is within the pH gradient range (from 2.80 to 1.33) generated in the first culture (Fig. 1). Thus, the calculated minimum final pH value (4.68) is in perfect agreement with the optimum final pH values (4.90 and 4.27) obtained for nisin synthesis in DW medium in batch and realkalized fed-batch cultures, respectively (Guerra et al. 2007b).

With regard to the addition of glucose, it can be noted that the *Gopt* value obtained (1.29 g/l) is the minimum value that favored bacteriocin production (Table II). Then, more addition of glucose in every realkalization and feeding cycle is needed to enhance nisin synthesis in fermentation I.

Lactic acid, acetic acid, and butane-2,3-diol. The signs of the lineal and quadratic terms in the empirical models obtained for these three metabolites were similar to those obtained for the dependent variables X and VCC. Thus, according to the predictions of model [7], the maximum final pH values for LA, AA and B productions were 4.70, 4.17 and 4.60, respectively.

Lactic acid production in the realkalized fed-batch culture I was minimal at final pH values between 4.62 and 4.83 (Fig. 2), which includes the maximum pH value (4.70) calculated from model [7]. Similarly, when the culture reached final pH values between 4.22 and 4.97 (12–84 h of incubation), the lowest AA and B productions were obtained, because, at these incubation times, the two fermentation metabolites had not been detected in the culture medium (Fig. 2). In fact, AA and B productions started when the culture reached a final pH value of 4.99 after 84 h of incubation (left side of Fig. 3).

In the same way, the minimum concentrations of glucose in the processes for high LA, AA and B production were 1.76, 1.41 and 2.80 g/l, respectively (Table II).

Validation of model [7]. The effectiveness of model [7] to describe the productions of biomass, bacteriocin and fermentation metabolites by *L. lactis* CECT 539 was validated by using the experimental data obtained from the second fed-batch culture. As can be observed, the empirical model [7] satisfactorily described the evolution of the dependent variables X, VCC, Nis, LA, AA and B (right side of Fig. 3), providing *RPDM* values < 4% and R^2 values > 0.979 (Table III). In addition, the maximum final pH values were similar (for X, VCC, LA and B) or almost similar (for AA) to the corresponding calculated values in the fed-batch culture I (see Tables I and II).

However, in the case of nisin synthesis, the optimum pH value calculated (4.88) could be considered as the maximum final pH value for high bacteriocin production in every realkalization and feeding cycle, since the value of the coefficient for VpH^2 had a positive sign. This indicates that nisin synthesis is favored in this type of fed-batch cultures in the pH range of 4.68 and 4.88, which is within the optimum pH range observed in previous studies for nisin production by *L. lactis* CECT 539 (Guerra et al. 2007b; Costas et al. 2016, 2018).

As shown in Table IV, the optimum final pH values for nisin production by other *Lactococcus* strains (e.g. *L. lactis* ATCC 11454 and ATCC 7962) were not always within the optimum final pH range calculated

Table III
Significant values ($p < 0.05$) for the constants in model [7] for the different dependent variables in the second fed-batch culture.

Parameter	Biomass	Viable cell counts	Nisin	Lactic acid	Acetic acid	Butane-2,3-diol
A_1	0.46 ± 0.043	0.58 ± 0.053	0.42 ± 0.040	10.19 ± 0.405	0.41 ± 0.032	0.23 ± 0.062
A_2	–3.32 ± 0.351	–1.75 ± 0.062	–27.69 ± 1.011	–8.10 ± 0.621	–2.19 ± 0.027	–3.15 ± 0.333
A_3	0.58 ± 0.059	0.45 ± 0.011	6.53 ± 0.462	1.79 ± 0.109	0.44 ± 0.024	0.63 ± 0.097
A_4	0.53 ± 0.038	0.26 ± 0.065	4.73 ± 0.516	–0.35 ± 0.017	0.42 ± 0.023	0.72 ± 0.065
A_5	–0.04 ± 0.005	–0.01 ± 0.003	–0.10 ± 0.013	0.03 ± 0.006	–0.02 ± 0.001	–0.04 ± 0.004
A_6	0.11 ± 0.006	NS	NS	NS	NS	NS
R^2	0.9973	0.9906	0.9950	0.9959	0.9794	0.9856
RPDM (%)	0.987	0.326	3.775	2.609	3.988	3.602
VpHopt	1.82	1.96	2.12	2.26	2.47	2.49
pHopt = 7.0 – *VpHopt*	5.18	5.04	4.88	4.74	4.53	4.51
Gopt (g/l)	10.55	11.10	22.83	5.30	11.17	10.27

Table IV
The optimal final culture pH values for different bacteriocins produced by lactic acid bacteria.

Bacteriocin	Producing strain	Optimum final pH	Culture medium	Reference
Mesenterocin 5	*Leuconostoc mesenteroides* UL5	4.24 to 4.34	Whey	Daba et al. 1993
Pediocin AcH	*Pediococcus acidilactici* LB42-923	3.70	TGE broth	Yang and Ray 1994
Nisin	*Lactococcus lactis* ATCC 11454	5.80	TGE broth	Yang and Ray 1994
Leuconocin Lcm1	*Leuconostoc carnosum* Lm1	5.00	TGE broth	Yang and Ray 1994
Sakacin A	*Lactobacillus sake* LB 706	4.50	TGE broth	Yang and Ray 1994
Nisin	*Lactococcus lactis* ATCC 7962	4.90	Whey permeate	Flôres and Alegre 2001
Carnocin KZ213	*Carnobacterium piscicola* 213	4.80 to 5.08	MRS broth	Khouiti and Simon 2004
Nisin	*Lactococcus lactis* ATCC 11454	4.60	MRS + milk	Penna et al. 2005
		4.80	M17 + milk	
Nisin	*Lactococcus lactis* ATCC 11454	4.65 to 4.96	Whey + YE (5 g/l)	Jozala et al. 2011

YE: yeast extract

for *L. lactis* CECT 539. In addition, other lactic acid bacteria, including the genera *Leuconostoc*, *Pediococcus*, *Lactobacillus*, and *Carnobacterium* produced the highest bacteriocin concentrations at final pH levels different to those observed for *L. lactis* strains. These results indicate that the effect of the final pH on the bacteriocin production depended on both the strain and culture medium used.

This different effect of the final pH values on the bacteriocin synthesis has been related with the need of an appropriate final pH range for the post-translational conversion of prebacteriocin to active bacteriocin (Yang and Ray 1994).

With regard to the glucose addition, it could be noted that with the exception of LA, the signs for the coefficients of G and G^2 terms in the models for the other dependent variables, had a positive and negative sign, respectively (Table III). Therefore, the calculated *Gopt* values are the maximum added glucose levels to obtain the maximum concentrations of X, VCC, Nis, AA and B. Therefore, with the use of a feeding medium (CMPWGP) with a concentration of glucose (400 g/l) higher than the CMPW medium (101.72 g/l), the amounts of glucose added to the growing culture in fermentation II were considerably higher than those added in fermentation I (Figs. 1 and 2). Thus, glucose levels higher than the calculated *Gopt* value in the second culture could produce substrate inhibition on the growth and product (Nis, AA and B) formation (Pongtharangkul and Demirci 2006; Costas et al. 2016, 2018) by *L. lactis* CECT 539. In addition, the inhibitory effect produced by higher levels of glucose on nisin production could be also related with the regulation that the carbon source produced on the synthesis or activity of prenisin-modifying enzymes (De Vuyst 1995).

These observations are consistent with the results obtained for the fed-batch production of nisin by *L. lactis* ATCC 11454 in a complex medium, with sucrose feeding at rates of 6, 7, 8, and 10 g/l/h (Lv et al. 2005). In this study, the growth was slightly affected by the different feeding rates, but the bacteriocin synthesis was different in the four cultures. Thus, the optimal

feeding rate for nisin production was 7 g/l/h, but the addition of sucrose at feeding rates of 8 and 10 g/l/h led to the accumulation of the carbon source in the culture medium during feeding that inhibited the bacteriocin synthesis. For a feeding rate of 6 g/l/h, the sucrose was almost completely consumed by the nisin-producing strain and its remaining level in the culture medium was close to zero in the period of feeding. This low sucrose availability limited the growth and bacteriocin production (Lv et al. 2005).

The results obtained with the use of model [7] are in perfect agreement with the affirmation that nisin is produced as a pH-dependent primary metabolite since its production depends on both the biomass synthesis and the final culture pH in the medium (Yang and Ray 1994; Guerra et al. 2007b). Thus, biomass production by *L. lactis* CECT 539 was favored at culture pH values above 5.0, but a final pH range of 4.68–4.88 was needed for high nisin synthesis.

Conclusions

From a practical point of view, the modeling procedure used in this work could allow: i) determining the optimum pH and glucose ranges to obtain high levels of biomass, nisin and fermentation metabolites in realkalized fed-batch cultures, ii) providing an accurate interpretation of the fermentation kinetics taking into account the effects of the amount of glucose added and the pH gradient generated in every realkalization and feeding cycle on the growth and product synthesis by *L. lactis* CECT 539 and, iii) design feeding strategies to produce highly concentrated probiotic products with high concentrations of viable cells and nisin.

ORCID
Nelson Pérez Guerra 0000-0002-8202-932X

Acknowledgements
This work was supported by the Research and Development Cluster for Agricultural and Food, Campus da Auga (CITACA), University of Vigo (Spain) and The Xunta de Galicia, Spain (project PGIDT00BIO1E).

Conflict of interest
The authors do not report any financial or personal connections with other persons or organizations, which might negatively affect the contents of this publication and/or claim authorship rights to this publication.

Literature

Alvarez-Olmos MI, Oberhelman RA. Probiotic agents and infectious diseases: a modern perspective on a traditional therapy. Clin Infect Dis. 2001 Jun 01;32(11):1567–1576. doi:10.1086/320518 Medline

Cabo ML, Murado MA, González M, Pastoriza L. Effects of aeration and pH gradient on nisin production: A mathematical model. Enzyme Microb Technol. 2001 Sep;29(4-5):264–273. doi:10.1016/S0141-0229(01)00378-7

Cho YH, Song JY, Kim KM, Kim MK, Lee IY, Kim SB, Kim HS, Han NS, Lee BH, Kim BS. Production of nattokinase by batch and fed-batch culture of *Bacillus subtilis.* N Biotechnol. 2010 Sep;27(4): 341–346. doi:10.1016/j.nbt.2010.06.003 Medline

Costas M, Alonso E, Outeiriño D, Guerra NP. Production of a highly concentrated probiotic culture of *Lactococcus lactis* CECT 539 containing high amounts of nisin. 3-Biotech. 2018;8:292.

Costas M, Alonso González E, Pérez Guerra N. Nisin production in realkalized fed-batch cultures in whey with feeding with lactose- or glucose-containing substrates. Appl Microbiol Biotechnol. 2016 Sep;100(18):7899–7908. doi:10.1007/s00253-016-7558-9 Medline

Daba H, Lacroix C, Huang J, Simard R. Influence of growth conditions on production and activity of mesenterocin 5 by a strain of *Leuconostoc mesenteroides.* Appl Microbiol Biotechnol. 1993 May;39(2):166–173. doi:10.1007/BF00228601

De Vuyst L, Vandamme EJ. Influence of the phosphorus and nitrogen source on nisin production in *Lactococcus lactis* subsp. *lactis* batch fermentations using a complex medium. Appl Microbiol Biotechnol. 1993 Oct;40(1):17–22. doi:10.1007/BF00170422

De Vuyst L. Nutritional factors affecting nisin production by *Lactococcus lactis* subsp. *actis* NIZO 22186 in a synthetic medium. J Appl Bacteriol. 1995 Jan;78(1):28–33. doi:10.1111/j.1365-2672.1995.tb01669.x

Garsa AK, Kumariya R, Kumar A, Lather P, Kapila S, Sood SK. Industrial cheese whey utilization for enhanced production of purified pediocin PA-1. Lebensm Wiss Technol. 2014 Dec;59(2): 656–665. doi:10.1016/j.lwt.2014.07.008

Guerra NP, Agrasar AT, Macías CL, Bernárdez PF, Castro LP. Dynamic mathematical models to describe the growth and nisin production by *Lactococcus lactis* subsp. *lactis* CECT 539 in both batch and re-alkalized fed-batch cultures. J Food Eng. 2007b Sep; 82(2):103–113. doi:10.1016/j.jfoodeng.2006.11.031

Guerra NP, Araujo AB, Barrera AM, Agrasar AT, Macías CL, Carballo J, Pastrana L. Antimicrobial activity of nisin adsorbed to surfaces commonly used in the food industry. J Food Prot. 2005 May;68(5):1012–1019. doi:10.4315/0362-028X-68.5.1012 Medline

Guerra NP, Bernárdez PF, Méndez J, Cachaldora P, Pastrana Castro L. Production of four potentially probiotic lactic acid bacteria and their evaluation as feed additives for weaned piglets. Anim Feed Sci Technol. 2007a Mar;134(1-2):89–107. doi:10.1016/j.anifeedsci.2006.05.010

Guerra NP, Pastrana L. Modelling the influence of pH on the kinetics of both nisin and pediocin production and characterization of their functional properties. Process Biochem. 2002 Apr;37(9): 1005–1015. doi:10.1016/S0032-9592(01)00312-0

Havilah EJ, Wallis DM, Morris R, Woolnough JA. A microcolorimetric method for determination of ammonia in Kjeldahl digests with a manual spectrophotometer. Lab Pract. 1977;26:545–547.

Flôres SH, Alegre RM. Nisin production from *Lactococcus lactis* A.T.C.C. 7962 using supplemented whey permeate. Biotechnol Appl Biochem. 2001 Oct 1;34(2):103–107. doi:10.1042/BA20010030 Medline

Jozala AF, Silva DP, Vicente AA, Teixeira JA, Júnior AP, Penna TCV. Processing of byproducts to improve nisin production by *Lactococcus lactis.* Afr J Biotechnol. 2011 Oct 26;10(66):14920–14925. doi:10.5897/AJB11.979

Khouiti Z, Simon JP. Carnocin KZ213 produced by *Carnobacterium piscicola* 213 is adsorbed onto cells during growth. Its biosynthesis is regulated by temperature, pH and medium composition. J Ind Microbiol Biotechnol. 2004 Jan 1;31(1):5–10. doi:10.1007/s10295-003-0104-7 Medline

Letort C, Nardi M, Garault P, Monnet V, Juillard V. Casein utilization by *Streptococcus thermophilus* results in a diauxic growth in milk. Appl Environ Microbiol. 2002 Jun 01;68(6):3162–3165. doi:10.1128/AEM.68.6.3162-3165.2002 Medline

Lowry OH, Rosebrough NJ, Farr AL, Randall RJ. Protein measurement with the Folin phenol reagent. J Biol Chem. 1951 Nov;193(1):265–275 Medline.

Lv W, Zhang X, Cong W. Modelling the production of nisin by *Lactococcus lactis* in fed-batch culture. Appl Microbiol Biotechnol. 2005 Aug;68(3):322–326. doi:10.1007/s00253-005-1892-7 Medline

Murado MA, Gonzalez MP, Pastrana L. Mussel processing wastes as a fermentation substrate. In: Martin AM, editor. Fisheries Processing: Biotechnological Applications. London (UK): Chapman and Hall; 1994. p. 311–343.

Murado MA, González MP, Vázquez JA. Dose–response relationships: an overview, a generative model and its application to the verification of descriptive models. Enzyme Microb Technol. 2002 Sep;31(4):439–455. doi:10.1016/S0141-0229(02)00109-6

Murphy J, Riley JP. A modified single solution method for the determination of phosphate in natural waters. Anal Chim Acta. 1962;27:31–36. doi:10.1016/S0003-2670(00)88444-5

Penna TCV, Jozala AF, De Lencastre Novaes LC, Pessoa A, Cholewa O. Production of nisin by *Lactococcus lactis* in media with skimmed milk. Appl Biochem Biotechnol. 2005;122(1-3):619–638. doi:10.1385/ABAB:122:1-3:0619 Medline

Penna TCV, Moraes DA. Optimization of nisin production by *Lactococcus lactis*. Appl Biochem Biotechnol. 2002;98-100(1-9): 775–790. doi:10.1385/ABAB:98-100:1-9:775 Medline

Pongtharangkul T, Demirci A. Effects of fed-batch fermentation and pH profiles on nisin production in suspended-cell and biofilm reactors. Appl Microbiol Biotechnol. 2006 Oct 20;73(1):73–79. doi:10.1007/s00253-006-0459-6 Medline

Poolman B, Konings WN. Relation of growth of *Streptococcus lactis* and *Streptococcus cremoris* to amino acid transport. J Bacteriol. 1988 Feb;170(2):700–707. doi:10.1128/jb.170.2.700-707.1988 Medline

Slavov AK. General characteristics and treatment possibilities of dairy wastewater. A review. Food Technol Biotechnol. 2017;55(1): 14–28. doi:10.17113/ftb.55.01.17.4520 Medline

Strickland JDH, Parsons TR. Determination of carbohydrate. In: Strickland JDH, Parsons TR, editors. A practical handbook of sea water analysis. Ottawa: Fisheries Research Board of Canada; 1968a. p. 173–174.

Strickland JDH, Parsons TR. Determination of total phosphorus. In: Strickland JDH, Parsons TR, editors. A practical handbook of sea water analysis. Ottawa: Fisheries Research Board of Canada; 1968b. p. 57–62.

Yang R, Ray B. Factors influencing production of bacteriocins by lactic acid bacteria. Food Microbiol. 1994 Aug;11(4):281–291. doi:10.1006/fmic.1994.1032

Supplementary materials are available on the journal's website.

Polish Journal of Microbiology
2019, Vol. 68, No 2, 281–284
https://doi.org/10.33073/pjm-2019-023

SHORT COMMUNICATION

Bacterial Diversity in Soybean Rhizosphere Soil at Seedling and Mature Stages

LIN WANG[1]*, ZHIYING LI[2], RUIRUI LIU[2], LULU LI[2] and WEIWEI WANG[2]

[1] Department of Medical Technology, Xi'an Medical University, Xi'an, Shaanxi, China
[2] Key Laboratory of Resource Biology and Biotechnology in Western China, Ministry of Education, Northwest University, Xi'an, Shaanxi, China

Submitted 5 December 2018, revised 3 March 2019, accepted 5 March 2019

Abstract

Changes in the structural diversity of bacterial communities in soybean rhizospheres play important roles in plant growth and crop productivity. However, there are only a few studies on different soybean growth stages. Here, we investigated the changes in the bacterial community of soybean rhizosphere soil at two stages using Illumina high-throughput sequencing. The results showed that the bacterial abundance and diversity in the seeding stage were higher than those in the mature stage and that the diversity changed significantly. *Actinobacteria*, *Acidobacteria*, and *Proteobacteria* were the dominant bacteria in the soybean rhizosphere soil. Additionally, changes in *Actinobacteria* and *Proteobacteria* abundances showed opposite trends.

Key words: soybean, growth stages, rhizosphere soil, bacterial community, Illumina high-throughput sequencing

Rhizosphere microbes are important components of soil ecosystems. These organisms are closely related to soil fertility and are essential indicators for evaluating soil health. Soil microbial community and diversity can reflect changes in the soil environmental quality and reveal differences in microbial ecological functions, which are critical for maintaining soil quality and ecosystem stability (Gertini 2005). Rhizosphere microorganisms can absorb the hydrogen released by nitrogen-fixing nodules of leguminous plants lacking hydrogenase. Experiments have shown that bacteria remove hydrogen (Mclearn and Dong 2002), and these bacteria were beneficial to the growth of plants (Dong et al. 2003; Abdellatif et al 2017). Therefore, studying the rhizosphere microbial diversity of legumes will improve our understanding of microbes that promote the growth of legumes.

Accordingly, in this study, Illumina high-throughput sequencing was used to investigate the microbial communities of rhizosphere soil samples. The soybean field was located in Xianyang, Shaanxi, NW China (107°38'–109°10' E, 34°11'–35°32' N), which is a typical warm temperate continental monsoon climate. The soil is dominated by ash-calcium soil. The soybean rhizosphere soil samples, numbered as S, were collected on June 24, 2016, when after more than half of the cotyledons were breaking out, and also the soil samples, numbered as M, were collected on September 30, 2016. At this time, the leaves and beans were dehydrated, demonstrating the inherent traits of the varieties.

The five-point sampling method was used to collect the rhizosphere soil samples according to the shake-off method of Riley et al. (1969). The soil sample was divided into two portions after filtering through a 2-mm sieve. One portion was stored in an –80°C refrigerator for soil microbial diversity analysis and was sequenced using an Illumina HiSeq 2500 at Biomarker Technologies (Beijing, China). The primers used for sequencing were 338F (5'-ACTCCTACGGGAGGCAGCA-3') and 806R (5'-GGACTACHVGGGTWTCTAAT-3') (Zhang et al. 2015); the other was naturally air-dried and sieved for soil physical and chemical properties analysis in a reference to Soil Agrochemical Analysis (Bao 2000).

Some physical and chemical properties of soil in different time are shown in Table I. There were significant differences in pH, available potassium, and soil

* Corresponding author: L. Wang, Department of Medical Technology, Xi'an Medical University, Xi'an, Shaanxi, China; **e-mail: w.w.wang@163.com**

Table I
Changes in basic physical and chemical properties of soils at different sampling times.

	S	M
Organic matter (g/kg)	1.40 ± 0.05a	1.51 ± 0.02a
Total nitrogen (g/kg)	2.05 ± 0.02a	2.13 ± 0.07a
pH	7.30 ± 0.04a	7.55 ± 0.03b
Available phosphorus (mg/kg)	7.54 ± 0.04a	7.59 ± 0.09a
Available potassium (mg/kg)	86.09 ± 0.93a	88.18 ± 0.40b
Soil temperature (°C)	18.48 ± 0.13a	23.65 ± 0.09 b
Moisture content (%)	30.58 ± 0.91a	31.27 ± 0.83a

temperature, whereas other indicators did not differ at the two sampling times. The contents of organic matter, total nitrogen, available phosphorus, and potassium, as well as the moisture in M soil samples were higher than those in S soil samples, and the pH and temperature increased in the M phase.

The coverage of each sample was greater than 99%, demonstrating that the sequencing results could reflect the real situation of the sample. The ACE ($P = 0.453$) index and the Chao1 ($P = 0.909$) index were higher at the S stage than at the M stage, indicating that the S stage soil samples were rich in microorganisms; however, the difference was not significant. The Shannon index of the S stage was larger than that of the M stage, and the P values between the S and M stages were the Shannon index ($P = 0.00074$) and Simpson index ($P = 0.0037$), respectively, indicating that the diversity of the bacteria were higher in the S stage.

As shown in Fig. 1, ten phyla including *Actinobacteria*, *Acidobacteria*, *Proteobacteria*, *Gemmatimonadetes*, *Bacteroidetes*, *Chloroflexi*, *Verrucomicrobia*, *Nitrospirae*, *Planctomycetes*, and *Armatimonadetes* were obtained from the six soil samples.

The dominant phyla at the S and M stages were *Actinobacteria*, *Acidobacteria*, and *Proteobacteria*. At the S stage, *Proteobacteria*, *Acidobacteria*, and *Actinobacteria* accounted for 27.7%, 27.2%, and 14.3%, respectively; at the M stage, *Proteobacteria*, *Actinobacteria*, and *Acidobacteria* accounted for 17.0%, 38.1%, and 21.8%, respectively. Compared with the soil samples collected at the S stage, the number of *Actinobacteria* increased by 165.6%, and the numbers of *Acidobacteria* and *Proteobacteria* decreased by 20.1% and 38.6%, respectively.

Bacteria are important soil microbes, and their types and quantities have direct effects on soil biochemical properties and soil nutrients. The Illumina high-throughput sequencing is widely used in the study of soil microbial diversity owing to its rapid, convenient, and highly accurate results. In this study, we analyzed the community and diversity of bacteria in rhizosphere soil from two different growth stages. We found that

Table II
Alpha diversity of samples.

	S	M
ACE	1,590.75 ± 6.14a	1582.79 ± 12.11a
Chao1	1594.44 ± 5.52a	1593.50 ± 9.42a
Shannon	6.31 ± 0.0100a	5.70 ± 0.0919b
Simpson	0.0047 ± 0.00a	0.0152 ± 0.0024b
Coverage	0.9993	0.9983

microbial abundance and diversity at the S stage were higher than those at the M stage. Many factors influence microbial diversity (Lupwayi et al. 2001; Schutter and Dick 2002; Lipson 2007; Peralta et al. 2013). Rasche et al. (2011) suggested that humidity and temperature are the main environmental factors affecting soil microbes in temperate forests, similar to the results of the present study. The appropriate soil temperature affects the availability of nutrients in the soil and the growth environment of microorganisms, further stim-

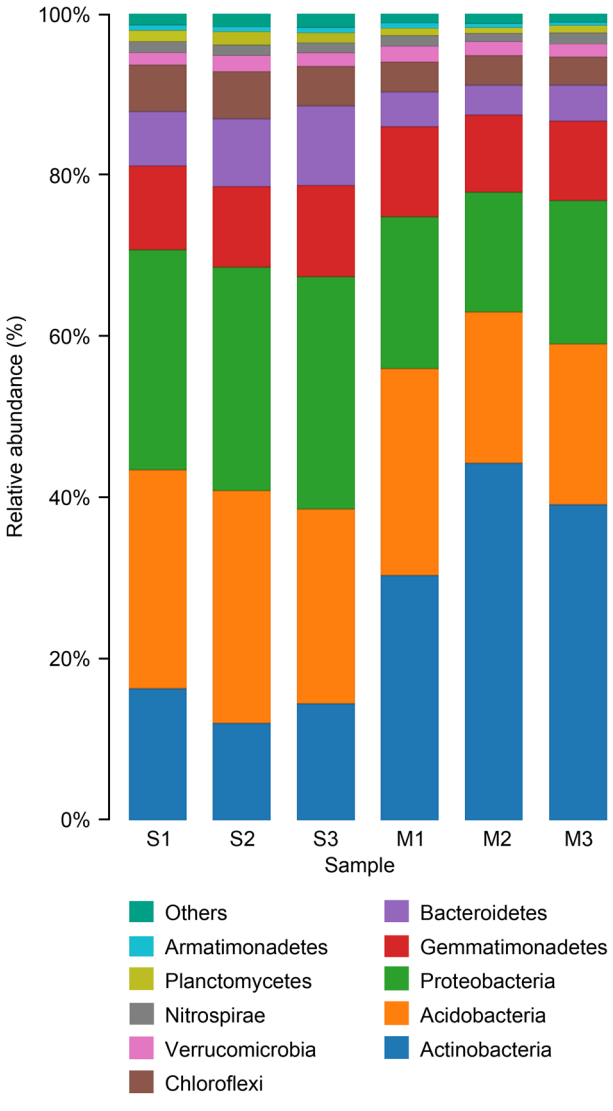

Fig. 1. Microbial communities at the phylum level.

ulating the activity of soil microbes and function of soil microbial communities (Luo et al. 2001; Melillo et al. 2002). Suitable water can significantly change the microbial community and activity. A certain degree of humidity in the soil plays an important role in cultivating strong seedlings and improving the ability to resist drought in the later period. In June, the temperature and rainfall in Xianyang were appropriate, which led to increases in the number of nodules, the emission of hydrogen gas during nitrogen fixation, and enhancement of the number of hydrogen-oxidizing bacteria (Dong and Layzell 2001; Dong et al. 2003). This caused soil microbial diversity and abundance to be high in June. In September, the soil temperature rose significantly to 23°C, which was beneficial for microorganism growth; however, the diversity was lower in the M stage than in the S stage. The reason for this result may be that the appropriate temperature enhanced microbial metabolism, changing some specific flora into the main flora. These dominant bacteria had a competitive advantage over other microbiota, resulting in the proliferation of a few dominant phyla, whereas others were inhibited or eliminated during competition. At the same time, there was heavy rain in Xianyang in September 2016. Unger et al. (2009) also found that continuous flooding conditions reduced soil microbial biomass and affected the soil microbial community, causing microbial diversity and abundance to decrease.

In this study, we found that compared with the S stage, the number of *Actinobacteria* increased, and both *Proteobacteria* and *Acidobacteria* decreased in the M stage. At the M stage, the nitrogen fixation capacity of soybean nodules is weakened, and the hydrogen concentration is lowered. Studies have shown that certain microorganisms in *Actinobacteria* (Constant et al. 2008; Constant et al. 2010) consume atmospheric tropospheric trace hydrogen at 0.553 ppmv. This may increase the number of *Pseudonocardia* and *Nocardioides*. Whether these two genera can absorb atmospheric trace hydrogen is worthy of further study. Li et al. (2018) found that in the original rhizosphere soil samples of *Medicago sativa* and the hydrogen-treated soil samples, changes in the abundances of *Actinobacteria* and *Proteobacteria* showed opposite trends. In this study, we found that soil samples from the rhizospheres of soybeans also showed similar trends. Further studies are needed to determine whether this trend exists in other legumes or other crops. Many studies have shown that the microbial community is related to the growth stage. For example, Duineveld et al. (2001) found that the microbial community structures of rhizosphere soils of young plants and mature plants differed. Additionally, Farina et al. (2012) found that the microbial community structure of canola differed accordingly to growth stage, with the greatest abundance during the rosette period. Xu et al. (2009) also found that the bacterial diversity in soybean rhizosphere increased primarily and then decreased; the increase was observed beginning from the flowering period, reached a maximum during the drum period, and was lowest during the maturity period.

In summary, the soybean growth period was found to have an important influence on the bacterial community in rhizosphere soil, and bacterial diversity was mainly affected by soil temperature and humidity. Changes in the abundances of *Acidobacteria* and *Proteobacteria* showed opposite trends. Our findings provided a theoretical basis for understanding the diversity and changes in the bacterial community in soybean rhizosphere soil.

Acknowledgments

This study is supported by the National Natural Science Foundation (Grant No. 41571243) and the project of young talents of science and technology association of Shaanxi province (Project Number: 20160232). We thank Biomarker Technologies for their excellent technical assistance.

Conflict of interest

The authors do not report any financial or personal connections with other persons or organizations, which might negatively affect the contents of this publication and/or claim authorship rights to this publication.

Literature

Abdellatif L, Ben-Mahmoud OM, Yang C, Hanson KG, Gan Y, Hamel C. The H_2-oxidizing rhizobacteria associated with field-grown lentil promote the growth of lentil inoculated with Hup+ rhizobium through multiple modes of action. J Plant Growth Regul. 2017 Jun;36(2):348–361. doi:10.1007/s00344-016-9645-7

Bao SD. Soil Agricultural Chemistry analysis. Beijing (China): Agriculture Press; 2000.

Constant P, Chowdhury SP, Pratscher J, Conrad R. *Streptomycetes* contributing to atmospheric molecular hydrogen soil uptake are widespread and encode a putative high-affinity [NiFe]-hydrogenase. Environ Microbiol. 2010 Mar;12(3):821–829. doi:10.1111/j.1462-2920.2009.02130.x Medline

Constant P, Poissant L, Villemur R. Isolation of *Streptomyces* sp. PCB7, the first microorganism demonstrating high-affinity uptake of tropospheric H_2. ISME J. 2008 Oct;2(10):1066–1076. doi:10.1038/ismej.2008.59 Medline

Dong Z, Layzell DB. H_2 oxidation, O_2 uptake and CO_2 fixation in H_2 treated soils. Plant Soil. 2001;229(1):1–12. doi:10.1023/A:1004810017490

Dong Z, Wu L, Kettlewell B, Caldwell CD, Layzell DB. Hydrogen fertilization of soils – is this a benefit of legumes in rotation? Plant Cell Environ. 2003 Nov;26(11):1875–1879. doi:10.1046/j.1365-3040.2003.01103.x

Duineveld BM, Kowalchuk GA, Keijzer A, van Elsas JD, van Veen JA. Analysis of bacterial communities in the rhizosphere of *chrysanthemum* via denaturing gradient gel electrophoresis of PCR-amplified 16S rRNA as well as DNA fragments coding for 16S rRNA. Appl Environ Microbiol. 2001 Jan 01;67(1):172–178. doi:10.1128/AEM.67.1.172-178.2001 Medline

Farina R, Beneduzi A, Ambrosini A, de Campos SB, Lisboa BB, Wendisch V, Vargas LK, Passaglia LMP. Diversity of plant growth-promoting rhizobacteria communities associated with the stages of canola growth. Appl Soil Ecol. 2012 Apr;55(1):44–52. doi:10.1016/j.apsoil.2011.12.011

Gertini G. Effect on properties of forest soils: a review. Oecologia, 2005;143(1):l–10.

Li Z, Liu X, Liu R, Li L, Wang L, Wang W. Insight into bacterial community diversity and monthly fluctuations of *Medicago sativa* rhizosphere soil in response to hydrogen gas using Illumina High-Throughput Sequencing. Curr Microbiol. 2018 Dec;75(12): 626–1633. doi:10.1007/s00284-018-1569-y Medline

Lipson DA. Relationships between temperature responses and bacterial community structure along seasonal and altitudinal gradients. FEMS Microbiol Ecol. 2007 Feb;59(2):418–427. doi:10.1111/j.1574-6941.2006.00240.x Medline

Luo Y, Wan S, Hui D, Wallace LL. Acclimatization of soil respiration to warming in a tall grass prairie. Nature. 2001 Oct;413 (6856): 622–625. doi:10.1038/35098065 Medline

Lupwayi NZ, Arshad MA, Rice WA, Clayton GW. Bacterial diversity in water-stable aggregates of soils under conventional and zero tillage management. Appl Soil Ecol. 2001 Mar;16(3):251–261. doi:10.1016/S0929-1393(00)00123-2

McLearn N, Dong Z. Microbial nature of the hydrogen-oxidizing agent in hydrogen-treated soil. Biol Fertil Soils. 2002 Jul 1; 35(6):465–469. doi:10.1007/s00374-002-0495-z

Melillo JM, Steudler PA, Aber JD, Newkirk K, Lux H, Bowles FP, Catricala C, Magill A, Ahrens T, Morrisseau S. Soil warming and carbon-cycle feedbacks to the climate system. Science. 2002 Dec 13;298(5601):2173–2176. doi:10.1126/science.1074153 Medline

Peralta AL, Ludmer S, Kent AD. Hydrologic history influences microbial community composition and nitrogen cycling under experimental drying/wetting treatments. Soil Biol Biochem. 2013 Nov;66(11):29–37. doi:10.1016/j.soilbio.2013.06.019

Rasche F, Knapp D, Kaiser C, Koranda M, Kitzler B, Zechmeister-Boltenstern S, Richter A, Sessitsch A. Seasonality and resource availability control bacterial and archaeal communities in soils of a temperate beech forest. ISME J. 2011 Mar;5(3):389–402. doi:10.1038/ismej.2010.138 Medline

Riley D, Barber SA. Bicarbonate accumulation and pH changes at the soybean (*Glycine max* (L.) Merr.) root-soil interface. Soil Sci Soc Am J. 1969;33(6):905–908. doi:10.2136/sssaj1969.03615995003300060031x

Schutter ME, Dick RP. Microbial community profiles and activities among aggregates of winter fallow and cover-cropped soil. Soil Sci Soc Am J. 2002;66(1):142–153. doi:10.2136/sssaj2002.1420

Unger IM, Kennedy AC, Muzika RM. Flooding effects on soil microbial communities. Appl Soil Ecol. 2009 May;42(1):1–8. doi:10.1016/j.apsoil.2009.01.007

Xu Y, Wang G, Jin J, Liu J, Zhang Q, Liu X. Bacterial communities in soybean rhizosphere in response to soil type, soybean genotype, and their growth stage. Soil Biol Biochem. 2009 May;41(5):919–925. doi:10.1016/j.soilbio.2008.10.027

Zhang X, Tian X, Ma L, Feng B, Liu Q, Yuan L, Fan C, Huang H, Huang H, Yang Q. Biodiversity of the symbiotic bacteria associated with toxic marine dinoflagellate *Alexandrium tamarense*. J Biosci Med (Irvine). 2015;03(06):23–28. doi:10.4236/jbm.2015.36004

Polish Journal of Microbiology
2019, Vol. 68, No 2, 285-290

INFORMACJE Z POLSKIEGO TOWARZYSTWA MIKROBIOLOGÓW

KONFERENCJA POD PATRONATEM PTM

Konferencja międzynarodowa:
8 Międzynarodowa Konferencja Weiglowska
Łódź, 26–28.06.2019

Konferencja organizowana jest przez Instytut Biologii Medycznej PAN,
Uniwersytet Łódzki oraz Uniwersytet Medyczny w Łodzi

The planned Conference is the eighth conference to commemorate the outstanding Polish microbiologist Prof. Rudolf Weigl, the creator of the first effective vaccine against typhus. The conference is devoted to selected medical, microbiological and biotechnology issues. As part of the conference, thematic sessions will be devoted to (i) Reinvention of bacteriophage therapy. Bacteriophages in control of infectious diseases (ii) From single cell to microbial communities studies, molecular basis of virulence in the complexity of microbiome, (iii) Medical and industrial biotechnology – research and development. Novel therapeutic strategies and practical applications. The conference will be a unique platform for meetings and discussions for researchers dealing with the molecular basis of selected diseases, for microbiologists investigating these processes at the level of virulence factor, but also for clinicians involved in everyday diagnostics and treatment of diseases. The conference will also create a unique opportunity to familiarize participants of the session, including students and doctoral students, with different perspectives of research on the same processes, from the human body to pathogenic or saprophytic microorganisms and their mutual interactions.

http://grupamedica.pl/8th-international-weigl-conference-26-28-06-2019/
www.twitter/grupamedica ; https://web.facebook.com/8thweiglconferene/

W dniu 25.03.2019 r. odbyło się trzecie zebranie
Zarządu Głównego Polskiego Towarzystwa Mikrobiologów kadencji 2016–2020.

Poniżej w punktach, w formie skrótowej przedstawiono omawiane sprawy.

1. Prezes PTM – prof. Stefan Tyski powitał zebranych – przybyli wszyscy członkowie ZG PTM (z wyjątkiem przedstawiciela Oddziału Puławy), a także 9 zaproszonych gości (dr Kamila Korzekwa, wiceprzewodnicząca Oddziału Wrocław, dr Elżbieta Stefaniuk – przewodnicząca Głównej Komisji Rewizyjnej, prof. dr hab. Jacek Bielecki – redaktor naczelny Postępów Mikrobiologii, dr Radosław Stachowiak – z-ca redaktora naczelnego PM, Pani Mariola Machowska-Kacprzak – księgowa PTM, dr Tomasz Zaręba, przewodniczący Sekcji Mikrobiologia Farmaceutyczna, dr Szymon Walter de Welthoffen, diagnosta laboratoryjny, Pan Zbigniew Kowal, Prezes firmy Global Congress oraz Panie Barbara Tutak i Joanna Stasiszyn również z firmy Global Congress. Firma ta będzie pomagać w organizacji XXIX Zjazdu PTM w 2020 r. w Warszawie.

Po przyjęciu programu zebrania nastąpiła prezentacja wszystkich uczestników spotkania.

2. Wybrano 2 osobową Komisję Skrutacyjną.

3. Minutą ciszy uczczono zmarłych zasłużonych członków PTM: prof. Marię Kozioł-Montewkę, prof. Józefa F. Kubicę, dr Wandę Michalską i dr Andrzeja Kasprowicza.

4. Prezes PTM przedstawił informację o działalności Prezydium PTM od poprzedniego zebrania ZG PTM w dniu 19.03.2018 r.:
   - omówiono Uchwały nr 26–45 z 2018 r., które poddano głosowaniu droga elektroniczną na kilku wirtualnych zebraniach Prezydium ZG PTM w 2018 r. i **Uchwałą nr 1-2019** zaakceptowano działalność Prezydium ZG PTM w okresie 19.03.2018 r. – 25.03.2019 r.
   - przypomniano, że informacje o bieżącej działalności PTM zamieszczano we wszystkich kolejnych numerach czasopism Postępy Mikrobiologii (PM) i Polish Journal of Microbiology (PJM), a także na facebooku PTM,
   - podano informację o złożeniu wniosku do MNiSW na działalność upowszechniającą naukę (DUN), dotyczącym organizacji konferencji 70 lat Oddziału PTM w Warszawie, jednakże wniosek ten nie uzyskał finansowania,
   - przedstawiono informację o dofinansowaniu z DUN czasopism PM i PJM w latach 2018–2019. Redakcje obu czasopism dokładają starań, aby podnieść ich poziom. Maszynopisy prac przesyłane do PM są tłumaczone za język angielski z dofinansowania MNiSW w 2019 r. Od przyszłego roku autorzy będą zobowiązani do przesyłania wersji angielskojęzycznych manuskryptów, ponieważ takie będą zamieszczane on-line na stronie wydawnictwa Exeley Inc.

5. Omówiono sprawę powołanych sekcji PTM, które w zasadzie nie działają. Pan dr Tomasz Zaręba przedstawił Sekcję Mikrobiologii Farmaceutycznej i konferencję, która miała się odbyć w maju, natomiast Pan dr Szymon Walter de Walthoffen przedstawił swoja wizję działalności Sekcji Diagnostów Laboratoryjnych.

6. Księgowa PTM Pani Mariola Machowska-Kasprzak przedstawiła informację o stanie finansowym PTM oraz bilans finansowy PTM za 2018 r.

7. Pani dr Elżbieta Stefaniuk Przewodnicząca Głównej Komisji Rewizyjnej PTM przedstawiła pozytywna opinię Komisji Rewizyjnej na temat bilansu finansowego PTM za 2018 r.

8. Omawiano sprawę możliwości przekazania pewnych środków finansowych do wydatkowania przez Oddziały PTM.
   - Prezes PTM poddał pod głosowanie **Uchwałę nr 2-2019** zmieniająca Uchwałę nr 33-2017 z dnia 30.08.2017 r. ZG PTM w sprawie udostępnienia Oddziałom Terenowym PTM od stycznia 2019 r., 50% kwoty uzyskanej z tytułu pozyskania sponsora, Członka Wspierającego PTM, darowizny, lub innej dodatkowej kwoty, na rzecz PTM, przez dany Oddział, na pokrycie kosztów prowadzenia działalności statutowej przez ten Oddział. Obecnie przyjęto **Uchwałę 2-2019** w brzmieniu: „Kwota środków przekazana na konto PTM z tytułu sponsorowania konkretnego wydarzenia w całości jest do dyspozycji Oddziału, który pozyskał takiego sponsora. W pozostałych przypadkach 50% kwoty uzyskanej z tytułu pozyskania; sponsora przekazującego środki na ogólne cele statutowe Towarzystwa, Członka Wspierającego PTM, darowizny na ogólne cele statutowe Towarzystwa, innej dodatkowej kwoty, pozyskanej na rzecz Towarzystwa, przez dany Oddział, udostępniane jest temu Oddziałowi. Zasady wydatkowania i rozliczania wszystkich pozyskanych funduszy przez Oddział Terenowy PTM muszą być zgodne z Regulaminem wydatkowania i rozliczania środków pieniężnych przez Oddziały PTM".
   - Sekretarz ZG PTM mówiła opracowany „Regulamin wydatkowania i rozliczania środków pieniężnych przez Oddziały Terenowe Polskiego Towarzystwa Mikrobiologów".
   - **Uchwałą nr 3-2019** zatwierdzono w/w Regulamin do stosowania począwszy od początku 2019 r. Tym samym Oddziały uzyskają możliwość wydatkowania środków finansowych, których wysokość uzależniona jest od liczby członków w Oddziale, na prowadzona przez siebie działalność statutową.

9. Przyjęto **Uchwałę nr 4-2019** w sprawie przyjęcia 35 nowych członków zwyczajnych.

10. Przyjęto **Uchwałę nr 5-2019** w sprawie usunięcia z grona członków PTM 78 osób oraz firmę Aesculap Chifa Sp. z o.o. – członka grupy B. Brown, z powodu nieopłacenia składki członkowskiej za 2018 r.

Podsumowując, składkę członkowską w PTM w 2018 r. opłaciło 856 osób, a przynależność do PTM w oddziałach kształtowała się następująco:

Oddział Terenowy PTM	Liczba			
	Członek Zwyczajny	Członek Zwyczajny, emeryt	Członek Honorowy	SUMA
Białystok	33	0	1	34
Bydgoszcz	70	1	0	71
Gdańska	47	2	2	51
Katowice	89	3	0	92
Kielce	23	0	0	23
Kraków	117	7	0	124
Lublin	55	0	1	56
Łódź	40	1	0	41
Olsztyn	28	2	1	31
Poznań	64	4	0	68
Puławy	15	1	2	18
Szczecin	56	1	2	59
Warszawa	157	8	7	172
Wrocław	31	1	1	33
Ogółem	825	31	17	873

11. Przewodniczący Zarządów Oddziałów Terenowych PTM przedstawili informacje z działalności swoich Oddziałów w okresie od 19.03.2018 r. do 25.03.2019 r. w tym o odbytych konferencjach pod patronatem PTM. Przedstawili również plany działalności Oddziałów w najbliższych latach.

12. Prezes PTM poinformował o planowanych konferencjach pod patronatem PTM:
    - VII Konferencji Naukowo-Szkoleniowej „Mikrobiologia Farmaceutyczna 2019", Gdańsk, 22–24 maj 2019 r.,
    - VIII Międzynarodowej Konferencji Weiglowskiej, Łódź, 26–28 czerwiec 2019 r.,
    - **Uchwałą nr 6-2019** udzielono poparcia IV Ogólnopolskiemu Sympozjum Mikrobiologicznemu „Metagenomy Różnych Środowisk", Lublin, 27–28 czerwiec 2019 r.

13. Przedstawiono wstępne informacje o XXIX Zjeździe PTM, planowanym na wrzesień 2020 r. w Warszawie**. Uchwałą nr 7-2019** na przewodniczącego Komitetu Organizacyjnego Zjazdu powołano Prezesa PTM – prof. S. Tyskiego, a na zastępcę Wiceprezes PTM – prof. E. Augustynowicz-Kopeć. Na przewodniczącą Komitetu Naukowego Zjazdu powołano prof. E. Augustynowicz-Kopeć, a na wiceprzewodniczącego – prof. S. Tyskiego. W skład Komitetu Naukowego Zjazdu wchodzą wszyscy członkowie ZG PTM. Logistycznie zjazd będzie wspierać firma Global Congress.

14. Prezes PTM, a jednocześnie delegat PTM do FEMS oraz IUMS – prof. S. Tyski podsumował 45 spotkanie „FEMS Council" organizowane po raz pierwszy w naszym kraju przez PTM, w dniach 7–8 września 2018 r. w Warszawie. Na nasze zaproszenie przyjechali przedstawiciele 35 europejskich towarzystw mikrobiologicznych przyjechał również cały zarząd FEMS – Prezydent FEMS prof. Bauke Oudega z Holandii oraz 7 dyrektorów FEMS wraz z 12 pracownikami FEMS. Wysokość składek do FEMS – 1,4 Euro i IUMS – 1,4 USD od członka PTM nie ulegają zmianie. Dużą stratą jest brak zgłoszeń osób na FEMS Research Grant na wyjazdy do naukowych ośrodków zagranicznych. Poinformowano o kongresie „8th Congress of European Microbiologists – FEMS2019", który odbędzie się w Glasgow, Szkocja 7–11 lipca 2019 r. Międzynarodowa konferencja „4th Congress of Baltic Microbiologists", organizowana 10–12.09.2018 r. w Gdańsku otrzymała dofinansowanie FEMS w wysokości 7.000 Euro. W **Uchwale nr 8-2019** wyrażono zgodę na pokrycie kosztów uczestnictwa prof. S. Tyskiego w FEMS Council 2019 w Mediolanie.

15. W tym roku kończy się kadencja Sekretarza Generalnego FEMS, jest to jedno z głównych stanowisk w Zarządzie Głównym FEMS. Pan prof. dr hab. Grzegorz Węgrzyn z Uniwersytetu Gdańskiego wyraził zgodę na kandydowanie na stanowisko Sekretarza Generalnego FEMS. W głosowaniu tajnym przyjęto **Uchwałę nr 9-2019** popierającą kandydaturę Pana profesora na stanowisko Sekretarza Generalnego FEMS.

16. W związku z rozmaitym podejściem stosowanym w Oddziałach do przyznawania punktów edukacyjnych, powołano Komisję w składzie prof. dr hab. Ewa Augustynowicz-Kopeć, dr hab. Edyta Podsiadły i dr Elżbieta Stefaniuk, do określania zasad przyznawania punktów edukacyjnych za uczestnictwo w zebraniach i seminariach organizowanych przez Oddziały PTM – **Uchwała nr 10-2019**.

17. Prezes PTM przedstawił informację o Konferencji Prezesów Towarzystw Lekarskich (nie należy mylić z Federacją Polskich Towarzystw Medycznych). Podjęto **Uchwałę nr 11-2019** o podpisaniu deklaracji o przystąpieniu PTM do KPTL.

18. W związku z pojawieniem się zachowań „nielicujących z dobrym imieniem członka PTM", przy braku statutowej komisji dyscyplinarnej, postanowiono powołać „Komisję do spraw etyki członków PTM" o składzie osobowym podobnym do Komisji konkursowej oceniającej materiały do nagrody naukowej PTM im. prof. Edmunda Mikulaszka, pod przewodnictwem Pani prof. dr hab. Stefanii Giedrys-Kalemby – **Uchwała nr 12-2019.**

19. W **Uchwale nr 13-2019** podjęto decyzje w sprawie przedłużenia zatrudnienia Pana mgr Adama Guśpiela jako Sekretarza Redakcji PJM do 30.09.2020 r.

20. Informacje o wydawanych czasopismach PTM i sytuacji w redakcjach przedstawili redaktorzy naczelni: PJM – Pani prof. dr hab. Elżbieta Anna Trafny i PM – Pan prof. dr hab. Jacek Bielecki. Omawiano problemy i plany związane z wydawaniem czasopism przez wydawnictwo amerykańskie Exeley Inc.

21. W związku z dużymi kosztami wydawania czasopism, podjęto **Uchwałę nr 14-2019** w sprawie zwiększenia opłat redakcyjnych za publikacje w PJM z 250 USD do 350 USD dla autorów korespondencyjnych – członków PTM i z 500 USD do 700 USD dla autorów korespondencyjnych nie będących członkami PTM. Zwiększona opłata dotyczyć będzie manuskryptów przysłanych do Redakcji PJM po 30.06.2019 r.

22. Dyskutowano nad informacją o stanowisku Konsultanta Krajowego w dziedzinie Diagnostyki Laboratoryjnej Pana prof. dr hab. Macieja Szmitkowskiego w sprawie absolwentów studiów na kierunku mikrobiologia. Stanowisko to jest sprzeczne ze stanowiskiem PTM opracowanym w ubiegłym roku i zamieszczonym na stronie PTM. Pani dr hab. Beata Anna Sadowska zobowiązała się do przygotowania odpowiedzi dla Pana prof. dr hab. M. Szmitkowskiego.

Po zebraniu Zarządu Głównego Polskiego Towarzystwa Mikrobiologów, w kolejnych miesiącach Prezydium ZG PTM zajmowało się następującymi sprawami:

1. Podjęto **Uchwałę nr 15-2019** w sprawie objęcia honorowym patronatem seminarium naukowego pt. „III Sesja Młodych Mikrobiologów Środowiska Łódzkiego", które odbędzie się w dniu 7 czerwca 2019 r. na Wydziale Farmaceutycznym Uniwersytetu Medycznego w Łodzi.

2. Podjęło **Uchwałę nr 16-2019** w sprawie przyjęcia firmy BART Sp. z o.o. Sp. K. do grona członków wspierających PTM, jako Członka Zwyczajnego.

3. Podjęło **Uchwałę nr 17-2019** w sprawie przyjęcia 6 nowych członków zwyczajnych PTM.

4. Informujemy, że PTM podpisało umowę z firmą EBSCO Publishing Inc. ze Stanów Zjednoczonych dotyczącą współpracy i umieszczenia czasopisma Polish Journal of Microbiology w międzynarodowych bazach naukowych EBSCO. Współpraca z firmą EBSCO powinna zapewnić wzrost popularności czasopisma (IF, punktacja) i jego umiędzynarodowienia, a także rozpoznawalności PJM i PTM. Bazy EBSCO są używane przez ponad 130 000 bibliotek akademickich, instytutów i szpitali na całym świecie (w tym Harvard Medical College, UCLA itp.).

5. Informujemy również, że Minister Nauki i Szkolnictwa Wyższego Pan dr Jarosław Gowin powołał Pana prof. dr hab. Grzegorza Węgrzyna z Uniwersytetu Gdańskiego, **członka PTM** na stanowisko Przewodniczącego Rady Doskonałości Naukowej (RDN) w kadencji 2019–2023. RDN zastępuje dotychczasową Centralną Komisję do spraw Stopni i Tytułów.
   Pan prof. Grzegorz Węgrzyn do RDN został wybrany w dziedzinie nauk ścisłych i przyrodniczych w dyscyplinie nauk biologicznych. Zainteresowania badawcze Pana profesora to mechanizmy replikacji DNA plazmidów i bakteriofagów, regulacja ekspresji genów w komórkach bakteryjnych oraz zastosowanie elektrycznych bio-chipów.

6. Ustalono, że **XXIX Zjazd PTM odbędzie się w dniach 15–18 września 2020 r., w Warszawie w Centrum Konferencyjno-Szkoleniowym przy ul. Bobrowieckiej 9.** Prosimy o zarezerwowanie tego terminu i przygotowanie ciekawych oraz wartościowych prac.

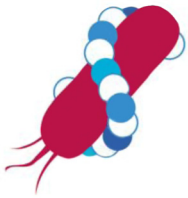

XXIX OGÓLNOPOLSKI ZJAZD
POLSKIEGO TOWARZYSTWA
MIKROBIOLOGÓW
15-18 WRZEŚNIA 2020,
WARSZAWA

SEKRETARZ
Polskiego Towarzystwa Mikrobiologów
dr hab. n. farm. Agnieszka E. Laudy

PREZES
Polskiego Towarzystwa Mikrobiologów
prof. dr hab. Stefan Tyski

CZŁONKOWIE WSPIERAJĄCY PTM

Członek Wspierający PTM – Złoty
od 27.03.2017 r.

HCS Europe – Hygiene & Cleaning Solutions
ul. Warszawska 9a, 32-086 Węgrzce k. Krakowa
tel. (12) 414 00 60, 506 184 673, fax (12) 414 00 66
www.hcseurope.pl

Firma projektuje profesjonalne systemy utrzymania czystości i higieny dla klientów o szczególnych wymaganiach higienicznych, m.in. kompleksowe systemy mycia, dezynfekcji, osuszania rąk dla pracowników służby zdrowia, preparaty do dezynfekcji powierzchni dla służby zdrowia, systemy sterylizacji narzędzi.

Członek Wspierający PTM – Srebrny
od 12.09.2017 r.

Firma Ecolab Sp. z o.o. zapewnia: najlepszą ochronę środowiska pracy przed patogenami powodującymi zakażenia podczas leczenia pacjentów, bezpieczeństwo i wygodę personelu, funkcjonalność posiadanego sprzętu i urządzeń. Firma jest partnerem dla przemysłów farmaceutycznego, biotechnologicznego i kosmetycznego.

Członek Wspierający PTM – Srebrny
od 12.12.2017 r.

Od ponad 100 lat siedziba Wodociągów Krakowskich mieści się przy ul. Senatorskiej. Budowę obiektu ukończono w 1913 roku. W 2016 r. do sieci wodociągowej wtłoczono ponad 56 mln m^3 wody. Szacuje się, że ponad 99,5% mieszkańców Gminy Miejskiej Kraków posiada możliwość korzystania z istniejącej sieci wodociągowej.

Członek Wspierający PTM – Zwyczajny
od 12.09.2017 r.

Merck Sp. z o.o. jest częścią międzynarodowej grupy Merck KGaA z siedzibą w Darmstadt, Niemcy i dostarcza na rynek polski od roku 1992 wysokiej jakości produkty farmaceutyczne i chemiczne, w tym podłoża mikrobiologiczne

Członek Wspierający PTM – Zwyczajny
od 06.06.2019 r.

BART Spółka z o.o. Sp. K
ul. Norwida 4, 05-250 Słupno
NIP: 1180741884, KRS: 0000573068
https://bart.pl/, email: info@bart.pl

Firma BART jest producentem i dystrybutorem surowców oraz dodatków dla przemysłu spożywczego i farmaceutycznego. Specjalizujemy się w probiotykach oraz surowcach uzyskiwanych metodami biotechnologicznymi.
Współpracujemy z renomowanymi producentami: Probiotical, Gnosis, Lesaffre